



Vertical deformation in hybrid timber high-rise structures

Main Thesis

Document information

Title : Vertical deformation in timber hybrid high-rise structures.
Document type : Main thesis
Reference : V3.0
Status : Definitive
Date : 05 January 2023

Graduation company : Aveco de Bondt
Burgemeester van der Borchstraat 2
7451 CH Holten



Educational Institution : Technical University Delft
Faculty Civil Engineering
Stevinweg 1
2628 CN Delft



Colophon

Author

Name : ing. R. (Rick) Schönthaler

Company supervisor

Name : ir. K.J. (Jeroen) ter Steege
Function : Senior constructor building constructions

University supervisor 1

Name : Dr. ir. G.J.P. (Geert) Ravenshorst
Function : Professor Biobased structures

University supervisor 2

Name : Prof. dr. ir. J.W.G. (Jan-Willem) van de Kuilen
Function : Professor Biobased structures

University supervisor 3

Name : Dr. ir. P.C.J. (Pierre) Hoogenboom
Function : Assistant professor structural engineering

Revision list

7 October 2022 – V1.0 – Concept version.

28 November 2022 – V2.0 – Definitive version 2.

05 January 2023 – V3.0 – Definitive version including feedback from the greenlight meeting.

Preface

Dear reader,

to conclude the master Structural Engineering, a graduation project has been carried out at Aveco de Bondt. This project comprises of the theoretical verification of differential vertical shortening in hybrid timber high rise buildings.

The system that is considered in this research consists of a concrete prefabricated core combined with a timber frame. The timber frame consists out of prefabricated timber modules which derive lateral stability from the core. Due to contrasting elastic, hygroexpansion and viscoelastic properties there is a notable difference in the vertical deformation of the concrete core and the timber units.

The impact of the vertical deformation differences will be outlined and possibilities to minimize the impact will be explored. This is done by means of a literature study followed by a case and parameter study.

Rick Schönthaler



Summary

At this day and age, climate control has become an important topic. In search of more durable building materials is timber becoming increasingly popular for structural building. During recent years a lot of progress has been made to standardize the quality of engineer timber to the point where it is competitive in the building industry. However, timber has quite a different set of properties including a relatively low stiffness compared to traditional building materials as concrete or steel. When building high-rise structures the stiffness of a structure becomes progressively important. Therefore a solution has been sought in the form of combining timber elements with concrete or steel, utilizing each material to their strengths.

A common applied system is to combine a concrete core with a lightweight timber frame. The timber frame is able to take all gravitational forces but derives its lateral stability from a stiff element like a concrete core. This prevents large complex connections and unnecessary bulky dimensions of the timber structure. As most high rise buildings require some sort of stiff element to house an elevator or emergency staircase a concrete core is perfectly suited for this application. However, concrete and timber differ quite a bit from each other. Where the concrete material properties are set in stone, is timber a natural composite with isotropic material properties.

During this research such a system, where a concrete core is combined with prefab timber units, has been researched. Due to contrasting elastic, hygroexpansion and viscoelastic properties there is a notable difference in the vertical deformation of the concrete core and the timber units. Following a theoretical desk study, a case study has been performed to determine the impact of the difference in vertical deformation. The case study comprises of a structure in Amsterdam which provided all raw data which could be used for further analysis.

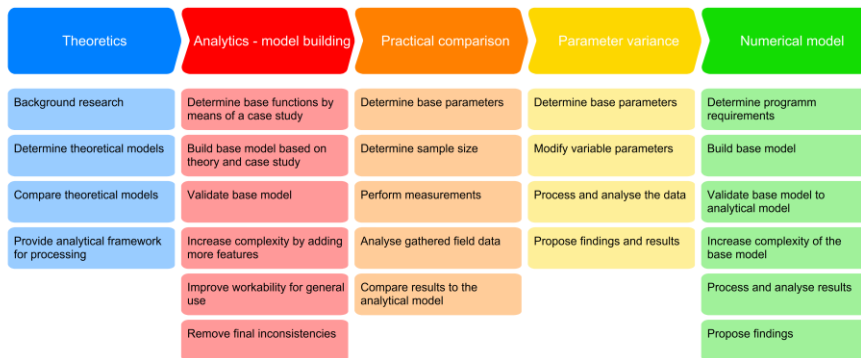
To determine the difference in vertical deformation several models have been researched to provide an upper and lower bound limit. The lower bound limit is based on the Eurocode and the upper bound limit is based on experimental research. While the elastic and hygroscopic deformation is identical in both models, the viscoelastic deformation differs. The impact of building order has also been taken into account within these models, whether it is possible to mitigate some of the elastic and viscoelastic deformations during this phase.

Analyzing the data following from the case study the following can be concluded:

- Depending on the building order, a certain amount of elastic and viscoelastic deformation can be mitigated during construction. Preloading the units can increase the amount of deformation that can be mitigated.
- Depending on the model used, the components that have the greatest impact on the differences are the elements loaded perpendicular to the grain (beams) and the acoustic felt. By limiting the contributions of these components the difference could be greatly reduced.
- The connection between the timber and concrete elements has a built in tolerance to account for any vertical deformations differences. This tolerance proved to be insufficient at the top levels, depending on which model has been applied. A risk analysis performed proved that when using the upper limit boundary conditions the connection was strong and ductile enough to withstand the added deformation.

General strategy and reading guide

For a project this size it is easy to lose sight of the initial objectives. In order to ensure proper flow of the thesis, a strategy has been set up. This strategy consists out of a set of topics that provide directional view and order to the thesis. A clear framework has been constructed which ensures the main objectives will be touched upon and all questions will be answered in an orderly fashion. An overview of the strategy can be found below.



The following topics will be covered:

- Chapter 1 – Introduction
The first chapter provides a brief introduction into timber highrise. The main and sub questions are formulated and boundary conditions are set.
- Chapters 2 and 3 – theoretics
These chapters contain the theory needed to get some insight into the materials and their deformation mechanics. These chapters provide background needed to setup an analytical model which describes the differences in vertical deformation in timber and concrete.
- Chapter 4 – Case study
This chapter consists out of a case study which combines the theoretics from chapters 2 and 3 with a real live example. An analytical model will be created based on the conditions set in this case study.
- Chapter 5 – Experimental testing
The ingress and discharge of moisture is one of the main topics that has a major influence on the project. A unique opportunity arose and allowed for some experimental testing of the moisture content in the loadbearing structure of the timber units. These tests are used to validate and explore the limitations of the analytical model made in chapter 4.
- Chapter 6 – Parameter variance study
A numerous amount of parameters and different components have impact on the amount of deformation that occurs. This chapter explores several parameters and determines their influence and a comparison will be made.
- Chapter 7 – Numerical modeling
This chapter consists out of numerical verification of the analytical model and a risk analysis for the connections. The worst case scenario will be examined and its impact will be assessed.
- Chapter 8 – Conclusion and recommendations
The last chapter consists out of a general conclusion of the thesis and corresponding recommendations.

Index

1	INTRODUCTION.....	9
1.1	HIGH-RISE BUILDINGS - A BRIEF INTRODUCTION	9
1.2	MOTIVATION - EXISTING TIMBER HIGH-RISE.....	11
1.3	PROJECT AIM	14
1.4	MAIN RESEARCH QUESTION	14
1.5	SUB RESEARCH QUESTIONS	14
1.6	PROJECT SCOPE	15
2	THEORETICS – WOOD.....	16
2.1	ABOUT WOOD.....	16
2.2	ENGINEERED TIMBER	19
2.3	MECHANICAL PROPERTIES	22
2.4	DEFORMATIONS	24
3	THEORETICS – CONCRETE	34
3.1	HISTORY OF CONCRETE	34
3.2	GLOBAL USE OF CONCRETE	35
3.3	PRODUCTION AND COMPOSITION.....	35
3.4	MECHANICAL PROPERTIES	38
3.5	DEFORMATIONS	40
4	CASE STUDY - PROJECT BUIKSLOTERHAM.....	45
4.1	GENERAL DESCRIPTION	45
4.2	FUNCTIONAL CONCEPT	47
4.3	STRUCTURAL CONCEPT	48
4.4	STABILITY	49
4.5	FIRE DESIGN.....	50
4.6	BUILDING PHYSICS.....	54
4.7	LOADS.....	57
4.8	FOUNDATION.....	65
4.9	CONCRETE STRUCTURE	67
4.10	TIMBER MODULAR UNITS	69
4.11	CONNECTIONS.....	70
4.12	BUILDING ORDER	71
4.13	FINDINGS	74
4.14	SUB-CONCLUSION	83
5	COMPARISON - PRACTICAL MOISTURE MEASURES VERSUS THEORETICAL MODEL	85
5.1	INTRODUCTION.....	85
5.2	MEASURING METHODS.....	87
5.3	PRODUCTION ASSEMBLY LOCATION ENSCHEDE	89
5.4	PROJECT LOCATION	89
5.5	MEASUREMENT SETUP	91
5.6	RESULTS	93
5.7	SUB-CONCLUSION	96
6	PARAMETER VARIANCE STUDY.....	97
6.1	INTRODUCTION.....	97
6.2	BASE AND VARIABLE PARAMETERS.....	97
6.3	VARIANCE IN DIMENSION	98
6.4	VARIANCE IN MOISTURE.....	101
6.5	VARIANCE IN STRENGTH.....	102
6.6	SUB-CONCLUSION	105
7	NUMERICAL MODELLING.....	107
7.1	BASE MODEL VALIDATION	107
7.2	RISK ASSESSMENT	111
8	LIMIT OF THE SYSTEM	122
8.1	SYSTEM AT HAND	122
8.2	SEVERAL LIMITS	122
8.3	OPTIMIZATIONS TO THE SYSTEM	124
9	CONCLUSION AND RECOMMENDATIONS	126
	BIBLIOGRAFIE	128

Attachments

Attachment A – Reading guide main and sub questions

Attachment B – Excel-tool guide

Attachment C – Manual verification timber straining

Attachment D – Creep in timber and loading direction

1 Introduction

1.1 High-rise buildings - a brief introduction

Today the most expensive apartments in a residential tower are situated at the top, the so-called penthouses. These apartments are very popular due to the view and sense of privacy they offer. Despite the technologies being adequate enough in the 19th century, making tall buildings was far from attractive.

1.1.1 Higher than five

At the beginning of the 19th century there was no elevator in the buildings and people therefore had to walk to the top floor. This ensured that making a building taller than 5 stories was practically unappealing. This was the case until Elisha Otis in 1853 a passenger safe hydraulic lift introduced. As it was now possible to climb 5 stories under a minute it became more attractive to build structures higher as 5 stories.

1.1.2 Loadbearing wall

The problem arose that with the newer higher buildings the forces would increase drastically. The first tall buildings were made by means of a load-bearing wall that would absorb all the forces. To be able to take the weight, the walls often became extremely thick at the expense of space. An example is the Monadnock building in Chicago (1889) shown in Figure 1. This 16-story brick tower was made with a load bearing wall that had to bear all the forces. The result was a wall over 1.8 meters thick at the bottom and 45cm at the top. Due to the extreme weight the building had settled over 51cm into the ground [1].



Figure 1 - Monadnock building from the north [1].

1.1.3 Mass producing steel

With the Bessemer process in 1860 a great leap was made in high-rise buildings. This process made it possible to produce steel on a large scale. Thanks to the high strength-to-weight ratio of steel it became possible to increase the construction height without losing a lot of space. The Home Insurance Company building built in 1885 by the architect William Le Baron Jenney was the first building to use a steel supporting structure. William was also the first architect to use a curtain wall [2]. This principle consists of a steel supporting structure with an outer cladding of masonry or other material that bears only its own weight and is fixed and supported by the steel skeleton.

1.1.4 International style

After the 2nd world war, the world economy started to gain momentum and with it the demand for high-rise buildings. It was around this time that the international style became popular. This architectural way of designing often consisted of rectangular buildings which provided a lot of light as can be seen in Figure 2. These buildings were stripped of decoration and were an expression of visual weightless quality. The construction mainly consisted of a combination of glass, steel and somewhat less visibly reinforced concrete. In the 1970s some architects began to notice the downsides of this style. The ‘glass boxes’ that were characteristic for this style were ridiculed and in response to this a new movement arose [3].



Figure 2 - International style in Chicago [4].

1.1.5 Modern architecture

In the 80s and 90s the complexity of the buildings started to increase. Building engineering became a multidisciplinary approach with different specializations for each project. The preparation processes for the design of a large building has become increasingly more complex and requires a range of preliminary studies of issues concerning sustainability, quality, finance and compliance of local laws. A construction of such magnitude can no longer be the design of one person but is designed by various disciplines. The design is no longer a personal philosophical or aesthetic imitation of individuals. Instead, the daily needs of the environment and use of new technologies are key focal points to create livable environment [3].

1.1.6 Timber high-rise

Timber has been used by mankind to build structures for as long as can be remembered. Being a natural composite, timber contains quite a lot of inadequacies which effect its quality. With the rise of engineered timber like CLT and LVL in the early 90’s it became possible to remove these impurities and increase the mechanical performance. Today’s engineered timber has a strength-to-weight ratio comparable to steel while weighing less [5]. Besides its improved mechanical performance it is a widely available renewable resource making it more sustainable than non-renewable materials. Engineered timber therefore became a good competitor as a building material compared to common materials like concrete and steel. This resulted in the construction of the 9-story high Murray Grove Stadthaus in the UK in 2009 which is considered the first timber high-rise residential building [6]. Since then 27 new timber high-rise buildings have been made.

1.2 Motivation - existing timber high-rise

1.2.1 Mjøstårnet in Brumunddal, Norway

The Mjøstårnet in Norway is an 18 story timber building. Completed in March 2019 it is to date the world's tallest timber building with a height of 85.4m. Besides looking aesthetically pleasing, the tower is also one of the most sustainable building structures. The building is primarily made from local materials using local suppliers like the Norwegian spruce, harvested from the forest close to the town. Besides the material use for construction the energy supply and internal water recycling system have both been designed to be green, autonomous, and waste- and pollution-free [7].



Figure 3 - The world's tallest timber building - Mjøstårnet in Brumunddal, Norway [7].

The main vertical loadbearing system is made entirely out of glued laminated (glulam) beams and columns. Trusses along the façade provide horizontal stiffness and stability to the structure. Surrounding the elevators and staircases a secondary loadbearing system is in place by CLT wall panels. The floors up to the 11th floor are made out of prefabricated wooden decks. The floors from the 12th to the 18th floor are made out of wide plate concrete slabs. Due to the low weight and slenderness of the building added mass was needed to meet serviceability requirements. The entire structure is situated on a huge concrete slab which is supported by concrete piles driven to the bedrock below. The connections between the timber elements are made out of slotted-in steel plates and dowels.

The structural timber is situated behind the prefab façade panels making the entire loadbearing structure compliance with climate class 1. Being protected from external environmental influences like sun and rain increases the durability and reduces maintenance.

1.2.2 Hoho in Wien, Austria

The Hoho building in Austria is the second highest timber building containing 24 stories and a total height of 84 meters. The building was designed as a response to the climate change as timber is able to store carbon dioxide. Approximately 75% of all the material used for construction is timber. On the outside the timber elements are supposed to evoke bark and on the inside hybrid flooring systems expose the CLT paneling so residents are fully conscious of the timber structure. After 1.5 years of construction the entire building was completed and ready for tenants to move in in march 2020 [8].



Figure 4 - Hoho building in Wien, Austria [8].

The main vertical loadbearing system is made out of glued laminated timber columns, cross-laminated timber walls and a vertical in-situ concrete core. The lateral stability of the structure is provided by the in-situ concrete core. All the lateral loads are transferred from the façade to the core by diaphragm action of the floors. Only the concrete core has been made in-situ, the rest of the building is mainly made out of prefabricated elements. The flooring system is a hybrid system of prefabricated clt on the bottom with prefab concrete plates on top.

1.2.3 HAUT in Amsterdam, The Netherlands

Situated in Amsterdam the residential tower HAUT contains 21 stories and is with 73 meter the highest timber residential tower in the world. In 2006, the municipality of Amsterdam issued a tender for the lot on the Amstel, in which sustainability and design would be rewarded. This tender was won by Team V architecture and Arup engineers. The tower has completed construction in March 2022



Figure 5 - HAUT residential tower in Amsterdam, The Netherlands [9].

The main vertical loadbearing system is made out of a combination of concrete and CLT panels. Concrete has only been used to construct the parking garage and the basement. Besides the garage and the basement is also the core made out of concrete. At first a wooden core was considered but to get the required stiffness the amount of steel required would negatively impact the CO₂-emissions, hence a concrete core was constructed [9]. The concrete core is also used to provide lateral stability. From the 1st story and up the entire substructure consists out of prefab CLT walls and floors.

In total HAUT is made out of 2800 m³ timber. It is estimated that if the entire building was made out of concrete it would have expelled 30% more CO₂ during the construction phase. This corresponds to approximately 1.1 million kilos of CO₂ equivalent.

1.3 Project aim

Timber constructions are becoming more popular in the context of sustainable and circular building. Following this trend, more and more timber high-rise structures are being made. With the increasing height of the structure several problems arise. Two of which is stability and serviceability. Several systems exist to keep a timber structure stable and upright. The one considered in this research combines a concrete core with a timber frame. The timber frame derives its horizontal stability from the concrete core, allowing relatively slender timber members and connections. Being two different materials, the elastic and time dependent deformations in longitudinal direction differ.

The aim of this research is to parameterize all the different elements, summarized within one model. The data for this model will be provided by means of a case study. This model will include elastic and time dependent straining of concrete and timber. Several load applications, parallel and perpendicular to the fibers and construction order will also be taken into the equation. Once all the vertical shortening strains are established and the model is valid, the optimization process will start in which the primary focus is to minimize these differences.

1.4 Main research question

Various studies have been conducted into hybrid high-rise structures with wood. This research examines the settlement differences between a concrete core and the timber frame structure. A case study will be done to comprise a theoretical model based on experimental data. To ensure a proper flow of this research a main research question has been composed:

How can vertical straining differences in timber hybrid high-rise structures be minimized in practice by optimizing parameters by exploring a theoretical model?

1.5 Sub research questions

As the main question will provide a wide range of answers and cannot be answered with a simple yes or no. To support the main question a number of sub questions have been formulated. These sub questions can be found below and will be addressed during the research.

Sub question 1 (SQ1): What kind of settlements have to be taken into account when assessing a timber high-rise structure?

SQ 1.1 What kind of settlements can be expected (elastic, plastic, time dependent etc.)?

SQ 1.2 What kind of models exist to estimate these settlements?

SQ 1.3 How do environmental influences impact the settlement?

SQ 1.4 What are the theoretical expected locations where the settlement occurs?

SQ 1.5 Where are the biggest settlements in practice?

SQ 1.6 What are the expected settlements of the concrete core per level?

Sub question 2 (SQ2): How does the height of the structure affect the settlement for each floor?

SQ 2.1 Is there a relation between the applied normal force and the expected deformation?

SQ 2.2 What is the difference in settlement between the concrete core and the timber loadbearing structure?

SQ 2.3 How does the elastic deformation relate to the total deformation?

SQ 2.4 How does the stiffness of the foundation impact the settlement and deformations of the timber units?

SQ 2.5 How does the stiffness of the core impact the settlement and deformations of the timber units?

Sub question 3 (SQ3): How will different load applications (parallel and perpendicular to the grain) influence the settlement behavior?

SQ 3.1 What is the settlement behavior of wood when loaded perpendicular to the grain?

SQ 3.2 What is the settlement behavior of wood when loaded parallel to the grain?

SQ 3.3 How do the dimensions of the loaded specimen relate to the stress distribution?

Sub question 4 (SQ4): What is the common applied building order of the structure and how will changing the order effect the settlement behavior?

SQ 4.1 What is the building order applied to Buiksloterham?

SQ 4.2 What is the expected deformation during construction?

SQ 4.3 Is there a relation between the building order and the expected deformation?

Sub question 5 (SQ5): What is the structural composition of the timber units and is it possible to improve settlement behavior by optimizing this composition?

SQ 5.1 What is the current structural composition of the timber modular units?

SQ 5.2 Can the structural composition be optimized by applying different kinds of wood (LVL, CLT)?

Sub question 6 (SQ6): How does the settlement impact the connections of the timber units?

SQ 6.1 What kind of connections are applied within the modular units?

SQ 6.2 What kind of loads do the applied connections transfer?

SQ 6.3 What kind of deformations/rotations are allowed in the connections?

SQ 6.4 What are the limitations to the connections currently applied within the system?

Sub question 7 (SQ7): How are the timber units attached to the concrete core?

SQ 7.1 What are the failure mechanisms of the connection?

SQ 7.2 How is vertical deformation allowed while limiting the horizontal deformation?

1.6 Project scope

To ensure a proper flow of the project some boundary conditions have to be formulated. These boundary conditions will be addressed below.

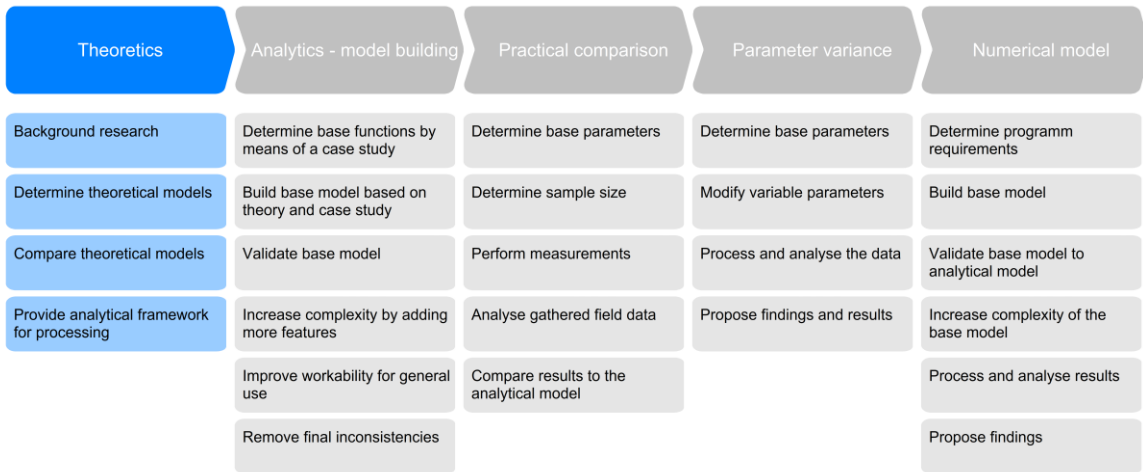
What belongs to the scope

- Case study to compare experimental data with practical examples.
- Theoretical investigation of several load applications consisting of loads applied parallel and perpendicular to the grain.
- Comparison commonly used building orders, belonging to the described stability system.
- Investigating whether the structural composition of the units can be optimized.
- Settlement impact on connections between the concrete core and the timber units as a function of the height of the structure.

What doesn't belong to the scope

- Other stability systems. Only the settlement difference in timber hybrid constructions with a stabilizing core in combination with a timber frame will be considered.
- Improving core stability, core detailing and or calculations. The focus of this research will be on the timber aspect of the construction.
- Other core materials. This research will consist of a concrete stability core in combination with a timber frame structure. If time should allow it, the research could be extended by exploring different core materials (steel, wood).

2 Theoretics – wood



2.1 About wood

Wood can be found all over the world. Forests cover approximately 31 percent of the global land area. More than half of the world’s forests are found in only five countries (Brazil, Canada, the United States of America, China and Russia) and nearly 66 percent in ten countries [10]. Forests are an important part of human society. Forests provide many benefits such as ecosystem services like storing carbon and nutrient cycling, they also maintain wildlife habitat and provide goods such as fuel and timber.

Wood is a natural composite produced by many botanical species including the angiosperms (hardwood) and gymnosperms (softwood). Hardwood is mainly used in furniture and finishes and softwood as a bulk material in construction. It can come in all shapes and sizes and has very appealing qualities like a high strength to weight ratio and workability. Being a biological product it also contains undesirable characteristics like the variability in quality and moisture uptake. To reduce these undesirable properties and to make the most out of wood, the structure and composition has to be studied. The anatomy of wood can be differentiated in several ranges, as can be observed in Figure 6.

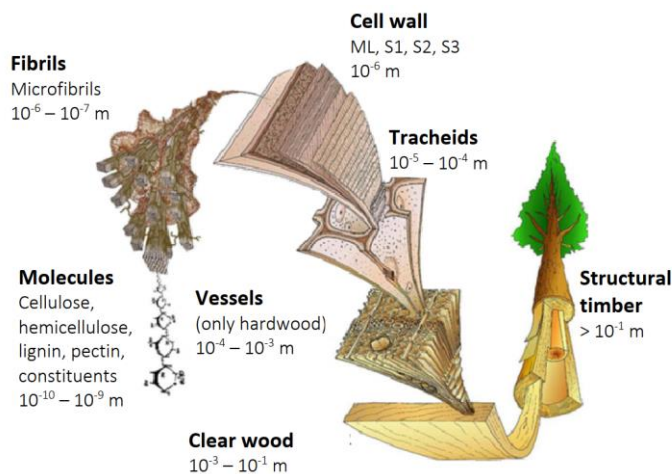


Figure 6 - Hierarchical levels of timber [11].

The most common species that are used in construction in the Netherlands are softwoods like the Douglas (*Pseudotsuga menziesii*), Spruce (*Picea abies*) and the Pine (*Pinus sylvestris*), all from different parts in Europe [12].

2.1.1 Macrostructure

A tree can be distinguished into three parts: Bark, sapwood and heartwood. Between the bark and the sapwood is the cambium located. The cambium is the growing part of the tree and is invisible to the naked eye. The stem is characterized by the annual rings. With each season the tree grows a new ring is formed. These rings vary in size depending on the environmental conditions of that season. The anatomy of a tree trunk can be seen in Figure 7.

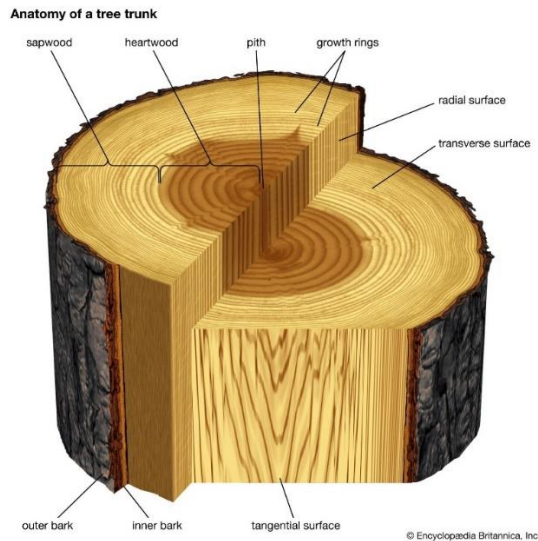


Figure 7 - Anatomy of a tree trunk [13].

Plane sections of wood

There are three plane sections to be distinguished, the radial, transverse and tangential sections. The transverse section, also known as the cross-section, is the section taken between the stem and the crown at a 90 degree angle. The radial section is a section taken in the longitudinal direction through the pit of the stem. The tangential surface is like the radial section taken in the longitudinal direction but not through the pith.

Heartwood and sapwood

The heartwood is the inner section and oldest part of the tree. This part is dead and no longer takes part in the nutrition cycle. Due to the absence of living cells and the fact that the cells tend to close make this part of the tree much more durable than the outer part. Sapwood is the younger, outer part of the tree and is used to transport water and nutrients up in the tree. With the growth of the tree more sapwood is converted to hardwood.

Pith

The pith is the center of the stem and is only a few millimeters in diameter. This part of the tree only supports growth at a very early stage of the developing tree.

Rays

Rays are canals running from the inner side (close but not to the pith) of the stem to the cambium in radial direction. Pith rays are rays connected to the pith, as the name indicates. The main function of these rays are to provide water and nutrition in radial direction.

Resin canals

Resin canals are canals that transport resin which is used as protection by the tree. These canals run in longitudinal as well as radial direction.

Annual rings

Annual rings are rings which are formed and indicate each grow season of the tree. The annual rings can be distinguished into two sections: Early- and latewood, see Figure 8. In the spring the leaves start to grow and a lot of water and nutrients have to be transported from to the top of the tree. This leads to large open canals running in longitudinal direction, also known as earlywood. Later in the season the tree focuses more on gaining strength and a more dense wood is created, known as latewood.

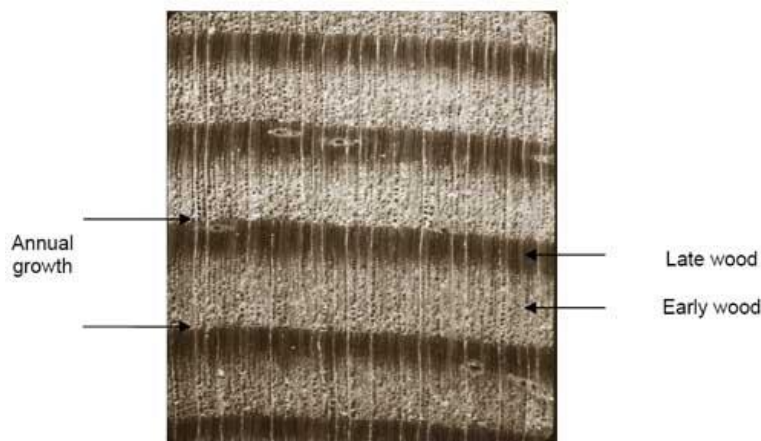


Figure 8 - Annual rings of a conifer (*Pseudotsuga menziesii*) [14].

2.1.2 Microstructure of softwood

Softwood comprises of tracheids (2 to 5mm) and parenchyma (10 to 50 μm). The longitudinal tracheids are predominantly present in the trees and run parallel to the trees axis. The parenchyma are present in longitudinal cense in some softwoods but are always present in radial direction. The parenchyma also forms the rays in radial direction. A schematic overview is presented in Figure 9.

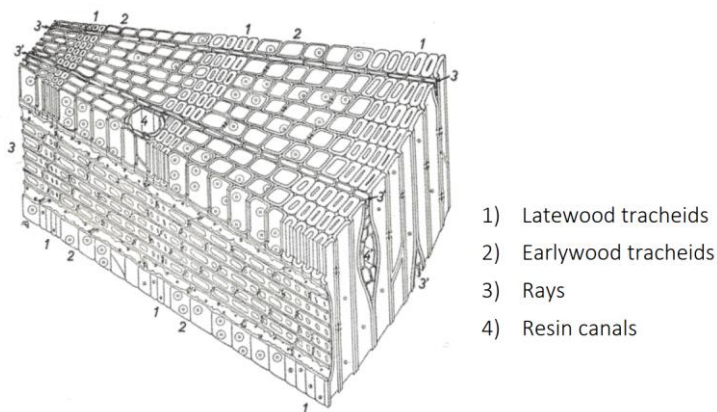


Figure 9 - Schematic structure and cell types of softwood [11].

2.2 Engineered timber

Originating from a natural living tree, the quality of timber does not only vary within species but also within the same tree. Several inadequacies can be found within a tree. Inadequacies like knots, reaction wood, tapered growth etc. cause deviations in the quality of the wood. Such deviations can be problematic when a constant quality is required. By removing these impurities the quality of the timber can be improved and a relatively constant quality can be acquired. Besides those impurities timber is also orthotropic by nature. Timber exhibits different material properties in several directions. The mechanical properties of timber therefore also are different in several directions making it a complicated material to design with. To improve the designability there are several products made and available on the market.

2.2.1 Sawn timber

Sawn timber is timber produced by sawing logs. These products can consist of square timbers, boards and planks. These sawn timber members visually inspected for any impurities after which they are dried in a kiln or naturally.



Figure 10 - Sawn square timber [15].

After drying they are subjected to machine or visual grade testing to determine their strength class. Table 1 represents the strength classes according to the EN388.

Table 1 - Strength classes according to the EN 388, in MPa and kg/m³.

	C14	C16	C18	C20	C22	C24	C27	C30	C35	C40	C45	C50
$f_{m,k}$	14	16	18	20	22	24	27	30	35	40	45	50
$f_{t,0,k}$	8	10	11	12	13	14	16	18	21	24	27	30
$f_{t,90,k}$	0.4	0.4	0.4	0.4	0.4	0.4	0.4	0.4	0.4	0.4	0.4	0.4
$f_{c,0,k}$	16	17	18	19	20	21	22	23	25	26	27	29
$f_{c,90,k}$	2.0	2.2	2.2	2.3	2.4	2.5	2.6	2.7	2.8	2.9	3.1	3.2
$f_{v,k}$	3.0	3.2	3.4	3.6	3.8	4.0	4.0	4.0	4.0	4.0	4.0	4.0
$E_{0,mean}$	7	8	9	9.5	10	11	11.5	12	13	14	15	16
$E_{90,mean}$	0.23	0.27	0.30	0.32	0.33	0.37	0.38	0.40	0.43	0.47	0.50	0.53
G_{mean}	0.44	0.50	0.56	0.59	0.63	0.69	0.72	0.75	0.81	0.88	0.94	1.00
ρ_k	290	310	320	330	340	350	370	380	400	420	440	460
ρ_{mean}	350	370	380	390	410	420	450	460	480	500	520	550

2.2.2 Glulam

Glued laminated timber (glulam) consists of several components of timber lamellae between 5 to 45mm thick. The lamellae are over the entire length glued on top of each other. With this process large imperfections are removed and all the lamellae have the same fiber orientation. This allows for a more homogeneous material without any of the natural undesired characteristics. Being an engineered product the laminated timber elements can be made in a variety of shapes and sizes.



Figure 11 - Curved glued laminated beams [16].

The timber lamellae are inspected and dried before glued together. To avoid cracks the moisture content of the timber is lowered to match the moisture content estimated in the final application. After gluing the glulam elements are mechanically tested to determine their strength class. Table 2 represents the strength classes according to the EN 14080.

Table 2 - Strength classes glued laminated timber according to the EN 14080, in MPa and kg/m³.

	GL20h	GL22h	GL24h	GL26h	GL28h	GL30h	GL32h
$f_{m,g,k}$	20	22	24	26	28	30	32
$f_{t,0,g,k}$	16	17.6	19.2	20.8	22.3	24	25.6
$f_{t,90,g,k}$	0.5	0.5	0.5	0.5	0.5	0.5	0.5
$f_{c,0,g,k}$	20	22	24	26	28	30	32
$f_{c,90,g,k}$	2.5	2.5	2.5	2.5	2.5	2.5	2.5
$f_{v,g,k}$	3.5	3.5	3.5	3.5	3.5	3.5	3.5
$E_{0,g,mean}$	8400	10500	11500	12100	12600	13600	14200
$E_{90,g,mean}$	300	300	300	300	300	300	300
$G_{g,mean}$	650	650	650	650	650	650	650
$\rho_{g,k}$	340	370	385	405	425	430	440
$\rho_{g,mean}$	370	410	420	445	460	480	490

2.2.3 CLT

Cross laminated timber is similar to the glued laminated timber. The main difference is the orientation of the lamellae. The orientation of the lamellae differs by 90 degrees within each layer, see Figure 12. By this alternating layup of the lamellae a material is created with near homogeneous properties in transvers and longitudinal direction. Due to the alternating layup CLT elements excellent at resisting lateral forces, making these elements perfectly suited for walls and floor slabs. The strength of CLT members is determined by the strength classes of the boards, presented in Table 2. Depending on the amount of layers and the orientation the strength properties change.



Figure 12 - Cross laminated timber slab [17].

2.2.4 LVL

Laminated veneer lumber is an engineered product that consists of 3mm thick plies glued together, creating a near homogeneous material. The plies are generally oriented all in longitudinal direction, sometimes with small deviations. A LVL panel can contain up to 20% transverse oriented plies.



Figure 13 - Laminated veneer lumber, Kerto LVL S-beam [18].

During production, the veneers are dried to a moisture content of approximately 5%. This is to ensure good bonding between the veneers and the adhesive agent. The members can be produced up to a length of approximately 25 meters, only limited by the mill building or the infrastructure after producing. Table 3 represents some mechanical properties for common LVL products.

Table 3 - Mechanical properties of common LVL products, all in MPa and kg/m³.

	LVL 48P beam	LVL 32P stud	LVL 36C panel	LVL 25C panel
$f_{m,0,edge,k}$	44	27	32	20
$f_{m,0,flat,k}$	48	32	36	25
$f_{m,90,flat,k}$	-	-	8	-
$f_{c,0,k}$	29	21	21	15
$f_{c,90,edge,k}$	6	4	9	8
$f_{t,0,k}$	35	22	22	15
$f_{v,edge,0,k}$	4.2	3.2	4.5	3.6
$f_{v,flat,0,k}$	2.3	2.0	1.3	1.1
$E_{0,mean}$	13800	9600	10500	7200
$E_{m,90,mean}$	-	-	2000	-
$G_{0,edge,mean}$	600	500	600	500
ρ_k	480	410	480	410
ρ_{mean}	510	440	510	440

2.3 Mechanical properties

Being an organic material, timber is a composite with anisotropic mechanical properties. These mechanical properties are not uniform as environmental conditions can introduce growth properties such as knots, tension and compression wood. As such, when spoken about the mechanical properties the referral is made to clear wood. A clear wood specimen with homogeneous properties will be assumed.

2.3.1 Density

The density of wood is highly influenceable by environmental conditions with moisture in particular. For this reason it is imperative to specify climate conditions when determining the density. Normal indoor climate conditions have a temperature of approximately 20°C and a relative humidity ranging between 40~65%. The density is determined as the ratio of the mass of the wood over the volume of the wood (including cavities). The main densities of interest are the oven-dry density ρ_0 and the density at a moisture content of 12% ρ_{12} .

$$\rho_u = \frac{m_u}{V_u} \quad \text{eq. 1}$$

ρ_u Density at moisture content u

m_u Mass of the wood at moisture content u

V_u Volume of the wood at moisture content u

The density of wood influences several key factors such as the strength, deformation capacity and moisture uptake. An increase in density leads to an increase of strength, decrease of deformability and decrease of maximum moisture content as is illustrated in Figure 14.

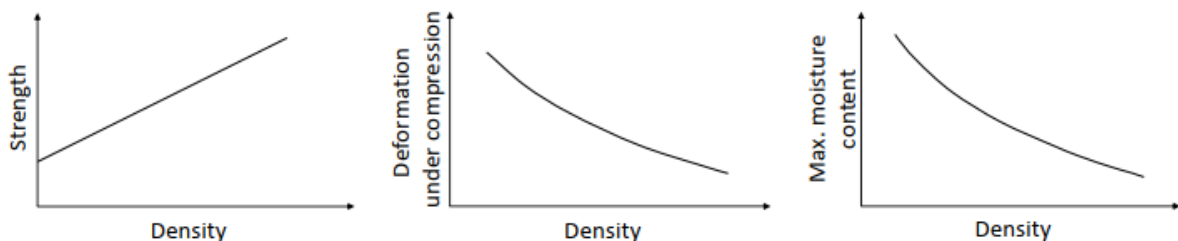


Figure 14 - Schematic overview influences of density on several factors [11].

2.3.2 Modulus of elasticity

Due to the orthotropic nature of wood the modulus of elasticity can be broken down into the three parts respective to their plane. E_L , E_T and E_R are the elastic moduli for the longitudinal, tangential and radial direction. The elastic moduli is normally obtained by axial or bending testing. However, within engineering practices it is common to only use E_{90} , which is a mix of both lateral E-moduli.

2.3.3 Poisson's ratio

With the application of a load in one direction, the element will deform in the unloaded directions. Poisson's ratio tells us how much this deformation will be. As with the elastic modulus, the Poisson's ratio can be distinguished into the longitudinal, radial and tangential Poisson's ratio. The ratio is affected by the specific gravity and moisture content and vary within species.

2.3.4 Compressive and tensile stresses

The resistance from wood to compressive and tensile forces differs per species and loading direction. As can be imagined, a bundle of straws is stronger in the longitudinal direction than to the radial and tangential direction. This is also the case for wood, the compressive and tensile resistance parallel to the grain are far greater than perpendicular to the grain, see Figure 15. To distinguish between the grain direction the following indices are used: $f_{t,0}$ where the first symbol indicates tension or compression and the second indicates the angle to the grain (0 is parallel to the grain, 90 is perpendicular to the grain).

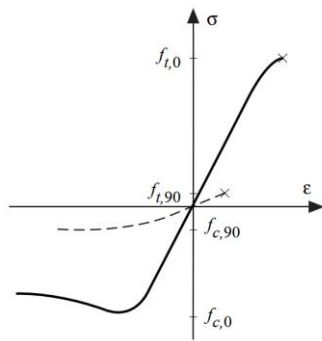


Figure 15 - Stress-strain curve of clear wood exposed to tensile and compressive stresses parallel and perpendicular to the grain [11].

It can be observed that when wood is exposed to tension it exhibits linear elastic behavior up until the point of failure. It therefore is classified as brittle behavior. The tensile strength resistance significantly reduces when pre-existing cracks are present.

It can also be observed that when loaded in compression along the fiber the wood shows ductile properties after the maximum strength is reached. This ductile behavior is due to the local buckling of the fibers in compression. When loaded perpendicular to the grain the fibers will get compressed up until the squash load while straining is still present.

2.3.5 Hankinson equation

When a load is applied at a defined angle other than 0 or 90 degrees the Hankinson equation [19] can be used. For compression and tension the index can be interchanged.

$$f_{i,\alpha} = \frac{f_{i,0} \cdot f_{i,90}}{f_{i,0} \cdot \sin^2 \alpha + f_{i,90} \cdot \cos^2 \alpha} \quad i = t, c \quad \text{eq. 2}$$

- $f_{i,\alpha}$ Stress at the defined angle alpha
- $f_{i,0}$ Stress parallel to the grain
- $f_{i,90}$ Stress perpendicular to the grain

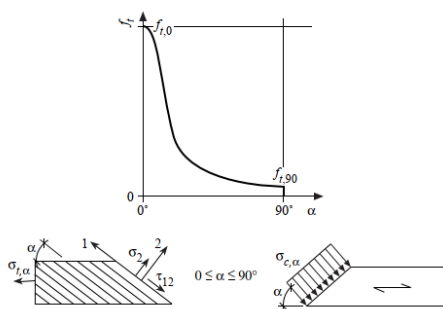


Figure 16 - Tensile and compressive strength depending on the angle alpha.

2.4 Deformations

A loadbearing structure is subjected to various mechanisms that may lead to deformation. Those mechanisms can be influenced by material properties like density, composition and strength properties or external factors like different types of loading and environmental influences. The overall deformation can be described in terms of straining, which is the ratio between the change in length to the original length. All the components which cause strain in a material are illustrated in Figure 17.

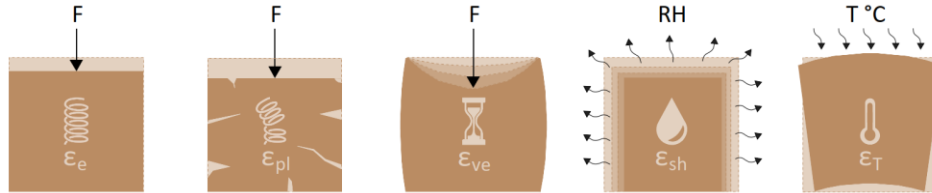


Figure 17 - Strain components.

The total strain ϵ can be described as the superposition of the elastic strain ϵ_e , the plastic strain ϵ_{pl} , the viscoelastic strain ϵ_{ve} , the hygroexpansion strain ϵ_u , the mechano-sorption strain ϵ_{ms} and the temperature strain ϵ_T .

The focal point of this research is on deformations as a result of elastic, viscoelastic and hygroexpansion straining. Deformations due to plastic, mechano-sorption and temperature straining are not taken into consideration based on the following assumptions:

- Stress values will not go past the elastic limit of the material.
- Cyclic loads due to wind or mechanical applications are sufficiently small to be disregarded.
- Indoor climate conditions provide a near constant temperature of approximately 20 °C.

2.4.1 Elastic straining

When a member is loaded it deforms. When members linearly deform when loaded it is called elastic deformation. During loading in the linear elastic regime the member will regain its original shape when it is unloaded, illustrated in Figure 18.

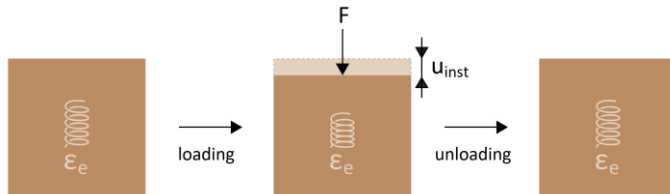


Figure 18 - Elastic deformation due to the load and unloading.

The change in length of a material in elastic regime can be derived from Hooke's law and is presented below.

$$\epsilon = \frac{\sigma}{E} \quad \text{eq. 3}$$

Solving for the change in length as a function of a members stiffness, area, length and applied force, eq. 3 can be rewritten into eq. 4. This formula will be governing to determine the elastic deformations of a member subjected to a static load.

$$u_{inst} = \frac{F \cdot L}{A \cdot E_{mean}} \quad \text{eq. 4}$$

- F Static load
- L Length of the loaded member
- A Cross-sectional area
- E_{mean} Mean elastic modulus

According to the NEN-EN 1995-1-1_2005 the elastic deformation u_{inst} has to be determined using the characteristic load combination according to the EN1990 6.5.3(2) and the mean modulus of elasticity [20].

2.4.2 Viscoelastic straining

Timber is as a viscoelastic material, meaning it has viscosity and elastic properties. When loaded timber therefore experiences straining, as illustrated in Figure 19.

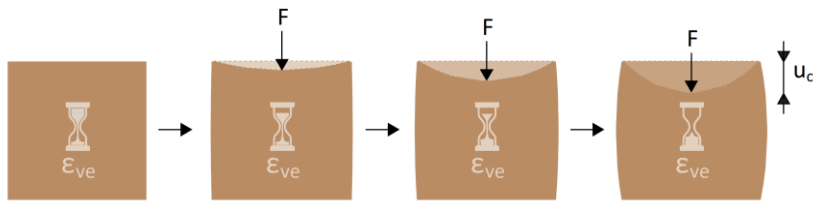


Figure 19 - Creep deformation due over time due to a constant load.

When under constant loading timber members will deform. This can even occur at very low stresses and is a continuous process. When the stresses increase the creep deformation will also occur faster. Creep also increases with the increase of temperature and moisture.

The creep curve can be divided into two areas: The instantaneous elastic deformation and the time dependent deformation due to creep. When the load should be removed after some time the elastic deformation should immediately recover and after some time the creep deformation should return to the original state as well, assuming ideal viscoelastic behavior. However, in reality this is not the case and some plastic deformation will occur, as can be observed in Figure 20.

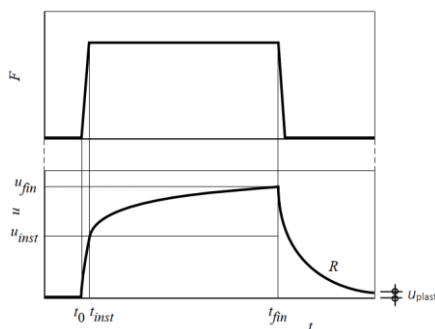


Figure 20 - Creep curve due to constant load [11].

2.4.2.1 Creep according to the Eurocode

The Eurocode includes creep deformation by multiplication of the elastic deformation, based on quasi-permanent loads, with the creep factor k_{def} . The values for the modification factor can be seen in Table 4.

Table 4 - Creep factor by the Eurocode for some materials based on climate classes.

Material	CC1	CC2	CC3
Sawn timber	0.6	0.8	2
CLT/GLh	0.6	0.8	2
LVL	0.6	0.8	2

Climate classes 1 to 3 take climate conditions and moisture variations into account.

- CC 1 is characterized by a moisture content in the materials corresponding to a temperature of 20°C and a RH that is only a few weeks per year above the 65%
- CC 2 is characterized by a moisture content in the materials corresponding to a temperature of 20°C and a RH that is only a few weeks per year above the 85%
- CC3 is characterized by climate conditions that lead to a higher relative humidity as in CC2.

The final creep deformation is determined by eq. 5.

$$u_{cr} = k_{def} \cdot u_{inst} \quad \text{eq. 5}$$

2.4.2.2 Creep parallel and perpendicular to the grain based on experiments

Creep calculations according to the Eurocode do not provide changes in creep over time. This is important because, as with concrete, most creep develops within the first period of time. To this extend there does not exist a norm which describes this time dependent behavior of creep. In order to gain insight in this behavior, a meta-analysis was performed by Okke Willebrands [21]. This analysis combined multiple timber creep experiments in an effort to more accurately describe this phenomenon. This research concluded that the creep factor according to the Eurocode was slightly progressive for 50 year service life for service class 1. A new creep factor has been constructed based on this analysis which includes a time dependency, see Figure 21.

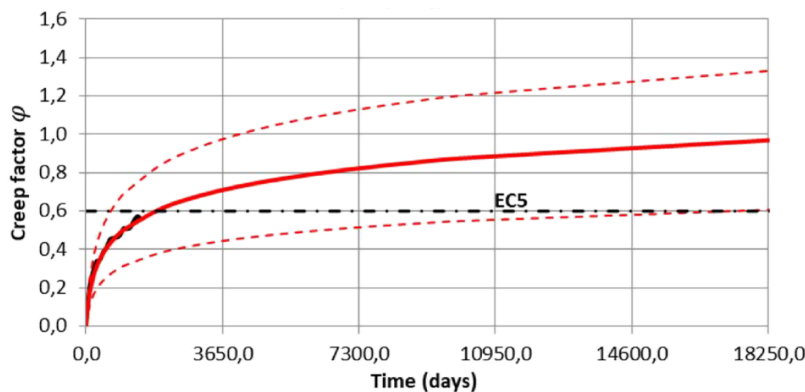


Figure 21 - Creep curve according to a meta-analysis performed by Okke Willebrands. [21]

It can be observed that within a 50 year time span the mean creep factor reaches a medium value of approximately 0.89. The 0.6 mark according to the Eurocode is passed after 2680 days. The creep curve is determined by the following formula:

$$\varphi(t) = 0.15 \cdot \ln(1 + 0.02 \cdot t) \quad \text{eq. 6}$$

That the creep factor of the Eurocode is on the lower side is also reflected when other standard timber building codes are considered. Across the world there are buildings being built with timber. Depending on region there are several standards provided in order to safely design timber structures. Standards like the Eurocode 5 (2004), New Zealand Timber Standard 3603 (1993) and National Design Specifications for Wood Construction (2018). These codes all provide standards for their own region for timber building. What these codes all have in common is that they take into account long term effects due to creep into their strength and deformation calculations.

In 2019 a comparison of the creep factor within these codes had been made by G. Granello and A. Palermo [22]. The creep factors for each of the codes can be observed in Table 5. It should be noted

that the New-Zealand code does not provide a distinction between service classes and is the same for all classes. The NDS only considers two service classes namely dry and wet.

Table 5 - Creep factors (intended as amplification factors of the elastic deflection).

Standard code	Service class I	Service class II	Service class III
NZS 3603	2	2	2
EC 5	1.6	1.8	3
NDS	1.5	2.41	2.41
Average	1.84	1.91	1.93
Max	NZS 3603	NDS	EC5
Min	NDS	EC 5	NZS 3603

The comparison concluded that generally there are no conservative codes. The Eurocode is most conservative for service class 3 but least conservative in service class 2. However, because the majority of the experiments in terms of creep are based on a period of observation lower than 10 years, it is difficult to identify which approach leads to the most accurate prediction over the life of a structure [22].

According to experiments done by Wanninger in 2014 [23] the timber creep when loaded perpendicular to the grain was observed to be 4.5 times as high as when loaded parallel to the grain, 2.8 and 0.6 respectively. These results concur with similar observations done by Schniewind and Barrett in 1972 [24]. According to experiments done by Massaro et al., a similar creep factor of 2.1 has been found when Norway spruce glulam specimens were loaded parallel to the grain [25]. An average factor of 2.45 has been used to determine the creep deflection for the beams loaded in compression perpendicular to the grain in following chapters. A more extensive elaboration about the creep factor perpendicular to the grain can be found in: Attachment D – Creep in timber and loading direction.

2.4.3 hygroexpansion straining

Due to its structure wood it is highly hygroscopic. It is able to absorb water in liquid form or as a vapor from the surrounding atmosphere. Unprocessed wood always contains moisture, either in the cell walls or the cavities. Moisture in the cavities does not affect the mechanical properties, the moisture content in the cell walls however are of importance as this property is linked to durability properties and volume changes, see Figure 22.

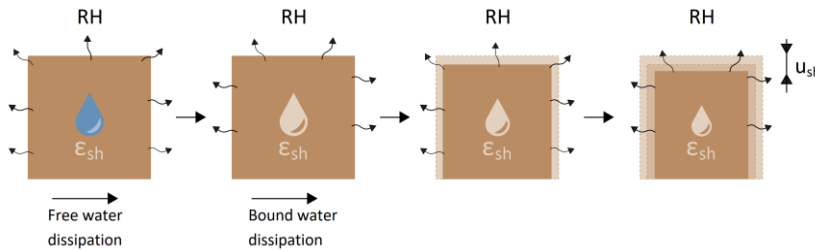


Figure 22 – Deformation due to bound water dissipation.

During the lifecycle there are a lot of different ways in which the wood comes into contact with moisture. It is imperative to protect the wood from high humidity to prevent biotic degradation by fungi, bacteria, insects and marine borders. Usually a MC over 20% for a long periods of time can create decay [26]. Moisture also affects various mechanical properties [11]. With an increasing moisture content; the stiffness and strength decrease, the creep deformation increases and the thermal conductivity rises. An overview of possibilities where wood is exposed to moisture during its lifecycle can be observed in Figure 23.

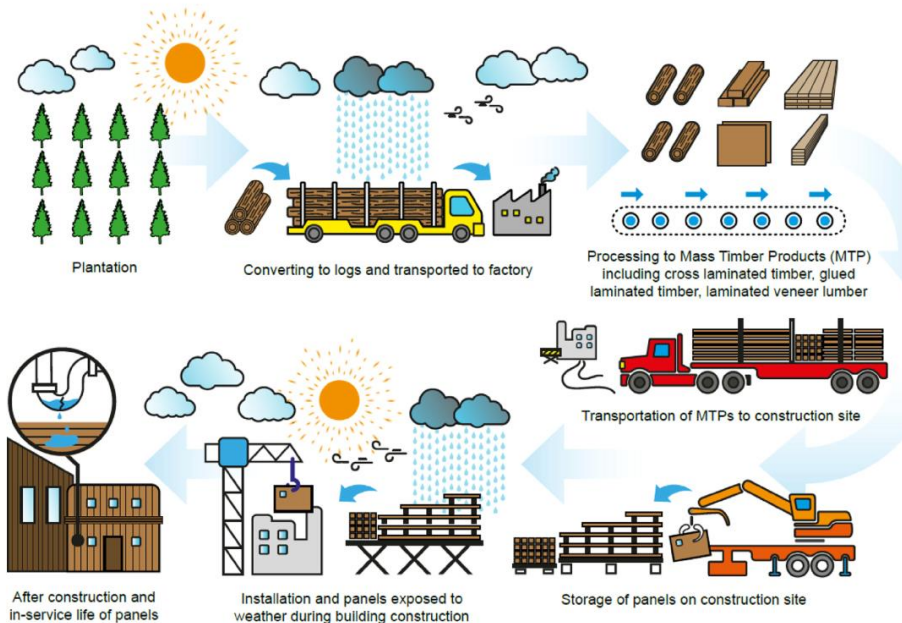


Figure 23 - Diagram of MTPs life cycle exposed to moisture (rain, flood, ground water, plumbing leaks, etc) [27].

2.4.3.1 Moisture content

The moisture content of wood can be expressed as the mass of the water in the wood over the mass of oven-dry wood.

$$MC = \frac{m_{water}}{m_{wood}} = \frac{m_{wet} - m_{dry}}{m_{dry}} \quad eq. 7$$

The moisture content in freshly cut wood or ‘green wood’ have completely saturated cells and possible additional water residing in the lumina. The moisture content of green wood can range from 30% to more than 200% [28]. In general, the moisture content is higher in sapwood than in heartwood, how much differs per species. The point where bound water in the cell walls remains and all other free water is removed is called the Fiber saturation point (MC_{fs}) [29].

2.4.3.2 Equilibrium moisture content

Equilibrium moisture content is the state of the wood in which the moisture content is in balance and is neither gaining nor losing moisture [28]. The EMC is calculated according to eq. 8 [28]. It can be observed that the equilibrium moisture content is determined by the temperature and the relative humidity of the surrounding air. This formula can be applied to wood of any species.

$$EMC = \frac{1800}{W} \cdot \left[\frac{Kh}{1 - Kh} + \frac{K_1Kh + 2K_1K_2K^2h^2}{1 + K_1Kh + K_1K_2K^2h^2} \right] \quad eq. 8$$

W	$349 + 1.29T + 0.0135T^2$
K	$0.805 + 0.000736T - 0.00000273T^2$
K_1	$6.27 - 0.00938T - 0.000303T^2$
K_2	$1.91 + 0.0407T - 0.000293T^2$
T	Temperature in degrees
h	Relative humidity

2.4.3.3 Liquid water absorption

Wood exposed to liquid water may be experience several changes. Due to capillary action liquid water is absorbed into the cells and replaces the air in the cavities. This may continue until the maximum moisture content is reached. The absorption rate depends on the direction of the side exposed to the water. Water is absorbed the fastest in the transversal plane. It also differs per species. The faster air can be displaced the faster water gets absorbed thus a more open structure is more beneficial for water absorption. The measuring rate of water absorption by wood is described in the ISO 15148. The general relation between the relative humidity and the moisture content can be observed in Figure 24.

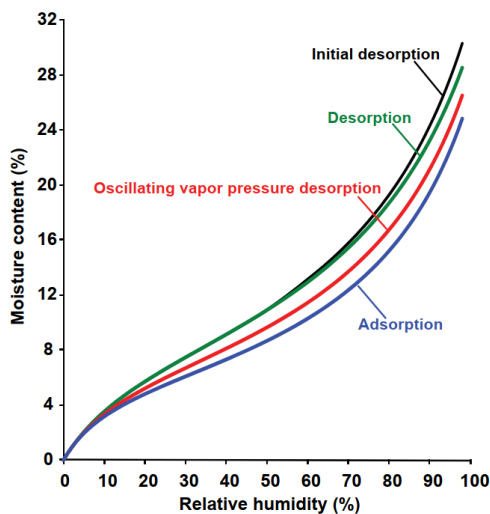


Figure 24 - Moisture content due to relative humidity under various desorption conditions [29].

2.4.3.4 Moisture absorption during construction

The Eurocode states that timber being used in construction needs to be dried to a moisture content which represents the final climatic conditions of the finished structure. Most timber after manufacturing ranges therefore between 10~15 percent. However, during construction is the timber shipped to the building site and exposed to outdoor climate conditions, i.e. higher relative humidity and possibly in direct contact with water. According to the wood handbook the average moisture content of the material can generally increase by 0.2% within the first 45 days if properly protected against the environmental influences by for instance plastic wrapping. After removal of the protective layers during construction the uptake of moisture can increase to almost 2% within the first 45 days. This result is confirmed by experimental testing [30] as can be observed in Figure 26.

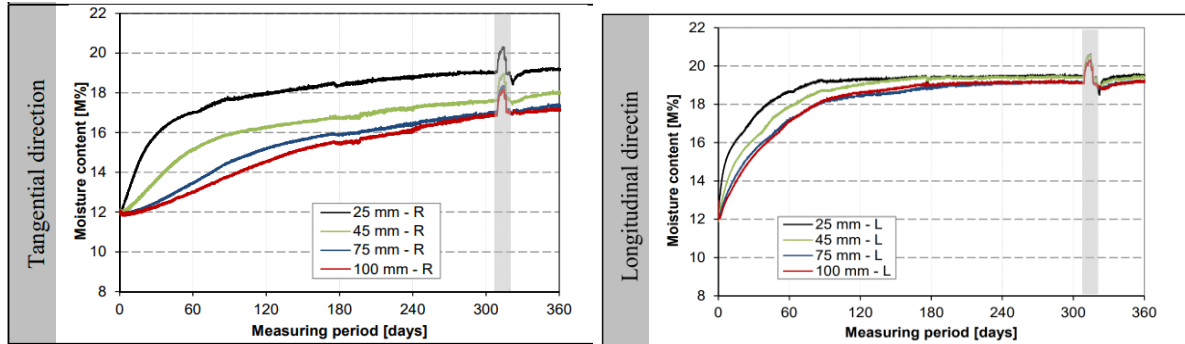


Figure 25 - Experimental results* on moisture diffusion in tangential (left) and longitudinal (right) direction. *it should be noted that the test chamber shortly broke down after 310 days (grey hatching).

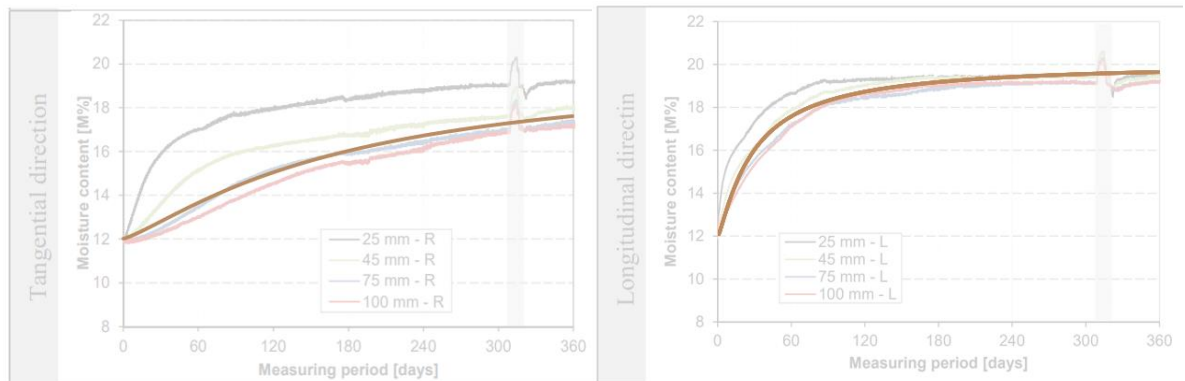


Figure 26 – Curve fitting of eq. 9 and eq. 10 to the results shown in Figure 25.

It can be observed that the diffusion rate over time decreases and differs in longitudinal and tangential direction. By means of nonlinear curve fitting the increase of MC over time can be approximated according to eq. 9 and eq. 10.

$$MC_{tangential}(t) = MC_{\infty} + \frac{MC_0 - MC_{\infty}}{1 + (\frac{t}{175})^{1.25}} \quad eq. 9$$

$$MC_{longitudinal}(t) = MC_{\infty} + \frac{MC_0 - MC_{\infty}}{1 + (\frac{t}{30})^{1.15}} \quad eq. 10$$

- t Time
- MC₀ Moisture content at t=0
- MC_∞ Moisture content at t=∞ according to eq. 8.

The moisture ingress rate differs depending on the size of the element. The formulas above are determined at a ingress depth of 75mm within a 200x200x200mm sample. This depth has been chosen as it is common practice to apply a charcoal layer to ensure fire safety. Since these elements are situated in high rise buildings the fire design states that the structure must hold for at least 120 minutes and with a constant ingress rate of 0.65 mm/min the charcoal layer will be approximately 78mm in width.

The relation mentioned in eq. 9 and eq. 10 can be used in conjunction with eq. 8 to determine the moisture uptake by the timber elements depending on the time the elements are stored at the building site and the corresponding average relative humidity and temperature at that time.

2.4.3.5 Moisture regression after construction

From the moment a structure is completed, the relative humidity inside the structure will drop due to heating of the building. Water vapor is dissipating and is expelled from the inside structure. Studies done in 2016 and 2009 about the moisture regression in timber in a newly constructed timber building provide experimental data [31], [32] which makes it possible to estimate moisture regression over time, see Figure 28.

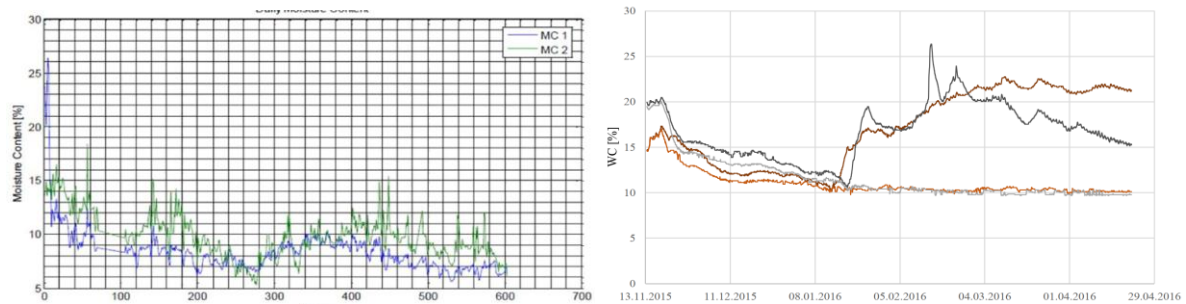


Figure 27 - Moisture regression experiment results from a newly constructed timber building.

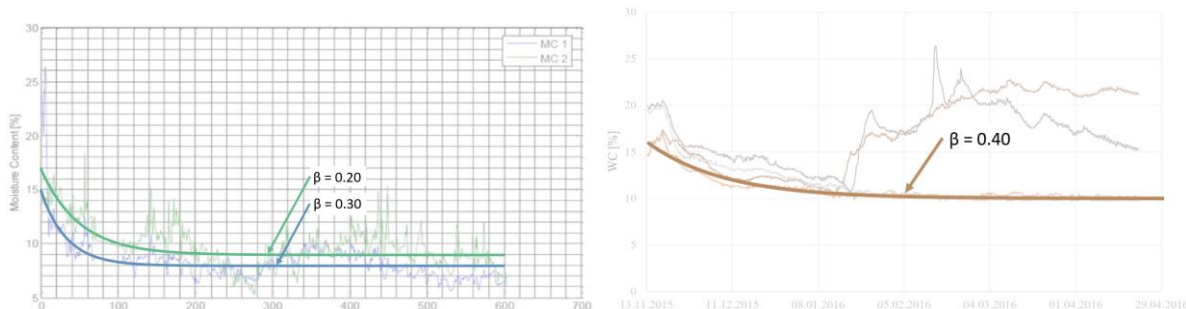


Figure 28 - Curve fitting moisture regression based on experimental data.

*It should be noted that in the graph presented on the right, the two diverging curves do not represent indoor climate conditions. These values represent the moisture content in timber elements placed outside of the insulations directly behind the cladding.

Both experiments are based on an initial relative humidity of approximately 85% with a temperature of roughly 14 °C, representing outdoor conditions. With the finish of construction, the timber elements had an initial moisture content of approximately 15%. With the heating of the structure the relative humidity dropped to an average of 45% after which it followed the seasonal cycles of heating and cooling in the summer and winter. It can be observed that the moisture content also follows a similar trend, with an average variation of 7-11% throughout the year which concurs with the provided recommendations according to the BS EN 942 [33]. The moisture regression curve is based on the formula presented in eq. 11.

$$MC(t) = \Delta MC \cdot e^{-\beta \cdot t} + MC_{\infty} \tag{eq. 11}$$

- t Time
- MC₀ Moisture content at t=0
- MC_∞ Moisture content at t=∞
- ΔMC Difference in MC₀ and MC_∞

2.4.3.6 Lower boundary moisture content

Outdoor conditions represent a cycle in which the relative humidity is higher in winter than it is in summer, see Figure 29.

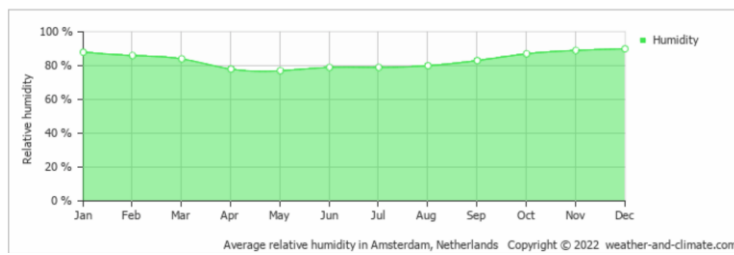


Figure 29 - Average outdoor relative humidity in Amsterdam the Netherlands 2022.

However, indoor conditions show a somewhat mirrored trend. This is due to the heating in winter which causes the relative humidity to drop. A study done in Germany in 2005 shows the relative humidity for indoor climate conditions subjected to outdoor conditions similar to what can be found in The Netherlands. The results can be seen in Figure 30. These results show an average of approximately 45% Relative humidity throughout the year. These results are similar to the results found in [31] and [32].

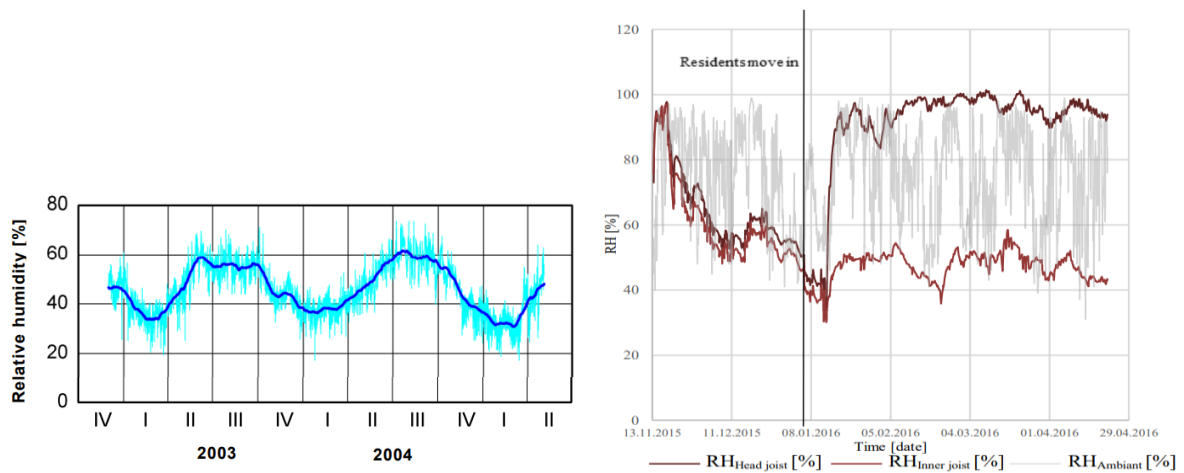


Figure 30 - Relative humidity shown in [34] and [31], left to right respectively.

As mean bottom boundary condition the average moisture content of the timber is based on 45% Relative humidity and 20 degrees Celsius. The corresponding MC of the timber therefore is 8,50%.

2.4.3.7 Dimensional change due to moisture regression

Depending on the direction, timber is less or more affected by shrinkage. Shrinkage in tangential direction is about twice as large as in radial direction. The shrinkage coefficient longitudinal direction is very small with average values from green to oven-dry are between 0.01 to 0.2 for most wood species [28]. The amount of shrinkage is dependent on many variables like size, shape and drying rate, but in general greater shrinkage is associated with greater density.

There is a considerable amount of variation in shrinkage for any species which makes it very hard to accurately describe the shrinkage of an individual piece of wood. However, the average shrinkage of a quantity of species can be predicted accurately.

The dimensional change of a timber element can be determined using the formula stated below:

$$u_{sh} = H \cdot \alpha \cdot (MC_0 - MC(t)) \quad \text{eq. 12}$$

H	Height of the member
MC ₀	Moisture content at t=0
MC(t)	Moisture content at time
α	Shrinkage coefficient

3 Theoretics – concrete

3.1 History of concrete

3.1.1 First remnants

The first remnants of concrete can be found in prehistoric times. Approximately 6500 B.C. concrete-like materials were already being used by the Nabataea traders in southern Syria north of the Jordan. Around 3000 B.C. it was the Egyptians who used limestone to construct the great pyramids of Giza [35].



Figure 31 - Pyramids of Gizeh [36].

3.1.2 Roman Pantheon

The first signs of concrete in its known form was made by the Romans. It is well known that the Romans had a wide variety of knowledge of infrastructure and architecture. By adding a combination of volcanic ash to limestone and water the Romans obtained a material that closely resembles today's concrete. The addition of steel was still unknown at this time so little tensile forces could be absorbed. This however was compensated by architectural design, as can be seen at the Pantheon temple where the dome has a span of 43.30 meters.

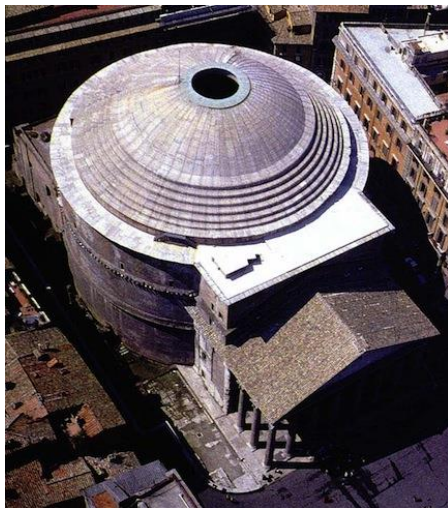


Figure 32 - Roman Pantheon [35].

3.1.3 Portland cement

In the mid-19th century another great leap was made in the development of concrete. Joseph Aspdin found that a mix of limestone, clay and steel clinker formed mortar that hardened under water. In 1824 Joseph obtained the patent on Portland cement, named after stone mined at the island Dorset in England [37].

3.1.4 Reinforced concrete

Although cement had been used in construction for centuries, reinforced concrete was not introduced until the 19th century. The development started in 1867 when the French gardener Joseph Monier applied for a patent for large concrete flower pots containing a net of iron wires. François Hennebique saw Joseph’s design and found a way to apply this material in construction. He started applying reinforced concrete floors in 1879 and in 1892 he patented the use of concrete reinforced with stirrups [38].

3.1.5 prefabricated concrete

Despite the long history of concrete, precast concrete didn’t became popular until the British engineer John Alexander patented the process of constructing precast paneled buildings in 1905 [39]. Although a few precast elements like girders and walls have been made in the 60s and 80s respectively, the precast industry development really started to grow with the invention of CAD (computer-aided design) and PLC (Programmable logic controller) systems in the 80s [40]. These systems would make it able to increase the speed and accuracy of the production process tremendously by automatization while maintaining a good quality.

3.2 Global use of concrete

Concrete has been used for generations to make concrete structures. Developments such as Portland cement and the application of reinforcing steel have made concrete the most widely used artificial material in the world today. Figure 33 shows the global cement production between 2000 and 2018.

GLOBAL CEMENT PRODUCTION (Mt)

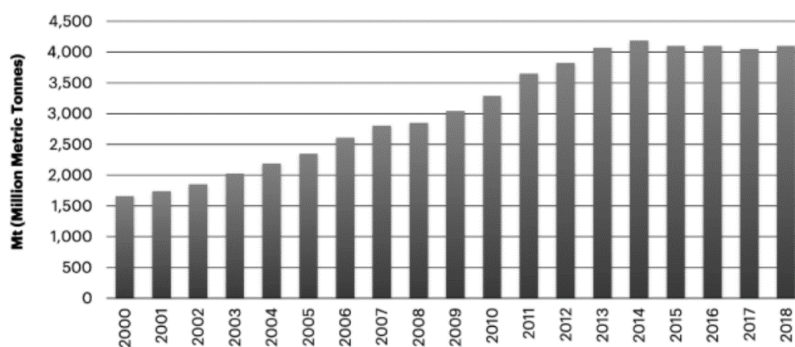


Figure 33 - Global cement production 2000-2018 [41].

3.3 Production and composition

3.3.1 Harvesting raw materials

The production process of concrete starts with the collection of limestone, the basic component of cement. Limestone is a sedimentary rock formed by the accumulation of remains of marine organisms. Limestone mainly consists of calcium carbonate (CaCo3) and depending on the geographic location of the mines. Limestones contain various other minerals such as iron, silica, alumina and clay. The raw materials are transported to the cement factory where the limestone is ground to the size of a golf ball.

3.3.2 Formation of hydraulic cement

This calcium carbonate is then heated in a kiln to 900 degrees. A process known as calcination which liberates a molecule of carbon dioxide from the calcium carbonate to form calcium and magnesium oxide. At 1400-1600 degrees the clinker forms. Gypsum can be added to lower the burning temperature of the raw materials [42]. A flow chart of the production process is presented in Figure 34.

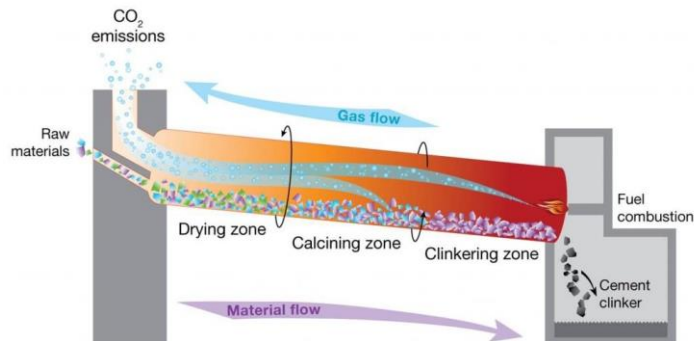


Figure 34 - Cement production flow chart [43].

3.3.3 A typical Portland cement clinker

A typical Portland cement clinker contains the following minerals:

- Tricalcium silicate $3\text{CaO}\cdot\text{SiO}_2$ (C_3S) → Responsible for the initial set and early strength. (alites)
- Dicalcium silicate $2\text{CaO}\cdot\text{SiO}_2$ (C_2S) → Hardens slowly, effect on strength after one week. (Belites)
- Tricalcium aluminate $3\text{CaO}\cdot\text{Al}_2\text{O}_3$ (C_3A) → Contributes to early strength, first compound to hydrate. This is the least desirable component due to the high heat generation and fast reactivity.
- Calcium ferro aluminate $4\text{CaO}\cdot\text{Al}_2\text{O}_3\cdot\text{Fe}_2\text{O}_3$ (C_4AF) → Lowers clinking temperature, contributes little to the strength despite rapid hydration.

3.3.4 Concrete production

The raw materials are mixed in the desired consistency at the concrete factory. To make the desired concrete one concrete plant has an extensive package of raw materials: Various types of cement, admixtures and additives. Most of the concrete plants are able to provide an extensive range of strength classes, colors, consistencies, all tailored to the client's needs.

After the mixing is complete and the concrete is according to the required specifications, the concrete is ready for transport to the construction site. Here the concrete is poured into the formwork and after curing it takes its final shape.

3.3.5 Concrete composition

The raw materials for conventional concrete usually consists of aggregates like grind and sand, cement, admixtures, additives and water. All depending on the properties and quality requested.



Figure 35 - Composition of raw materials concrete [44].

3.3.5.1 Aggregates

Depending on the desired quality and behaviour of the concrete there are various aggregates. A distinction is made between coarse and fine aggregates. Below are some examples of coarse and fine aggregates displayed.

Coarse aggregates 4/32

- River gravel
- Concrete granulate (recycled)
- Sea gravel
- Hard limestone
- Granite
- Expanded clay granules (for lightweight concrete)

Fine aggregates 0/4

- River sand
- Concrete crusher sand
- Sea sand
- Expanded clay granules

3.3.5.2 Supplementary cementitious materials (SCM)

A number of scm's can be used in The Netherlands. The most famous are fly ash and blast furnace slag. Blast furnace cement reacts more slowly at low temperatures than Portland cement and faster at high temperatures. Fly ash is a by-product of burning coal and due to its spherical shape increases the workability and reduces the water/cement ratio. Fly ash also has a pozzolanic effect which increases the chemical reaction between lime and water.

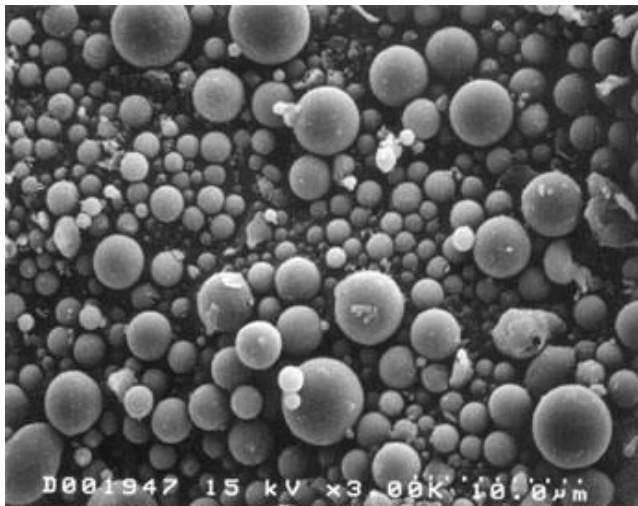


Figure 36 - Photomicrograph made with a scanning electron microscope at 2000x magnification [45].

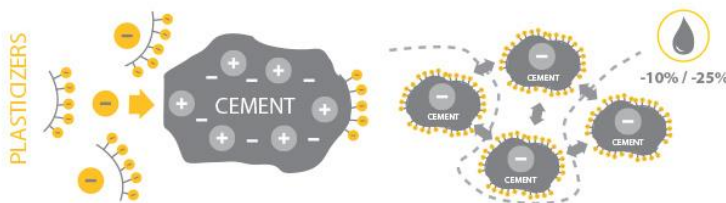
3.3.5.3 Admixtures

Admixtures can be added to a concrete mix during the mixing stage to improve the mechanical properties of the concrete. Admixtures like accelerators, set-retarders and (super)plasticizers can be added.

- Accelerators accelerate the hardening of the concrete. Compounds like calcium chloride (CaCl_2) can be added which acts like a catalyst in the hydration between the C_3S and C_2S . The heat increases a lot at small volumes, at approximately 3%

- Set-retarders decelerate the setting time of the concrete. By modifying the crystal growth or morphology so the barrier around the cement is more efficient. Although the development of early strength is delayed, the final strength is hardly influenced.
- Plasticizers decrease the water/cement ratio of the concrete. The cement gets negatively charged which create a dispersing effect which allows more water permeation. There are three generations available: Water reduces (-10% water), plasticizers (-25% water) and super-plasticizers (-40% water). The mechanism is shown in

1st & 2nd GENERATION PLASTICIZERS


 Figure 37 - Mechanism of 1st and 2nd generation plasticizers [46].

3.4 Mechanical properties

The compressive strength is arguably the most important quality parameter of concrete. Many quality aspects are related to the compressive strength. Concrete has a high compressive strength and a relatively low tensile strength. The bending tensile strength is respectively 10% of the compressive strength. Table 6 comprises some of the mechanical properties based on the concrete class.

 Table 6 - Mechanical properties concrete according to the NEN-EN 1992-1-1 (N/mm²)

Concrete class	f_{ck}	$f_{ck,cube}$	f_{cd}	f_{ctd}	f_{ctm}	$f_{ctk,0.05}$	E_{cm}
C8/10	8	10	5.3	0.56	1.20	0.84	25300
C12/15	12	15	8.0	0.73	1.57	1.10	27100
C16/20	16	20	10.7	0.89	1.90	1.33	28600
C20/25	20	25	13.3	1.03	2.21	1.55	30000
C25/30	25	30	16.7	1.20	2.56	1.80	31500
C30/37	30	37	20.0	1.35	2.90	2.03	32800
C35/45	35	45	23.3	1.50	3.21	2.25	34100
C40/50	40	50	26.7	1.64	3.51	2.46	35200
C45/55	45	55	30.0	1.77	3.80	2.66	36300
C50/60	50	60	33.3	1.90	4.07	2.85	37300
C55/67	55	67	36.7	1.97	4.21	2.95	38200
C60/75	60	75	40.0	2.03	4.35	3.05	39100
C70/85	70	85	46.7	2.15	4.61	3.23	40700
C80/95	80	95	53.3	2.26	4.84	3.39	42200
C90/105	90	105	60.0	2.36	5.05	3.54	43600

f_{ck} Characteristic cylinder compressive strength after 28 days.

$f_{ck,cube}$ Characteristic cubic compressive strength after 28 days.

f_{cd} Design compressive strength.

f_{ctd} Design tensile strength.

f_{ctm} Mean cylinder tensile strength.

$f_{ctk,0.05}$ 5th percentile of the characteristic tensile strength.

E_{cm} Mean elastic modulus

3.4.1 Density

Depending on the composition, the density of concrete can be divided into a number of categories:

- Lightweight concrete 800-2000 kg/m³
- Normal concrete 2000-2600 kg/m³
- Heavy concrete >2600 kg/m³

The density of concrete is highly determined by the aggregates inside the concrete matrix (approximately 75%). In general for plain concrete without reinforcement a density of 2400 kg/m³ is assumed and 2500 kg/m³ for reinforced concrete.

3.4.2 Modulus of elasticity

Concrete is a heterogeneous material, consisting of aggregates embedded in a cement matrix. The modulus of elasticity is largely determined by the type and content of aggregates. However, when hardened the concrete may be approximated to be a homogeneous material with one elastic modulus. The elastic modulus can be determined using the mean cubic compressive strength. This relation is defined in eq. 13, according to the Eurocode.

$$E_{cm} = 22 \cdot \left(\frac{f_{cm}}{10} \right)^{0.3} \quad \text{eq. 13}$$

Concrete has a non-linear stress-strain distribution, see Figure 38. It can be observed that concrete exhibits linear-elastic behavior in the compressive as well as in the tensile section. This elastic behavior is present until the elastic stress limit is reached after which it will exhibit non-elastic behavior. After the ultimate stress limit is reached there is a softening curve in which the stress decreases and the strain increases. According to the Eurocode a bi-linear relationship may be used.

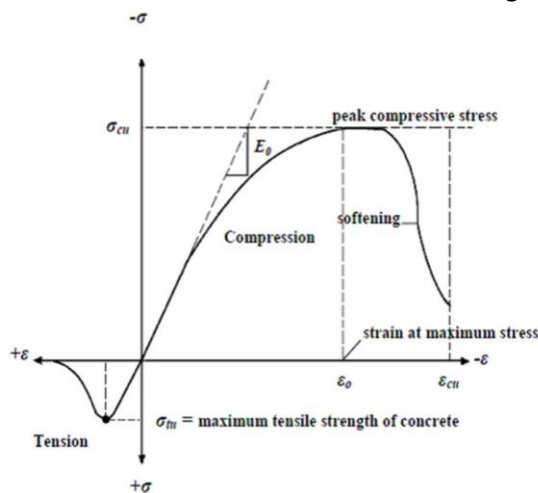


Figure 38 - Typical stress-strain curve concrete [47].

3.4.3 Poisson's ratio

When concrete is subjected to compressive or tensile in one direction, dimensional changes occur in the lateral direction. Poisson's ratio describes the ratio of the strain in axial direction compared to the strain in lateral direction. Generally, the Poisson's ratio for lightweight and normal concrete resides between the 0.15 and 0.20.

3.4.4 Compressive and tensile strength

The compressive strength of concrete is dependent on several factors like: Age, shape, boundary conditions, speed of testing (higher speed is higher strength) and the size effect (the greater the size the lower the strength). The compressive strength is nearly ten times as strong as its tensile

strength. Concrete failure in compression is therefore caused by splitting forces between the particles, as illustrated in Figure 39. To compensate for the low tensile forces steel reinforcement is added.

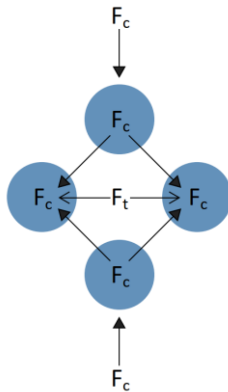


Figure 39 - Concrete compressive failure due to splitting forces.

3.5 Deformations

Just like timber is concrete subjected to various mechanisms that cause strain. Some depend on time, others on load and some on a combination of both.

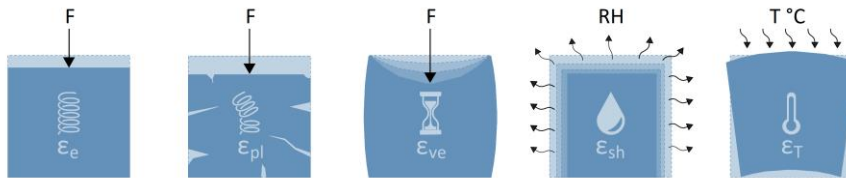


Figure 40 - Strain in concrete.

As is the case with timber, the final strain consists of a superposition of the strains mentioned above. Deformation due to exceeding the elastic limit and temperature differences are assumed to be sufficiently small to be disregarded.

3.5.1 Elastic straining

Just like with timber, concrete also elastically deforms. During loading in the linear elastic regime the member will regain its original shape when it is unloaded, illustrated in Figure 18.

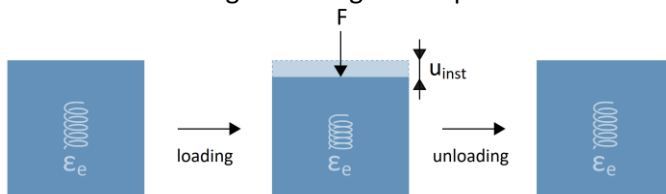


Figure 41 - Elastic deformation due to the load and unloading.

The change in length in the elastic regime can be observed in eq. 14. The derivation can be found in chapter 2.4.1.

$$u_{inst} = \frac{F \cdot L}{A \cdot E_{cm}} \tag{eq. 14}$$

According to the NEN-EN 1995-1-1_2005 the elastic deformation u_{inst} has to be determined using the characteristic load combination according to the EN1990 6.5.3(2) and the mean modulus of elasticity [20].

3.5.2 Viscoelastic straining

Like timber, concrete also is a viscoelastic material, meaning it has viscosity and elastic properties. When subjected to a constant loading the concrete therefore experiences straining, as illustrated in Figure 19.

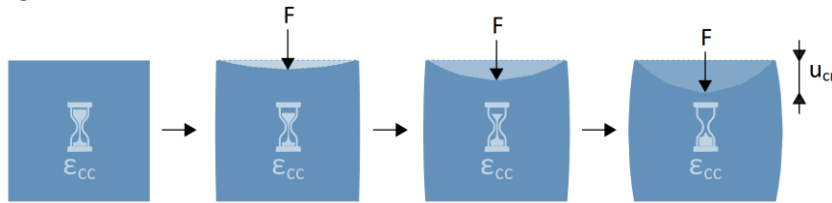


Figure 42 - Creep strain due over time due to a constant load.

Creep deformation in concrete is not related to stress, shrinkage or thermal deformations. Creep is related to the elastic deformation by the secant elastic modulus. The amount of creep is mainly influenced by the cement paste, the water cement ratio and the relative humidity of the surrounding air.

- As aggregates are not liable to creep, their main function is to restrain the creep in the concrete, depending on the elastic modulus and volumetric proportion [48]. Consequently if the volume of aggregates is higher or if the aggregates are stiffer the less creep will occur.
- Creep is also influenced by the water cement ratio. As a lower water cement ratio reduces the porosity of the concrete and thus increases its strength. Since concrete strength is related to the amount of creep, the lower the w/c ratio the lower the creep deformation.
- A lower relative humidity results in more creep. A saturated cement paste will not remain dimensionally stable due to lowering of the internal relative humidity and this increases creep.

3.5.2.1 Viscoelastic straining according to the Eurocode

Creep in the Eurocode is represented as a multiplication of the instant elastic strain by the creep factor $\varphi(t, t_0)$. The elastic strain is dependent on the magnitude of the load and by extension the creep strain. Because not all the load is always present, the load taken into account has to be based on quasi-permanent load factors. When the compressive resistance is higher than 0.45 times the applies compressive stress the creep coefficient may be considered nonlinear.

The final creep deformation can be calculated according to eq. 15.

$$u_{cc} = \phi(\infty, t_0) \cdot u_{inst}^* \quad \text{eq. 15}$$

*Provided the instantaneous deflection is determined according the quasi-permanent loads.

Final creep coefficient at intimate time

The final creep coefficient $\varphi(\infty, t_0)$ at infinite time is obtained by setting the time development coefficient $\beta(t, t_0)$ equal to one. The final creep coefficient is therefore equal to the notional creep coefficient φ_0 .

$$\phi_{(\infty, t_0)} = \phi_0 \cdot \beta_c(t, t_0) \quad \text{eq. 16}$$

Notional creep coefficient

The notional creep coefficient φ_0 is the fictitious creep coefficient. This coefficient takes the effects of the concrete strength, the age of loading and the relative humidity into account by the factors $\beta(f_{cm})$, $\beta(t_0)$ and φ_{RH} respectively.

$$\phi_0 = \phi_{RH} \cdot \beta(f_{cm}) \cdot \beta(t_0) \quad \text{eq. 17}$$

Time development creep coefficient.

The time development creep coefficient $\beta(t, t_0)$ describes the time aspect of the creep development. This factor takes the size effect, concrete strength and relative humidity of the surrounding air into account by the factors h_0 , α_i and β_H .

$$\beta_c(t, t_0) = \left(\frac{(t - t_0)}{\beta_H + t - t_0} \right)^{0.3} \quad \text{eq. 18}$$

Intermediate factors

- The factor ϕ_{RH} accounts for the effect of relative humidity.

$$\phi_{RH} = \left(1 + \frac{1 - RH/100}{0.1 \cdot \sqrt[3]{h_0}} \cdot \alpha_1 \right) \cdot \alpha_2 \quad \text{eq. 19}$$

- The coefficient h_0 accounts for the notional size of the cross-section.

$$h_0 = \frac{2 \cdot A_c}{u} \quad \text{eq. 20}$$

- The coefficients α_1 , α_2 and α_3 that consider the influence of concrete strength.

$$\alpha_1 = \left(\frac{35}{f_{cm}} \right)^{0.7}, \alpha_2 = \left(\frac{35}{f_{cm}} \right)^{0.2}, \alpha_3 = \left(\frac{35}{f_{cm}} \right)^{0.5} \quad (\alpha_i = 1 \text{ for } f_{cm} \leq 35 \text{ MPa}). \quad \text{eq. 21}$$

- The effect of cement type is taken into account by adjusting the concrete age at loading t_0 . The coefficient α depends on the cement type. For cement type Class S, N and R alpha is -1, 1.0 and 1, respectively.

$$t_0 = t_0 \cdot \left(\frac{9}{2 + t_0^{1.2}} + 1 \right)^\alpha \quad \text{eq. 22}$$

- The factor $\beta(f_{cm})$ takes into account the effect for concrete strength.

$$\beta(f_{cm}) = \frac{16.8}{\sqrt{f_{cm}}} \quad \text{eq. 23}$$

- The factor $\beta(t_0)$ allows for the effect of concrete age at the time of loading.

$$\beta(t_0) = \frac{1}{0.1 + t_0^{0.20}} \quad \text{eq. 24}$$

- The factor β_H depends on the relative humidity and the notional member size h_0 .

$$\beta_H = 1.5 \cdot (1 + (0.012RH)^{18}) \cdot h_0 + 250 \cdot \alpha_3 \leq 1500 \cdot \alpha_3 \quad \text{eq. 25}$$

3.5.3 Shrinkage straining

The total shrinkage of a concrete specimen is the sum of drying shrinkage and autogenous shrinkage. Autogenous shrinkage is a reduction in volume due to cement hydration without any moisture migration from or to the concrete. Drying shrinkage is the volume reduction of the cement paste due to water migration when the internal relative humidity is larger than the relative humidity of the surrounding air. The shrinkage strain is illustrated in Figure 43.

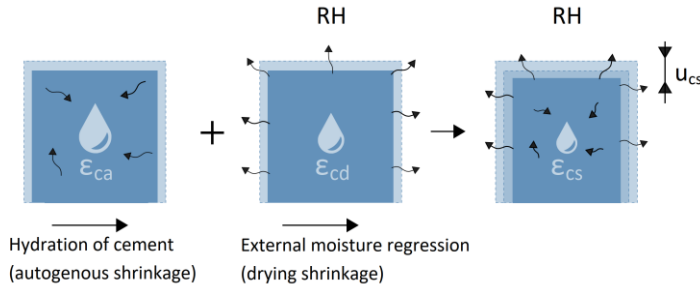


Figure 43 - Autogenous and drying shrinkage strain illustration.

Drying shrinkage is similar to autogenous shrinkage where both occur due to loss of water. The difference between drying and autogenous shrinkage is that drying shrinkage is due to water exchange with the surrounding environment and autogenous shrinkage is due to internal moisture migration. The drying shrinkage is therefore mainly dependent on the relative humidity ratio and can largely be prevented by proper curing methods, the type of aggregates and admixtures. The autogenous strains are largely influenced by the w/c ratio and occur where there is a rise in capillary suction pressure due to self-desiccation.

The final shrinkage deformation can be calculated according to eq. 15.

$$u_{cs} = \varepsilon_{cs}(\infty, t_s) \cdot L \quad \text{eq. 26}$$

Total shrinkage coefficient at intimate time

The final shrinkage coefficient ε_{cs} at infinite time is obtained by superposition of the autogenous and drying shrinkage. This corresponds to setting the time development coefficients $\beta_{ds}(t, t_s)$ and $\beta_{as}(t)$ to 1.

$$\varepsilon_{cs}(\infty, t_s) = \varepsilon_{cd}(t) + \varepsilon_{ca}(t) \quad \text{eq. 27}$$

Time development of shrinkage strain

The time development curve of the drying shrinkage and autogenous shrinkage is described by the time development coefficients $\beta_{cd}(t)$ and $\beta_{ca}(t)$ respectively.

$$\varepsilon_{cd}(t) = \beta_{ds}(t) \cdot k_h \cdot \varepsilon_{cd,0} \quad \text{eq. 28}$$

$$\varepsilon_{ca}(t) = \beta_{as}(t) \cdot \varepsilon_{ca}(\infty) \quad \text{eq. 29}$$

Basic drying shrinkage strain

The basic drying shrinkage strain $\varepsilon_{cd,0}$ is described in the equation below. This equation takes the external relative humidity, concrete strength and cement properties into account by the factors β_{RH} , f_{cm} and α_{dsi} , respectively.

$$\varepsilon_{cd,0} = 0.85 \cdot \left[(220 + 110 \cdot \alpha_{ds1}) \cdot e^{-\alpha_{ds2} \cdot \frac{f_{cm}}{f_{cm0}}} \right] \cdot 10^{-1} \cdot \beta_{RH} \quad \text{eq. 30}$$

Basic autogenous shrinkage strain

The basic autogenous shrinkage strain $\varepsilon_{ca}(\infty)$ is described in the equation below. This equation does take into account the concrete strength only.

$$\varepsilon_{ca}(\infty) = 2.5 \cdot (f_{ck} - 10 \text{MPa}) \cdot 10^{-6} \quad \text{eq. 31}$$

Intermediate factors

- The time dependent factor for drying shrinkage $\beta_{ds}(t)$

$$\beta_{ds}(t, t_s) = \frac{t - t_s}{t - t_s + 0.04 \cdot h_0^{3/2}} \quad \text{eq. 32}$$

- The time dependent factor for autogenous shrinkage $\beta_{as}(t)$

$$\beta_{as}(t) = 1 - e^{-0.2 \cdot t^{0.5}} \quad \text{eq. 33}$$

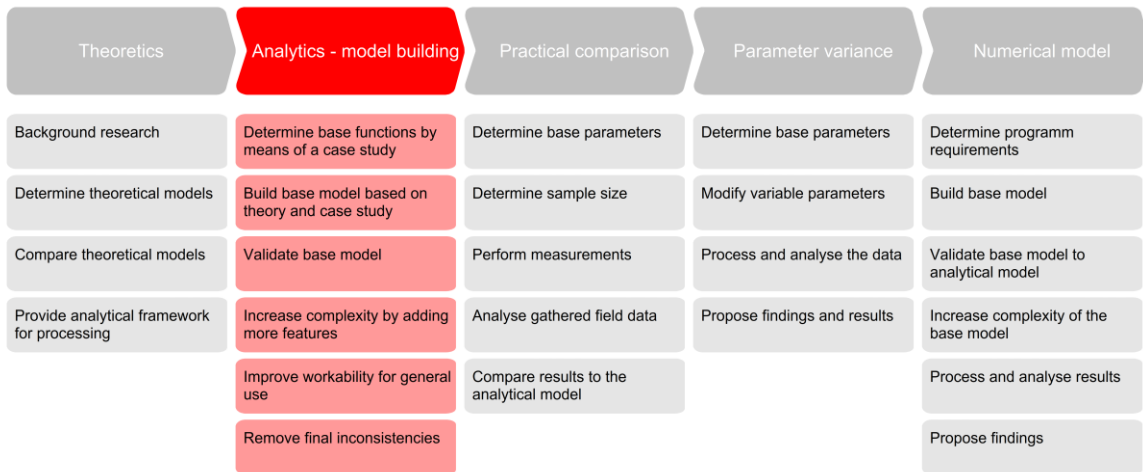
- The factor k_h accounts for the size effect. h_0 according to eq. 20.

h_0	k_h
100	1
200	0,85
300	0,75
500	0,7

- The coefficients α_{ds1} and α_{ds2} consider the influence of cement type.

	S	N	R
α_{ds1}	3	4	6
α_{ds2}	0.13	0.12	0.11

4 Case study - Project Buiksloterham



4.1 General description

In the context of circular building, the municipality of Amsterdam is revising the neighborhood ‘Buiksloterham’. Buiksloterham is changing from an industrial business park into a circular city district focused on living and working. The area on the northern bank of the IJ is one of the most promising areas in Amsterdam to build. The area development will run until approximately mid-2030 and will provide a maximum of 8575 homes. Architect Finch Buildings has been asked to make the design for lot B3, see Figure 44.



Figure 44 - Project overview Buiksloterham&Co by the municipality of Amsterdam [49].

Aveco de Bondt and De GrootVroomshoop were asked to construct the design made by Finch Buildings. The design consists of a hybrid timber-concrete residential structure, see Figure 45. The tower has a height of 23 meters, consists of 7 levels and contains 22 apartments. The plinth offers space for offices and commercial use.



Figure 45 - Architectural design of the hybrid timber-concrete residential tower in Buiksloterham [50].

This hybrid timber tower has been built by means of a concrete core which provides lateral stability in combination with timber modular units. The structure consists of a concrete beam grid with a pile foundation. The ground floor, first floor and core consist entirely of prefabricated concrete. The construction from the first floor to the roof consists of timber modular units. These modular units are prefabricated and are already equipped with installations and sanitary facilities, see Figure 46.



Figure 46 - Finch Buildings modular timber unit [51].

General dimensions

Height of the building	: 23 meter
Width	: 18,55 meter
Depth	: 15,35 meter
Central cores (2)	: 1,36 m ² and 1,56 m ² (C and I shaped cores)
Gross area	: 285 m ²
Number of floor levels	: 7

4.2 Functional concept

The functional concept is based on a bicycle storage and office spaces at the ground floor and appartements at all other levels. The ground floor has an open layout to provide flexibility for the office spaces. The floor plans of the 1st floor up to the 6th floor are identical and provide 4 appartements per level, with the exception of the location of the balconies. The top floor provides 2 penthouses with an outdoor deck. The apartments consist out of prefab timber modules. The layout of each floor is provided in Figure 47.

The building provides the following spaces:

- Office space : gross floor area 197 m²
- Bicycle storage : gross floor area 58 m²
- Modular apartment A : Gross floor area 44 m²
- Modular apartment B : Gross floor area 65 m²
- Modular apartment C : Gross floor area 71 m²
- Modular apartment D : Gross floor area 49 m²
- Modular apartment E : Gross floor area 66 m²
- Modular apartment F : Gross floor area 80 m²



Figure 47 – Functional layout of the ground floor (top left), floors 1,3&5 (top right), floors 2&4 (bottom left) and floor 6 (bottom right).

4.3 Structural concept

The main structure consists out of one layer of prefab concrete while the other 6 layers consists out of stacked prefab timber units, see Figure 48. The structure is supported by a concrete pile foundation in combination with a concrete roster. The ground floor is made out of hollow core slabs situated between the concrete foundation beams. The vertical support structure at the ground floor entirely consist out of prefab concrete walls and columns. The concrete cores runs from the ground floor to the 6th floor and house vertical transport options including elevators and stairwells. The core also provides lateral stability to the structure. From the 1st floor up, the apartments consist of prefab timber modular units. The modular units are located between the concrete core and the façade.

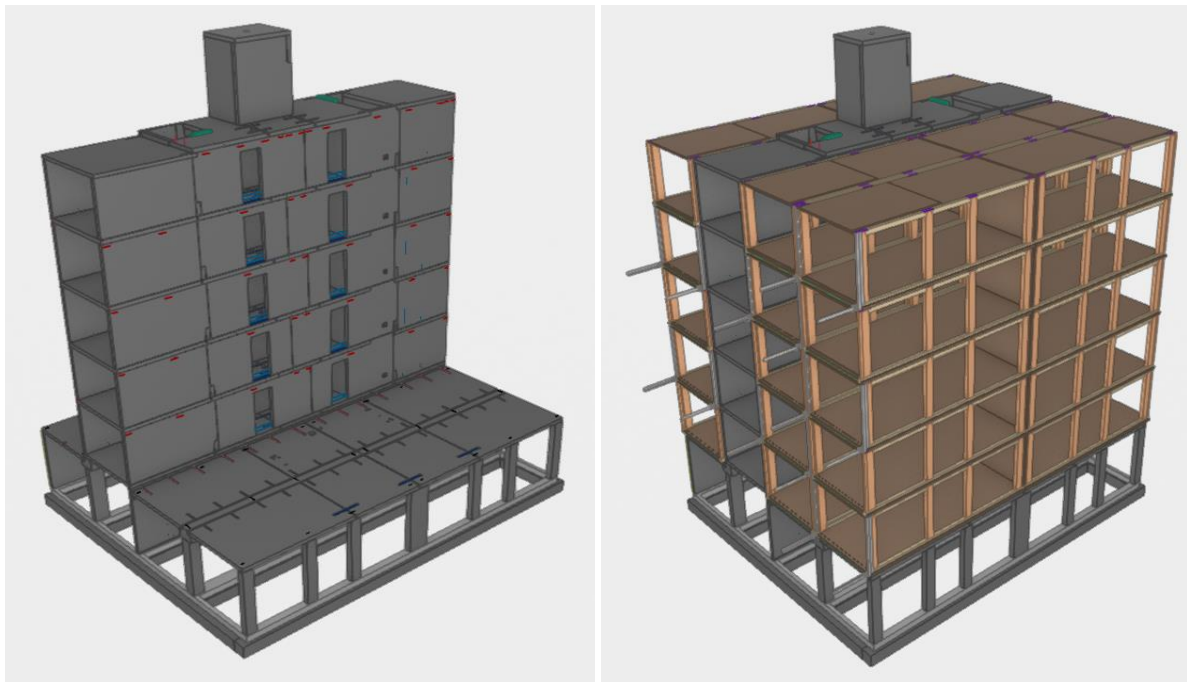


Figure 48 - Structural overview of Buiksloterham, concrete structure (left), including the timber units (right).

The following elements are present in the structure:

- Roof construction : Prefab timber + HSB + CLT.
- 1st – 6th floors : Finch units.
- 1st floor : Prefab concrete slab (beneath finch unit).
- Ground floor : Isolated hollow core slabs.
- Foundation : DPA Pile foundation + in-situ concrete beam roster.
- Façade : Bi-panel: HSB + prefab cladding.
- Internal walls : Lightweight metal stud walls.
- Core : Prefab concrete walls
- Columns : Prefab concrete columns.

4.4 Stability

The stability of the structure in lateral direction is provided by two cores (indicated in blue) and shear walls (indicated in green), see Figure 49. As there are sufficient stability walls in longitudinal direction this direction will not be decisive. A stability calculation will be made for the wind load in lateral direction. The load in lateral direction will be transferred through the floors to the cores. The concrete cores of the Buiksloterham building have to stabilize the complete building and have to withstand all horizontal loads, caused by wind, inclination or eccentricities and second order effects.

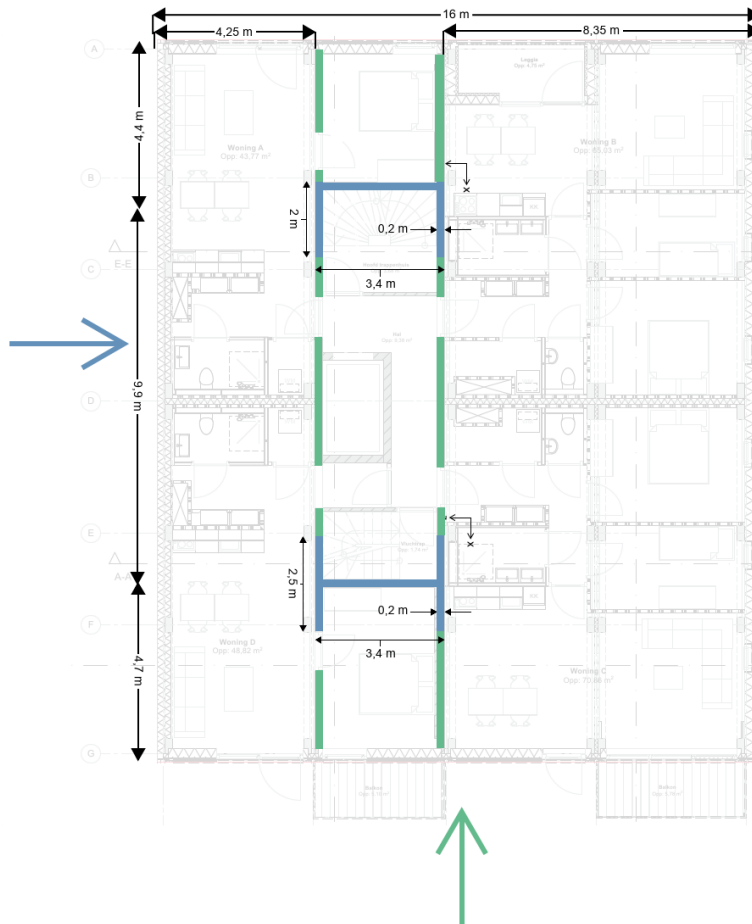


Figure 49 - Stability provisions for several wind directions.

As the structure is located in Amsterdam it is located in wind area II. The corresponding wind load coefficient to a structure in a rural area in wind area II with a height of 23m is 1.11, according to the NEN-EN 1991-1-4.

4.5 Fire design

During the design of a structure, the choice of construction materials has a major influence on the development of a fire. Depending on the material used for the main loadbearing structure several actions need to be undertaken to ensure a fire safe design.

Important aspects that affect the design are:

- Fire resistance with regard to collapse of the main loadbearing structure.
- Fire resistance of the façade.
- Limiting the spread of fire.
- Design of smoke-free escape routes.

The development of a fire is described according to the NEN 6069 [52] and can be observed in Figure 50. This is the standard ISO-curve which describes heat development due to a fire over time. It can be observed that a temperature of approximately 800 degrees is reached after just 30 minutes.

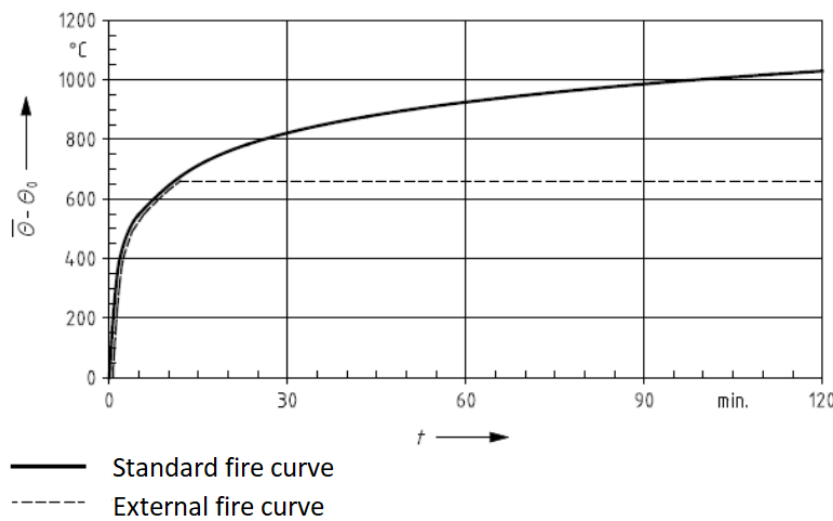


Figure 50 - Fire curve according to the NEN 6069.

4.5.1 Fire classes

The NEN-EN 13501-1:2019 classifies several fire classes for construction materials. These classes are part of the European fire propagation class. The classes run from A1 to F, with A1 being the highest and F the lowest ranking. A non-combustible material therefore belongs in the A1 category and materials that are highly flammable belong to class F. Materials of which no information is available belong in category F as well. Table 7 indicates the fire classes according to the Eurocode.

Table 7 - Fire classes according to the NEN-EN 13501-1:2019

Class	Description	Example
A1	Materials that don't contribute at any stage of the fire, even with a fully developed fire.	Stone-like materials like gypsum, brick and concrete.
A2	Materials in this class do not contribute to a fully developed fire to the fire load and fire spread. Practically non-combustible.	Plasterboard.
B	Materials that are difficult to combust, which provide a limited contribution.	PVC flooring, some textile floor coverings, painted plasterboard, fire retardant MDF.
C	Materials in this class exhibit limited lateral flame spread when exposed to flames. Combustible materials	Heavier woods, plasterboard with wallpaper.

	that contribute to fire hazard.	
D	Materials in this class provide longer resistance to a small flame without substantial flame spread taking place. In addition, they are also able to withstand exposure to radiation heat with sufficient delayed and limited heat release. Good combustible materials that make a major contribution to fire hazard.	Most wood species.
E	Materials in this class make a very high contribution to the fire. The materials are resistant to fire without significant flame spread for a small period of time. Very good combustible materials that make a major contribution to a fire hazard.	Plastic, fire retardant EPS.
F	Materials for which no response to fire propagation requirements are determined. Highly flammable materials.	Non-tested materials, EPS.

4.5.2 Fire resistance duration

When designing a structure, the main loadbearing structure has to be fire resistance for a certain amount of time to ensure people have a chance to get out safe. The Dutch building degree describes the fire resistance against collapse as: ‘the time during which a structural part can withstand the loads its subjected to when heated according to the standard fire curve’. The standard fire curve according to the ISO834. These fire resistance times vary from 0,30,60,90 to 120 minutes, see Figure 51.

It should be noted that a distinction is made between the main loadbearing structure and the rest. When determining the main loadbearing structure it is important to determine the effect of collapse of a fire compartment. A fire compartment spanning maximal 3 levels may collapse as long as the rest of the compartments remain unaffected. The reason for this is that when the structural elements are on the brink of collapse the fire is hot enough to ensure no people would be alive anymore.

The fire resistance requirement can be lowered by 30 minutes when inflammable materials are used.

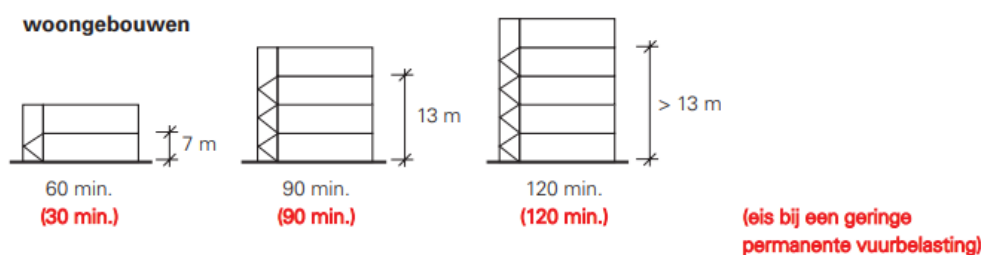


Figure 51 - Fire resistance times according to the Dutch building degree.

In most cases the top floor is not considered to be part of the main load bearing structure. If this is the case the static load of this compartment should be taken into account when designing the compartment directly below.

4.5.3 Concrete elements

Concrete is extremely suitable for making a fire resistant structure due to the following qualities:

- Concrete is inflammable.
- Concrete has a high fire resistance

- Concrete is (heat)isolating
- Concrete doesn't allow molten material to drip and allow fire to spread.

As the material does not contribute to a (fully developed) fire, concrete falls within the category A1. The steel within the concrete however is very sensible to high temperatures so a sufficient cover is therefore required. The design of the concrete elements regarding fire resistance is done according to the tables provided in the NEN-EN 1992-1-2.

4.5.4 Steel elements

Steel is like concrete inflammable and therefore is also classified in the A1 category. Unlike concrete however is steel extremely susceptible to high temperatures. From approximately 300 degrees the strength and stiffness start to decline and at 800 degrees there is approximately 10% of the original strength left. This can be observed in Figure 52. Appropriate action has to be taken to increase the fire resistance, differentiating between active and passive measurements.

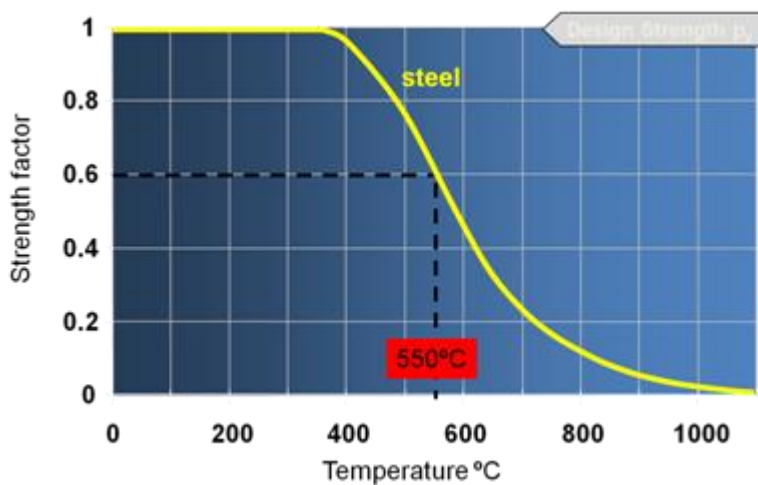


Figure 52 - Steel strength in fire. [53]

Active measurements:

- Detection
- Extinguishing media
- Smoke and heat extraction (SHE) installations

Passive measurements:

- Increasing the dimensions
- Placement (internal or external construction)
- Structural integration
- Fireproof isolation

From the designers point of view the passive measurements are most interesting. Especially structural integration and fireproof isolation are cheap and common practice.

4.5.5 Timber elements

Unlike concrete and steel contributes timber to a fire hazard. For this reason softwood is classified as a class D material. The question therefore arises whether it would be safe to build with timber. Whether it is safe to build with timber depends on the requirements of the structure. What kind of function does it have to fulfill? According to the Eurocode the aim of structural safety during a fire hazard is to ensure a safe evacuation of the people inside the structure. It should be noted that the Eurocode does not describe the state of the building after a fire. The standard ISO-curve is designed

to ensure a self-burnout when the fuel in the building is consumed. However, when the structure of the building itself acts as fuel, the question arises whether the structural integrity of the building will remain intact during a fire. This problem however is beyond the scope of this research and only the design criteria according to the Eurocode will be taken into account, which is ensuring there is sufficient time for evacuation of the structure.

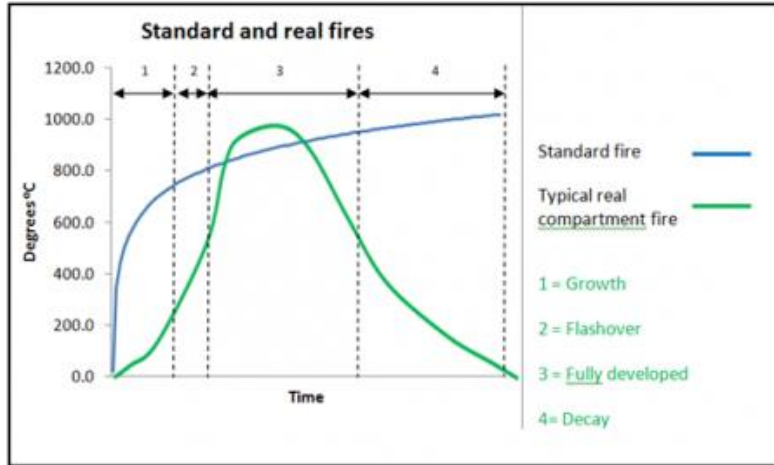


Figure 53 - ISO-standard curve versus real compartment fire. [54]

Like steel there are several ways to design a structure for such a calamity. Active and passive measures can be taken to shield the timber from the heat. Passive measures like encapsulating the timber works relatively well. By encapsulating the temperature can be kept below the 200 degrees Celsius to prevent pyrolysis.

Another way to ensure a safe design is to make use of char. Char acts as an insulator between the timber and the fire, see Figure 54. The char does not have any structural integrity and is no longer able to resist any stresses. The charring rate of timber has been extensively researched and is well documented. A common way of designing for fire is to take into account a disposable layer which is allowed to char, ensuring that enough structural timber remains.

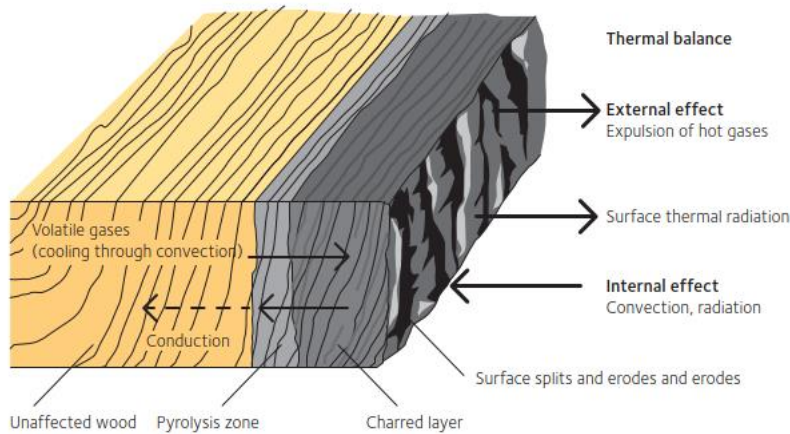


Figure 54 - Charring process of timber. [55]

The charring depth of a member subjected to a single-sided fire is defined according to eq. 34. In case of a multi-sided fire β_n is used instead of β_0 . Values for the charring rates are given in Table 8.

$$d_{char,0} = \beta_0 \cdot t \tag{eq. 34}$$

β_0 One dimensional charring rate [mm/minute]
 t Time [minutes]

Table 8 - Design charring rates of timber according to the NEN-EN 1995-1-2

	β_0 [mm/min]	β_n [mm/min]
Softwood and beech		
Solid timber with $\rho \geq 290 \text{ kg/m}^3$	0.65	0.8
Glulam with $\rho \geq 290 \text{ kg/m}^3$	0.65	0.7
Hardwoods		
Solid or glued timber with $\rho \geq 290 \text{ kg/m}^3$	0.65	0.7
Solid or glued timber with $\rho \geq 450 \text{ kg/m}^3$	0.50	0.55
LVL		
With a density $\geq 480 \text{ kg/m}^3$	0.65	0.7
Panels*		
Wood paneling	0.9	
Plywood	1.0	
Wood-based other than plywood	0.9	
*Minimum panel thickness of 20mm		

4.6 Building physics

Noise from outside or neighbours can be particularly annoying. Especially in cities there are increasingly more noise sources. To prevent excessive noise nuisance, the Dutch Building decree has determined acoustic requirements for new residential buildings with respect to the following elements:

- Sound from the façade and roof
- Allowable sound from installations
- Sound between apartments and buildings
- Limiting resonance in common rooms

This chapter focuses on the sound between apartments, specifically airborne and impact sound. Generally speaking, if a structure has good impact sound insulation the airborne sound insulation will also meet the requirements.

4.6.1 Mass requirement

According to the NEN5077 there needs to be at least a 52 dB difference between adjacent apartments. In order to fulfil this requirement there are numerous details described in the NPR5070. These details however require excessive designing or require expensive systems and can complicate the matters during execution. An alternative option is to apply a certain minimum mass instead. Generally speaking this will also be the cheapest option. The following mass requirements are being used:

Table 9 - Mass requirements for sound design

	Single-family home	Residential building
House-dividing wall (solid)	250mm concrete	250mm concrete *
House-dividing wall (cavity)	2x100mm concrete	2x160mm concrete
Inner cavity wall	100mm concrete	110mm concrete(800kg floor) / 160mm (550kg floor)
Inner wall, load bearing	100mm concrete	110mm concrete
Floor solid (>800kg/m ²)	280(70) / 300(50) / 320VBI(70)	280(70) / 300(50) / 320VBI(70)

Floating floor (>550kg/m ²)	230(70) / 260VBI(50)	230(70) / 260VBI(50)
---	----------------------	----------------------

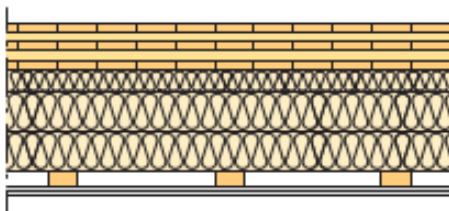
* Also for connection to walkways inside the building

- Around an elevator always 214 limestone + 150 cavity
- Open gallery as inner cavity wall
- Closed gallery as house-dividing wall

4.6.2 Timber building physics

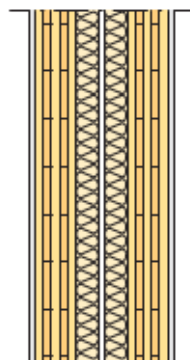
The mass of timber is very low compared to concrete so the mass requirement as described in the chapter above doesn't really apply. A few systems exist to still fulfil the requirements for airborne and impact sound level reduction. These systems include:

- (1) Insulation. A structural timber slab combined with a floating timber deck or suspended ceiling with acoustic isolation. In case no structural timber has to be exposed gypsum can be added to the ceiling to increase the fire resistance. This method is also very common for timber walls. [55]



Top to bottom:

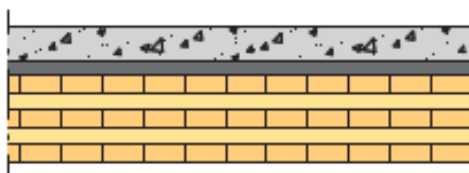
- 140 CLT slab
- 70 insulation
- 45 x 220 studs, self-supporting
- 2 x 95 insulation
- 28 battens
- 2 x 13 gypsum plasterboard



Left to right:

- 13 plasterboard
- 120 CLT panel
- 45 insulation
- 20 cavity
- 45 insulation
- 120 CLT panel
- 13 plasterboard

- (2) Hybrid concrete-timber flooring with acoustic matting in between. This has been done in HAUT in Amsterdam. The structural timber can be exposed at the ceiling. This method is not suitable for walls.



Top to bottom:

- 80 concrete
- 30 acoustic matting
- dynamic stiffness < 9 MN/m³
- 200 CLT slab

- (3) Acoustic decoupling. This is done in the case of Buiksloterham in Amsterdam. The modules are decoupled so no impact sound is able to transfer horizontally or vertically between the apartments. The width of the cavity depends on the thickness of the structural elements, as can be observed in Figure 55.

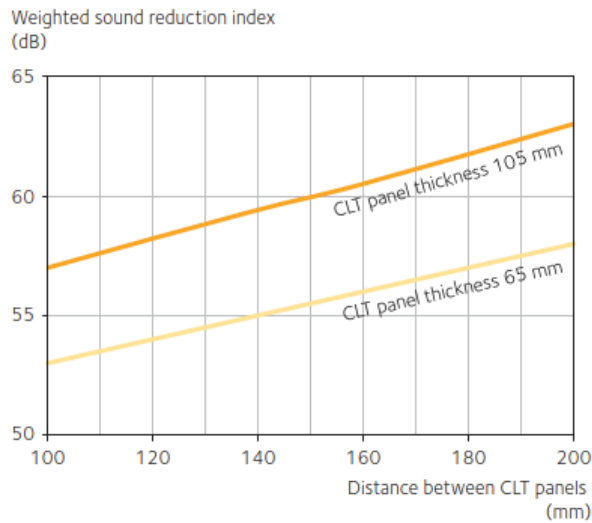


Figure 55 - Weighted sound reduction index for CLT based on the width of the cavity. [55]

Attention has to be given to the design of the nodes as no acoustic decoupling can take place. To reduce flanking transmission an acoustic insulation layer can be applied. This insulation layer can be in the form of an elastic as well as a non-elastic bearing.



Figure 56 - Example of a steel bearing that reduces flanking transmission. [55]

4.7 Loads

When designing a structure there are multiple loads that need to be considered. For a structure this size there main three loads are the wind load, snow load and self-weight of the structure. These loads are all applied to the structure in a different way.

4.7.1 Snow load

According to the NEN-EN1991-1-3 the load case for snow in the Netherlands is as follows:

$$s = \mu_i \cdot C_e \cdot C_t \cdot s_k$$

μ_i is the snow load coefficient, this coefficient depends on the shape of the roof.

C_e is the exposure coefficient, 1 in The Netherlands

C_t is the warmth coefficient, 1 in The Netherlands

s_k is the characteristic value of snow load on the ground, 0.7 in the Netherlands

The variable μ_i depends on the shape of the roof.

$$\mu_i = \begin{cases} 0.8, & 0^\circ \leq \alpha \leq 30^\circ \\ 0.8 \cdot \frac{60-\alpha}{30}, & 30^\circ < \alpha < 60^\circ \\ 0, & \alpha \geq 60^\circ \end{cases}$$

4.7.2 Wind load

According to the NEN-EN 1991-1-4 there are several wind areas in the Netherlands. Depending in which area the building is built the thrust of the wind that needs to be taken into account differs. The wind load coefficient depends on the height of the building and the shape of the roof. The wind load is always applied normal to the façade and the roof.



Figure 57 - Wind areas in The Netherlands

As the structure is located in Amsterdam it is located in wind area II. The corresponding wind load coefficient on the façade to a structure in this area with a height of 23m is 1.11, according to the NEN-EN 1991-1-4. The wind load has a distribution as indicated in Figure 58.

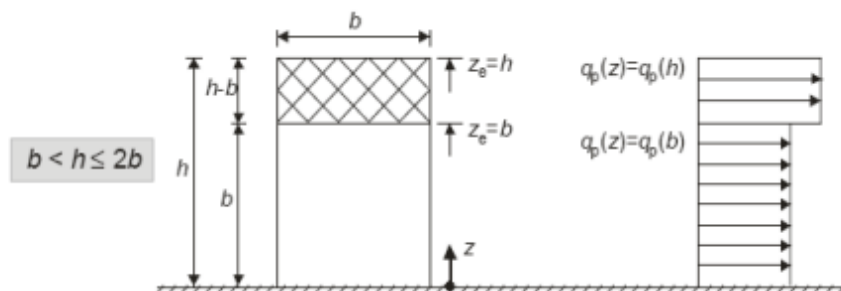


Figure 58 - Distribution of wind loads on the facade as a function of the height.

The loads on the façade can be viewed in Figure 59. The wind load has to be taken by the cores and the concrete stabilizing walls. Due to the eccentricity between the application of the load and the cores, a moment is generated which is taken by compressive and tensile forces in the connections, indicated as F1-4 in the figure below. The following parameters were used to determine these forces:

- Area : Area II, rural
- $q_{p(h)}$: 1.112, based on a height of 23m.
- $q_{p(b)}$: 0.998, based on a width of 19m.
- pressure : +0.8
- negative pressure : -0.5
- overpressure : +0.2
- under pressure : -0.3
- safety factor : 1.5

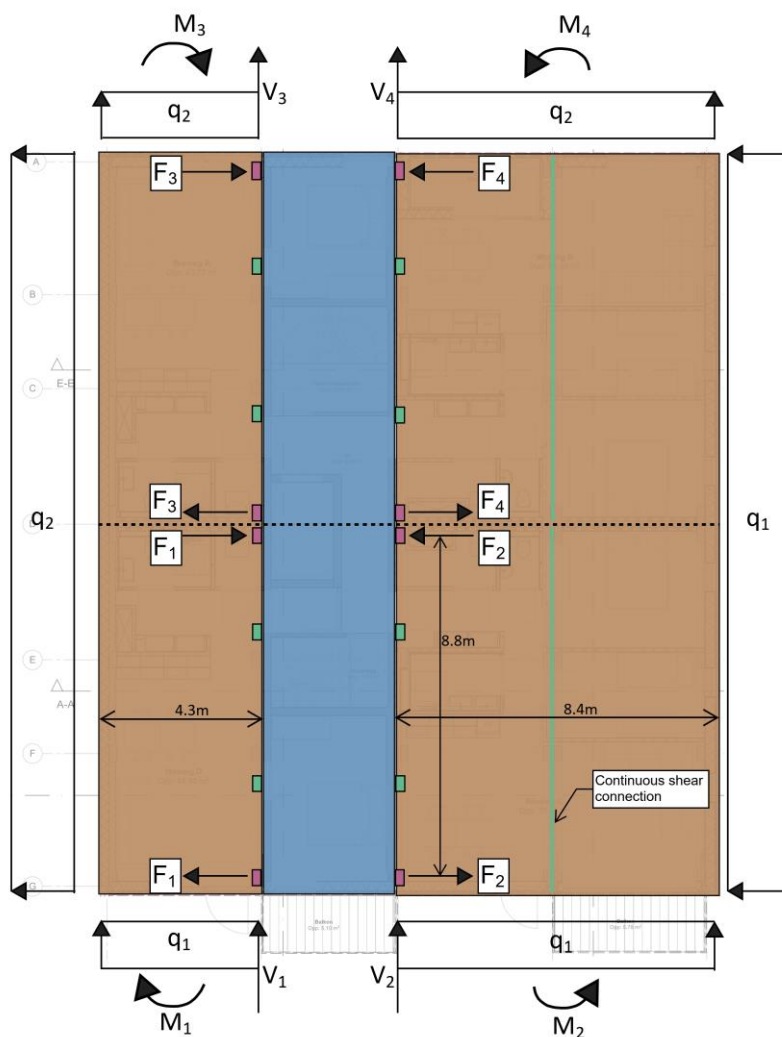


Figure 59 – Overview of forces on façade and connections due to the wind.

The wind load creates tensile and shear forces in the connections between the concrete core and the timber units. These forces are transferred via designated tensile and shear connections, see chapter 4.11. There are two tensile (indicated in red) and two shear (indicated in green) connections per module. The results of the forces in the connections can be observed in Table 10.

Table 10 – Forces acting on the façade and connections due to the wind for each level, all in kN and m.

Level	Height from 0	Pressure height	$q_{p(z)}$	Left side			Right side			$F_{c,1/3}$	$F_{t,1/3}$
				$V_{1/3}$	$M_{1/3}$	$F_{1/3}^*$	$V_{2/4}$	$M_{2/4}$	$F_{2/4}^*$		
Roof	23	2	1.11	11.5	24.7	2.8	22.4	94.2	10.7	12.7	7.9
6	19	3.5	1.11	20.1	43.2	4.9	39.2	165	18.7	22.2	13.9
5	16	3	1.00	15.4	33.2	3.8	30.2	127	14.4	17.1	10.7
4	13	3	1.00	15.4	33.2	3.8	30.2	127	14.4	17.1	10.7
3	10	3	1.00	15.4	33.2	3.8	30.2	127	14.4	17.1	10.7
2	7	3	1.00	15.4	33.2	3.8	30.2	127	14.4	17.1	10.7
1	4	3.5	1.00	18.0	38.8	4.4	35.2	148	16.8	19.9	12.4
0	0	2	1.00	10.3	22.1	2.5	20.1	84.5	9.6	11.4	7.1
				20.1	43.2	4.9	39.2	165	18.7	22.2	13.9

*Forces due to the bending moment.

The following can be observed:

- The maximum shear force in a connection is $39.2/4 = 9.8$ kN.
- The maximum tensile force in a connection is 18.7 kN due to the generated moment $M_{2/4}$.
- The maximum compressive force in a connection is 22.2 kN due to the wind in lateral direction.

The wind load in lateral direction has to be taken solely by the concrete cores. With a dilatation in the middle of the structure each core takes half the load. The corresponding mechanical scheme and moment distribution can be seen in Figure 60. The maximum moment at the base of the core is 3378 kNm (characteristic value).

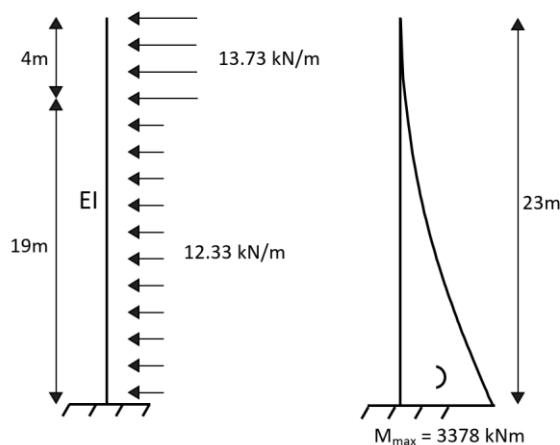


Figure 60 – Mechanical scheme and moment distribution in the cores due to the wind load.

4.7.3 Dead and live loads

Part	Deadload g_k [kN/m ²]	Live load q_k [kN/m ²]	Q_k [kN/m ²]	ψ -values		
				ψ_0	ψ_1	ψ_2
Roof						
Solar panels	0.15					
Decking + isolation + rafters	0.50					
Installation and finishing	0.15					
	0.80	1.00	2.00	0.00	0.00	0.00
1st t/m 6th floor (Finch)						
Finish (60mm)	1.20	1.75	<i>Persons</i>			
Isolation	0.10					
CLT plates 120mm (floor)	0.60					
CLT plates 80mm (ceiling)	0.40	0.80	<i>Separations</i>			
	2.30	2.55	3.00	0.40	0.50	0.30
Floors stairwell						
Finish (130mm)	3.25	1.75	<i>Persons</i>			
Prefab concrete floor 200mm	5.00	0.80	<i>Separations</i>			
	8.25	2.55	3.00	0.40	0.50	0.30
1st floor (concrete)						
Prefab concrete floor 200mm	5.00	1.75	<i>Persons</i>			
		0.80	<i>Separations</i>			
	5.00	2.55	3.00	0.40	0.50	0.30
Other floors (concrete)						
Prefab concrete floor 200mm	5.00	1.75	<i>Persons</i>			
Floor finish 130mm	3.25	0.80	<i>Separations</i>			
	8.25	2.55	3.00	0.50	0.50	0.30
Ground floor (office)						
Floor finish 80mm	1.60	2.50	<i>Persons</i>			
Isolated hollow core slab 200	3.10	1.20	<i>Separations</i>			
	4.70	3.70	3.00	0.50	0.50	0.30
Balcony						
Timber rafters	1.00	2.50	3.00	0.40	0.50	0.30
6th floor (terrace)						
Tiles	1.20	0.0				
Floor finish (80mm)	1.60	2.50	<i>Persons</i>			
Timber rafters	0.50	0.80	<i>Separations</i>			
	3.30	3.30	3.00	0.50	0.50	0.30

Per material

Concrete wall (200mm) : 5.00 kN/m²

CLT walls HSB (100mm) : 0.50 kN/m²

Façade timber framing : 1.00 kN/m²

Façade panels : 0.50 kN/m²

Window framing incl. glass : 1.00 kN/m²

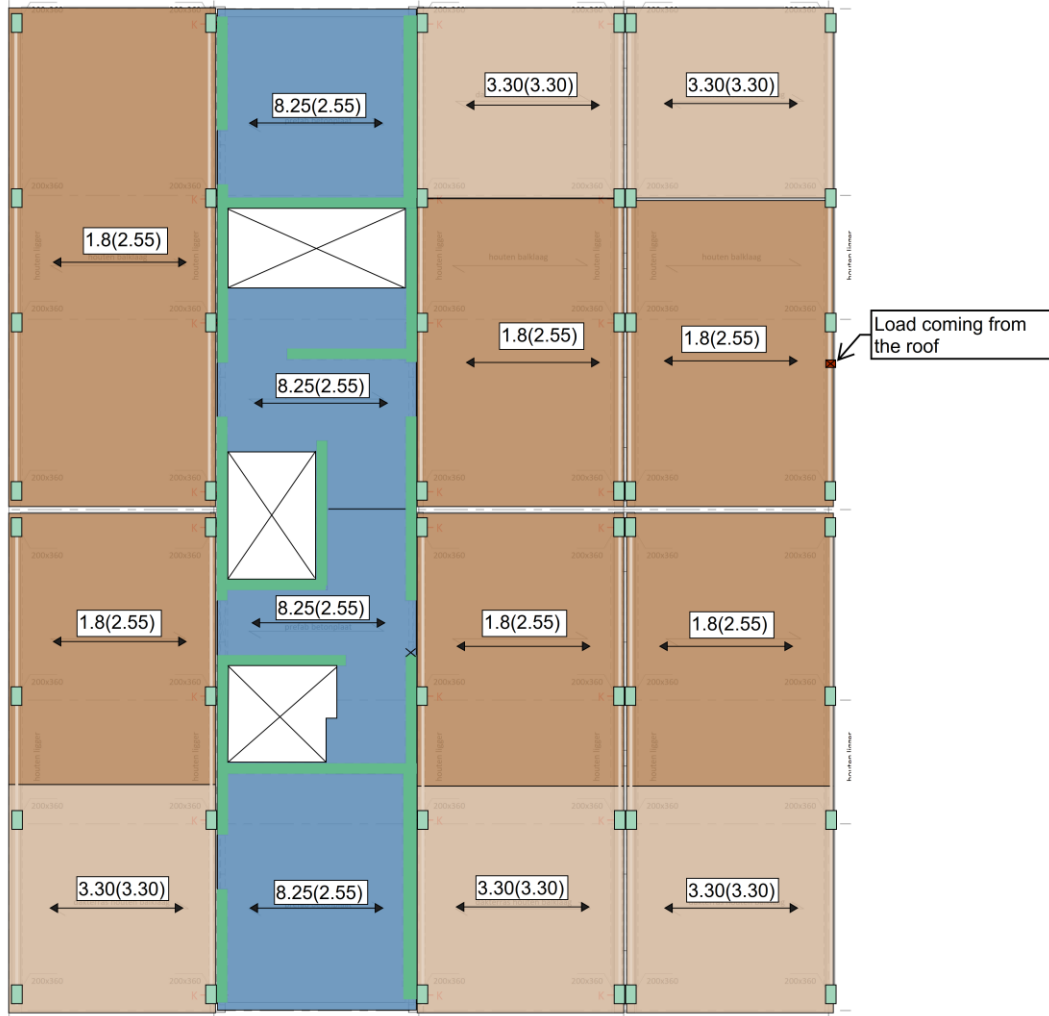
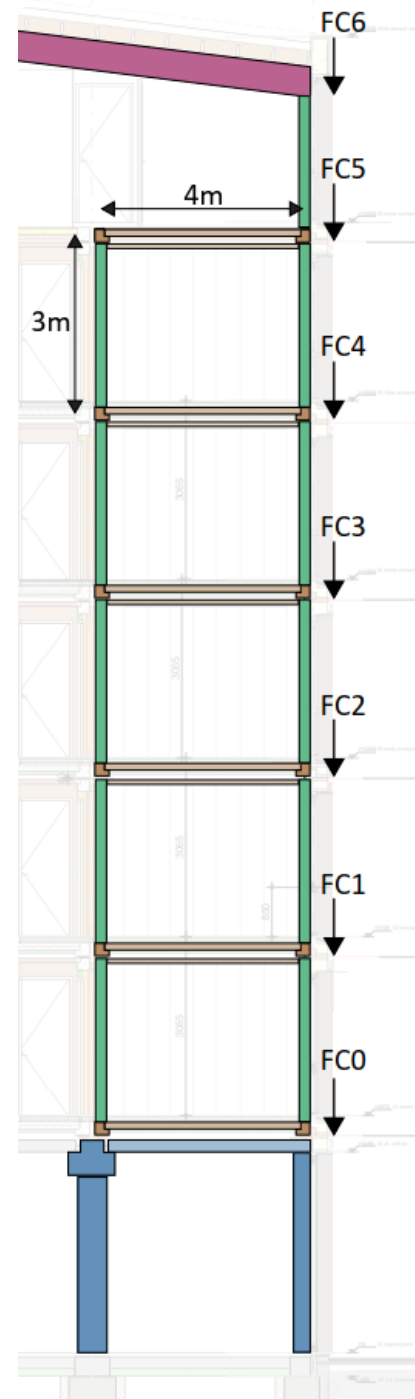


Figure 61 – Characteristic loads in plan view of 6th floor.

Table 11 - Loads on the glulam columns for each level.

Load#	Type	g_k	q_k	m^2	F_{gk}	F_{qk}	F_k
FC6	Roof	0,80	0,56	17,00	14	10	24
FC5	FC6				14	10	24
	CLT ceiling (80mm) + isolation	0,50	0,00	5,60	3	0	3
	Facade panels	0,50	0,00	10,95	5	0	5
	CLT floor (120mm) + finish (60mm)	1,80	2,55	9,00	16	23	39
					38	23	61
FC4	FC5				38	23	61
	CLT ceiling (80mm) + isolation	0,50	0,00	5,60	3	0	3
	Facade panels	0,50	0,00	10,95	5	0	5
	CLT floor (120mm) + finish (60mm)	1,80	2,55	9,00	16	23	39
					63	46	108
FC3	FC4				63	46	108
	CLT ceiling (80mm) + isolation	0,50	0,00	5,60	3	0	3
	Facade panels	0,50	0,00	10,95	5	0	5
	CLT floor (120mm) + finish (60mm)	1,80	2,55	9,00	16	23	39
					87	55	142
FC2	FC3				87	55	142
	CLT ceiling (80mm) + isolation	0,50	0,00	5,60	3	0	3
	Facade panels	0,50	0,00	10,95	5	0	5
	CLT floor (120mm) + finish (60mm)	1,80	2,55	9,00	16	23	39
					112	64	176
FC1	FC2				112	64	176
	CLT ceiling (80mm) + isolation	0,50	0,00	5,60	3	0	3
	Facade panels	0,50	0,00	10,95	5	0	5
	CLT floor (120mm) + finish (60mm)	1,80	2,55	9,00	16	23	39
					136	73	209
FC0	FC1				136	73	209
	Facade panels	0,50	0,00	10,95	5	0	5
	CLT floor (120mm) + finish (60mm)	1,80	2,55	9,00	16	23	39
					158	83	240

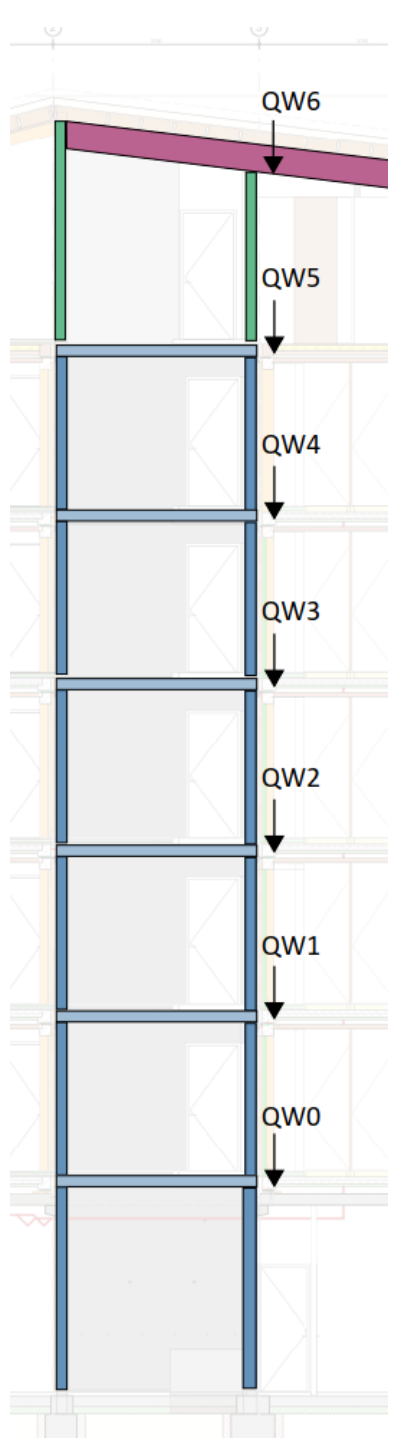


Notes:

- The bottom LVL beam of the modules are a continuous beam with 4 supports. The middle supports attract 60% of the total load. The effective width therefore is taken as 4.5m, opposed to the 2.8m for the top beams which are schematized as a beam on two supports.
- The façade panels are assumed to be secured to the top and bottom beams from the modules, corresponding effective widths 2.8m and 4.5m respectively.
- According to the Eurocode, the live load of two floors need to be fully included. Any additional floors will be taken into consideration with their respective phi-factor of 0.4.

Table 12 - Loads on the prefab concrete walls for each level.

Load#	Type	g_k	q_k	m	q_{gk}	q_{qk}	q_k
QW6	Roof*	0,80	0,56	28,00	22	16	38
QW5	QW7				22	16	38
	Finish (130mm)	3,25	1,75	1,90	6	3	10
	Prefab concrete floor 200mm	5,00	0,80	1,90	10	2	11
					38	7	45
QW4	QW6				38	7	45
	Finish (130mm)	3,25	1,75	1,90	6	3	10
	Prefab concrete floor 200mm	5,00	0,80	1,90	10	2	11
	Prefab concrete wall 200mm	5,00	0,00	3,00	15	0	15
					69	10	78
QW3	QW5				69	10	78
	Finish (130mm)	3,25	1,75	1,90	6	3	10
	Prefab concrete floor 200mm	5,00	0,80	1,90	10	2	11
	Prefab concrete wall 200mm	5,00	0,00	3,00	15	0	15
					99	12	111
QW2	QW4				99	12	111
	Finish (130mm)	3,25	1,75	1,90	6	3	10
	Prefab concrete floor 200mm	5,00	0,80	1,90	10	2	11
	Prefab concrete wall 200mm	5,00	0,00	3,00	15	0	15
					130	14	144
QW1	QW3				130	14	144
	Finish (130mm)	3,25	1,75	1,90	6	3	10
	Prefab concrete floor 200mm	5,00	0,80	1,90	10	2	11
	Prefab concrete wall 200mm	5,00	0,00	3,00	15	0	15
					161	16	176
QW0	QW2				161	16	176
	Finish (130mm)	3,25	1,75	1,90	6	3	10
	Prefab concrete floor 200mm	5,00	0,80	1,90	10	2	11
	Prefab concrete wall 200mm	5,00	0,00	3,00	15	0	15
					191	17	209



Notes:

- * The concentrated load from the roof is assumed to be spread through the wall at 45 degrees, resulting in a line load at position FW6 of approximately 5.3 kN/m^1 .
- According to the Eurocode, the live load of two floors need to be fully included. Any additional floors will be taken into consideration with their respective phi-factor of 0.4.

Total load of the structure

To determine the 2nd order effects of the concrete core the total load of the structure needs to be determined. The total load will be roughly estimated. The total load of the entire structure including live load is approximately 15000 kN

Table 13 – Total load of the structure.

Load#	Type	g_k	q_k	m^2	P_{gk}	P_{qk}	P_k
7	Roof	0,80	0,56	203	162	114	276
6-1	Finch units	2,3	2,55	1260	2898	3213	6111
	Concrete stairs	5	2,55	420	2100	1071	3171
	concrete walls	5		1044	5220	0	5220
							14778

4.8 Foundation

The foundation consists of a pile foundation with a concrete beam roster. The pile foundation consists of 51 DPA screw piles with a diameter of 410mm. The in-situ piles are made out of concrete with class C20/25 and have a length of 21 meter. An overview of the layout of the piles is provided in Figure 62.

The beams are made out of in-situ concrete, class C30/37. The width varies between 400 to 800mm with a standard height of 600mm. The standard detail of the foundation beams with the piles and isolated hollow core slabs can be found in Figure 63.

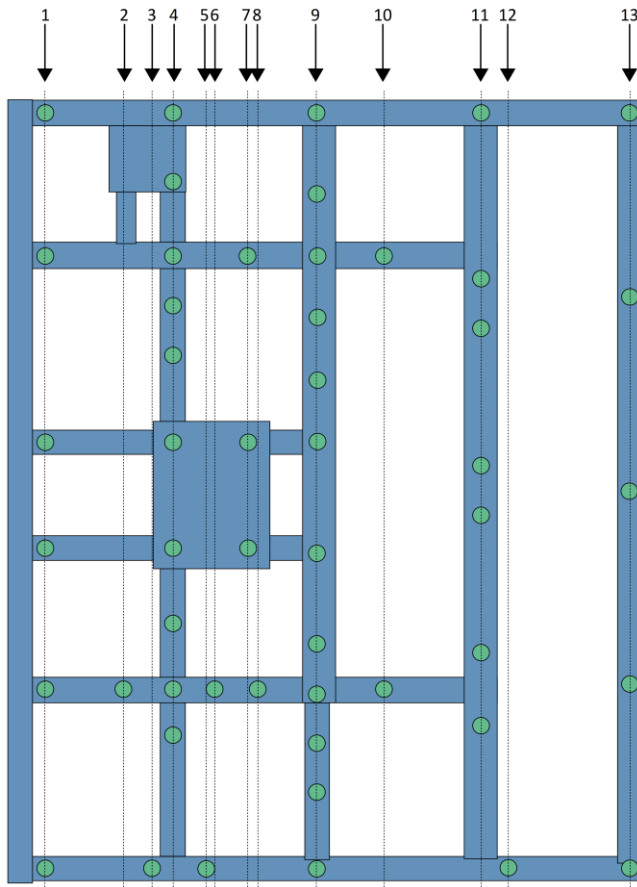


Figure 62 - Pile foundation layout

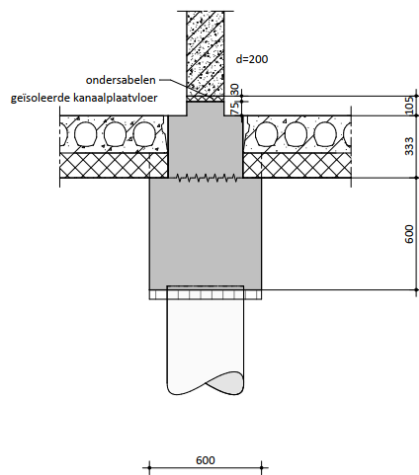


Figure 63 - Standard detail of foundation, ground floor and walls.

4.8.1 Estimation of rotational stiffness

In order to get an approximation for the rotational stiffness of the foundation the piles the polar moment of inertia is determined about the center of the core. By means of the polar moment of inertia the rotation can be estimated based on the moment due to the wind load.

$$I_p = \sum_{i=1}^n \cdot a_i^2$$

When dividing the layout in Figure 62 is divided into gridlines in which each gridline contains at least 1 pile the layout will be divided into 13 gridlines. The center moment of rotation is taken at the center of the concrete cores which coincides with gridline 7, see Figure 62. Table 14 provides an overview for the piles and their respective locations.

Table 14 - Foundation piles and location.

Gridline	# of piles	a [m]	a ² [m ²]	# of piles · a ²
1	6	4.9	24.01	144.06
2	1	3.0	9	9
3	1	2.3	5.29	5.29
4	10	1.8	3.24	32.4
5	1	1.0	1	1
6	1	0.8	0.64	0.64
7	3	0.0	0	0
8	1	0.3	0.09	0.09
9	12	1.7	2.89	34.68
10	2	3.3	10.89	21.78
11	7	5.6	31.36	219.52
12	1	6.3	39.69	39.69
13	5	9.3	86.49	432.45
				I_p
				940.6

The corresponding rotational stiffness of the foundation therefore is:

$$c = \frac{M}{\phi} = \frac{3378}{2.93 \cdot 10^{-5}} = 11.54 \cdot 10^7 \text{ kNm/rad}$$

With

Force in the outer piles : $P_n = \frac{M \cdot a_i}{I_p} = \frac{3378 \cdot 9.3}{940.6} = 33.4 \text{ kN}$

Elastic shortening : $\Delta l = \frac{P_n \cdot l_p}{E \cdot A_p} = \frac{33.4 \cdot 10^3 \cdot 21000}{31476 \cdot 160000} = 0.27 \text{ mm}$

Rotation : $\phi = \frac{\Delta l}{a_i} = \frac{0.27}{9300} = 2.93 \cdot 10^{-5} \text{ rad}$

4.9 Concrete structure

The concrete structure consists out of prefab concrete elements. A cross section of the concrete core in combination with the timber frame structure is provided in Figure 64.

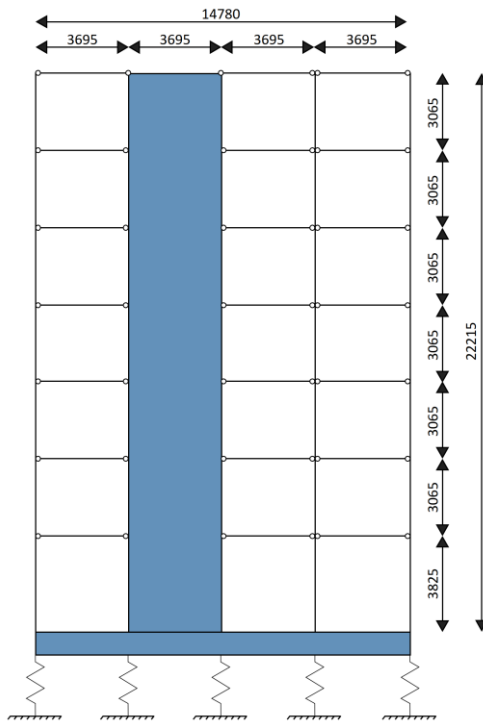


Figure 64 - Structural layout of the concrete core with frame.

4.9.1 Core slenderness

The building has a gross floor area of approx. 290m², (15,5 x 18,8). With a width of 3,7 meters and with a height of 22 meters the core slenderness is approx. 6. This core is therefore not very slender so dynamic influences will have a minor influence. The core can be schematized as a rod with a bending stiffness with a rotational spring at the base. The rod is subjected to a lateral load w and a normal force q . The mechanical scheme of the core can be seen in Figure 65.

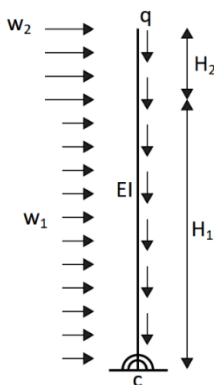


Figure 65 - Mechanical scheme of the core incl. the rotational stiffness of the foundation.

Due to the first order moment the concrete cores deflect in lateral direction. This deflection causes the mass of the structure to eccentrically load the core which causes a secondary bending moment. The main parameters to reduce the secondary bending moment are the stiffness of the core and the rotational stiffness of the foundation. Due to the wind load the first order bending moment as described in chapter 4.7.2 is 3378 kNm. The corresponding deflection is approximately 0.54mm as can be observed in Figure 66.

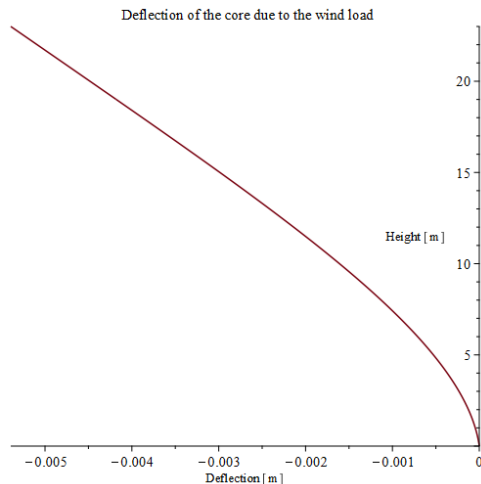


Figure 66 - Deflection curve concrete core due to the wind load.

Due to this deflection a secondary bending moment is generated by the eccentric loading of the entire mass of the structure. With the mass of the entire being approximately 15000 kN (see Table 13) and the corresponding secondary bending moment is 74 kNm. The total bending moment on the core therefore is 3452 kNm and the ultimate deflection 56mm.

4.9.2 Ground floor

The ground floor consists of isolated hollow core slabs, $h = 200\text{mm}$, which are situated between the in-situ concrete foundation. See Figure 63 for a standard detail of the foundation and ground floor connection. The cross section of the isolated hollow core slabs can be found in Figure 67.

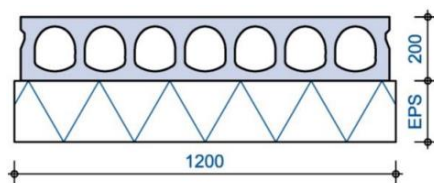


Figure 67 - Standard cross-section isolated hollow core slabs [56].

4.9.3 1st floor

The first floor consists of prefabricated concrete slabs, class C55/67, with a height of 200mm. The concrete slabs provide a workplace to place the timber units. In the final situation the concrete slabs are not subjected to any variable loads as the timber units contain their own structural floor, see chapter 0.

4.9.4 Vertical support structure

The vertical support structure consists of prefabricated walls and columns. The prefabricated concrete walls have a standard thickness of 200mm and a concrete quality of C55/67. Some walls are part of the horizontal support structure, see chapter 4.4.

Columns are present where the office spaces are located, see Figure 47 (top left). With the addition of columns instead of walls, an open structure provides the required flexibility for office spaces. These columns are made of the same material as the walls, prefabricated concrete C55/67. The columns do not provide any horizontal stability measures to the structure and are only loaded in normal direction.

4.10 Timber modular units

The timber structure consists of prefabricated timber units which only provide vertical stability. Horizontal forces such as wind load are transferred to the core by means of diaphragm action of the floors and beams. This means that all connections between the timber frame and the concrete core can be considered as simple connections. These connections will be elaborated further in chapter 4.11. The modular units consist of a column-beam load bearing structure. The layout of the timber units is provided in Figure 68.

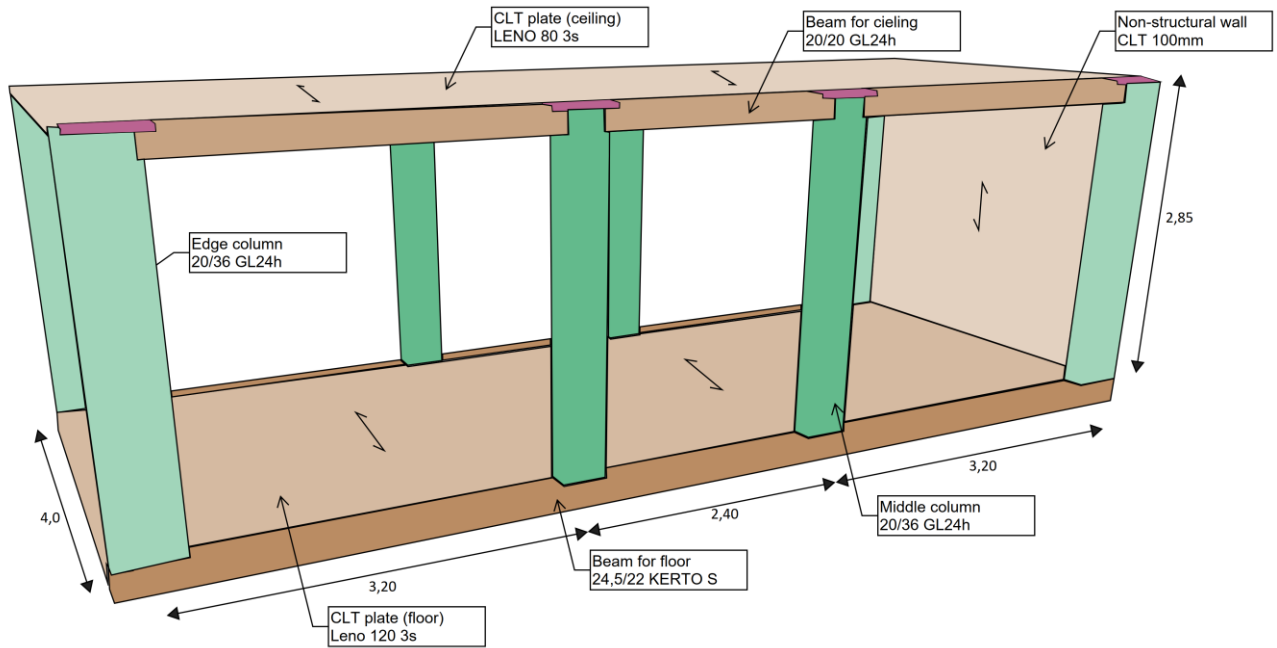


Figure 68 - Timber prefab modular unit

The floors span unidirectional and are simply supported at both ends by a LVL beam. This beam is a continuous beam with 3 spans and 4 supports which transfers the load to the columns. There are 8 columns in total. The CLT wall at the end of the module is non-structural and is placed for practical reasons only.

Lateral forces are transferred through the slabs to the stabilizing core. The units are connected to the stabilizing core using shear and tensile connections. The connections are made such that vertical deformation can occur while the horizontal deformation is restricted. The mechanical scheme of the timber units is provided in Figure 69.

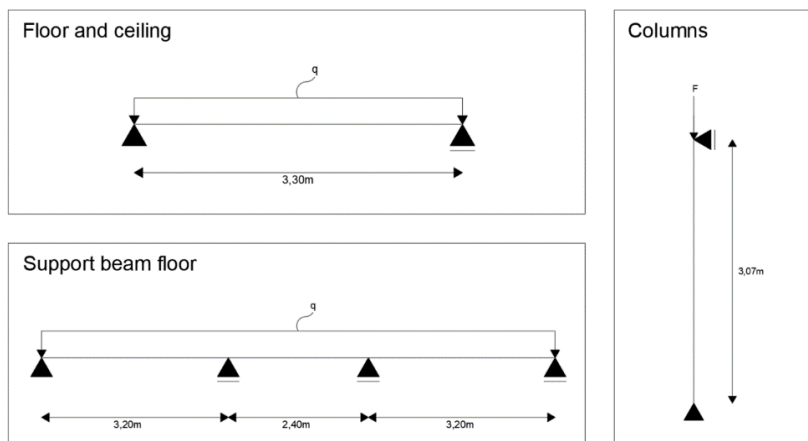


Figure 69 - Mechanical scheme modular units.

4.11 Connections

There are several connections present. An overview of the connections is provided in Figure 70. The connections between the modules and the concrete core consist out of 2 tensile (red) and 2 shear (green) connections per module, situated at the top of the columns and beams respectively. The modules are coupled to each other by a continuous shear connection (light green) at axis 4 and tensile coupling connections near the columns (cyan). With the absence of shear connections at axis D no shear can be transferred at this location. Standard details of the connections are provided in Figure 71 and Figure 72.

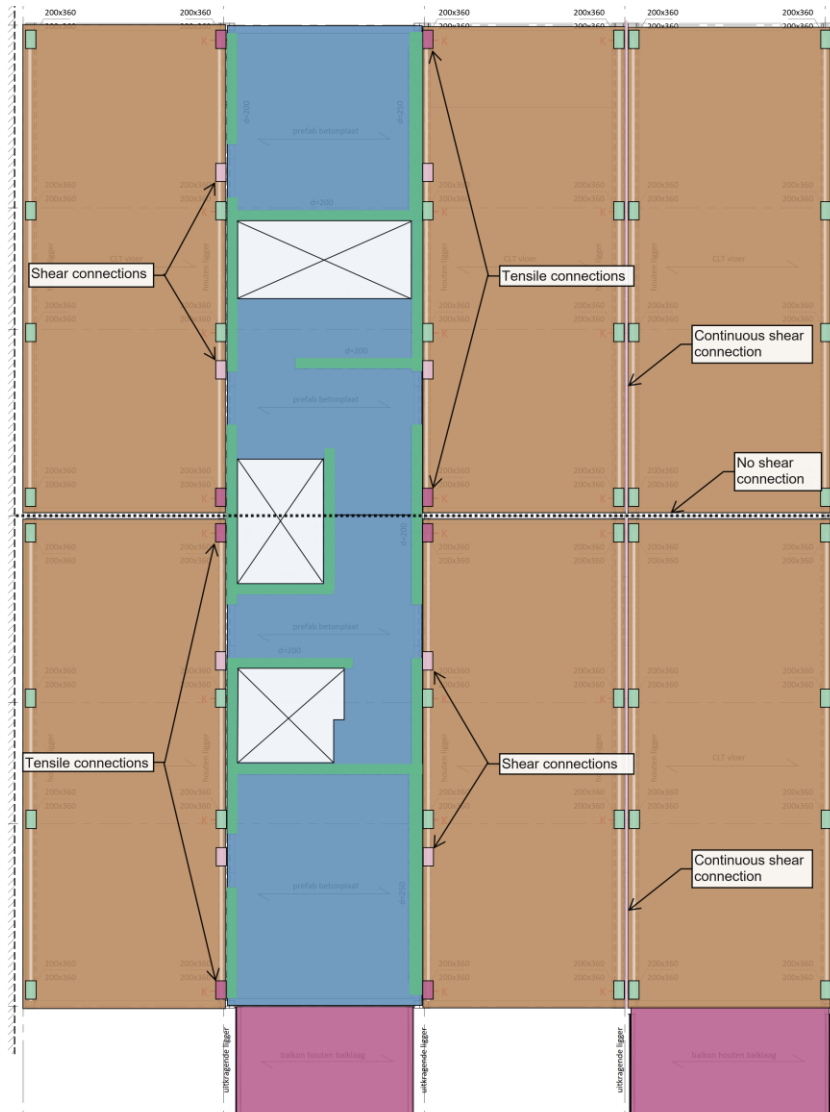


Figure 70 – Connection overview.

It can be observed that the tensile and shear connections have provisions taken to ensure vertical translation can take place. This is done by adding slotted holes or ‘slobgaten’ in Dutch. These slotted holes provide a vertical translation up to 35mm. Out of those 35mm is 15 mm reserved to properly align the units and an additional 20mm is provided for vertical tolerance.

It can also be observed that the modules only connect at the location of the columns, otherwise they do not touch. In the columns a blind anchor is placed to take up vertical tensile forces if needed. To ensure acoustic uncoupling an acoustic felt is placed in between the columns.

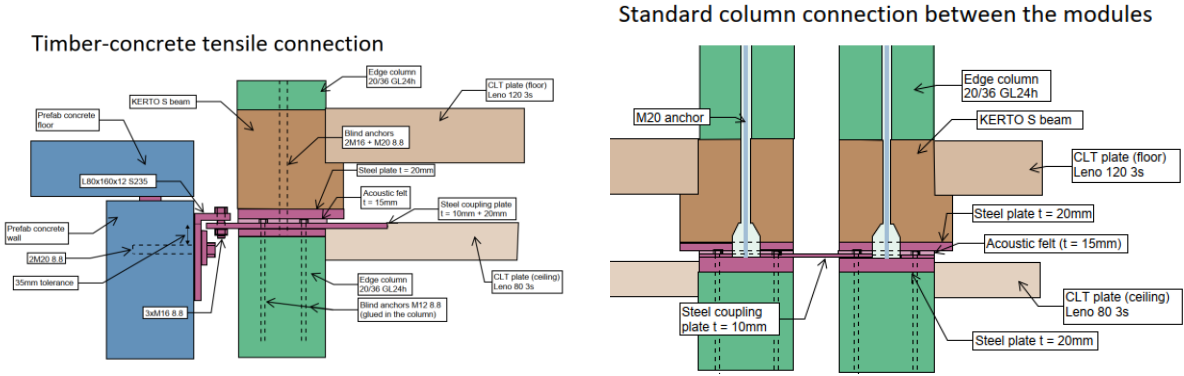


Figure 71 – Tensile connections concrete-timber and between the timber modules (not to scale).

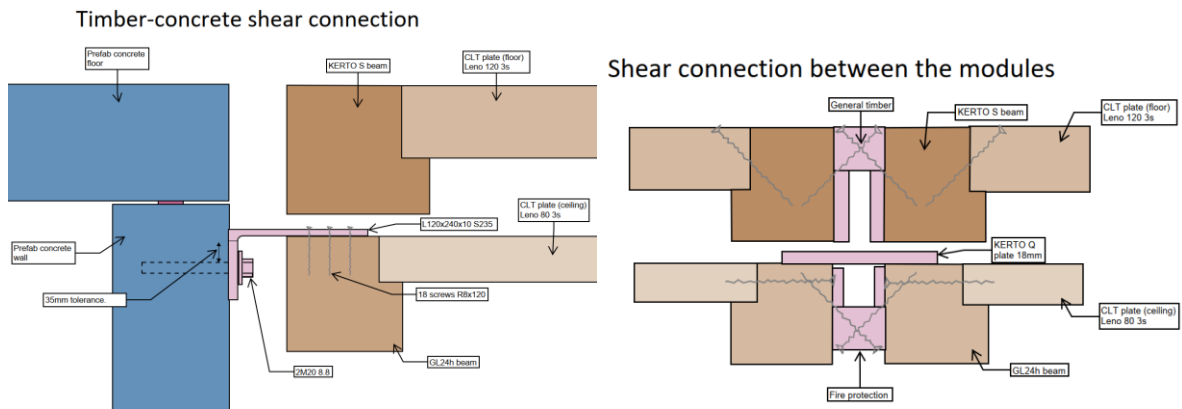


Figure 72 – Shear connections concrete-timber and between the timber modules (not to scale).

4.12 Building order

For a system like this, a concrete core in combination with a timber frame, there are two main approaches that can be taken namely: Building the concrete core first after which the timber modules are connected or building the structure floor by floor.

The first method consists of building the concrete core first, after which the timber modules are installed. This way the concrete core can be used as a member that provides stability during the construction.

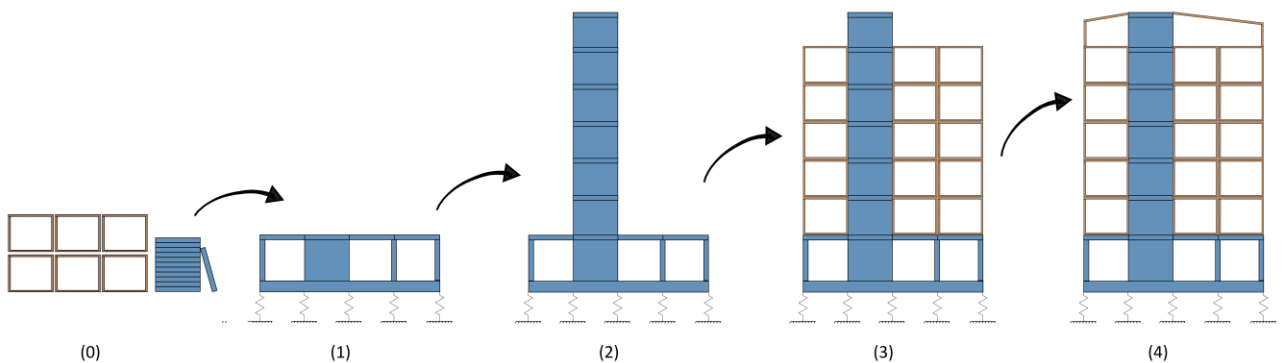


Figure 73 - Building order first method, ie. installing the concrete core first.

The second method is to build the floors level by level. The concrete core and the timber units are installed at the same time.

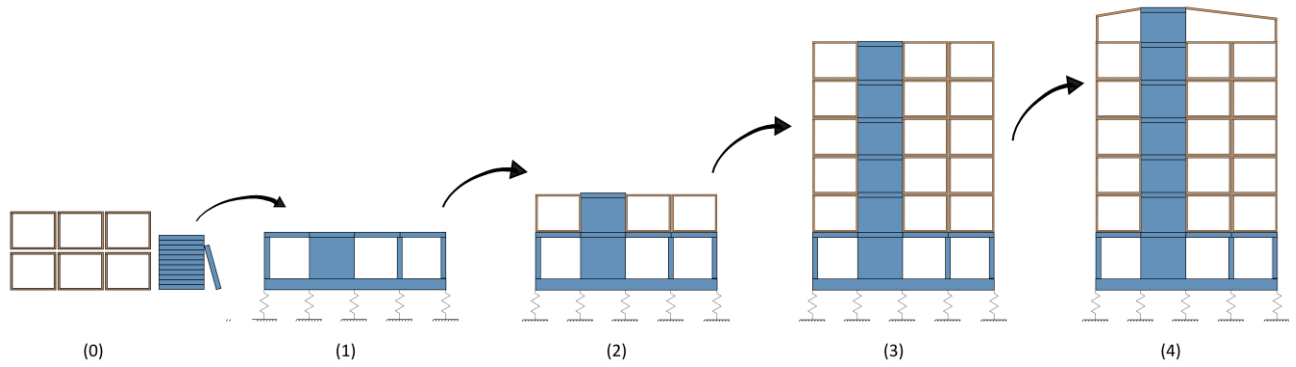


Figure 74 - Building order second method, ie. installing floor by floor.

In the case of the Buiksloterham the second method is used. In other words, the concrete core and the timber units were installed at the same time. Each week another level could be installed. The start of the construction started early 2021 at 15 January with the site preparation. At this time the preliminary design was already finished and the final design was nearly completed. The timber production at the factory started at 10 May 2021, just shy of 4 months before installing the units. The ground floor and foundation were finished approximately mid-September and the week after at 13 September the concrete core and timber units were installed in a weekly cycle, see Table 15. Using this method all six floors were installed within 9 weeks.

Table 15 - Weekly cycle for placing each floor.

Activity	day
Placing scaffolding	1,2
Measuring anchors timber modules	3
Placing timber modules	4
Placing concrete core	5
Placing stairwell, landing and façade.	6
Finishing concrete and façade.	7

4.12.1.1 Deformation during construction

It is possible to reduce vertical deformation during the construction phase. During construction when one unit is stacked on another unit, the load from the top unit causes elastic and creep strain deformation in the unit below it. By increasing the height of the top unit to the required level these strains can be mitigated. This could be done by means of filler material or set anchors. The principle is shown in Figure 75.

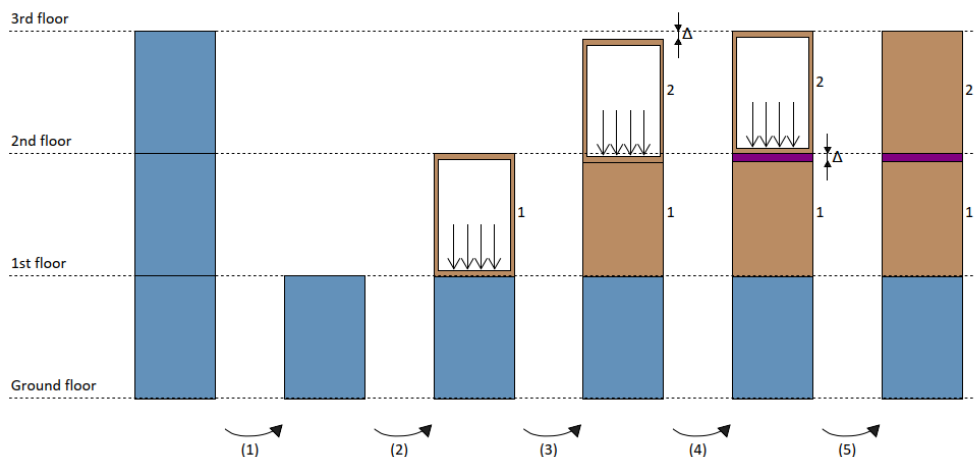


Figure 75 - Mitigation of elastic and creep deformation during the construction stage.

- (1) Placing and installing ground floor.
- (2) Placing and connecting unit number 1. Due to the distribution of the load the amount of deformation is negligible. After connecting, no vertical deformation can be mitigated anymore.
- (3) Placing unit 2. Unit 1 experiences loading from unit 2 and will therefore deform an amount delta.
- (4) The deformation delta can be mitigated by increasing the height of unit 2.
- (5) Unit 2 is now connected and no deformation can be mitigated in this connection anymore.

It can be observed that the amount deformation that could be mitigated within a certain level is due to the weight added within that same level. Up until the moment that the connection in a level is connected, the deformation could be mitigated. The amount of weight added however is not limited to the dead load of the unit. Additional weight could be added to the units for 'preloading' so the amount of deformation that can be mitigated gets increased.

4.12.1.2 *Comparing the two building methods*

When comparing the two building methods there are some differences worth mentioning. A choice can be made to build the core first according to method 1. Using this method allows for a more streamlined construction as the two disciplines which install the core and the timber units won't interfere with each other. This limits the amount of risk on possible delays and mistakes. Another upside of this method is that the elastic deformation in the core can be minimized. However, when building above approximately 60 meters special cranes need to be acquired to hoist all the elements.

When building according to building method 2 the construction can be sped up compared to the first method. As the next layer is installed, installations in the layers beneath can already commence. Lastly, this method also provides working platforms for the next level. This can be beneficial when building at extreme heights.

4.13 Findings

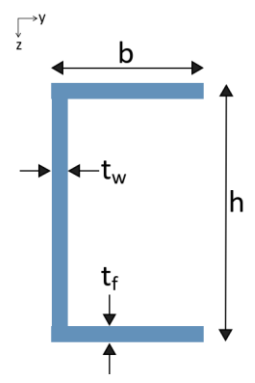
To determine the vertical deformation the following mechanisms are taken into account: Elastic strain, viscoelastic strain and strain due to a fluctuating relative humidity of the surrounding air. The total deformation is a result of a superposition of these strains.

4.13.1 Parametrics

This chapter provides an overview of all the structural elements and the properties which formed the basis for the calculations. The cross sectional properties of the core and timber elements can be found in Table 16 and Table 17 respectively. Material properties can be found in Table 18 and the properties of the applied acoustic felts can be found in Table 19.

Table 16 - Cross sectional properties concrete cores

C-shaped concrete core	
Material	Concrete
A [m ²]	1.4
b [m]	2.0
h [m]	3.4
t _w [m]	0.2
t _f [m]	0.2
I _z [m ⁴]	2.50
I _y [m ⁴]	0.55
W _z [m ³]	1.47
W _y [m ³]	0.39



I-Shaped concrete core	
A [m ²]	1.64
b [m]	2.5
h [m]	3.4
t _w [m]	0.2
t _f [m]	0.2
I _z [m ⁴]	3.01
I _y [m ⁴]	0.52
W _z [m ³]	1.77
W _y [m ³]	0.42

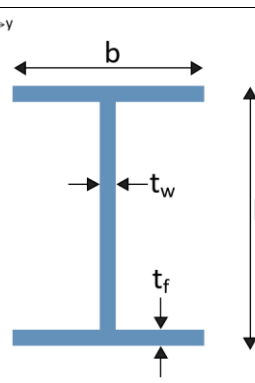
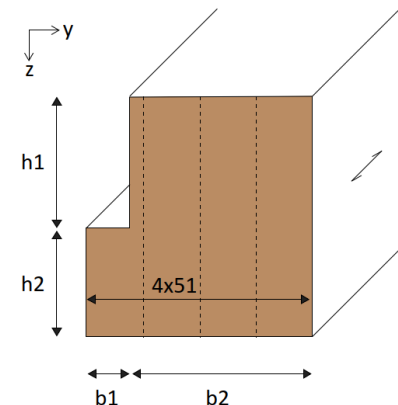
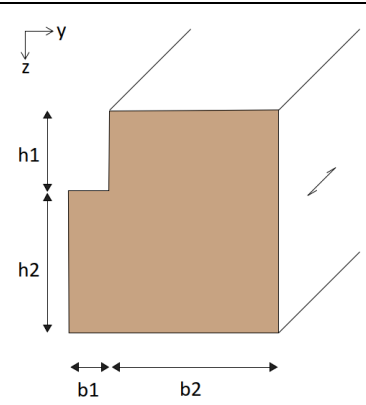


Table 17 - Cross sectional properties timber elements.

Beam floor	
Material	KERTO S
A [mm ²]	40080
b ₁ [mm]	40
b ₂ [mm]	164
h ₁ [mm]	120
h ₂ [mm]	100
I _z [·10 ⁴ mm ⁴]	16182
I _y [·10 ⁴ mm ⁴]	11886
W _z [·10 ³ mm ³]	1395
W _y [·10 ³ mm ³]	1063



Beam ceiling	
Material	GL24h
A [mm ²]	36800
b ₁ [mm]	40
b ₂ [mm]	160
h ₁ [mm]	80
h ₂ [mm]	120
I _z [$\cdot 10^4$ mm ⁴]	11910
I _y [$\cdot 10^4$ mm ⁴]	11065
W _z [$\cdot 10^3$ mm ³]	1132
W _y [$\cdot 10^3$ mm ³]	1034



Columns	
Material	GL24h
A [mm ²]	72000
b [mm]	200
h [mm]	360
I _z [$\cdot 10^4$ mm ⁴]	77760
I _y [$\cdot 10^4$ mm ⁴]	24000
W _z [$\cdot 10^3$ mm ³]	4320
W _y [$\cdot 10^3$ mm ³]	2400

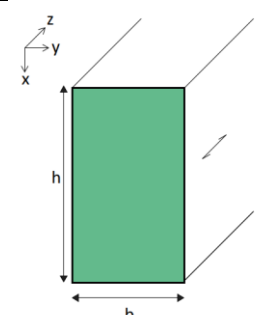


Table 18 - Material properties.

Properties	Concrete (C55/67)		KERTO S		GL24h	
Density ρ [kg/m ³]	2500		510		420	
Young's modulus [MPa]	E _{cm,t=0}	38214	E _{0,k}	11600	E _{0,mean}	11500
	E _{cm,t=30}	23059	E _{0,mean}	13800	E _{90,mean}	300
			E _{c,90,edge,k}	350		
			E _{c,90,edge,mean}	2400		
Shear modulus [MPa]	15923		G _{0,edge,k}	400	G _{mean}	650
Poisson ratio ν	0.2		-		-	
Bending str. [MPa]	-		f _{m,0,edge,k}	44.0	f _{m,0,k}	24
Compressive str. [MPa]	f _{ck}	55	f _{c,0,k}	35.0	f _{c,0,k}	24
			f _{c,90,edge,k}	6.0	f _{c,90,k}	2.5
Tensile str. [MPa]	f _{ctm}	4.21	f _{t,0,k}	35,0	f _{t,0,k}	19.2
			f _{t,90,edge,k}	0.8	f _{t,90,k}	0.5
Shear str. [MPa]	-		f _{v,90,edge,k}	4.2	f _{v,90,k}	3.5
Coefficient of linear thermal expansion α	10 x 10 ⁻⁶ °K ⁻¹		3.5 x 10 ⁻⁶ °K ⁻¹		5 x 10 ⁻⁶ °K ⁻¹ (0)	
					30-70 x 10 ⁻⁶ °K ⁻¹ (90)	

Table 19 - Acoustic felt properties.

Properties	CDM-106	CDM-105	CDM-911	CDM-910
Density ρ [kg/m ³]	810	820	835	750
Young's modulus [MPa]	17	9.2	8.16	4.57
Shear modulus [MPa]	1.93	1.15	-	-
Floors	1 st – 3 rd	4 th	5 th	6 th

4.13.2 Concrete straining

To determine the concrete straining a few parameters have to be determined. For project Buiksloterham the concrete core consists out of prefabricated concrete elements. These elements are poured and demolded within 48 hours. Although curing is possible this isn't common practice. After demolding the elements are stored and await their transport to the building site. This can take up to half a year, with an average of 10 days. The following assumptions are made to determine the time dependent properties of the elements:

- Cement class: R
- Average age at time of loading: 10 days
- Day at which curing ended: day 1

4.13.2.1 Elastic strain

The elastic strain is determined using characteristic loading factors, using the formulas provided in chapter 3.5.1. The total deformations due to elastic loads can be observed in Table 20. Due to the applied construction method described it is possible to mitigate some of the elastic deformations during the construction.

Table 20 - Elastic deformations concrete due to characteristic loads. $A = 200000 \text{ mm}^2$, $E_{cm,t=28} = 38214 \text{ N/mm}^2$.

Story	Height [m]	z [mm]	QW [kN] $\psi=0,4$	Elastic def. [mm]	Mitigation during construction [mm]	Elastic def. final [mm]
Roof	23	0	0	0	0	0
6 th	19	3000	12.7	0.005	0	0.005
5 th	16	3000	42.4	0.017	0.012	0.005
4 th	13	3000	76.9	0.030	0.012	0.019
3 rd	10	3000	108.5	0.043	0.012	0.031
2 nd	7	3000	140.1	0.055	0.012	0.043
1 st	4	3000	171.7	0.067	0.012	0.056
Total				0.217	0.058	0.159

4.13.2.2 shrinkage strain

Based on these assumptions the shrinkage and creep curve can be determined based on the formulas provided in chapters 3.5.2 and 3.5.3, see Figure 76.

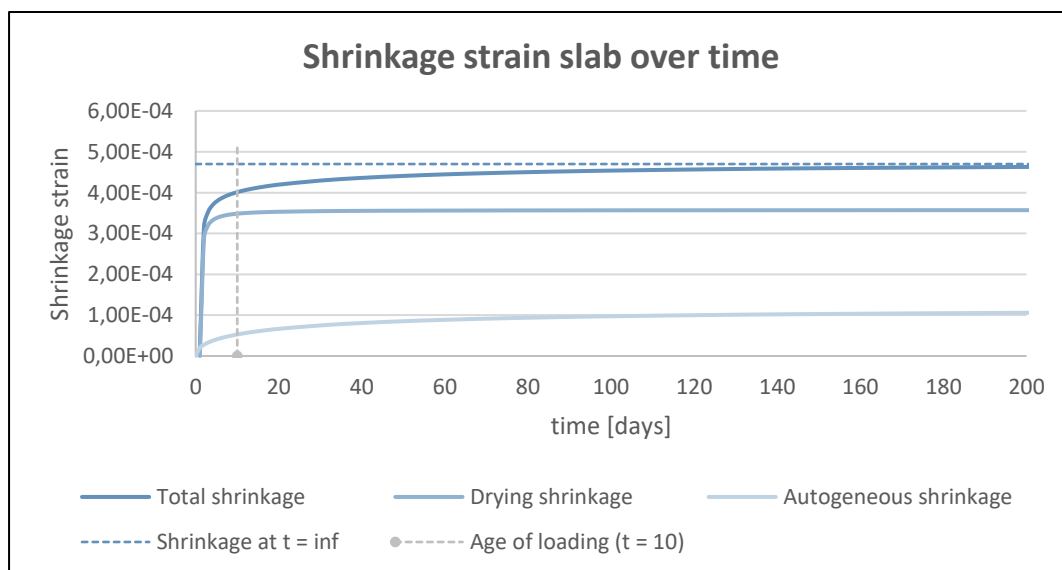


Figure 76 - Shrinkage strain of concrete, $f_{ck} = 55$, cement class R, RH 65%.

It can be observed that at day 10 approximately 85% of the total shrinkage already took place. It can also be observed that the final shrinkage strain is approximately $4.70 \cdot 10^{-4}$. The remaining strain which still has to take place can be observed in Table 21.

Table 21 - Shrinkage deformations concrete. $A = 200000 \text{ mm}^2$, $\epsilon_{sh} = 0.00047$.

Story	Height [m]	z[mm]	Shrinkage deformations [mm]	Mitigated during construction [mm]	Shrinkage def. final [mm]
Roof	23	0	0	0	0
6 th	19	3000	1.41	1.20	0.206
5 th	16	3000	1.41	1.27	0.139
4 th	13	3000	1.41	1.29	0.119
3 rd	10	3000	1.41	1.30	0.106
2 nd	7	3000	1.41	1.32	0.094
1 st	4	3000	1.41	1.33	0.085
Total			8.46	7.71	0.749

4.13.2.3 Creep factor

According to the Eurocode the creep factor can be linearly determined when the stresses are less than 45% of the design stress, which is the case. The notional creep factor is determined using quasi-permanent loading factors.

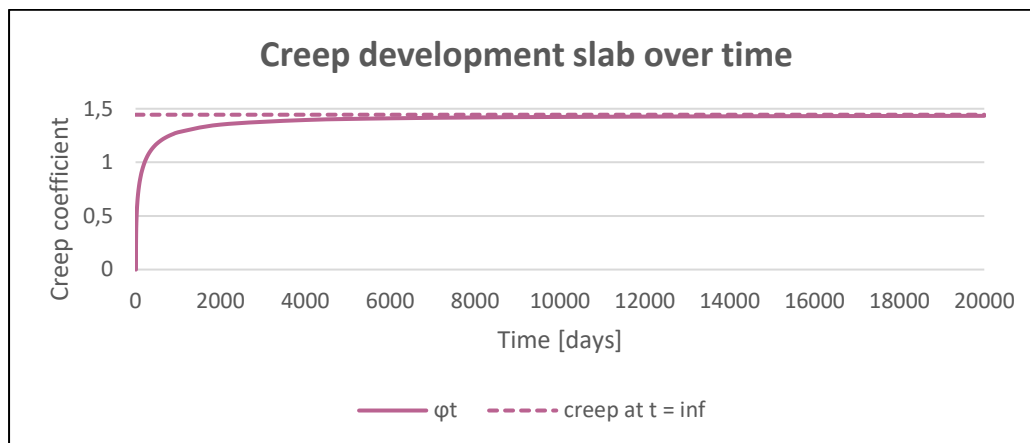


Figure 77 - Creep development over time.

It can be observed that the final creep will be reached after a much longer period than for the shrinkage. The notional creep factor according to the Eurocode is 1.44. The corresponding creep deformations can be found in Table 22.

Table 22 - Creep deformations concrete. $A = 200000 \text{ mm}^2$, $E_{c,t=28} = 40125 \text{ N/mm}^2$.

Story	Height [m]	z[mm]	QW [kN] $\psi=0,3$	Creep deformations [mm]	Mitigated during construction [mm]	Final creep def. [mm]
Roof	23	0	0	0	0	0
6 th	19	3000	12.7	0.007	0	0.007
5 th	16	3000	42.4	0.023	0.004	0.018
4 th	13	3000	76.9	0.042	0.004	0.037
3 rd	10	3000	108	0.058	0.004	0.054
2 nd	7	3000	139	0.075	0.004	0.071
1 st	4	3000	170	0.092	0	0.092
Total				0.272	0.016	0.256

4.13.2.4 Total deformations

The total deformation of the concrete in the concrete due to the elastic and time dependent properties can be found in Figure 78.

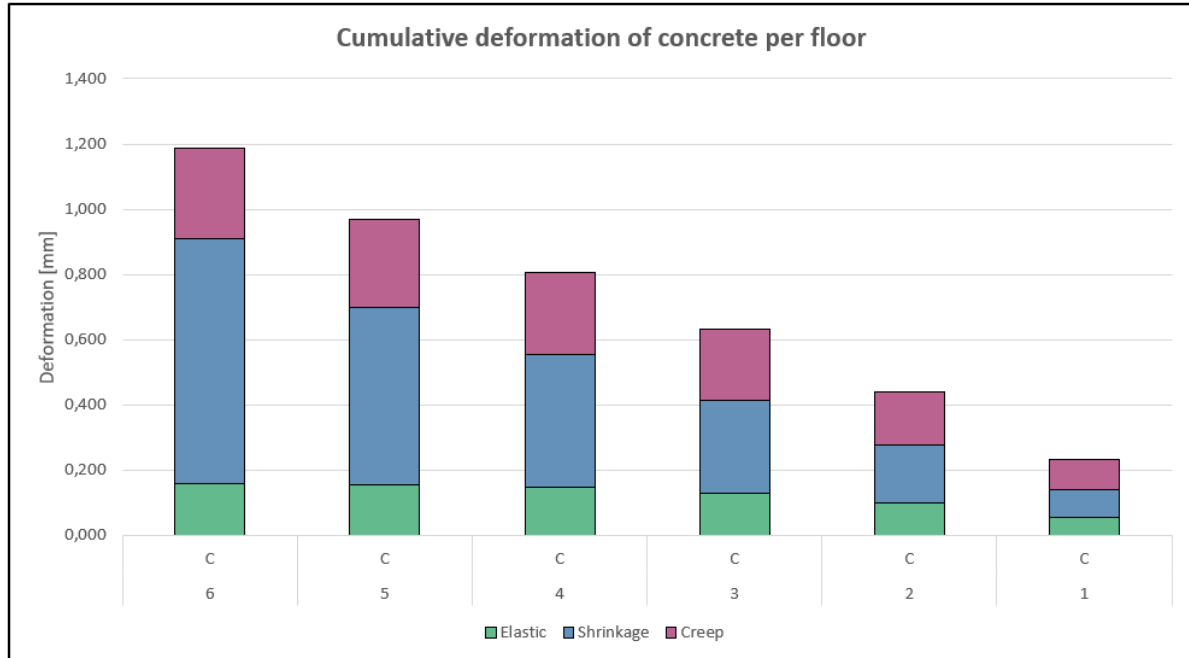


Figure 78 - Total deformation concrete core including correction due to construction.

4.13.3 Timber straining

The deformation of the timber modules consists of three separate parts namely the columns, beams and acoustic felt. Each of these components are subjected to elastic and time dependent straining which cause deformations. The timber columns are loaded parallel and the beams perpendicular to the fiber.

4.13.3.1 Elastic straining

The elastic deformations are calculated using the formulas provided in 2.4.1. For all components has the mean young's modulus been used. To determine the stress in the LVL beams the area has been adjusted according to the NEN-EN 1995-1-1:2005 eq. 6.4 which states that the effective pressure area may be extended by 30mm on each side to take into account the continues beam effect. Table 23 provides an overview of the elastic deformations for all components.

Table 23 - Elastic deformations timber elements and acoustic felt due to characteristic loads.

Story	Height [m]	FC [kN] $\psi=0,4$	column [mm]	Beam [mm]	Acoustic felt [mm]
Roof	23	0	0	0	0
6th	19	23	0.08	0.03	1.09
5th	16	61	0.21	0.07	1.56
4th	13	108	0.37	0.12	2.44
3rd	10	142	0.49	0.15	1.73
2nd	7	176	0.60	0.19	2.14
1st	4	209	0.71	0.23	2.55
Total			2.47	0.78	11.51

During the construction however it is possible to reduce the elastic deformations. These deformations are due to the dead loads as described in 4.12. The elastic deformations which can be accounted for during construction can be found in Table 24.

Table 24 - Elastic deformations that can be accounted for during construction.

Story	Height [m]	FC [kN] $\psi=0,4$	column [mm]	Beam [mm]	Acoustic felt [mm]
Roof	23	0	0	0	0
6th	19	23	0	0	0
5th	16	61	0.08	0.03	0.62
4th	13	108	0.08	0.03	0.55
3rd	10	142	0.08	0.03	0.30
2nd	7	176	0.08	0.03	0.30
1st	4	209	0.08	0.03	0.30
Total			0.42	0.13	2.05

It can be observed that the total elastic deformation can be mitigated by a small amount during construction. It can also be observed that the main elastic deformation is due to the acoustic felt.

4.13.3.2 Shrinkage straining

Timber is extremely susceptible to moisture uptake. To prevent large fluctuations within the structural timber, manufacturers try to get the MC as close to the final MC after construction. The timber however still has to be transported to the construction site and therefore is able to increase a little in moisture content. According to findings presented in chapter 2.4.3.4 it is assumed that timber approximately gains 0.2% in MC during transportation and storage on the construction site. This is under the assumption that the modules are covered and stored at a dry location. After installment however the timber units are not covered anymore and are thus subjected to outdoor environmental elements. With the construction cycle during approximately 42 days the internal moisture content of the wood increases approximately by 1% for the timber beams and 2.6% for the timber columns. After installing the equilibrium moisture content of the timber will drop to an average of 9.27% (corresponding to a RH of 50% and a temperature of 20 degrees) with a variation of 8 to 10% throughout the year.

The shrinkage values are calculated based on the formulas presented in chapter 2.4.3. The following input parameters have been used:

- Production MC Glulam column 12%
- Production MC LVL beam 10%
- Average time stored at the construction site 2 month (+0.2%)
- MC Glulam column after construction 14.58%
- MC LVL beam after construction 10.91%
- MC after completion 9.27%

- Longitudinal shrinkage coefficient glulam 0.011
- Perpendicular shrinkage coefficient LVL 0.32

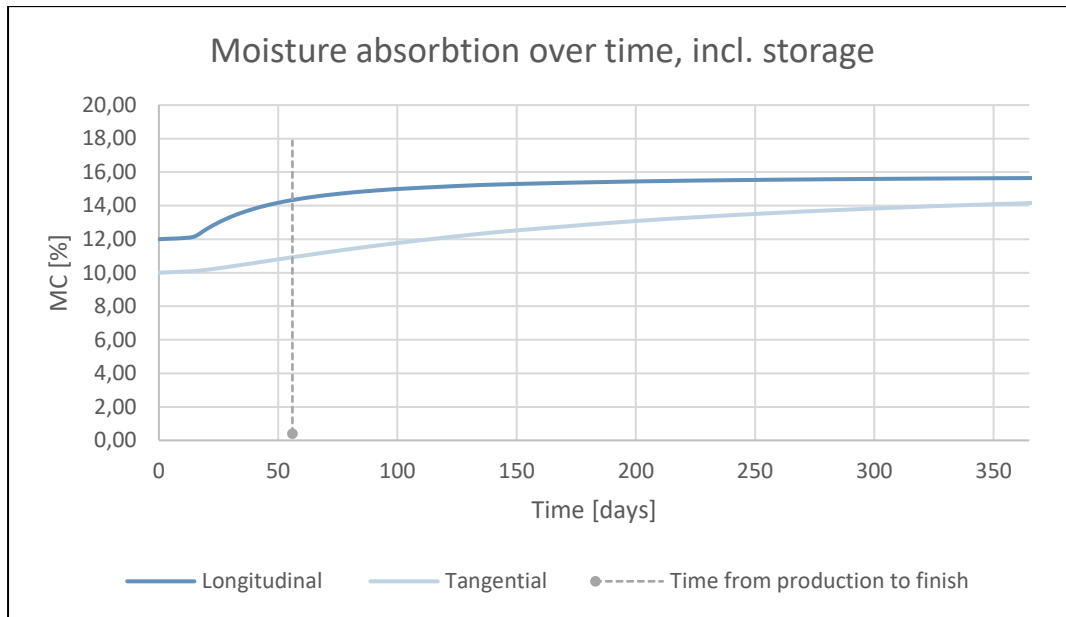


Figure 79 - Moisture absorption in tangential and longitudinal direction during storage and construction.

Based on the parameters provided above the shrinkage deformations according to Table 25 can be expected. The acoustic felt is not susceptible to shrinkage or swelling.

Table 25 - Shrinkage deformations timber columns and beams.

Story	Height [m]	FC [kN] $\psi=0,4$	column [mm]	Beam [mm]
Roof	23	0	0	0
6th	19	23	0.90	0.58
5th	16	61	0.90	0.58
4th	13	108	0.90	0.58
3rd	10	142	0.90	0.58
2nd	7	176	0.90	0.58
1st	4	209	0.90	0.58
Total			5.41	3.48

4.13.3.3 Timber creep

According to the Eurocode the amount of creep is determined by modifying the elastic deformation using quasi permanent loads and the modification factor k_{def} . This factor is dependent on the service class of the timber, which is class 1 for this project. Creep development of the fiber elements over time is determined according to chapter 2.4.2.2.

The expected creep of the acoustic felt is approximately 12% of the elastic deformation according to specifications provided by the supplier. The expected creep development curve can be seen in Figure 80 and the expected creep deformations can be observed in Table 26.

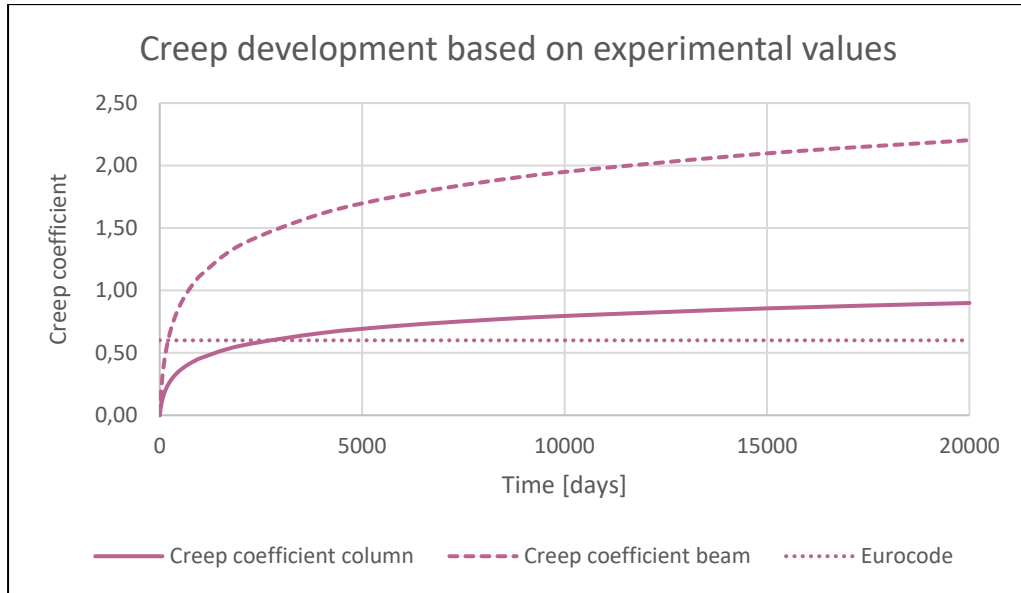


Figure 80 – Timber creep development curve over time based on experimental work and the EC 5.

Table 26 - Creep deformations timber elements based on quasi permanent loads and experimental development.

Story	Height [m]	FC $\psi=0,3$ [kN]	column [mm]	Beam [mm]	Acoustic felt [mm]
Roof	23	0	0	0	0
6th	19	23	0.07	0.12	0.14
5th	16	61	0.19	0.30	0.20
4th	13	108	0.33	0.53	0.31
3rd	10	140	0.43	0.68	0.21
2nd	7	171	0.53	0.83	0.26
1st	4	203	0.62	0.99	0.31
Total			2.17	3.45	1.42

During construction it is possible to mitigate some of the creep early on in the process. The amount of creep deformation that can be mitigated for each floor can be found in Table 27

Table 27 - Creep deformation mitigation timber modules during construction.

Story	Height [m]	FC $\psi=0,3$ [kN]	column [mm]	Beam [mm]	Acoustic felt [mm]
Roof	23	0	0	0	0
6th	19	23	0	0	0
5th	16	61	0.002	0.003	0.035
4th	13	108	0.002	0.003	0.030
3rd	10	140	0.002	0.003	0.020
2nd	7	171	0.002	0.003	0.020
1st	4	203	0.002	0.003	0.020
Total			0.007	0.014	0.12

4.13.3.4 Total deformations

The total deformation of the concrete in the timber elements and acoustic felt due to the elastic and time dependent properties can be found in Figure 81. Depending on the model applied, the creep contribution varies. This can be observed in Figure 81 and Figure 82.

Cumulative deformation of timber per floor based on a time dependent creep factor

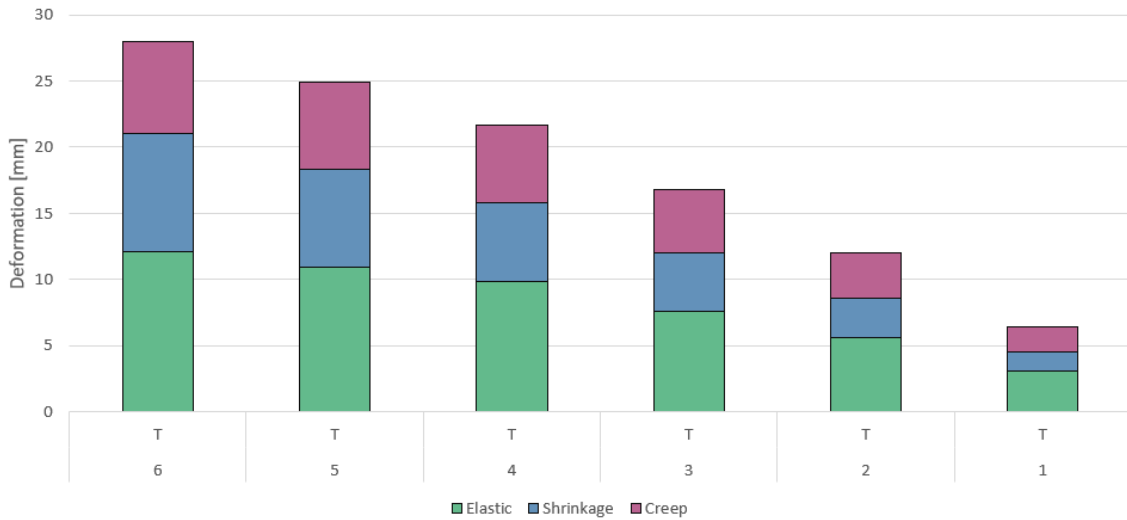


Figure 81 - Total timber deformations for each level, based on experimental values.

Cumulative deformation of timber per floor based on a creep factor of 0.6

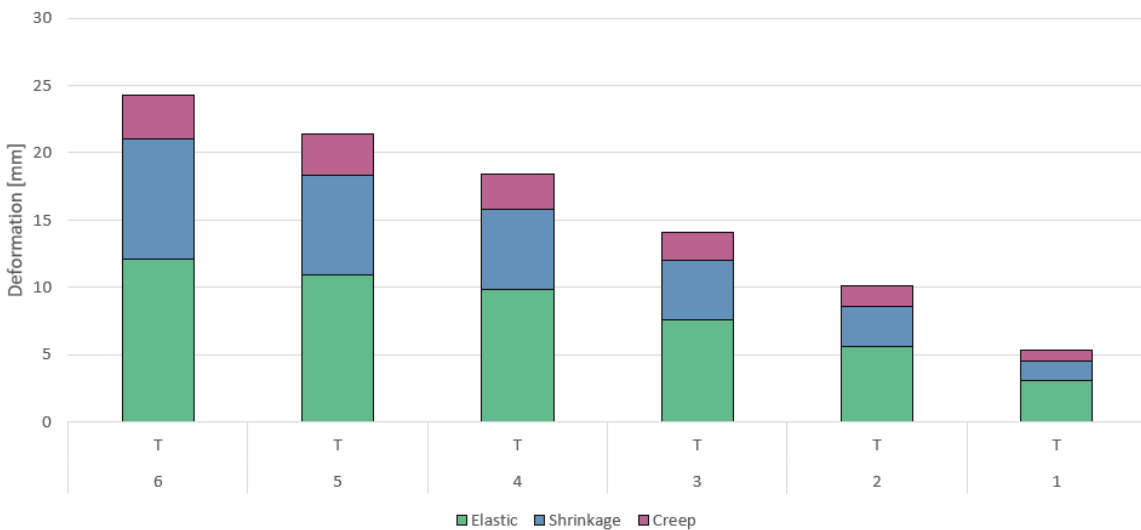


Figure 82 - Total timber deformations for each level, based on creep calculations according to the Eurocode.

4.14 Sub-conclusion

4.14.1 Experimental model – upper bound limit

When applying the system described, ie. prefabricated timber modules with prefabricated concrete columns, large differences between the two can be observed, see Figure 83. The basis for the calculations of these differences are mainly based on the Eurocode. The absorption rate of the timber elements are based on experimental values, as is the time based factor of the timber creep. The calculations include the rotational stiffness of the foundation, construction order, choice of materials and time (in)dependent behavior.

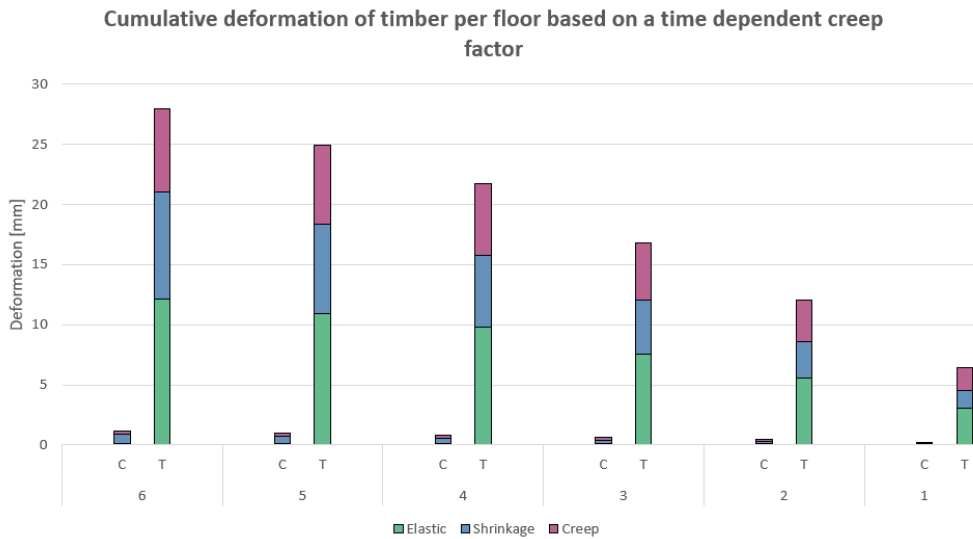


Figure 83 - Deformation of concrete and timber per floor with creep experimentally determined.

The vertical shortening of the timber units is largely determined by elastic and shrinkage deformation. Unlike shrinkage and elastic deformation, creep cannot be addressed in the production process or building order.

The vertical shortening of the timber modules is determined by three separate components, namely the timber columns and beams and the acoustic felt. Out of the three components the timber sections are responsible for approximately 59% of the total deformation, see Figure 84. The shortening is largely determined by creep, with its main benefactor being creep due to loading perpendicular to the fiber in the beam. Unlike shrinkage and elastic deformation, creep cannot be addressed in the production process or building order.

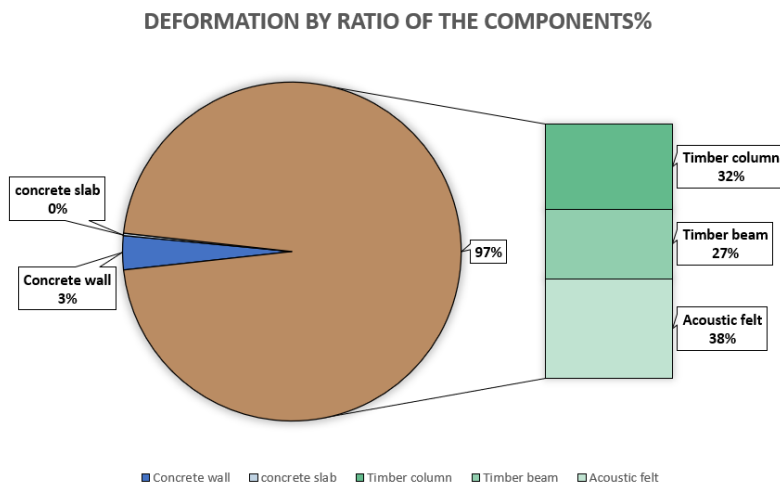


Figure 84 - Contribution of each element to the total deformation.

4.14.2 Eurocode model – lower bound limit

A different scenario occurs when the Eurocode model is used for determining the deflections. Within this model all the calculations are the same as in the experimental model except the creep development. The Eurocode does not provide a way to describe the time dependent behavior of creep and only describes the final creep coefficient. Unlike the experimental model however, there is no distinction between loading parallel and perpendicular to the fiber. When the same system is considered the deformations are therefore substantially lower in comparison with the experimental model, see Figure 85.

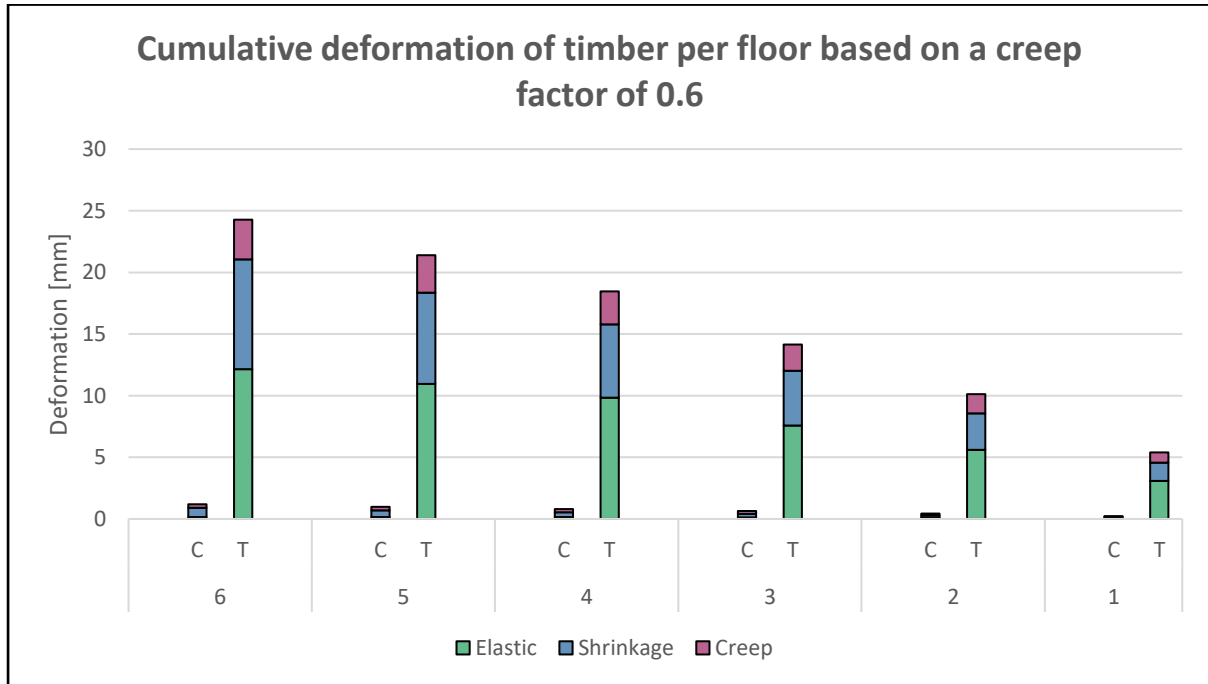


Figure 85 - Deformation of concrete and timber per floor with creep according to the Eurocode.

It can be observed that the total deformation is much less than when the experimental model is applied. The main contributor to the vertical shortening is the shrinkage of the timber column and beam. It can also be observed that the contribution of the beam to the total shortening is much less (see Figure 86) compared to the experimental model.

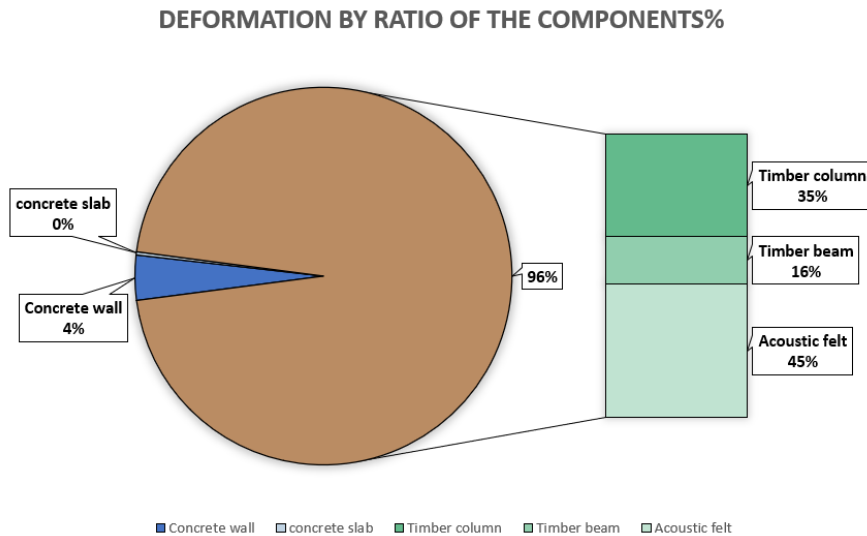
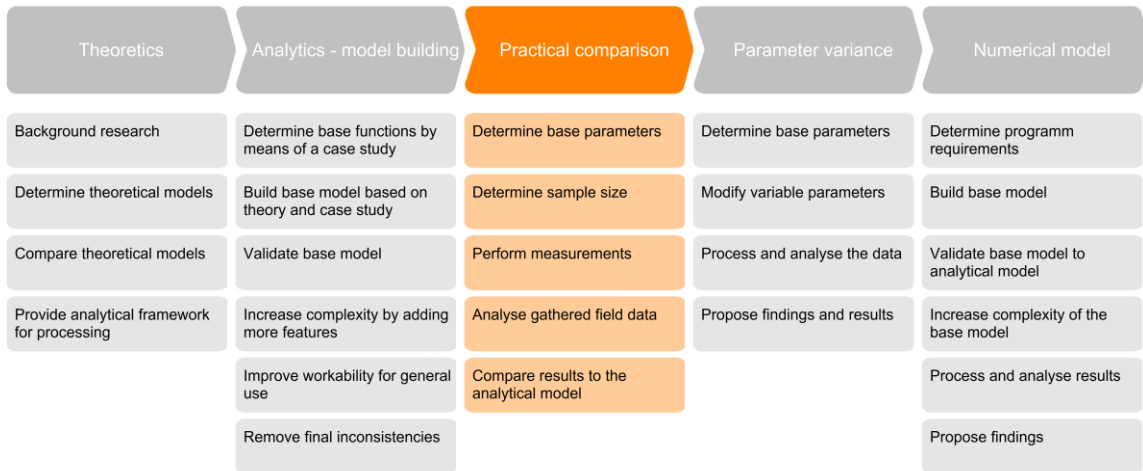


Figure 86 - Contribution of each element to the total deformation.

5 Comparison - practical moisture measures versus theoretical model



5.1 Introduction

As part of this research, moisture measurements were taken to validate and compare the theoretical model to practical values. At the time of writing, similar units to the one used in Buiksloterham are being installed in a project in Alkmaar. With this project a unique opportunity arose to do moisture measurements both at the factory in Enschede and at the construction site in Alkmaar.

In a span of 20 weeks a total of 260 modules are being produced and installed, resulting in approximately 130 apartments. Unlike in Buiksloterham, one side of the module is fitted with a CLT wall instead of columns. The other side however consists of an identical column-beam structure. The columns and beam contain the same dimensions and properties as used in the units in Buiksloterham, making them ideal for testing. The layout of the modules can be seen in Figure 87. The properties of the columns and beams can be found in Table 28.

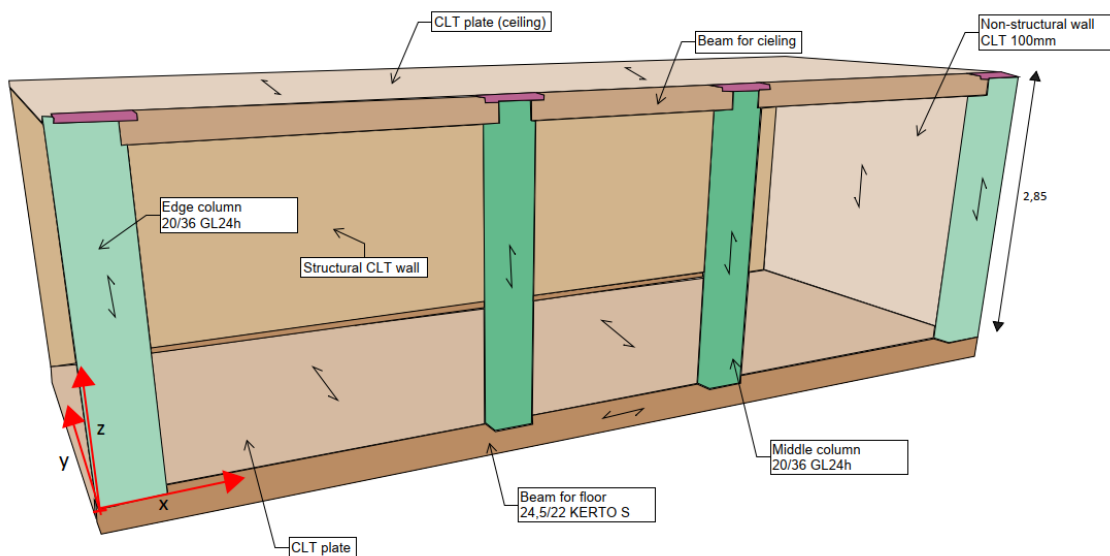
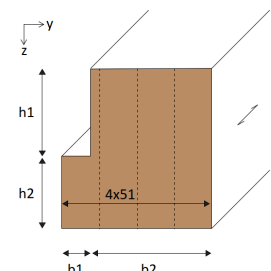
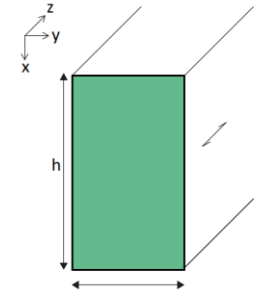


Figure 87 – Timber prefab modules layout.

Table 28 - Properties columns and floor beam.

Beam floor		
Material	KERTO S	
A [mm ²]	40080	
b ₁ [mm]	40	
b ₂ [mm]	164	
h ₁ [mm]	120	
h ₂ [mm]	100	
Density [kg/m ³]	510	
Columns		
Material	GL24h	
A [mm ²]	72000	
b [mm]	200	
h [mm]	360	
I _z [$\cdot 10^4$ mm ⁴]	77760	
I _y [$\cdot 10^4$ mm ⁴]	24000	
Density [kg/m ³]	500	

5.2 Measuring methods

Two measurement methods were available to approximate the moisture content of the columns and beams. These measurement methods make use of the FMD and FMW-T equipment by Brookhuis. Both measurements techniques are described in the following chapters.

5.2.1 FMD

Perhaps the more traditional method of approximating the moisture content in a timber element is by using the FMD moisture detector, see Figure 88. This method measures the moisture content by placing two electrodes in the material, up to a depth of 40mm, through which an electrical current is sent and the resistance is measured. The detector has several calibration lines for a numerous amount of wood species.



Figure 88 - FMD Moisture meter by Brookhuis. [57]

The moisture detector has the following specifications according to the supplier.

Measuring range	5 ~ 99%
Measuring accuracy	0,2%
Measuring depth	0 – 40mm
Operating temperature range	0 ~ 50 °C
Amount calibration lines	Approximately 450 species
Calibration	Adjustment period to surrounding climate is approx. 10 minutes.

The following settings can be specified before measuring.

- Temperature input
- Wood species and calibration lines
- Calibrate setting
- Allows for multiple measurements which the average is taken of.

5.2.2 FMW-T

The FMW-T is a wireless moisture meter which uses an electromagnetic arc to determine the resistance of the specimen. By assigning a density to the material, the moisture content is determined. Being wireless allows for measurements in exposed timber areas which cannot be damaged. The results are shown within half a second which allows for a large amount of measurements within a short period of time. Unlike the FMD however there are no calibration lines present and the results solely rely on the set density. Because of the variation density within the timber due to several factors including pressure and tension wood and more, this device is slightly less accurate than the FMD meter.



Figure 89 - FMW-T moisture meter by Brookhuis. [58]

The moisture detector has the following specifications according to the supplier.

Measuring range	2 ~ 30%
Measuring accuracy	0,5%
Operating temperature range	0 ~ 50 °C
Measuring depth	25mm (non-adjustable)
Calibration	Adjustment period to surrounding climate is approx. 10 minutes. After which the RH base is set after starting.
Amount of measurements the	At least 10 measurements must be made to comply with the
	measuring accuracy of 0,5%.

The following settings can be specified before measuring

- Temperature adjustment
- Set density
- Specimen depth (max is 20mm)
- Ability to show max or average values

5.3 Production assembly location Enschede

The timber elements ie. the walls, columns and floors are produced in Austria and assembled at the factory of The Groot Vroomshoop in Enschede. At the time of arrival the prefab elements are approximately a week old. During transit from Austria to Enschede the elements are wrapped in plastic to protect it from environmental influences. After arrival the plastic is removed and the elements are assembled in a production hall. Within 6 days a unit is assembled, electricity wiring and isolation is fitted and EPDM is applied to the roof after which the units are sealed in plastic again and are ready for storage. The units are stored for a maximum of 10 days before being transported to the construction site.



Figure 90 - Units wrapped in plastic and getting ready for storage and transport.

The assembly line has 18 separate stations and allows for 3 units to be completed per day. The assembly hall is a large warehouse like hall with an open front end and 3 closed sides. It could be stated that the indoor climate conditions in the hall are closely related to the outside climatic conditions in terms of relative humidity and temperature. Due to only one side being open the wind is not free to roam which is beneficial to prevent excessive surface drying of the timber.

5.4 Project location

After production the covered units are stored in outside weather conditions for approximately two weeks. During these two weeks the units are transferred from the production location in Enschede to the building site in Alkmaar, see Figure 91.

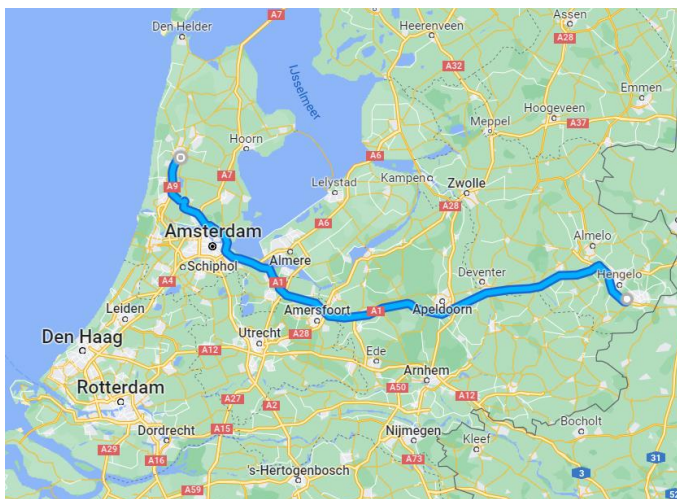


Figure 91 - Transit from production to building site, Enschede to Alkmaar respectively.

On site the plastic protection layer is removed and the units are directly installed. At this stage, the units are exposed to outdoor environmental conditions. Approximately 3 units are installed daily. After instalment the timber in the units is much less exposed as only the outsides are not properly covered. The outsides are fitted with a layer that provides limited protection against direct rainwater contact, see Figure 92.



Figure 92 - On site installed units in Alkmaar.

Approximately 4 weeks after the units are placed and prepared, a cement screed is fitted in the units to provide a nice finish see Figure 93. However, with the placement of the screed the relative humidity inside the units noticeably increases. For this reason, the measurements done after the cement screed has been placed will proved a new 'baseline' for the drying process.



Figure 93 - Units before and after the cement screed is placed, left to right respectively.

The increase of moisture content does not impact the vertical differential between the concrete columns and the timber units because at the time of casting all levels are already installed. This means that the timber modules will increase in height as a whole but will also decrease to the original position at time of instalment and will likely decrease from that point onward.

5.5 Measurement setup

Initially, measurements would be taken using both the FMD and FMW-T meters. When on site however, the non-exposed timber was unreachable and the FMD therefore could not be used. In addition, the floor beams were also unreachable so only the columns were measured. For this reason, only the FMW-T provided enough data for reliable results.

Each unit contains 4 columns. For each of the four columns 6 measurements were done at specific heights of 20, 50, 100, 150, 200 and 250cm measured from the bottom of the column, see Figure 94. With 24 measurements per unit and 28 tested units a total of 672 measurements were done. See Table 29 and Table 30 for project specific conditions and Table 31 for the FMW-T measurement settings.

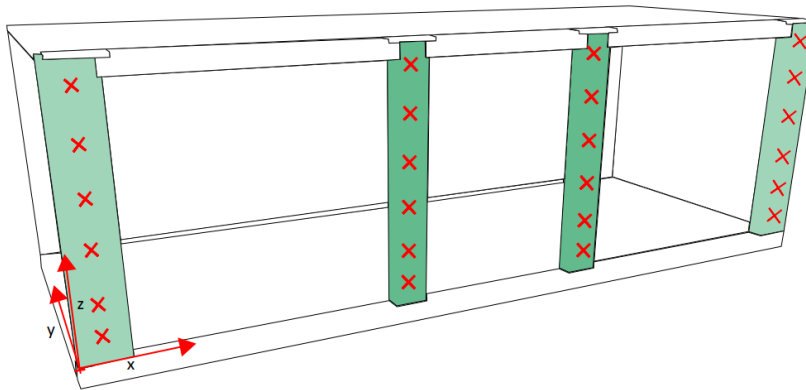


Figure 94 - Measurement locations.

Table 29 - Project specifics per location

Assembly	
Location	Marssteden 20 7547 TC Enschede
Measuring dates	11-07-2022 (results not shown) 18-11-2022
Outside temperature	23 °C
Outside relative humidity	78%
Units	1-14

Construction site	
Location	Koelmalaan 310 1813 JE Alkmaar
Measuring dates	14-07-2022
Outside temperature	18 °C
Outside relative humidity	69%
Units	15-28

Table 30 - Age of the units and concrete screed.

Unit	Age [weeks]	Production week	Concrete screed	Screed age
1-14	0	29	No	N/A
15-18	2	26		
19-21	4	24	Yes	1
22-23	8	20		5
24-25	12	16		8
26-28	14	14		10

Table 31 - FMW-T meter settings (uniform for all locations)

FMW-T settings	
Density ρ [g/m ³]	0,5
Thickness [mm]	20 (max)
Measuring method	PH0 (average values)

5.5.1 Metrological data

It is imperative to take into account the metrological data during production and instalment of the units. Because of limited data from within Alkmaar at this period, the climatological data from Wijk aan zee has been provided instead. The following climatic conditions were present, according to the KNMI. [59] See Figure 95 for the daily temperature, Figure 96 for the daily relative humidity and Figure 97 for the daily rainfall. For weekly values corresponding to the time of instalment of the units see Table 32.

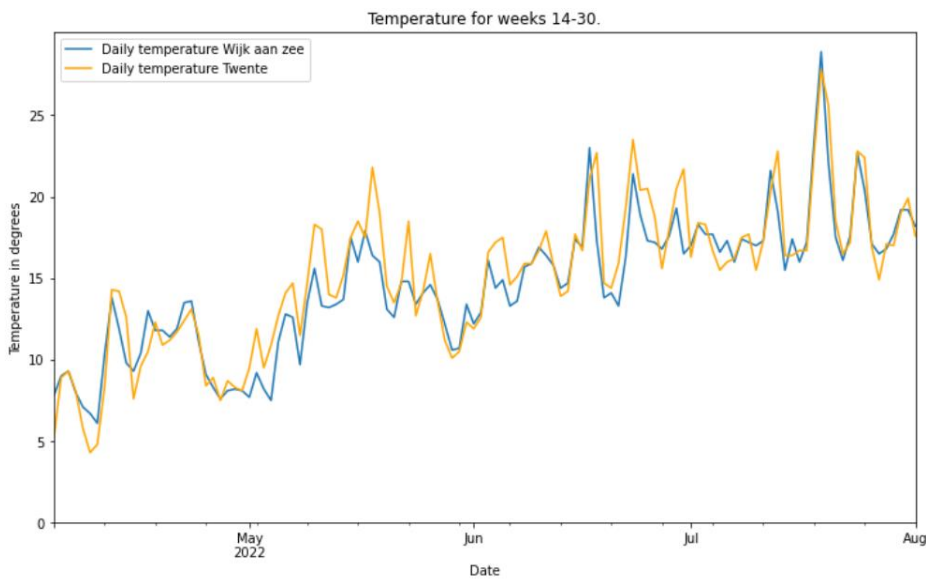


Figure 95 - Daily temperature weeks 14-30 Wijk aan zee and Twente according to KNMI.

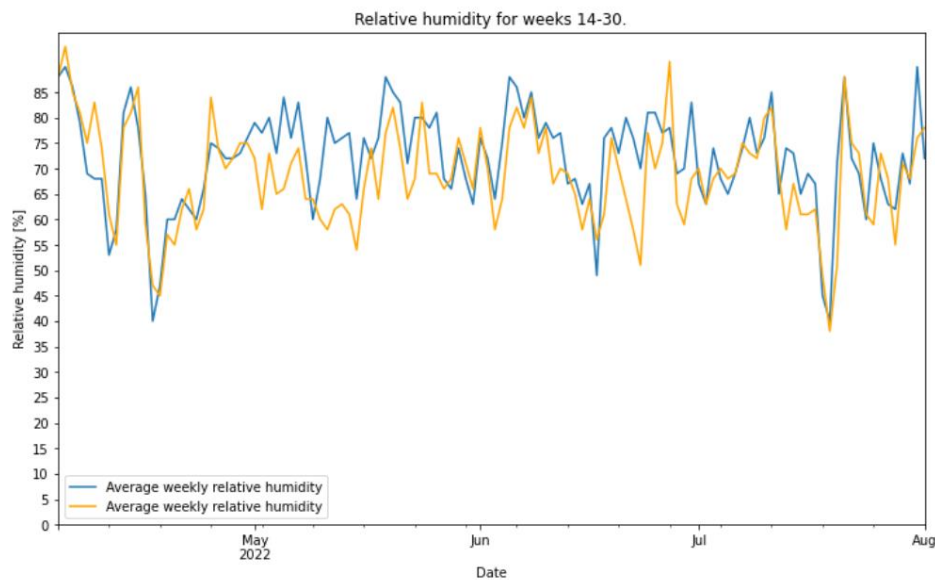


Figure 96 - Daily relative humidity weeks 14-30 Wijk aan zee and Twente according to KNMI.

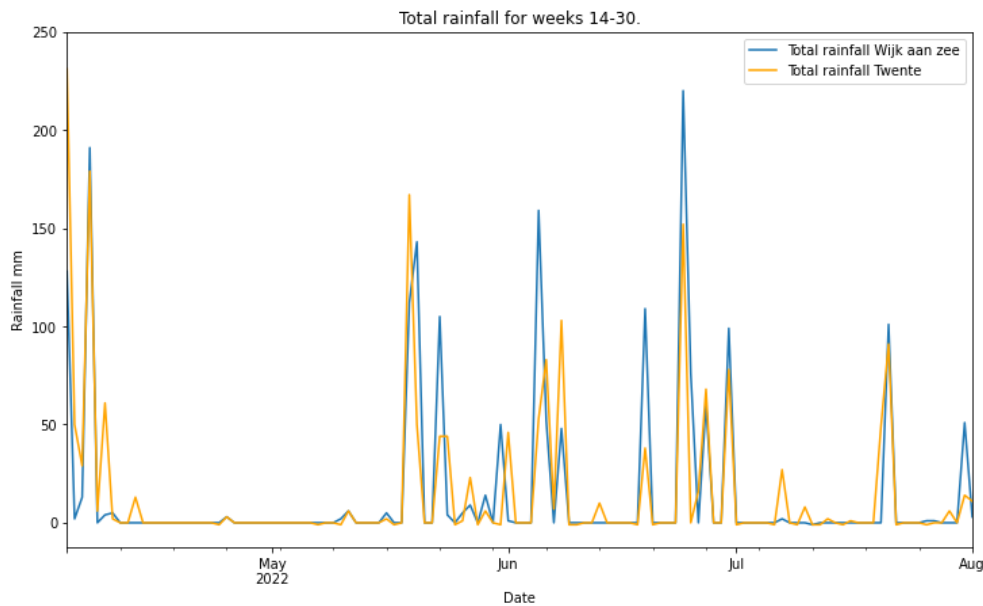


Figure 97 - Daily rainfall weeks 14-30 Wijk aan zee and Twente according to KNMI.

Table 32 - Metrological data during instalment of the units.

Unit	Production week	Instalment week	Temperature °C	RH [%]	Rainfall [mm]
1-14	29	31	18,2	72,0	3
15-18	26	28	17,7	71,1	0
19-21	24	26	17,6	72,0	159
22-23	20	22	13,5	72,3	210
24-25	16	18	10,2	77,9	0
26-28	14	16	12,5	59,9	0

5.6 Results

The results can be distinguished into two phases. The first phase is defined as the period from the assembly to first installment after two weeks. The second phase is defined as the period directly after casting. This way two comparisons can be made, the evolution of the MC during production and transit and the evolution of drying after the screed has been applied.

5.6.1 MC during production and transit

In total 336 measurements are were taken at the factory and 96 two weeks after at the building site. The following results were obtained:

Table 33 - Results for phase 1

Units	Age	Mean MC	Standard deviation
1-14	0 weeks (assembly)	10,48	0,87
15-18	2 weeks (after transit)	10,14	0,72

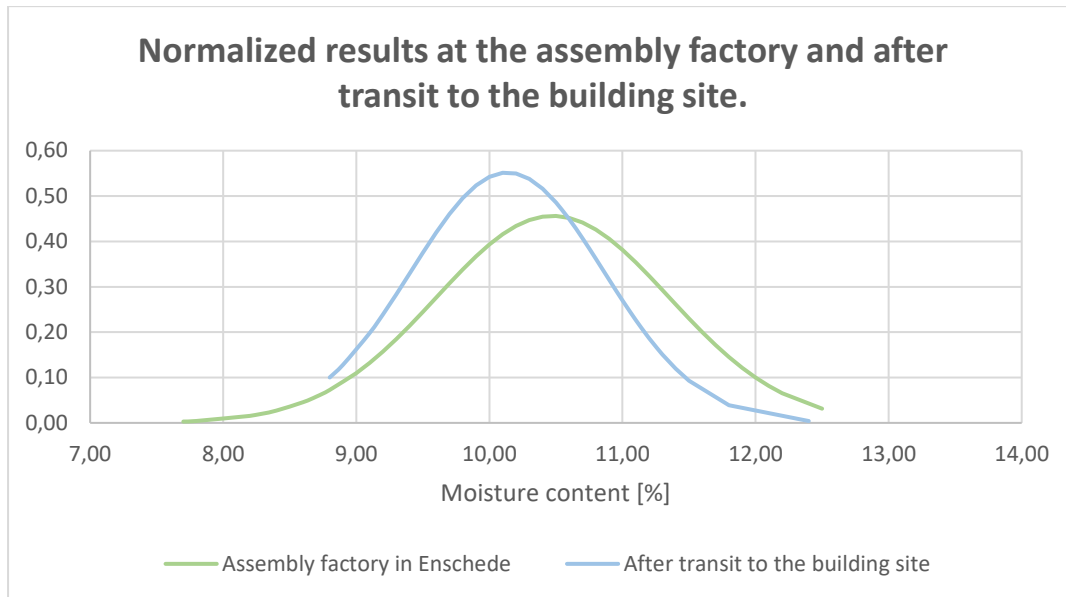


Figure 98 - Normalized results of the measurements at the assembly factory and after transit.

It can be observed that the average moisture content of the columns in the assembly factory contains a relatively large spread. It can also be observed that the moisture content is below the 12% requirement for approximately 95%.

It can also be observed that the moisture content is lower after transit to the building site. There are no large climatological abnormalities at this time. Little to no rainfall was present and the relative humidity and temperature differ only slightly.

5.6.2 MC after the casting of the screed

4 weeks after installment the screed was casted. Since the drying evolution of the units cannot be measured based on the baseline provided during assembly and transit a new baseline is provided after the screed has been placed. The following results have been obtained:

Table 34 - Results for phase 2

Units	Age after casting	Mean MC	Standard deviation
19-21	1 week	12,32	1,03
22-23	4 weeks	11,66	0,63
24-25	8 weeks	10,76	0,71
26-28	10 weeks	10,42	0,76

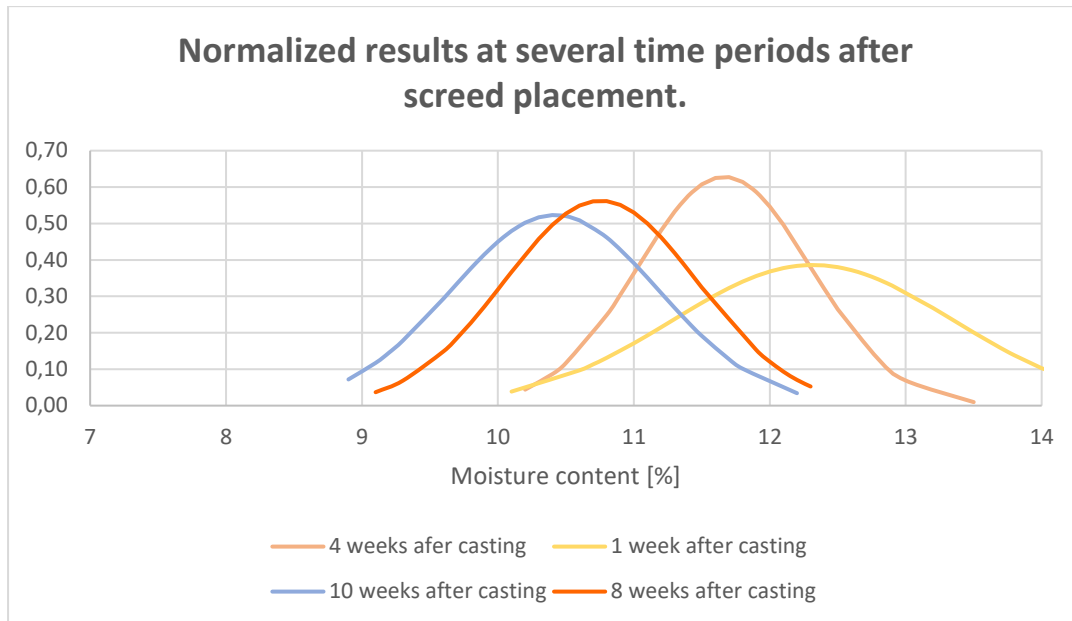


Figure 99 - Normalized results of the measurements after screed placement.

It can be observed that within the first week after casting the moisture content has increased by approximately 2,2% compared to directly before casting. There is however a large spread noticeable with a standard deviation of 1,03%.

It can also be observed that there is a downward trend from the time of casting onward. This is to be expected as over time the relative humidity in the units will drop after casting and the moisture content in the timber will follow the same trend. After approximately 10 weeks the moisture content is approximately back to the original MC measured before casting.

5.6.3 Model versus measurements

Because of the increase in moisture content after pouring the screed it is not possible to monitor the MC from production to finish. It is however possible to observe the shrinkage of the timber from this point forward.

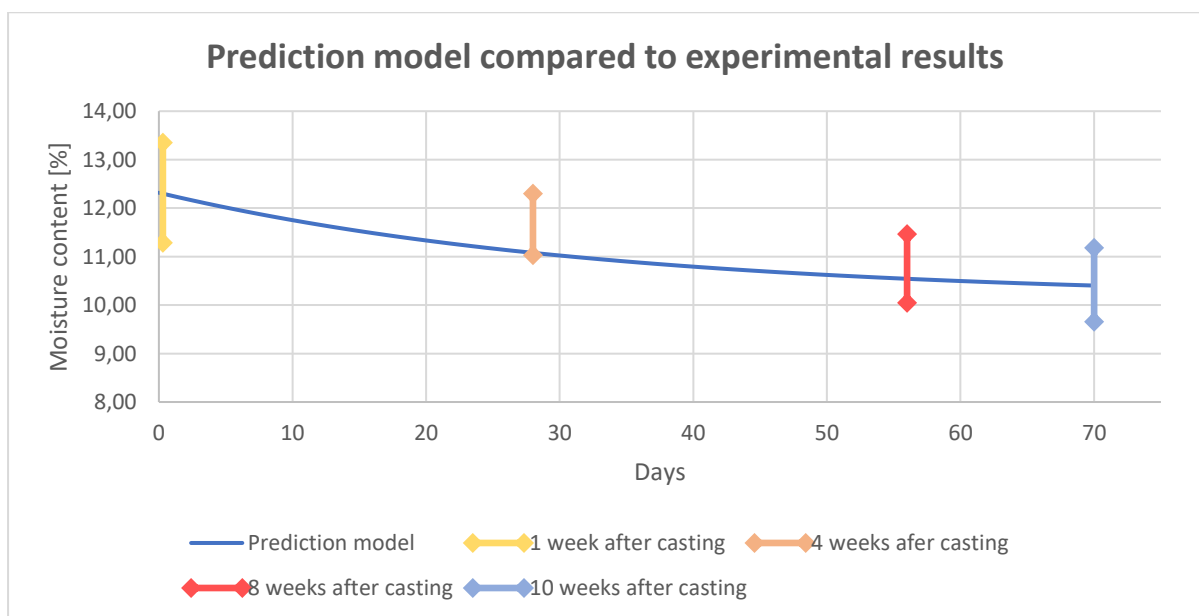


Figure 100 - Prediction model compared to experimental results.

The range of the experimental results contains 1σ or an equivalent of 68,27% of all the measurements. The prediction model is according chapter 2.4.3.5. The following parameters have been used:

MC high	12,32% (according to units 19-21)
MC low	10,14% (according to units 15-18)
Beta	0,03

It can be observed that the model quite accurately describes the drying process and passes all the datapoints which contain approx. 70% of all the measurements.

It should be noted that during installment of the units during week 1 and week 4 there was rainfall present that week of 159 and 210mm, respectively. This could cause the input moisture content to be slightly higher tot begin with.

5.7 Sub-conclusion

Initially, measurements would be carried out using both the FMD and FMW-T meters. However, due to a lack of measurements done with the FMD meter these results were not presented. In total 28 units were tested and a total of 672 measurements were done with the FMW-T meter. It should be stated that these tests were carried out in an attempt to approximate the moisture content. The measurements taken are mend to extract a general trend of moisture diffusion within the timber elements and not to obtain its absolute values. The only way to accurately measure the moisture content is by means of the oven dry method.

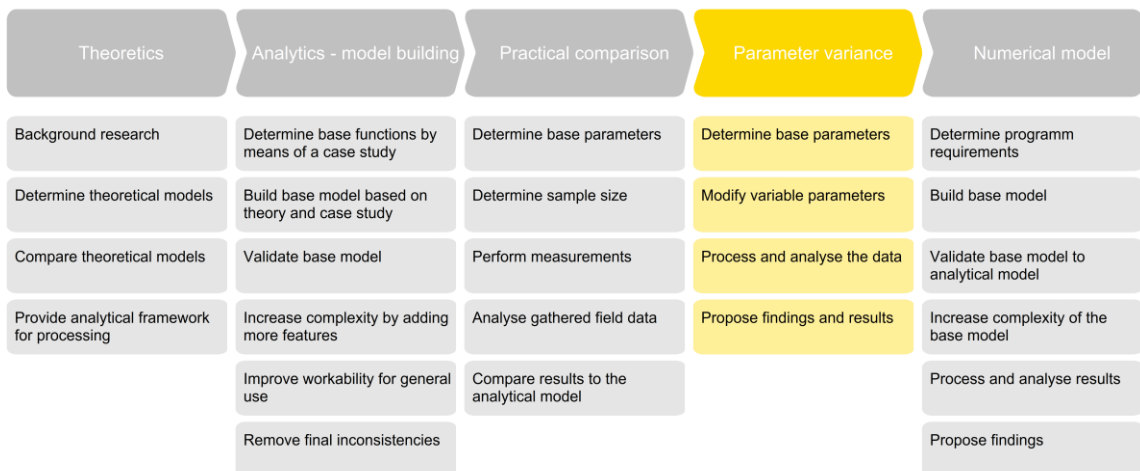
The average standard deviation of all measurements combined is 0,79%, this does not include the deviation of 0,5% by the manufacturer. The FMW-T meter does not contain any calibration lines and solely bases the moisture content on the density of the element. This could arise some problems as being an natural composite timber could contain large variations in density, due to environmental conditions like pressure or tension wood, growth period, knots etc. Due to these large variations it is not possible to accurately describe the relatively small moisture content changes during transit.

The difference in moisture content of the specimens in the assembly factory compared to the specimens after transit could be due to numerous factors. As the diffusion due to the relative humidity is a relatively slow process compared to for instance diffusion due to wind blowing across the surface.

After the units are installed and the screed is poured however there is a noticeable downward trend to be observed. This trend is closely related to the prediction model described in chapter 2.4.3.5. Any deviations could again be due to a number of factors. For instance if the windows were opened, for how long and how much direct sunlight was emitted in the unit.

In the end it can be concluded there is a visible and noticeable trend. However, there are a lot of aspects that influence the absorption or drying rate.

6 Parameter variance study



6.1 Introduction

In order to minimize the vertical deformation differences between the core and the units, a parameter study is done to determine the influences of several parameters. It has already been determined in the previous chapter (chapter 4.13) that the most gain can be made with the timber units. The total deflection of the units could be approximately 21-38 times as high as the total deflection of the concrete core, depending on the applied calculation method. It is as such that the parameter variation study only comprises variation within the scope of the timber units. All comparisons are done compared to the deformation described in the case study while using the experimental creep values.

6.2 Base and variable parameters

In order to accurately describe the changes in deformation, a baseline is chosen and the measurements are increased in steps of 5%. All the base parameters are according to chapter 4.13.1 but are mentioned in the results as well. With a set increase of 5% the change in deformation will also be measured in percentage of change compared to the base line. Only one parameter will be altered, the rest will return to the base parameters. It should be noted however that the acoustic felt is always present between the column and beam. With an increase in dimensions of the column or beam the dimensions of the acoustic felt also increase by the same amount.

Base parameters:

F_{gk}	134,6 kN
F_{qk}	73,1 kN
F_k	207,7 kN
$F_{qk,creep}$	66,3 kN
$F_{k,construction}$	120,58

The following parameters will be altered:

Dimensions:

- Column width (base 200mm)
- Column height (base 360mm)
- Beam width (base 204mm)
- Beam height (base 220mm)
- Felt height (base 15mm)

Moisture:

- Column initial moisture content (base 12%)
- Beam initial moisture content (base 10%)
- Final moisture content (base 9,27%)

Strength:

- Column strength class (base GL24)
- Acoustic felt strength increase (base 17Mpa)

6.3 Variance in dimension

6.3.1 Column width

Deformation difference due to column width variation

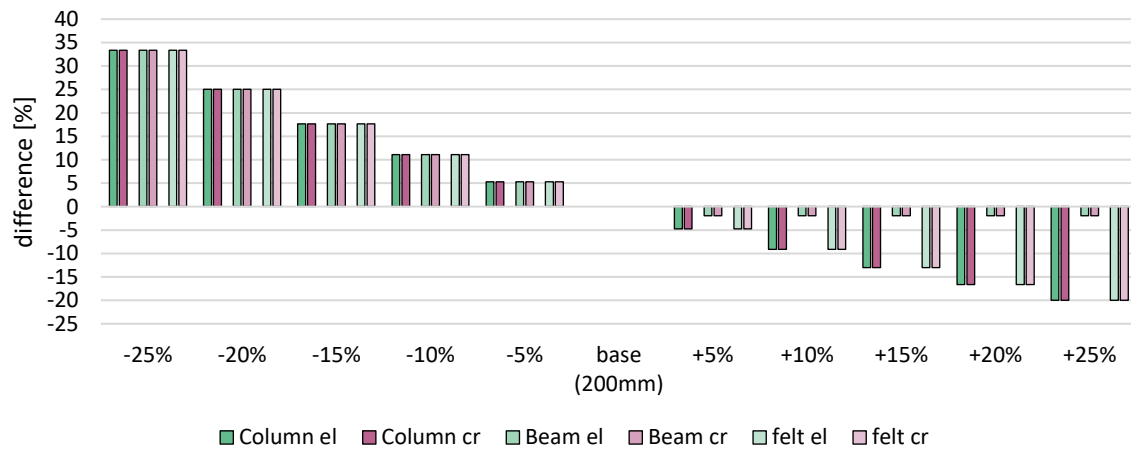


Figure 101 -Difference in deformation of the column, beam and felt by changing the column width, relative to 200mm.

As the column width impacts the amount of stress that is exerted on the beam and felt a change is noticeable in the column beam and felt. A linear relation can be observed for the decrease in column width for all three elements. As the column width is increased the same linear relation can be observed for the column and felt. As the width of the column starts to exceed the beam width (204mm), the stress in the beam stays constant regardless of the width of the column. As expected, the deformation due to change in moisture remain unaffected.

6.3.2 Column height

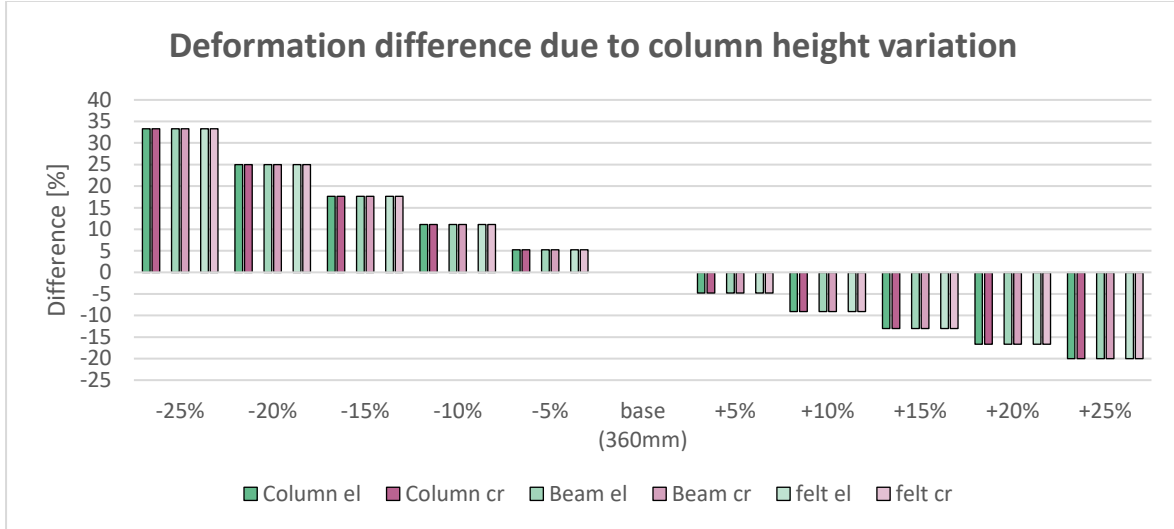


Figure 102 - Difference in deformation of the column, beam and felt by changing the column height, relative to 360mm.

The same linear relationship can be found for the change in deformation for the felt and column. This increase is due to the area of the two is linearly dependent to the deformation. A noticeable difference in the beam can be observed. This is due to the fact that in the approximation it is assumed that the beam is able to redistribute forces up to 30mm to both sides. The deformation due to change in moisture remain unaffected.

6.3.3 Beam width

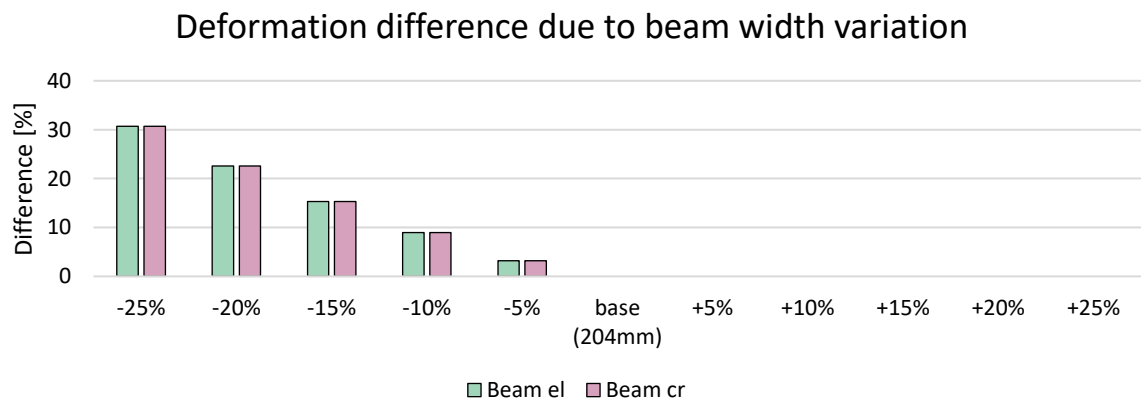


Figure 103 - Difference in deformation in the beam by changing the beam width, relative to 204mm.

It can be observed that the width of the beam does increase when it gets reduced. The pressured area gets smaller and thus the stress increases. However, when the dimensions increase nothing changes. This is due to the fact that in the approximation the beam does not redistribute any forces along its width. This means that increasing the width beyond the width of the column is futile. No change has been found in the acoustic felt or column as their area remains unaffected.

6.3.4 Beam height

Deformation difference due to beam height variation

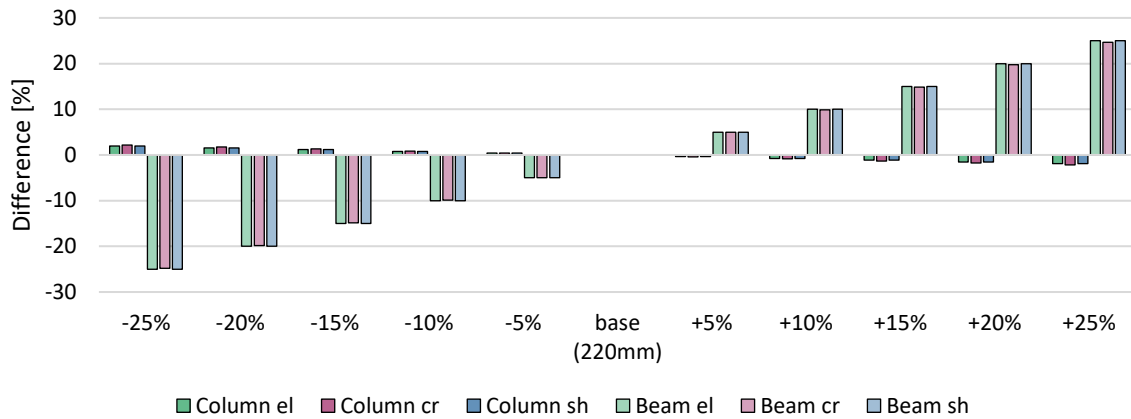


Figure 104 - Difference in deformation in the column, beam and felt by changing the beam height, relative to 220mm.

It can be observed that a linear relation exists between the change in height of the beam and the deformation. As the height of the beam decreases the difference becomes less. It can be observed that with the decrease of the beam height the column length increases and therefore a small increase in deformation is noticeable.

6.3.5 Felt height

Acoustic felt height variation in percentage

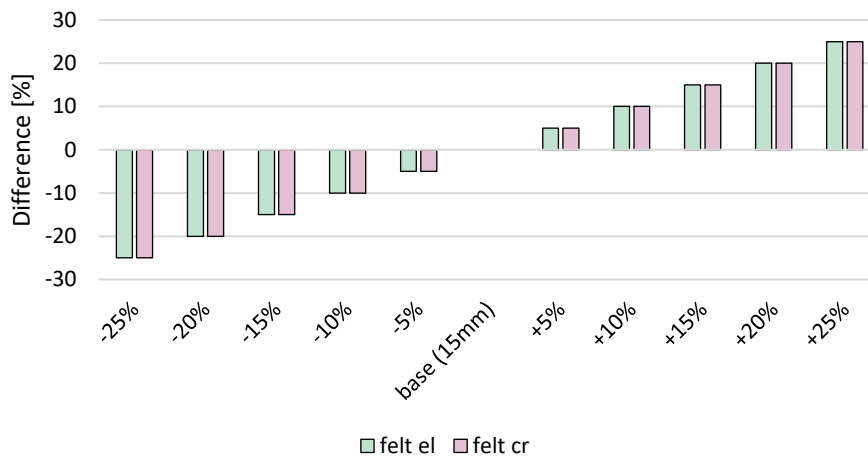


Figure 105 - Difference in deformation in the felt by changing the felt height, relative to 15mm.

Although the change in height should affect either the height of the beam or the length of the column with this approximation these changes are neglected. The change in height poses a linear relation to the elastic and creep deformation.

6.4 Variance in moisture
6.4.1 Column initial moisture content

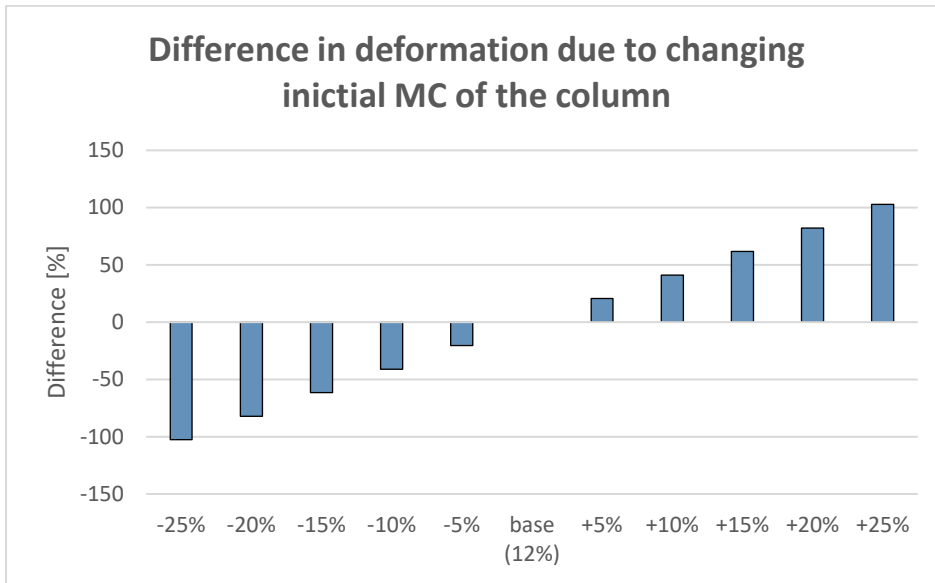


Figure 106 - Difference in deformation in the column by changing the initial MC, relative to 12%.

A linear relationship exists between the initial moisture content and the deformation due to the change in moisture. It is therefore expected to see this linear relation again in the figure above. As expected no change in elastic or creep deformation exists in any of the elements.

6.4.2 Beam initial moisture content

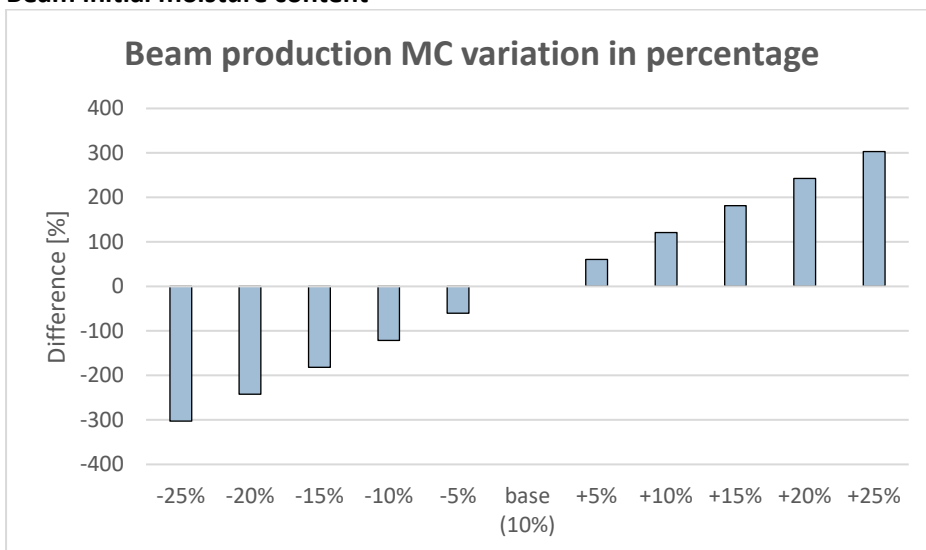


Figure 107 - Difference in deformation in the beam by changing the initial MC, relative to 10%.

It can be observed that like in the case of the column there is a linear relationship between the change in initial moisture content and the final deformation difference. It can also be observed that the amount of difference is much greater than is the case with the column.

It should be noted that the increase is relative to the base so a 25% increase represents a MC of 12,5%.

6.4.3 Final moisture content

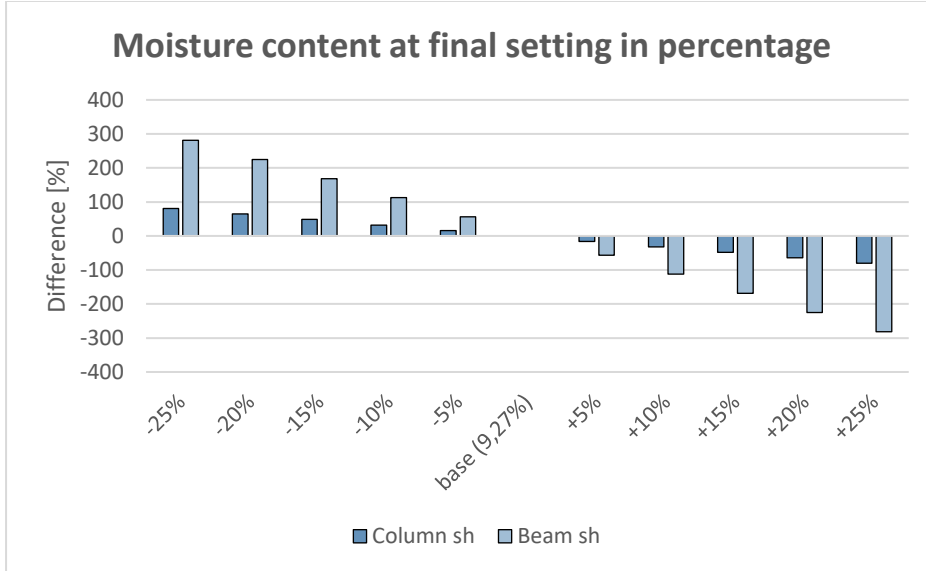


Figure 108 - Difference in deformation in the column and beam by changing the final MC, relative to 9,27%.

Figure 108 depicts the change in deformation relative to the core for the beam and the column. It can be observed that the change in the beam is approximately 3 times as high as for the column. This is to be expected as the perpendicular shrinkage coefficient is approximately 3 times as high as the longitudinal shrinkage coefficient.

6.5 Variance in strength

6.5.1 Column strength class

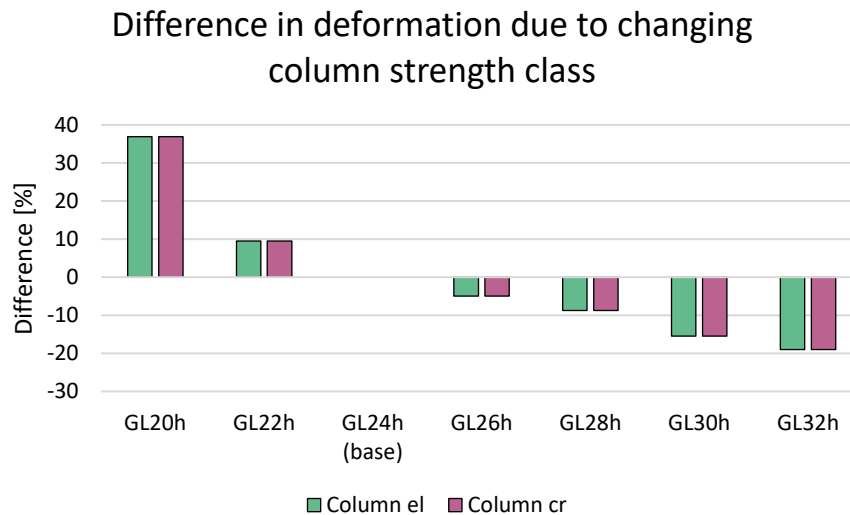


Figure 109 - Difference in deformation of the column to the core due to varying strength classes.

It can be observed that the column strength class does have a nonlinear relation with the amount of deformation. An approximate 40% difference can be observed for strength class GL20h. With an increasing strength class the amount of change could be up to 20% when GL32h were to be applied. The discontinuity of the linear trend at the GL20h is solely due to the difference in stiffness compared to the others.

6.5.2 Acoustic felt strength class

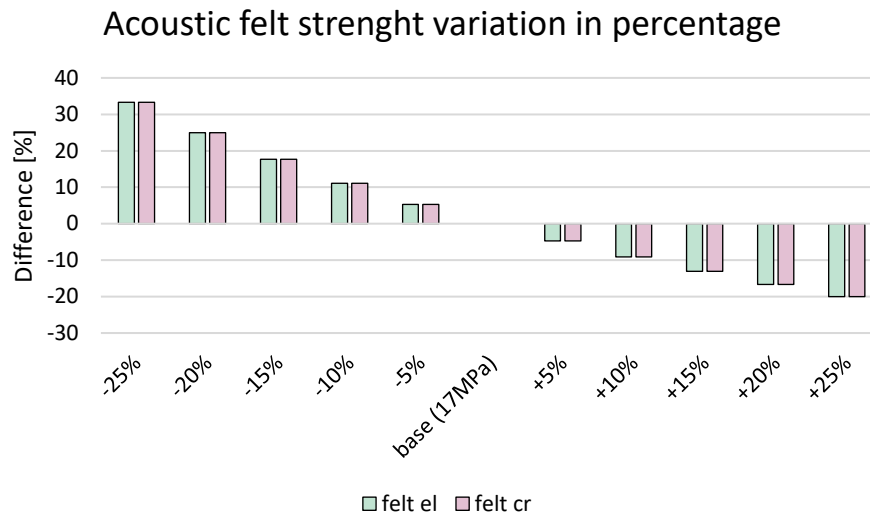


Figure 110 - Difference in deformation of the acoustic felt to the core due to varying strength classes.

A linear relationship can be observed when increasing the strength of the acoustic felt. As the creep coefficient is linearly dependent on the elastic stress the amount of difference should be the same as the elastic difference.

6.5.3 Absent beam

Within the current system the beam is part of the loadbearing structure. Because the beam is loaded perpendicular to the fiber relatively large deformations are present compared to the deformations due to the column (which is loaded parallel to the fiber). An interesting approach would be to remove the beam out of the loadbearing structure. The beam would be situated between the columns instead. The total load on the columns would not change, however, the length of the columns would slightly increase.

The structural loadbearing system of the units would change as the floor beam would be situated between the columns, as can be observed in Figure 111. The results of this analysis can be found in Figure 112.

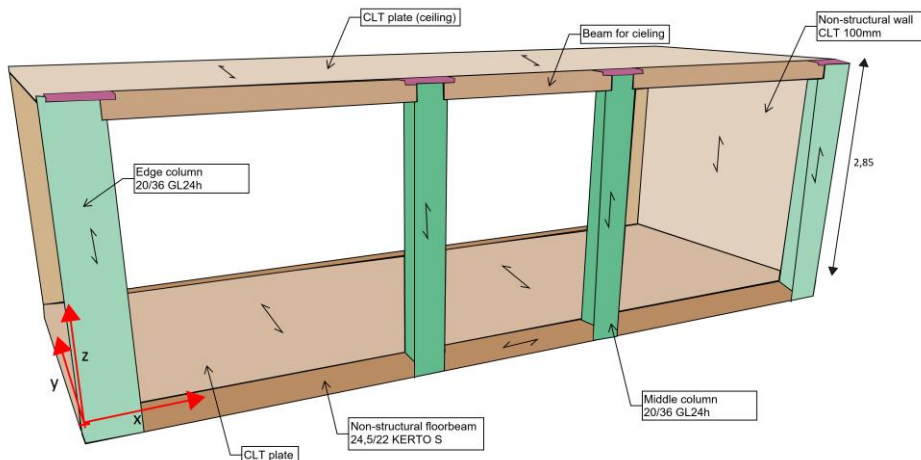


Figure 111 - Structural system of the timber units excluding the floor beam.

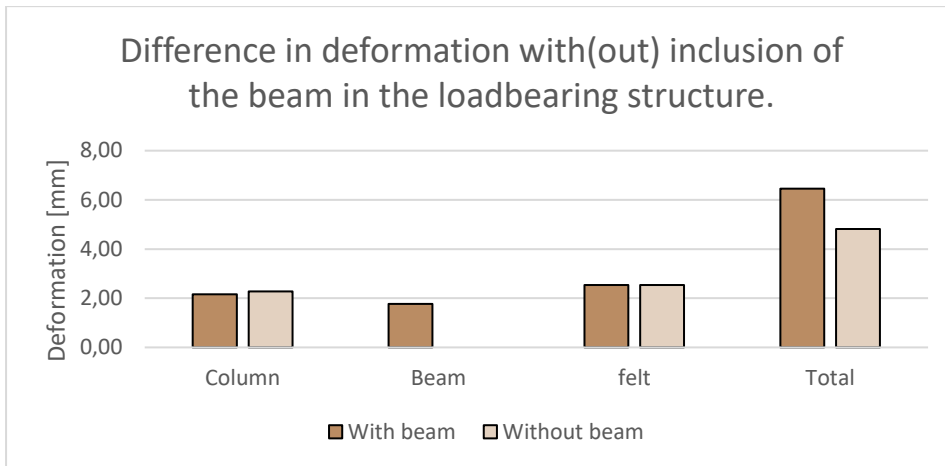


Figure 112 - Difference in deformation with the beam excluded from the loadbearing structure compared to included.

It can be observed that the absence of the floor beam in the loadbearing system leads to a slight increase in deformation of the column. This is to be expected since the length increases slightly. It can also be observed that the total deformation in the system is reduced. The total deformation is approximately 34% less when the beam is excluded from the loadbearing structure.

6.6 Sub-conclusion

It should be noted that all the values presented are represented as change relative to a set base value. This way it is possible to observe the impact of each percentual change to the entire structure and the relative changes can easily be compared to each other, see Figure 114.

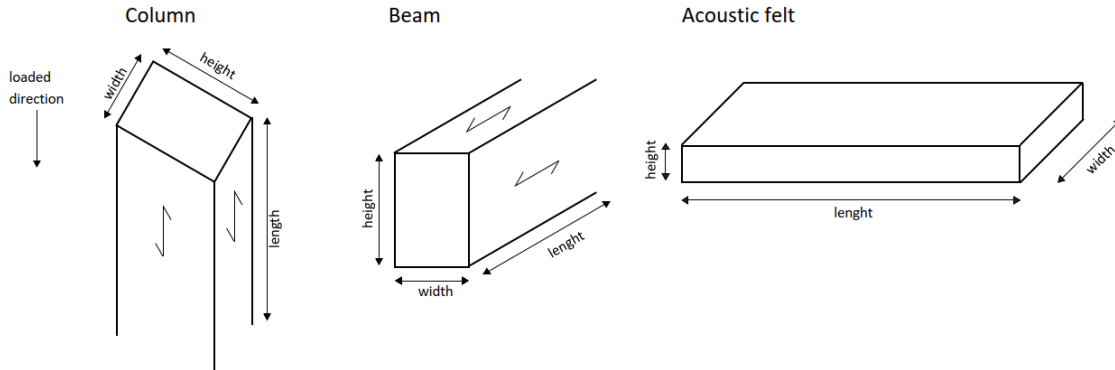


Figure 113 - Definitions of dimensions for the column, beam and acoustic felt.

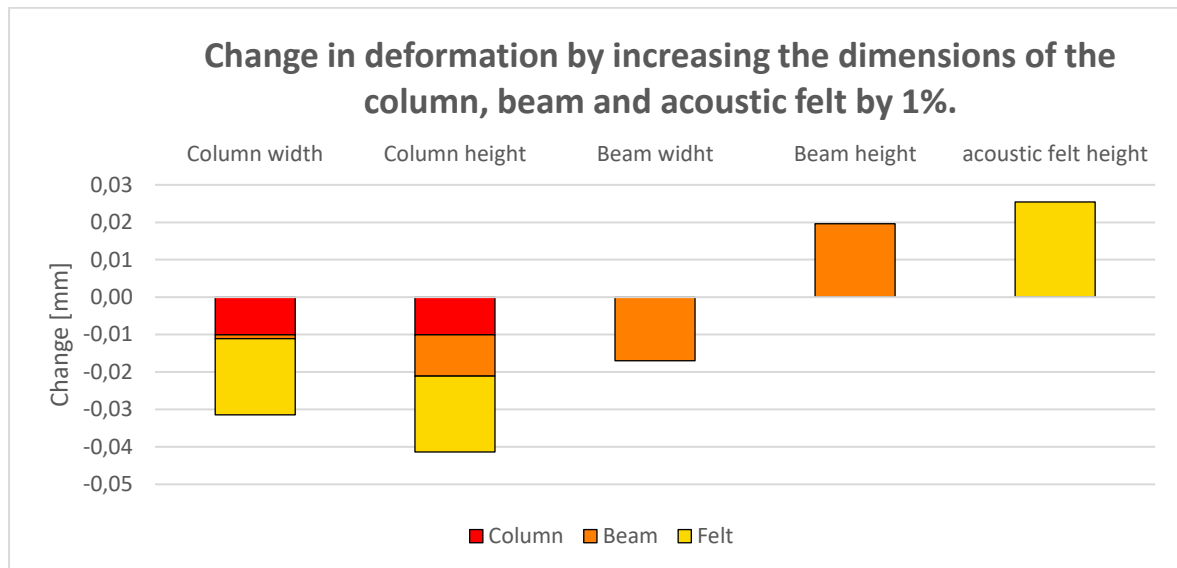


Figure 114 - Impact of increasing the dimensions of the elements by 1% relative to their base.

The figure above depicts the total change in deformation by increasing the dimensions of an element by 1%. It should be noted that the acoustic felt is always present between the contact area of the column and the beam. Therefore, by increasing the width or height of the column the acoustic felt increases as well. However, as the width of the beam is larger than the column, changing the width of the beam even further does not impact the stress distribution of the acoustic felt or column and only impacts the stress within the beam itself, as can be observed above.

The following can be observed:

- Increasing the cross sectional dimensions of the column and beam, ie. column width, column height and beam width decreases the stresses and thus the deformation.
- Increasing the height cross section of the column decreases the stress within the column, beam and felt.
- Increasing the cross section of the beam only alters the stress distribution within the beam.
- Increasing the beam and acoustic felt height increases the deformation. This is due to the increase of compressible material in loaded direction.

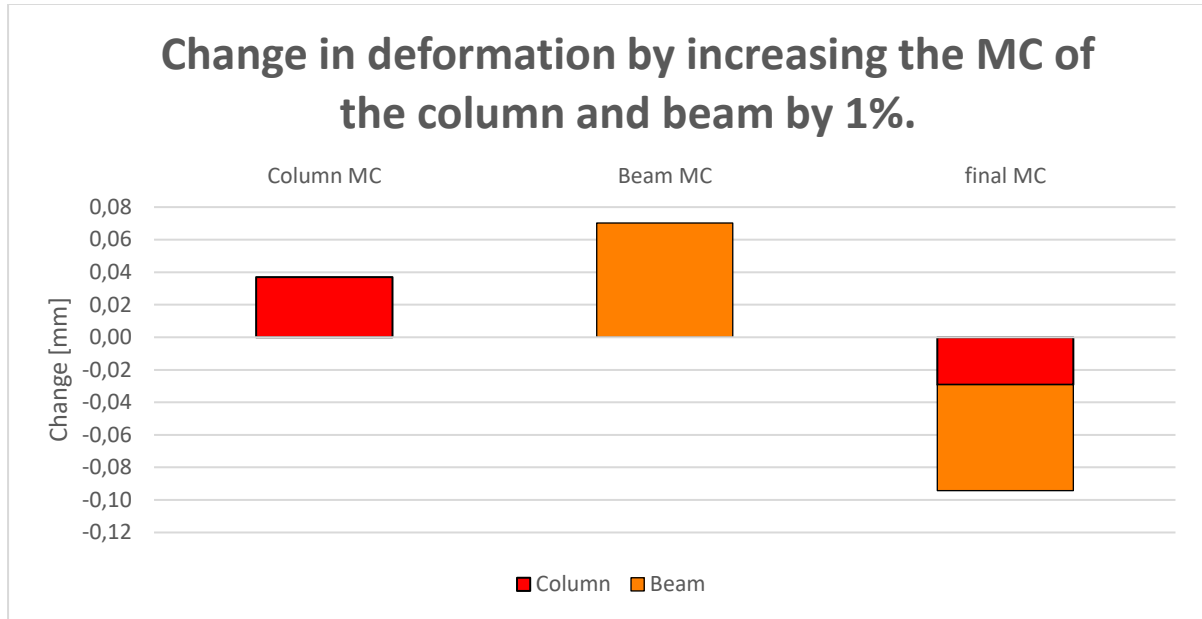
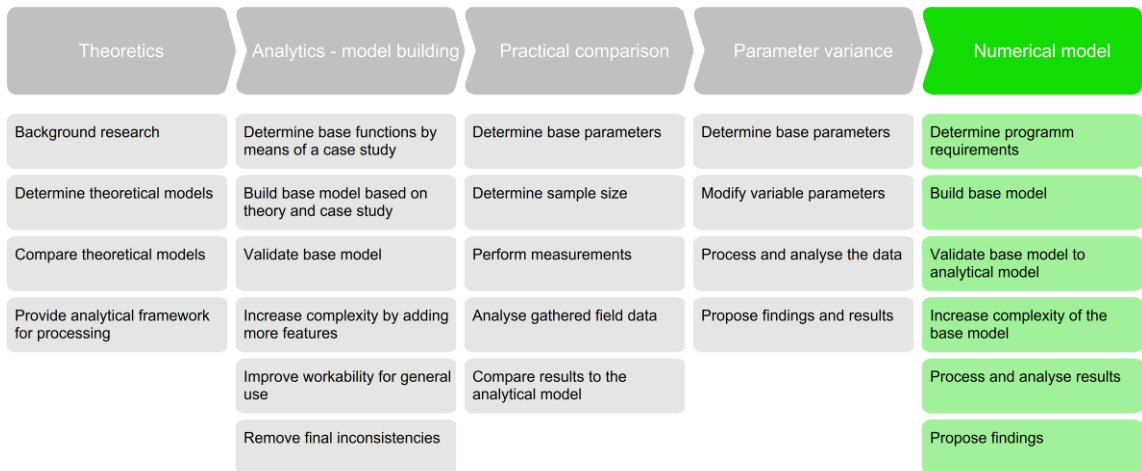


Figure 115 - Impact of increasing the MC by 1% relative to their base.

It can be observed that by changing the moisture content of the column and beam an increase in deformations is to be expected. This is in line with the expectations as the amount of accumulation and dissipation of moisture will increase with an increased difference in internal MC and surrounding environment. Were the final moisture content to be increased the moisture content will come closer to the MC at time of installment and thus the amount of deformation will decrease.

Within the current system it can be concluded that the most optimal way to reduce deformations is to increase the column height. If the system were to be adjusted to a column-only loadbearing structure where the beam is no longer included a reduction of approximately 34% could be achieved.

7 Numerical modelling



7.1 Base model validation

At first a base model has been made to validate the results from the excel-tool. This base model will consist of a column-beam structure made out of 3D solid elements with isotropic material properties. The setup can be observed in Figure 116. Several analysis will be performed using the Finite Element Program DIANA.

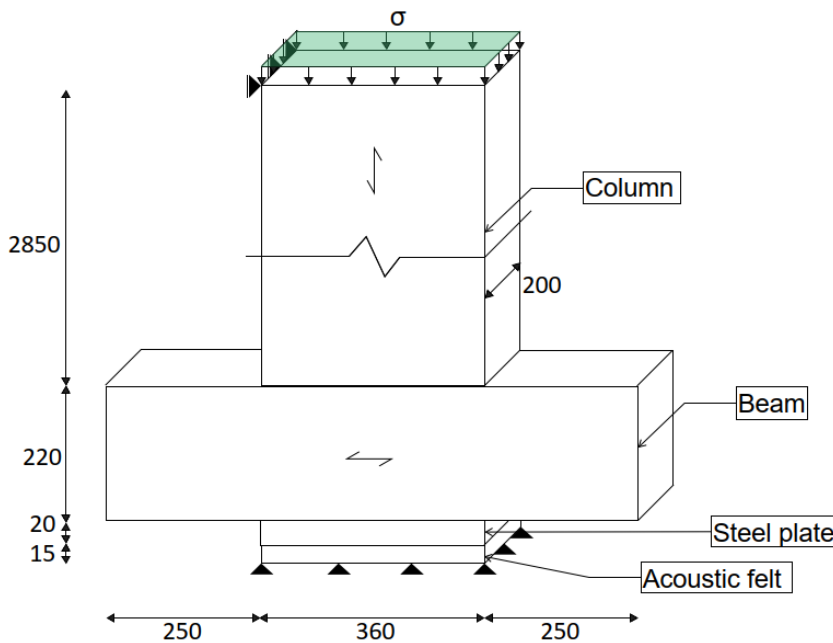


Figure 116 - Column-beam setup.

The aim of this analysis is to verify the excel tool made in previous chapters. A total of two analysis will be performed. The first analysis will determine the elastic deformations by means of a linear elastic analysis. The second analysis will be non-linear and will describe the shrinkage deformations. Unfortunately there isn't a package available to verify the creep deformations. The results will be analyzed and verified using analytical results.

7.1.1 Analysis method

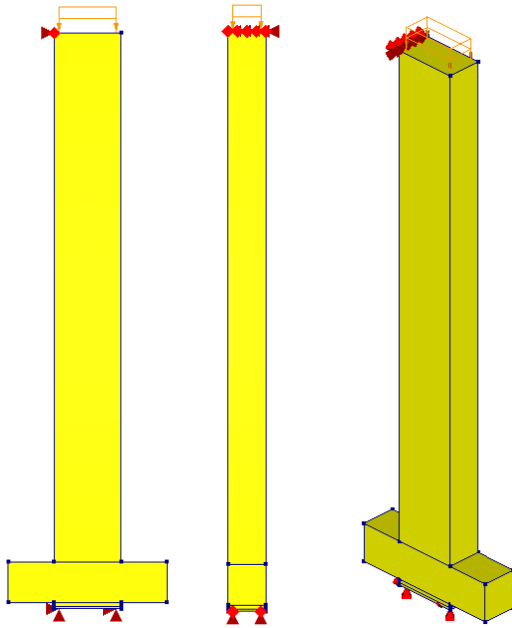


Figure 117 - From left to right: Front view, side view & isometric view.

Table 35 - Used elements and their characteristics.

Element type	Solid brick elements (HX24L)
Degrees of freedom	8x3
Interpolation scheme	Linear interpolation
Integration scheme	2x2x2
Shape dimension	3D
Stress components	$\sigma_{xx}, \sigma_{yy}, \sigma_{zz}, \sigma_{xy}, \sigma_{yz}, \sigma_{zx}$
Nr. of elements	15440
Nr. of nodes	18810
Av. element size	50mm

Table 36 - Material properties

	Acoustic felt	GL24h	LVL Kerto-S	Steel
Young's modulus [N/mm ²]	17	11500	2400	210000
ν	0	0	0	0.3
Mass density [T/mm ³]	$8.1e^{-10}$	$4.2e^{-10}$	$5.1e^{-10}$	$7.85e^{-9}$

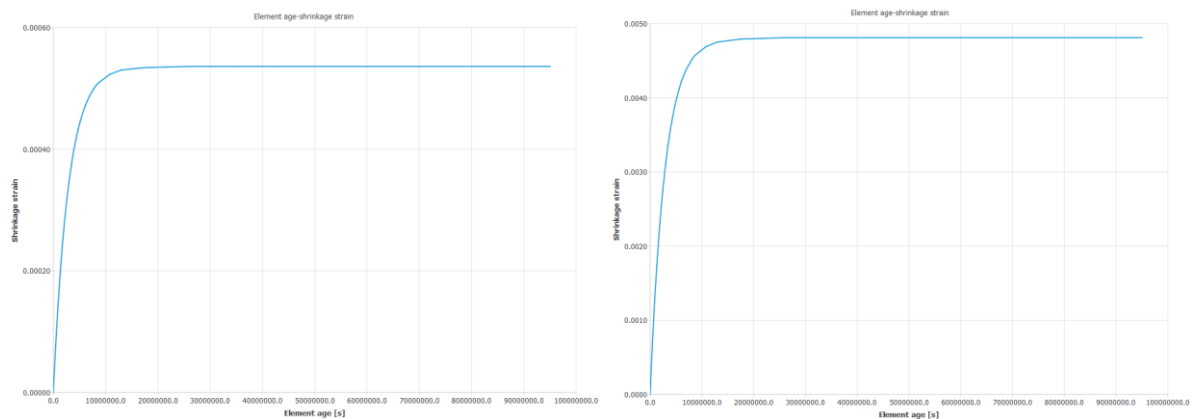


Figure 118 - Shrinkage strain over time for GL24 and LVL, left to right respectively.

The model used represents the loadbearing structure of the units. Lateral supports at the top and vertical supports at the bottom provide boundary conditions which represent the actual model. A distributed load of 2.89 N/mm^2 will be applied at the top of the column. This represents a characteristic dead load of 134.6 and a live load of 73.1 kN, corresponding to the loads present at the first level.

The material properties can be found in Table 36. It should be noted that besides the shrinkage strain, only linear elastic properties are used. It should also be noted that the poisson's ratio of both timber elements and of the acoustic felt is set to 0. The reason for this is because the base model serves as a check for the excel model and the poisson ratio is nonexistent in this model as well.

There are two different analysis performed on this model. One linear elastic and one nonlinear elastic. The nonlinear elastic analysis was performed to determine the shrinkage of the model. The nonlinear analysis was performed using force and displacement control with 100 time increments of 864000 or 10 days. Convergence criteria was based on the regular Newton-Raphson method.

7.1.2 Analytical results

According to the analytical model the following results are to be expected for the elastic and shrinkage deformation.

Deformation	Column	Beam	Felt	Total
Elastic [mm]	0.710	0.227	2.550	3.487
Shrinkage [mm]	1.526	1.057	-	2.584
Total [mm]	2.226	1.284	2.550	6.071

Any deformation due to the steel plate is neglected. The shrinkage values are determined after approximately 1000 day period.

7.1.3 Numerical results

7.1.3.1 Linear elastic analysis results

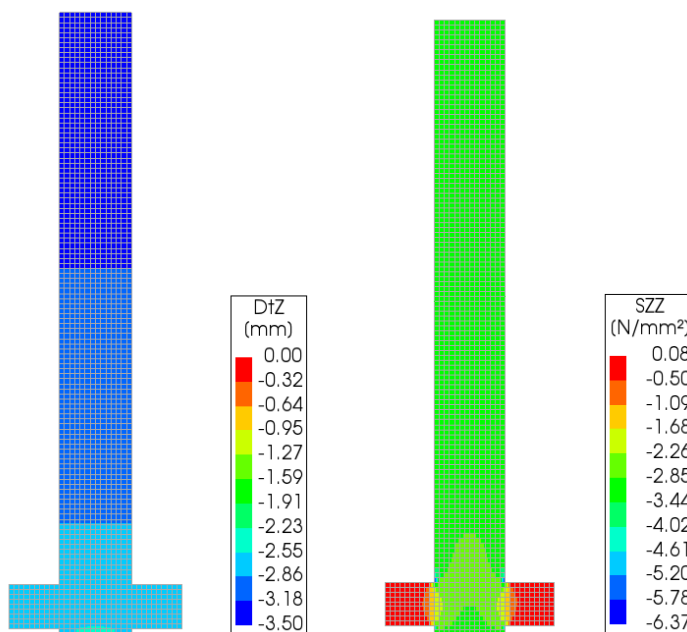


Figure 119 - Numerical results of the linear elastic analysis. Left to right: Deformations and vertical stresses.

It can be observed that the total elastic deformation in the model is nearly identical to the expected elastic deformation determined analytically. As to be expected, the main portion of the deformation is due to the acoustic felt.

It can be observed that the vertical stresses are 0 in the ends of the beams. Noticeable spread at an angle of approximately 60 degrees is present near the column beam boundary. In the analytical model, for a continuous beam the area could be increased by 30mm on each side. The numerical results indicate this is the right approach.

7.1.3.2 Nonlinear elastic results

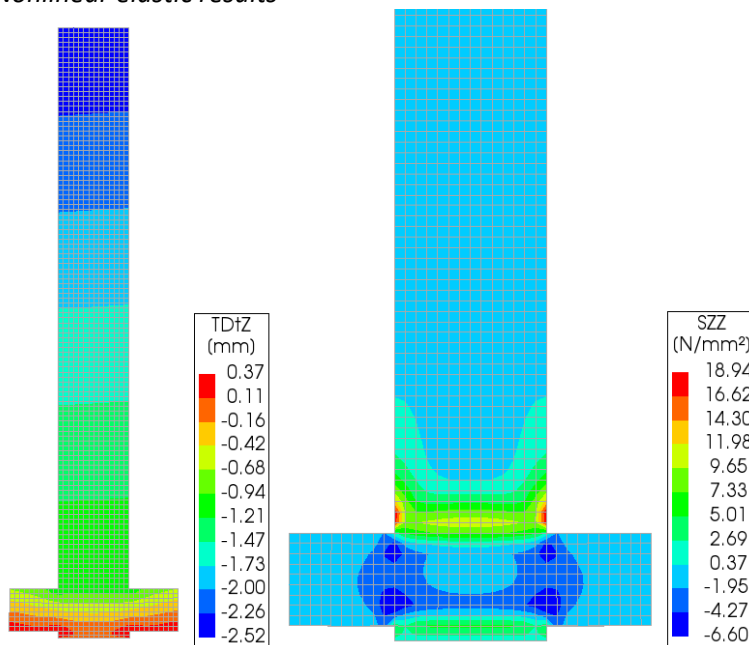


Figure 120 - Numerical results of the nonlinear analysis. Left to right: Deformations and vertical stresses.

It can be observed that the total shrinkage deformation is approximately 2.52mm which is nearly identical to the expected result. It can also be observed that there are quite large compressive stresses in the column near the connection of the beam.

7.1.4 Conclusion

Two analysis have been performed, one linear elastic and one nonlinear. The material properties of the model are identical to the material properties in the analytical model.

It can be concluded that the results of the linear elastic analysis and shrinkage are very closely related to analytical results. This indicates that the numerical model is correct. No imperfections were modelled.

It can also be concluded that the initial assumption to increase the width of the contact area by 30mm on each side for the beam has been validated by the numerical model.

7.2 Risk assessment

A second model is made to determine the ductility of the connection assessing the worst case scenario. That is, the tolerance of 20mm is exceeded. According to the case study done in chapter 4 this tolerance is exceeded by 5 millimeter if the upperbound limit is taken. The deformation difference has to be taken by the connections between the timber and concrete elements. It is therefore imperative to explore the connections and determine their behavior when subjected to these loads. It is important to note that the connection has a built in tolerance. A total of 35mm tolerance is taken into account of which 15mm is to ensure proper alignment and 20mm is to account for the deformation differences, see Figure 121 top left. Another important note is that the blind anchors in the column are situated in the acoustic felt. This indicates that the forces are being transferred by the anchors instead of the acoustic felt. This chapter outlines this force transfer through these connections.

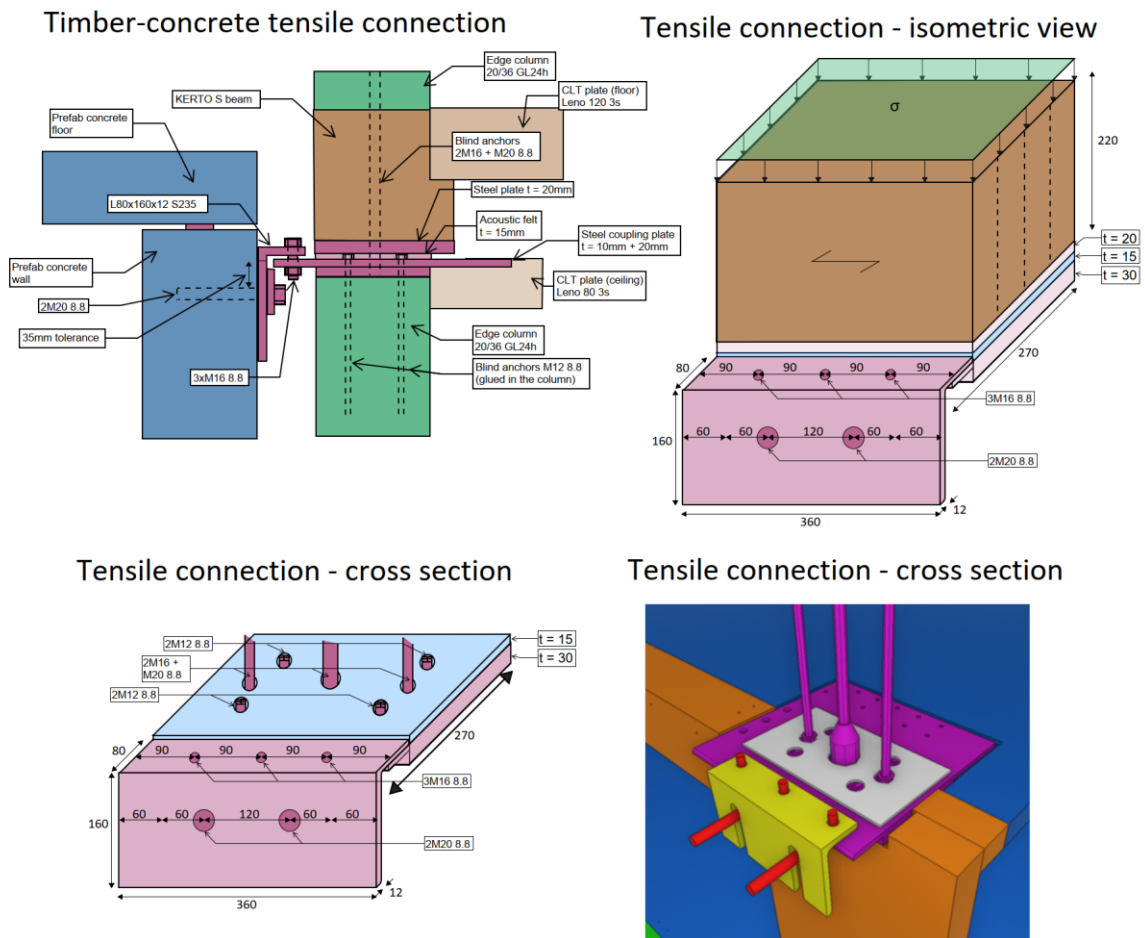


Figure 121 - Tensile connection - side and isometric view, left to right respectively.

The aim of this analysis is to determine the strength capacity of the connection in case the maximum built in tolerance of 20mm is exceeded. In addition, the forces in the anchors will be determined and the ductility of the whole connection will be assessed. To describe this behavior a nonlinear elastic analysis will be performed. This analysis will consider a combination of physical and geometrical nonlinear effects.

The model presented in Figure 121 represents the tensile connection between the units and the prefabricated concrete walls. The model consists out of an L-profile, bolted to a coupling plate which is bolted to the timber columns via 4M12 anchors. These set anchors protrude approximately 10mm

into the acoustic felt. An acoustic felt separates the coupling plate and the steel bearing plate for the timber floor beam. In the acoustic felt several anchors are present which are used for connecting the coupling plate to the overall connection. These anchors (2M16 and 1M20) are however tensile anchors and are not glued to the column which means they do not provide any resistance when the units move downward. When assessing the model it is assumed that due to the elasticity of the acoustic felt the connection mainly transfers the stresses through the anchors 4M12 anchors and not through the 2M16 and M20 anchor.

The following elements will be modelled:

- Concrete wall
- L-profile
- Bolts
- Connecting plate
- Acoustic felt
- Steel plate
- LVL beam

7.2.1 Analysis method

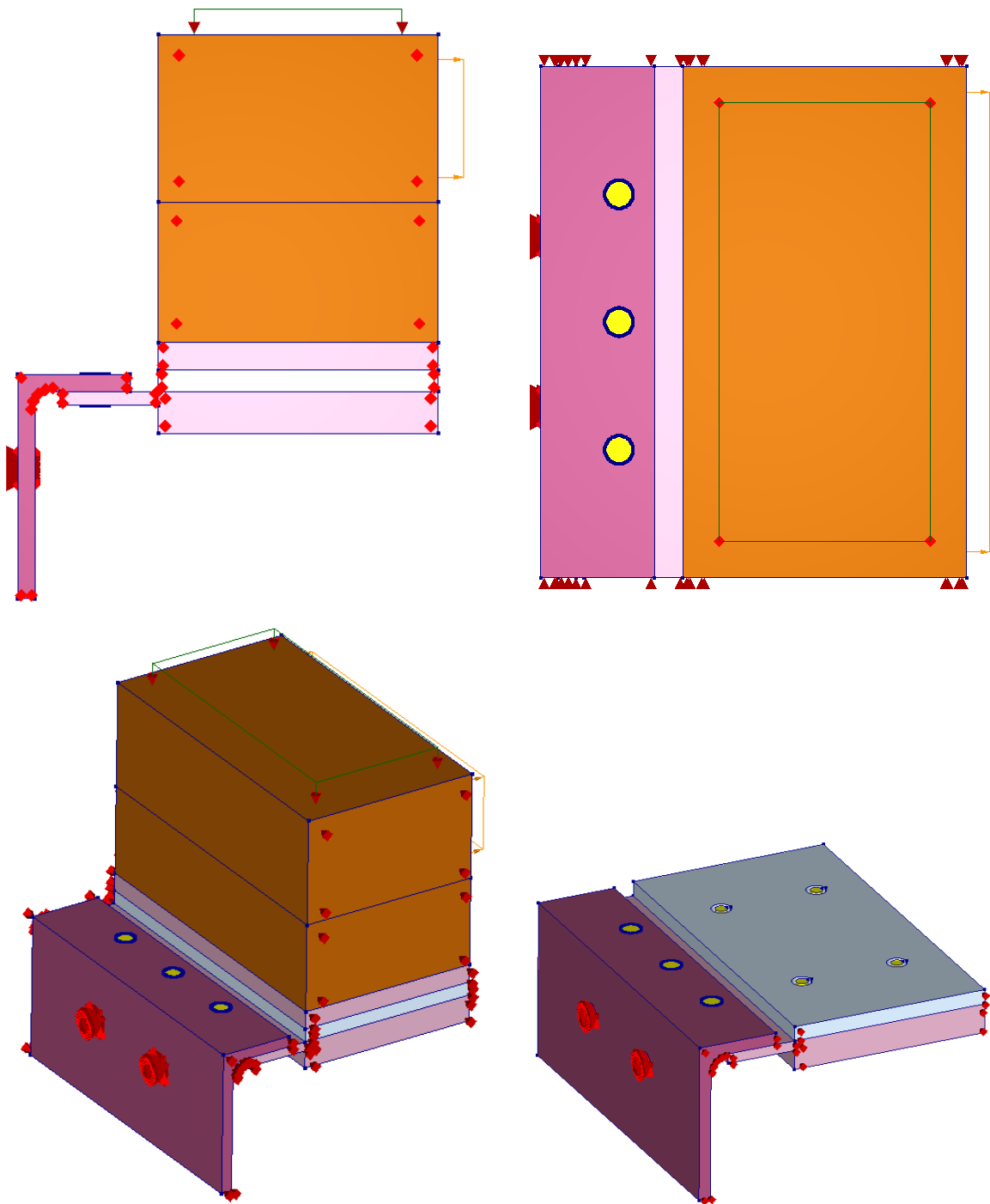


Figure 122 - From left to right, top to bottom: Side view, top view, isometric view and cross sectional view.

7.2.1.1 Displacement control

To assess the ductility, an imposed vertical deformation will be applied to the connection. A displacement of 5mm will be applied using an incremental procedure. The maximum number of iterations allowed is 25. The equilibrium method is based on full Newton-Raphson and convergence tolerance is based on energy, force and displacement equilibrium.

7.2.1.2 Materials

Table 37 - Material properties

Material	E [N/mm ²]	ν	Mass density [T/mm ³]	f_y [N/mm ²]	f_u [N/mm ²]	ϵ_u
Steel (S355)	210000	0.3	$7.85e^{-9}$	355	490	0.15
Bolts	210000	0.3	$7.85e^{-9}$	-	-	-
Acoustic felt	17	0	$8.10e^{-10}$	-	-	-
Concrete	35000	0.2	$2.5e^{-9}$	-	-	-
LVL	2400	0	$5.10e^{-10}$	-	-	-
8.8 Anchors	210000	0.3	$7.85e^{-9}$	640	800	0.15

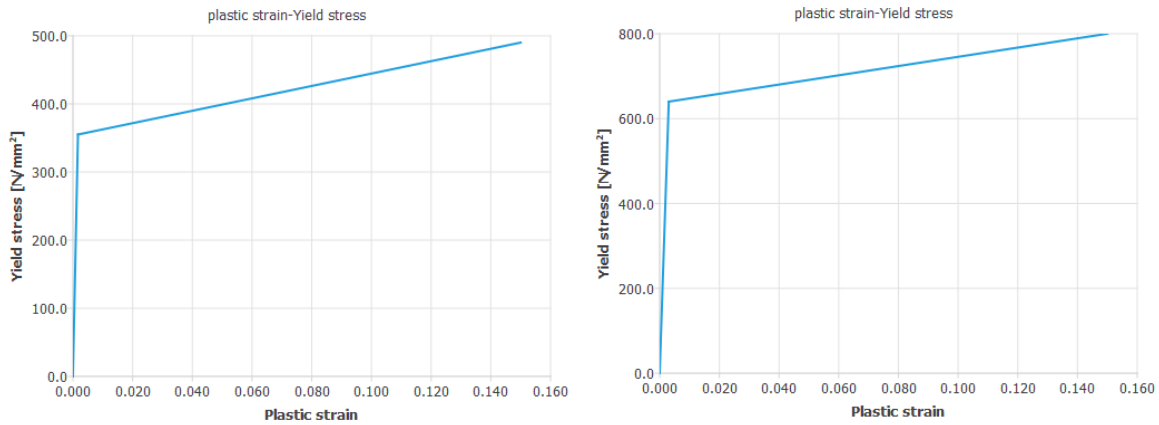


Figure 123 – Bi-linear stress strain relationship for the material steel S355 and 8.8 anchors, let to right.

An overview of the material properties can be found in Table 39. It can be observed that only the steel (S355 and 8.8 bolts) have a non-linear stress-strain relationship. Any stress distribution of the washers has been neglected in this model so stress concentrations and singularities at the location of the anchors and bolts are to be expected.

As the non-elastic material behavior of the LVL beam cannot be described accurately nor is the failure mechanism of interest in this model, the timber elements only exhibits isometric linear elastic properties. The stress in the timber will be checked whether the linear elastic stress limits gets exceeded.

Both the L-profile and the connecting plate are made out of steel with a grade of S355. It is imperative to assign non-elastic material properties to ensure proper deformation in the connection. The material properties of the steel can be found in Figure 123.

Two interface elements have been added to the model. One between the connecting plate and the L-profile and one between the L-profile and the concrete wall. The first is to provide a compressive restraint between the bolted plates while still allowing tensile freedom. The second is to provide a compressive restraint which is present due to the concrete wall. The interface between the steel plates has been given a young's modulus of 210000 and the interface between the concrete wall and the L-profile a young's modulus of 35000, both in normal direction and only in compression.

7.2.1.3 Restraints and supports

A concrete wall has been modelled using a 3D membrane. This membrane is uniformly supported in all translational DoFs. No restriction has been added to the rotational DoFs. The L-profile has been connected to the concrete wall with the use of interface elements and bolts. These interface elements allow for compressive forces but not for tensile forces, the bolts allow transfer of compressive, tensile and shear forces.

The anchors in the concrete have been modelled as translational restrains in x and z direction within the anchor holes. No restriction has been added to the rotational DoFs.

Although the timber floor would allow some restrained in lateral direction due to clamping moments within the column-beam structure of the units this is to be neglected.

A translational restraint in y-direction has been added to one side of the model in order to prevent lateral deflections.

7.2.1.4 Mesh

Table 38 - Mesh properties

Shapes	Nr. of elements	Nr. of nodes	Size x-dir. [mm]	Size y-dir. [mm]	Size z-dir. [mm]
L-profile	14868	9667	2.5	10	2.5
Connecting plate	35949	23586	2.5	10	2.5
Acoustic felt	8712	6309	2.5	10	2.5
Steel plate	23688	14022	2.5	10	2.5
Timber beam	75177	71904	5	10	5
Concrete wall	1044	1114	2.5	10	2.5
Anchors	84	231	2.5	2.5	2.5

Table 39 - Elements and their characteristics.

Element	DoF	Interpolation	Integration	Stress components	Shape
HX24L	8x3	Linear	2x2x2	$\sigma_{xx}, \sigma_{yy}, \sigma_{zz}, \sigma_{xy}, \sigma_{yz}, \sigma_{zx}$	Cube
PY15L	5x3		5 point		Pyramid
TE12L	4x3		1 point		Tetrahedron
TP18L	6x3		1x2		Wedge
Q12GME	4x2		2x2		Rectangle
T9GME	3x2		3 point		Triangle
Q24IF	4x2		3x3	t_n, t_t	Rectangle
T18IF	4x2		3 point	t_n, t_t	Triangle

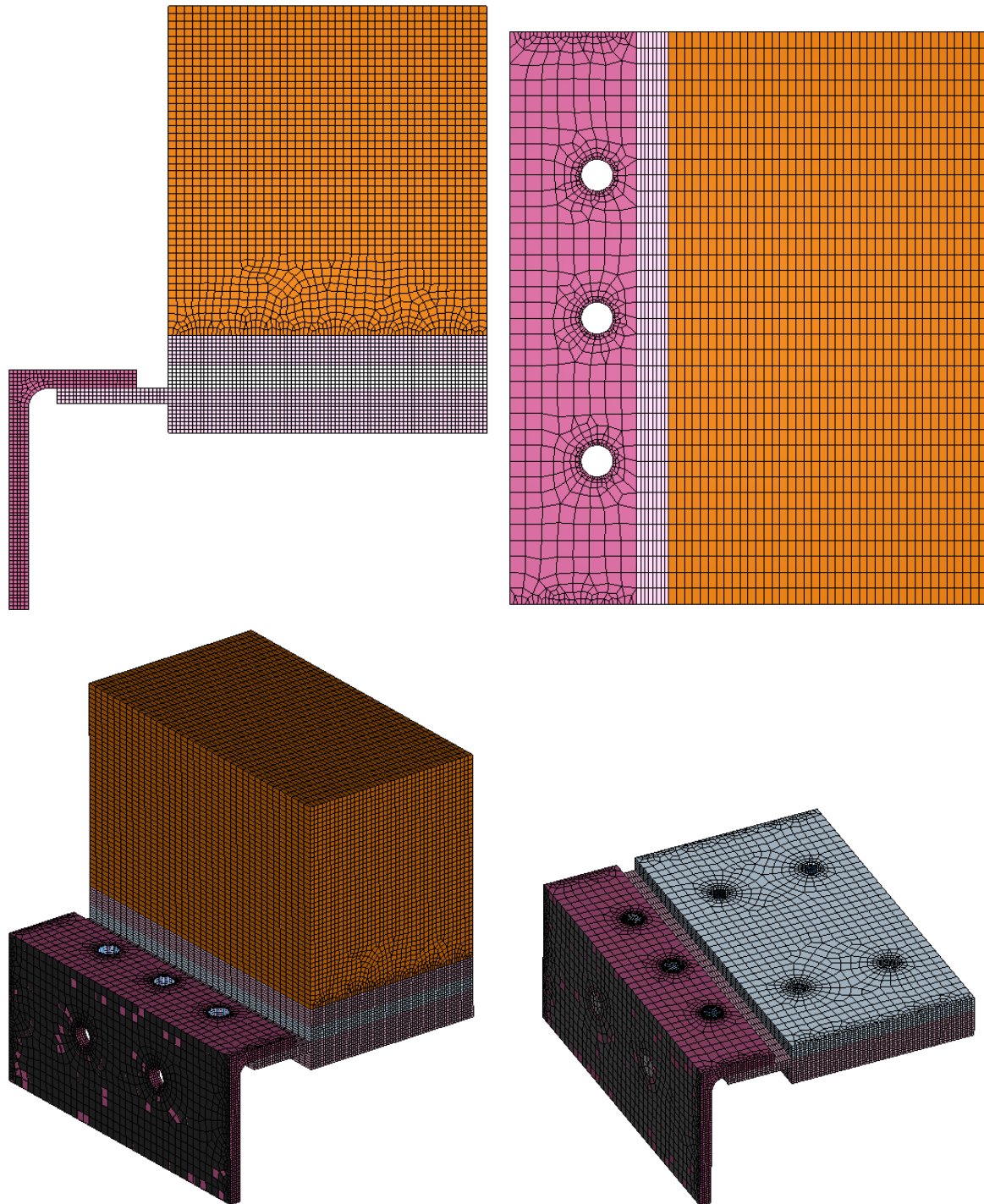


Figure 124 - From left to right, top to bottom: Side view, top view, isometric view and cross sectional view.

In order to accurately describe the stresses it is preferred to obtain at least 3 elements over the thickness of each shape. This is reflected in the average element size as depicted in Table 38.

7.2.2 Numerical results

The following results are obtained using the analysis method described according. The results will be given for the case with displacement and force control combined. An overview will be provided for 4 different points A to D. At approximately 0.25 times the load factor the maximum deflection is reached when the Eurocode is applied and at a load factor of 1 the experimental model. All results will be shown with a normalized deformation of 0.05.

Table 40 - Provided datapoints and their respective imposed deformation and force.

Point	Load factor	Vertical deformation
A	0.25	1.25mm
B	0.5	2.5mm
C	0.75	3.75mm
D	1	5mm

7.2.2.1 Displacement

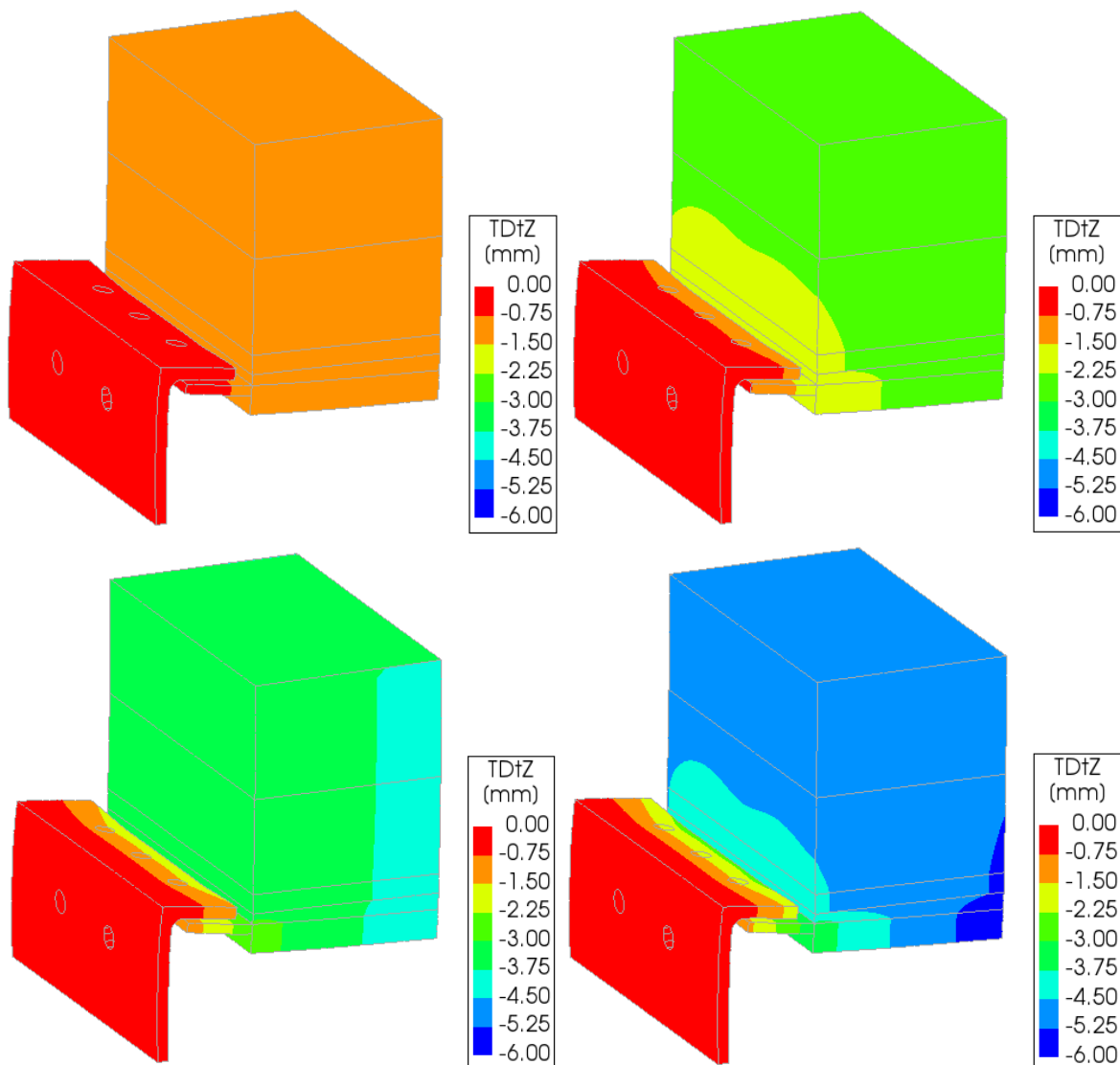


Figure 125 – Isometric view of vertical deformation at locations A to D, left to right top to bottom respectively.

It can be observed that the entire connection translates vertically downward. In addition, some rotation between the steel plates where the anchors are located is visible. The L-profile rotates inward and down and near the connections with the connecting plate some additional deformation is visible.

7.2.2.2 Plastic strains

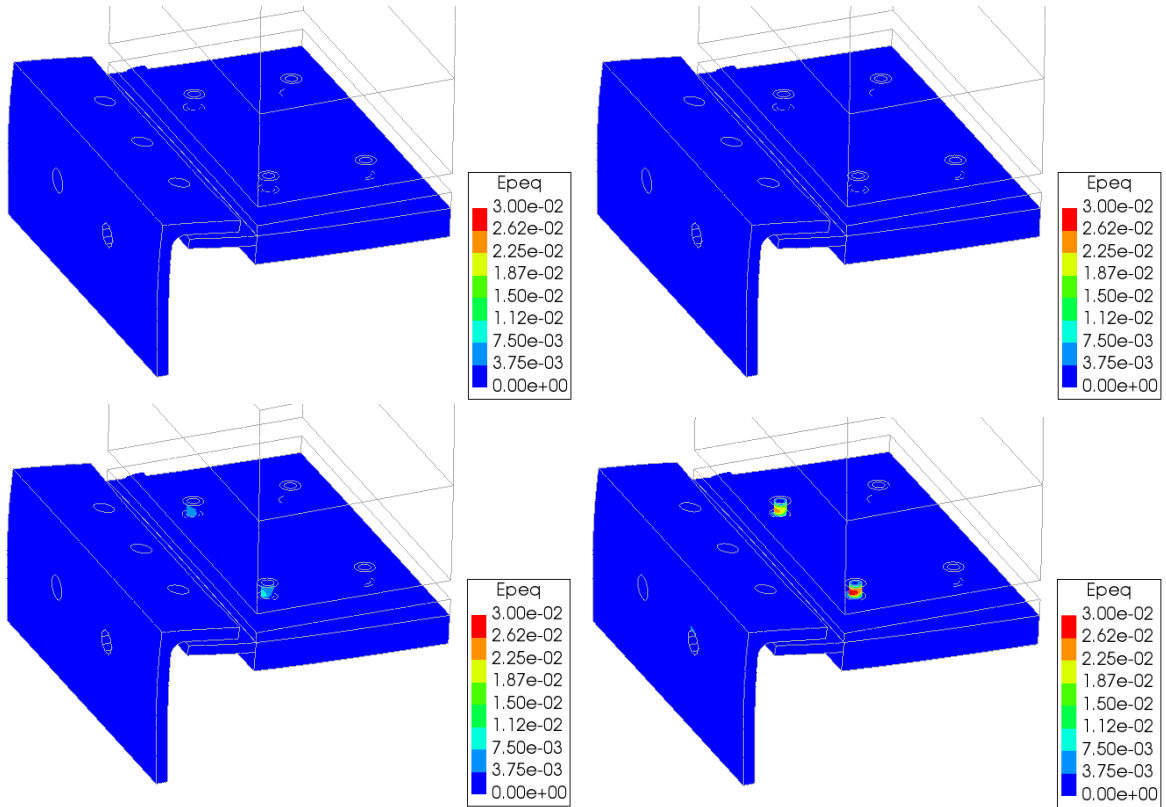


Figure 126 - Equivalent plastic strains at points A to D, left to right top to bottom respectively.

It can be observed that the anchors close to the side experience plasticity when the maximum deformation is reached. This is to be expected as the increase of forces causes the connection to rotate slightly and increases the exerted stress on the inner bolts. No other signs of plasticity in any of the other elements is visible.

7.2.2.3 Interface tractions

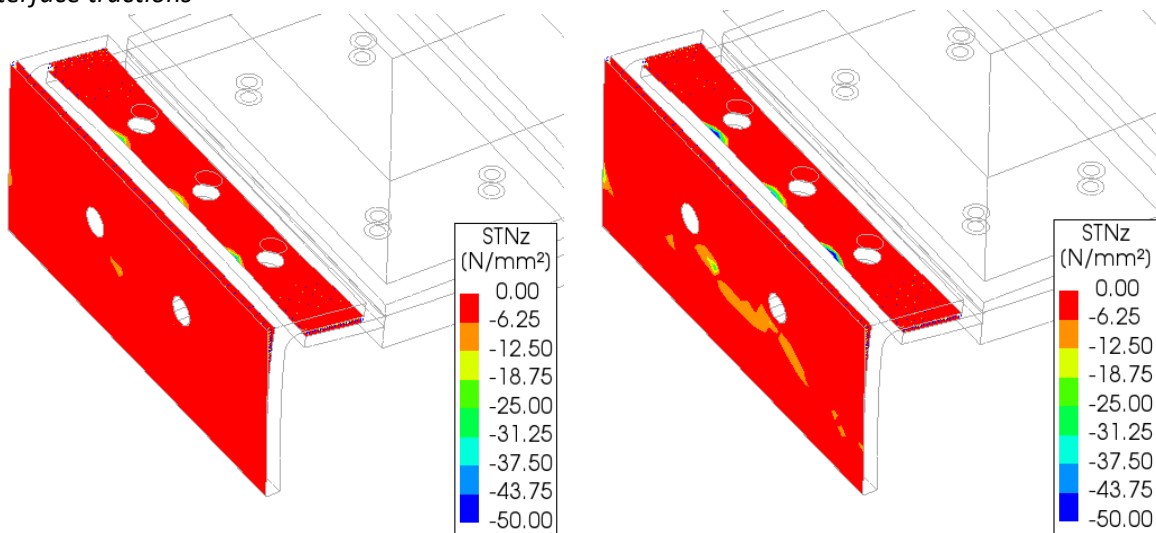


Figure 127 - Interface tractions at points B and D, left to right respectively.

It can be observed that the interfaces work as intended as there is no tension present. A compressive strut has developed below the anchors which is to be expected as the entire

connection is prone to rotation around the anchors. At deformation in x-direction is restrained by the concrete wall.

It can also be observed that near the location where the L-profile is bolted to the connecting plate the plates get compressed to each other. These are highly locally compressive forces and do not pose an issue with the connection.

7.2.2.4 Von mises stresses

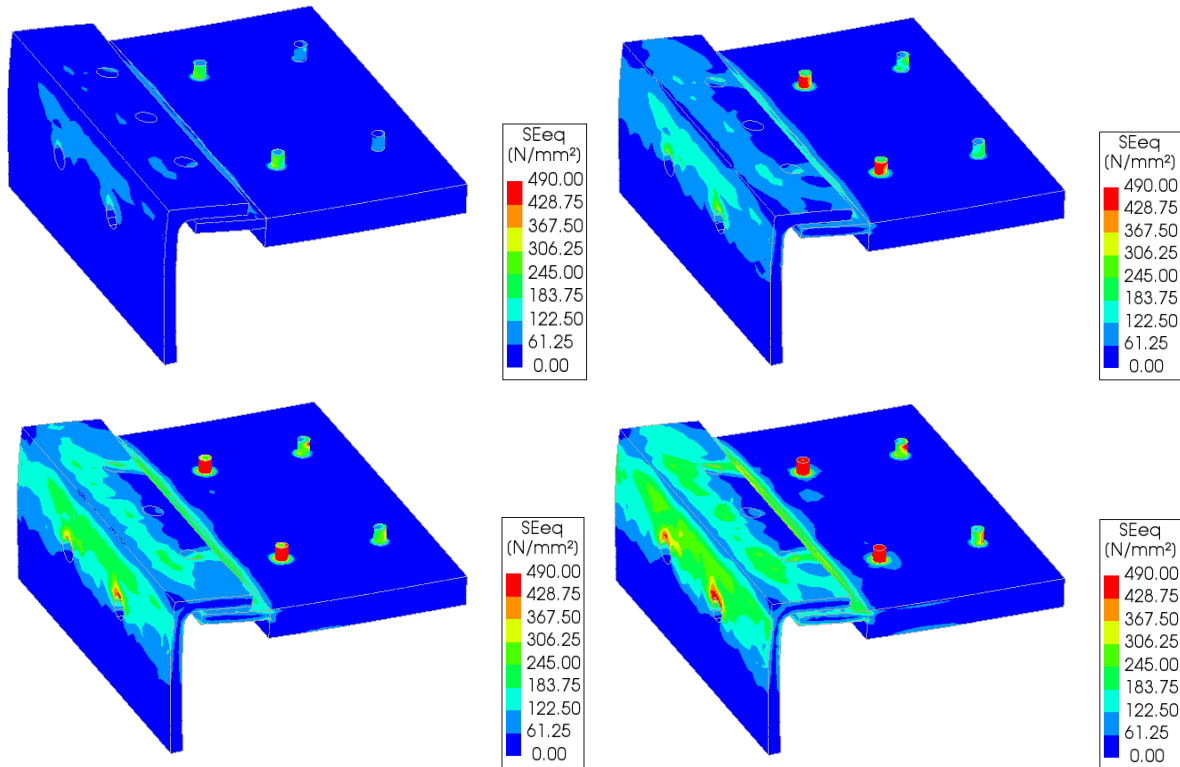


Figure 128 - Von mises stresses at points A to D, left to right top to bottom respectively.

The anchors close to the middle of the connection reach plasticity first. This is reflected in the von mises stresses as well. The stress in the plate material stays within the prescribed limit of 355Mpa with localize peaks of 490 Mpa where plasticity occurs which implies that the material properties are taken into account correctly.

7.2.2.5 Anchor reaction forces

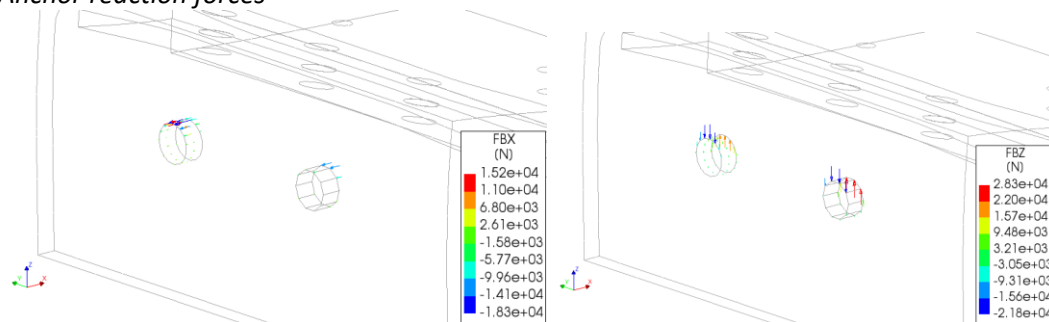


Figure 129 – Anchor forces at point D in global z and x axis, left to right respectively.

The anchor forces are modelled using a translational restraint in z and x-direction within the plate material of the L-profile. As no washers or contact distributors are modelled any singularities within the plate material at these locations are to be neglected.

The sum of forces within the anchors combined is 99,8kN and -61,7kN in z and x-direction respectively, mind the direction of the forces in the global axis of the model. This would account for a total exerted force of 50kN and -30.8kN per anchor.

7.2.3 Analytical solution

The numerical solution can be checked analytically. To observe the ductility of the connection the force needed to ensure a mechanism can be determined. A mechanism forms at the most critical points in the connection. In this case the mechanism forms at points MP1 and MP2, see Figure 130.

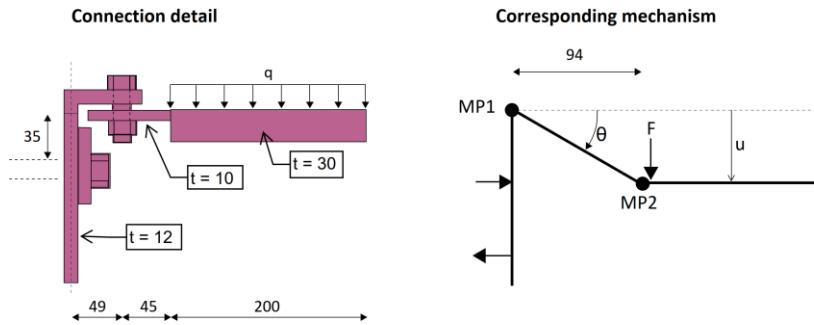


Figure 130 - Connection details and corresponding mechanism, left and right respectively.

The corresponding plastic moments to MP1 and MP2 are determined by the following equations:

$$MP1 = \frac{1}{4} \cdot b \cdot t^2 \cdot f_y = \frac{1}{4} \cdot 360 \cdot 12^2 \cdot 355 = 4.60 \text{ kNm} \quad \text{eq. 35}$$

$$MP2 = \frac{1}{4} \cdot b \cdot t^2 \cdot f_y = \frac{1}{4} \cdot 360 \cdot 10^2 \cdot 355 = 3.20 \text{ kNm} \quad \text{eq. 36}$$

With $\theta = u/l$ the virtual work equation can be expressed as follows:

$$MP1 \cdot \theta + MP2 \cdot \theta = F \cdot u \quad \text{eq. 37}$$

Solving for F the maximum shear force that leads to this mechanism is 83 kN. However, it should be noted that the yield stress could be higher which would increase the amount of shear force. It can be observed that at approximately 80kN the system is leaving its elastic regime and the first plastic nodes have been formed, see Figure 131.

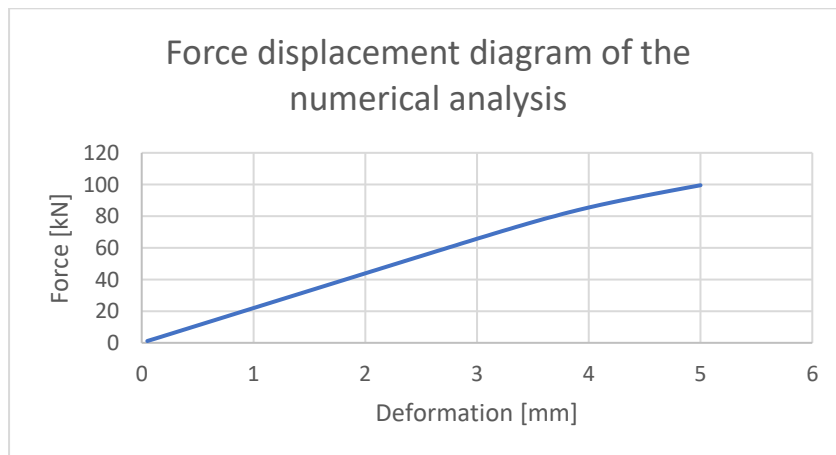


Figure 131 - Vertical force displacement results of the system.

7.2.4 Discussion

A total of 3 analysis have been performed. All the analysis were performed using nonlinear material and geometrical nonlinear properties. The geometrical nonlinearity only considers geometrical imperfections in the model while the material nonlinearity only considers nonlinear material behavior of the steel elements. The effects of these nonlinearities is clearly shown.

Two different solution methods have been used for all the analysis, namely Full Newton-Raphson and modified Newton-Raphson. The main difference between the methods is that the FNR method evaluated the stiffness at every iteration while the MNR assumes a constant stiffness for all iterations within the load step. The final results are based on the FNR method as the MNR was not able to find convergence in multiple load steps.

The first analysis has been performed using displacement control only where a vertical deformation has been applied to the model. The second analysis used force control where a lateral force is applied at the top half of the timber beam, representing wind loading. The third and final analysis was made using a combination of displacement and force control, combining both the vertical deformation and the horizontal force.

Displacement control restricts that degree of freedom in the area. This didn't pose a problem in this case as the vertical degree of freedom at the top of the beam is also restricted in the same direction in the case discussed.

The second aspect to consider is that no washers are modeled so any high stress concentrations near the bolts which connect the L-profile to the connecting plate and near the anchor locations where the anchors are connected to the L-profile are to be neglected.

7.2.5 Sub conclusion

The finite element program DIANA is suitable to perform nonlinear analysis. Geometrical and physical nonlinearity has been taken into account in the analysis. However, DIANA is not suitable to describe creep within timber elements as there are no standard packages available at this time. There are methods to write a sub program which can be imported by DIANA, however no such actions are attempted.

All vertical deformation due to elastic and shrinkage deformation can be taken by the slotted holes and the remainder of the deformation is due to creep of the timber elements. Depending on which model is being used, ie. Eurocode or experimentally, the remaining deformations exerted on the connecting is 5mm.

The amount of deformation exerted on the connection is based on the upper bound limit in which 5mm vertical deformation is to be expected in the connection. The connection itself is ductile enough to withstand the 'worst case scenario', ie. vertical deformation combined with a static wind loading. Some plasticity is to be expected, especially due to the vertical deformation but this doesn't pose any major issues in the connection between the concrete and timber elements.

Due to the eccentricity of the applied load to the location of the anchors due to mechanical theorem a large amount of the vertical forces would transfer to horizontal forces exerted on the anchors. The anchor forces in the concrete are subjected thus to substantial vertical and horizontal forces, as is to be expected.

8 Limit of the system

An interesting question arises, what are the limitations of the current system. In other words, how high can we built? In order to investigate this, the definition of the limit has to be defined first. There are a few criteria that could be considered regarding strength and stability. The stress in the timber columns and beam may not exceed the maximum stress limit of the materials. The second criteria is flexural buckling of the timber columns. The external applied load cannot exceed the buckling load.

8.1 System at hand

When determining the limit of the system it is important to ensure the behavior of the system is as it is intended to be. The current system consists of a concrete core and a timber frame. As intended, the timber frame derives its lateral stability from the concrete core, see Figure 132. The vertical loads are taken by the timber frame itself. Deformation differences must be allowed to occur to prevent unintended stresses in the connections.

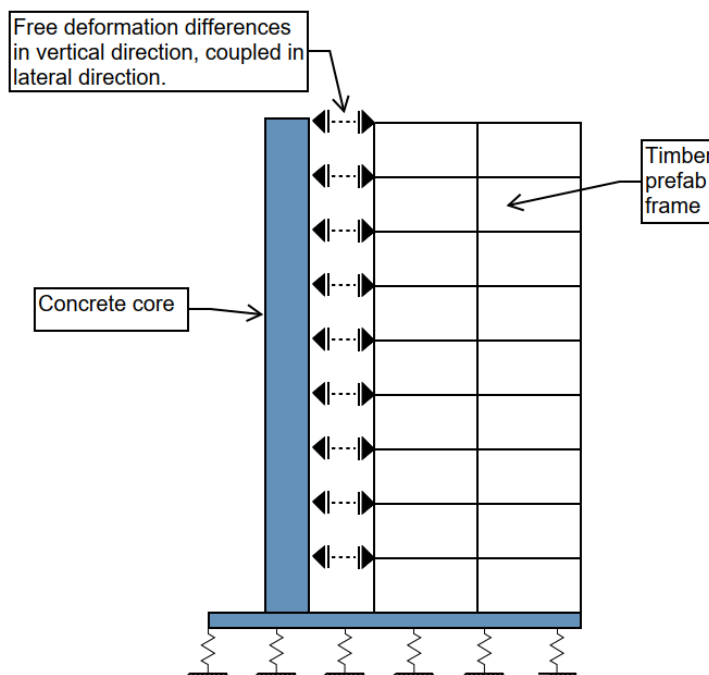


Figure 132 - System at hand with a concrete core and prefabricated timber frame.

8.2 Several limits

There are a few criteria that determine the limit of a system. These criteria can be distinguished into strength and stability limits. The strength criteria limits the amount of stress transferred through the system to the maximum stress limit allowed by the materials. The stability criteria limits the amount of stress through a column to ensure it doesn't buckle. The smallest load of these checks will determine the maximum load that can be applied to the system.

8.2.1 Stress limit Column

The column $b \times h = 200 \times 360 \text{ mm}$ GL24h is parallelly loaded to the fiber. The maximum allowable stress limit $f_{c,0,k}$ is 24Mpa. The maximum allowable stress is defined by the following equation

$$\sigma_{c,0,d} \leq f_{c,0,d}$$

$$f_{c,0,d} = k_{mod} \cdot \frac{f_{c,0,k}}{\gamma_m} = 0,6 \cdot \frac{24}{1,25} = 11,52 \text{ MPa} \quad \text{eq. 38}$$

The maximum allowable force on the system therefore is $F_d \leq f_{c,0,d} \cdot A = 11,52 \cdot 72000 = 830 \text{ kN}$

Beam

The Kerto-S beam $b \times h = 200 \times 420 \text{ mm}$ is perpendicularly loaded to the fiber. The maximum allowable stress limit $f_{c,90,k}$ is 6 Mpa. The maximum allowable stress is defined by the following equation $\sigma_{c,0,d} \leq k_{c,90,k} \cdot f_{c,0,d}$

$$f_{c,0,d} = k_{mod} \cdot \frac{f_{c,90,k}}{\gamma_m} = 0,6 \cdot \frac{6}{1,2} = 3,0 \text{ MPa} \quad \text{eq. 39}$$

The maximum allowable force on the system therefore is $F_d \leq k_{c,90,k} \cdot f_{c,0,d} \cdot A_{eff} = 1,75 \cdot 3,0 \cdot 84000 = 441 \text{ kN}$

8.2.2 Buckling load

The maximum buckling load of the column is determined by determining the maximum buckling load. This load cannot be exceeded. A combination of axial load in combination with bending should also be checked.

The following parameters are used in the calculations:

$f_{c,0,k} = 24 \text{ Mpa}$

$L_{buc} = 2850 \text{ mm}$

Width = 200 mm

Height = 360 mm

$E_{0,05} = 9600 \text{ Mpa}$

In the current system there is no moment present on the columns. However as is done in common engineering practice a moment of 0.02F will be assumed on the column to determine the maximum buckling load. Another assumption is done in regards that the columns cannot buckle around their weak axis.

$$\lambda = \frac{l_{buc}}{\sqrt{I/A}} = \frac{2850}{103,92} = 27,42 \quad \text{eq. 40}$$

$$\lambda_{rel} = \frac{\lambda}{\pi} \cdot \sqrt{\frac{f_{c,0,k}}{E_{0,05}}} = \frac{2850}{\pi} \cdot \sqrt{\frac{24}{9600}} = 0,44 \quad \text{eq. 41}$$

$$k = 0,5 \cdot (1 + 0,2 \cdot (\lambda_{rel} - 0,3) + \lambda_{rel}^2) = 0,61 \quad \text{eq. 42}$$

$$k_c = \frac{1}{k + \sqrt{k^2 - \lambda_{rel}^2}} = 0,97 \quad \text{eq. 43}$$

The maximum allowable stress is determined according to $k_c \cdot f_{c,0,d} = 11,15 \text{ Mpa}$.

The corresponding design load is approximately $F_d = 600 \text{ kN}$

8.2.3 System deformations

Based on the calculations done in chapters 8.2.1 and 8.2.2, the maximum design load is 441 kN for the beam. For the current system this means a maximum of 10 stories excl. ground floor. The corresponding deformations to this system with 10 stories will be determined.

A few notes have to be provided however. Due to the low stiffness of the acoustic felt the increase in loading creates unrealistic large deformations. The stiffness of the acoustic felt presented in previous chapters is not suitable for the limits explored in this chapter. Therefore, when determining the deformations the **elastic deformation of the acoustic felt is limited to 1.5mm**. This value is the same as is tried to achieve for the project Buiksloterham. This means that when searching for the limit of the system the stiffness of the acoustic felt should be such that the elastic deformation is approximately 1.5mm.

The deformation difference corresponding to a 10 story apartment building is 46mm when the upperbound theory is applied an 37mm when the Eurocode is applied.

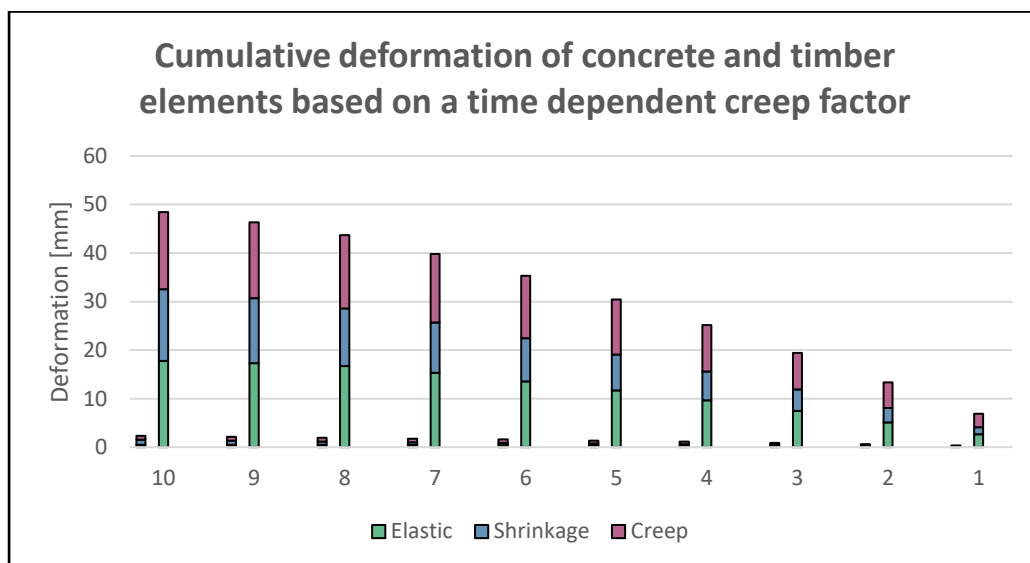


Figure 133 - Deformation of timber and concrete elements per floor based on a time dependent creep factor.

8.3 Optimizations to the system

These deformations are quite large and could be taken properly taken care of. A few optimizations to the current system could be made:

Changing the loadbearing structure

By changing the loadbearing structure to a column only structure the loading on the system can be increased. The length of the column slightly increases so the buckling load will decrease to 590 kN. However, an additional 3 stories can be added to the system, bringing the total to 13. The structural beam is a large benefactor to the total deformation. Removing the beam will decrease the total deformation drastically, see Figure 134.

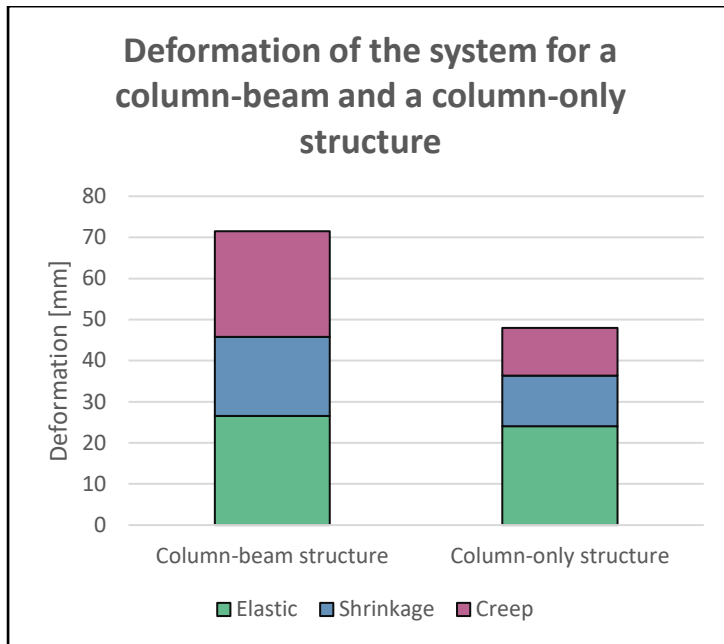


Figure 134 - Deformations for a column-beam structure and a column-only structure.

Optimizing the connection

Allowing the deformation to occur is one of the key points of this system. Allowing free vertical deformation of the timber frame in relation to the concrete core prevents unwanted stresses in the system. The current connection assumes a sliding connection where vertical deformation is allowed by means of a slobgat. However, an assumption is made that the connection, or specifically the L-profile is able to slide freely against the concrete. If this would not be the case due to friction between the L-profile and the concrete, a moment connection would arise, clamping the connection. To ensure a sliding connection, any friction should be addressed. This could easily be done by applying a layer of Teflon or similar product between the concrete and the steel profile, see Figure 135.

Another optimization of the connection is not one of structural nature but rather of building physics. There are 4M12 anchors present to align the units. These anchors protrude into the acoustic felt, assuming a rather standard nut + washer the anchors protrude approximately 10-12mm into the acoustic felt. With an increasing deformation a 'leak' will arise if the sound is traveling through the anchors instead of the acoustic felt. To ensure this doesn't happen the 4M12 anchors should be recessed into the coupling plate, see Figure 135.

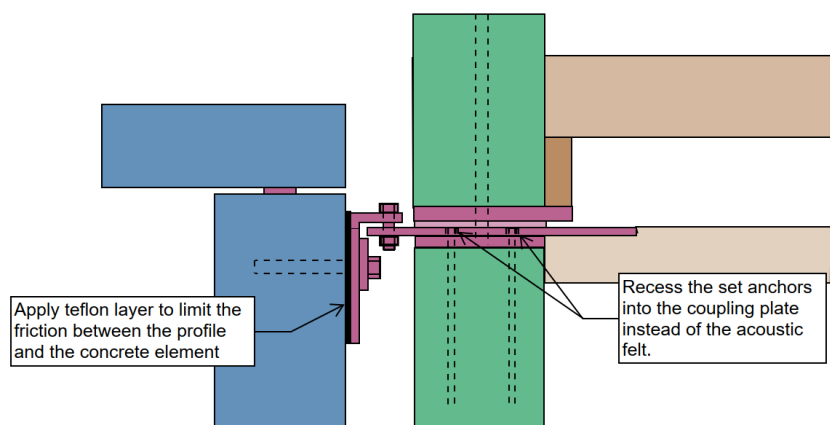


Figure 135 - Timber-column tensile connection with optimizations.

9 Conclusion and recommendations

Two models have been constructed to determine the amount of vertical deformation in the timber elements. The first one is based on the Eurocode and the second one is based on experimental research. These models provide an upper and lower limit. Both models are taken into consideration during this research. Both models have been analytically derived and are numerically validated. As of yet, there is limited research supporting the experimentally based model. However, the experimentally based model does distinguish between loading parallel and perpendicular to the grain which the Eurocode does not. When applying the models to the system considered within this thesis the expected deformation differences between the timber units and concrete core are between 24 and 28mm at the first floor.

Depending on the model used, the components that have the greatest impact on the differences are the structural beams and the acoustic felt. By limiting the contributions of these components the difference could be greatly reduced.

- Instead of a column-beam structure, a column-only structure where the beam is situated between the columns would greatly improve the vertical deformation. A reduction of 34% in vertical deformation of the timber system can be expected when the beam is no longer part of the main loadbearing structure.
- Optimizing the connection to allow for greater deformations. This could be done to introduce a 'sliding' connection where the tolerance of the connection is greatly improved. To ensure the connection is working properly, a layer of Teflon could be applied to prevent the connection from clamping.
- Although for smaller projects an elastic acoustic felt can be used, the amount of elastic deformation produced by this component is substantial (up to 40% within the lower bound model). For increasingly larger projects another type of loadbearing acoustic limiter should be applied.

Both models take into account hydrogenic properties of timber. In attempt to model and validate this behavior, several measurements were taken in the assembly factory and at the construction site. Research recommends taking into account an increase of MC of the timber elements during construction by 0.2% per month when fully wrapped. However, this highly depends on various parameters including but not limited to: The way the units are wrapped and stored after assembly, the relative humidity and temperature of the surroundings, the amount of exposure to wind, the density of the timber units itself. It can be concluded that this value should strictly be taken as a guideline. It should also be noted that the timber elements always should be stored and installed with care and should never be exposed to the elements.

After installing the units, the rate of diffusion is difficult to model as numerous variables play a role. It is therefore recommended to determine the overall shrinkage during its entire lifetime instead. In the case of an increased moisture content within the units, for instance due to the pouring of a concrete slab, the creep is likely to increase due to mechano-sorptive creep, this phenomenon has however not been explored as it was outside the scope of this thesis. The temporary increase of the timber volume has no impact on the total deformations as the units are already connected to the concrete core.

Depending on the building order, a certain amount of elastic deformation can be mitigated during construction. Preloading the units can increase the amount of deformation that can be mitigated. Theoretically a small amount of viscoelastic deformation could also be negated by preloading of the units but the amount is negligible.

The connection between the timber and concrete elements has a built in tolerance to account for any vertical deformations differences. A tolerance of 35mm has been added above the anchor, in which 15mm is reserved for fitting and adjustment and 20mm for vertical deformation differences. This tolerance proved to be more than sufficient, provided that the behavior of the connection is as it is intended. This means that the connection is free to move in vertical direction while providing resistance in lateral direction. To ensure this 'sliding' behavior, the connection could be improved by adding a layer of elastomeric bearing (a layer of Teflon for instance) between the concrete and the connection.

The ductility of the connection has been numerically explored. The connection proved ductile enough to withstand the forces in case the tolerance of 20mm is exceeded. A mechanism will form in the connection at a shear force of approximately 83kN. This value has been analytically derived and verified by numerical results. It should be noted that in practice this value could be higher as the yield stress of the steel will increase and the stresses will be redistributed within the material. This has also been shown in the numerical results. However, the force required to obtain this mechanism is much lower as the elastic limit of the timber elements, 441 kN for the beam and 600 kN for the column. This means that the connection will deform much faster than the timber elements.

The limit of the system in its current state has been explored. This limit is defined by its ULS requirements. The main limiter of the system is the crushing load of the beam at approximately 441 kN. If the beam were absent the main limiter would be the column which can withstand a load of 600 kN. This translates to a system of roughly 10-13 stories. In order to extend this system to its limit the deformations must be free to occur. Any hindrance of vertical deformation differences induces unintended large and complex forces into the system. Advice on how to prevent these forces has been given by optimizing the connection.

Recommendations

- The Eurocode does not provide a time dependency for creep nor does it differentiate creep originating from loading perpendicular or parallel to the grain of the timber. Although some research has been done regarding this topic, standardization is yet nonexistent.
- At this moment in time there are very limited options to model creep in timber elements. Standardization of modelling these phenomenon's is needed to improve numerical modelling.
- The ingress and egress of moisture during construction and after installing should be treated as an approximation. Extensive research could be undertaken to determine the swelling and shrinkage rate during and after construction under varying conditions.

Bibliografie

- [1] "Monadnock building," [Online]. Available: https://en.wikipedia.org/wiki/Monadnock_Building.
- [2] The editors of Encyclopedia Britannica, "Skyscraper building," [Online]. Available: <https://www.britannica.com/technology/skyscraper>.
- [3] Wikipedia, "Architecture," [Online]. Available: <https://en.wikipedia.org/wiki/Architecture>.
- [4] Pixabay, "Pixabay," [Online]. Available: <https://pixabay.com/nl/photos/chicago-architectuur-stad-449021/>.
- [5] M. F. L. Mallo and O. Espinoza, "Outlook for Cross-laminated timber in the United States.," *Departement of bioproducts and biosystems engineering. University of Minnesota*.
- [6] M. McLaren, "The world's tallest wooden buildings," 2022. [Online]. Available: <https://www.designbuild-network.com/analysis/worlds-tallest-wooden-buildings/#:~:text=%E2%80%9CMurray%20Grove%20was%20named%20the,prefabricated%20cross%20laminated%20timber%20panels.%E2%80%9D>.
- [7] "Beautiful and sustainable wooden skyscrapers," 27 10 2021. [Online]. Available: <https://www.webuildvalue.com/en/global-economy-sustainability/mjostarnet-wooden-skyscrapers.html>.
- [8] Lindner, "Hoho vienna," [Online]. Available: https://www.lindner-group.com/en_GB/references/detail/hoho-vienna-32712/.
- [9] H. Wind, "HAUT: De uitdagingen van hoogbouw in hout," 25 03 2022. [Online]. Available: <https://www.jpvanesteren.nl/nl/haut-de-uitdagingen-van-hoogbouw-hout>.
- [10] Food and Agriculture Organization of the United Nations, The state of the world's forests, Food and Agriculture Organization of the United Nations, 2020.
- [11] H. B. a. C. Sandhaas, Timber Engineering principles for design, KIT Scientific publishing, 2017.
- [12] Wikipedia, "Softwood," 11 04 2022. [Online]. Available: <https://en.wikipedia.org/wiki/Softwood>.
- [13] Britannica encyclopedia, "Wood as a material," [Online]. Available: <https://www.britannica.com/science/wood-plant-tissue/Wood-as-a-material>.
- [14] W. propertiew, "Wood properties," [Online]. Available: <https://www.fao.org/3/j8289e/J8289E05.htm>.
- [15] Pixabay, "Pixabay," [Online]. Available: <https://pixabay.com/nl/photos/bar-houten-balken-borden-61846/>.
- [16] Pinterest, "Pinterest," [Online]. Available: <https://nl.pinterest.com/pin/621567186055006427>.
- [17] "HRB," [Online]. Available: <https://www.hrb.be/wat-is-clt/>.
- [18] MetsaWood, "Kerto LVL S-beam," Kerto, [Online]. Available: <https://www.metsawood.com/nl/producten/Kerto/Pages/Kerto-S.aspx>.
- [19] R. Hankinson, "Investigation of crushing strength of spruce at varying angles of grain.," 1921.
- [20] "NEN-EN1995-1-1_2005," in *Eurocode 5*, p. 2.2.3.
- [21] O. Willebrands, "Differential vertical shortening in timber-concrete high-rise structures," 2017.
- [22] G. Granello and A. Palermo, "Creep in Timber: Research overview and comparison between code provisions," 2019.
- [23] W. F, F. A and F. M, "Long-term behavior of post-tensioned timber connections," *Journal of Structural engineering*, 2014.
- [24] S. A. P. and B. J., "Wood as a linear orthotropic viscoelastic material.," *Wood science and technology*, 1972.
- [25] F. Massaro and K. Malo, "Long-term behavior of Norway spruce glulam loaded perpendicular to the grain," 2019.
- [26] M. D. Meijer and H. Militz, "Moisture transport in coated wood. Part 1: Analysis of sorption rates and moisture content profiles in spruce during liquid water uptake.," 2000.
- [27] M. Shirmohammadi, W. Leggate and A. Redman, "Effects of moisture ingress and egress on the performance and service life of mass timber products in buildings: a review," *Construction and building materials*, p. 14, 2021.
- [28] S. V. Glass and S. L. Zelinka, "General Technical report FPL-GTR-190," in *Wood Handbook - Wood as an Engineering material.*, 2010, p. 508.
- [29] "Fibre saturation point," 2015. [Online]. Available: https://en.wikipedia.org/wiki/Fibre_saturation_point.
- [30] B. Franke, S. Franke, M. Schiere and A. Müller, "Moisture diffusion in wood - Experimental and

- numerical investigations," *WCTE 2016 World conference on Timber Engineering*, 2016.
- [31] M.-L. Sortland, "Moisture induced deformations in prefabricated wooden building modules,," 2016.
- [32] Z. Xiong Yu, R. Su Xin and O. Sabri, "Vertical displacements in a medium high-rise timber building," 2009.
- [33] Trada Technology, "Trada moisture in timber - wood information sheet," 2011.
- [34] H. M. Künzel, "Indoor Relative Humidity in Residential Buildings – A Necessary Boundary Condition to Assess the Moisture Performance of Building Envelope Systems," 2005.
- [35] K. Shepard and N. Gromicko, "The history of concrete," n.d.. [Online]. Available: <https://www.nachi.org/history-of-concrete.htm#ixzz31V47Zuuj>.
- [36] Pixabay, "Pixabay," [Online]. Available: <https://pixabay.com/nl/photos/gizeh-piramide-piramides-1756946/>.
- [37] n.d., "Cement history," [Online]. Available: <https://www.understanding-cement.com/history.html>.
- [38] A. Swenson, "Construction building," [Online]. Available: <https://www.britannica.com/technology/construction>.
- [39] n.d., "Precast concrete history," [Online]. Available: <https://www.metromont.com/precast-concrete-history/>.
- [40] "The history of precast concrete elements - The development of industrialized construction with precast concrete,," [Online]. Available: <https://www.prihofer.com/precast-history>.
- [41] n.d., "Cementing growth in an oversupplied market," 2019. [Online]. Available: <https://www.accenture.com/us-en/blogs/chemicals-and-natural-resources-blog/cementing-growth-in-an-oversupplied-market>.
- [42] "Cement, how it is made,," 2007. [Online]. Available: <https://www.youtube.com/watch?v=n-Pr1KTVSXo>.
- [43] Civiljungle, "Civiljungle," [Online]. Available: <https://civiljungle.com/cement-ingredients/>.
- [44] B. Mahajan, "Concrete," n.d.. [Online]. Available: <https://civiconcepts.com/blog/concrete>.
- [45] Ceramica, "Ceramica," [Online]. Available: https://ceramica.fandom.com/wiki/Fly_ash.
- [46] Bestsupportunderground, "Bestsupportunderground," [Online]. Available: <https://bestsupportunderground.com/plasticizers-concrete/?lang=en>.
- [47] M. Bangash, "Concrete and concrete structures: Numerical modelling and applications," 1989.
- [48] A. Neville and J. Brooks, "Concrete Technology - second editon," 2010.
- [49] Municipality of Amsterdam, "Buiksloterham&Co: woningen en bedrijfsruimten," n.d.. [Online]. Available: <https://www.amsterdam.nl/projecten/buiksloterham/deelproject/buiksloterham-co/>.
- [50] De Groot Vroomshoop, "Start hoogbouw met houtmodulebouw in buiksloterham," 2022. [Online]. Available: <https://degrootvroomshoop.nl/groep/start-hoogbouw-met-houtmodulebouw-in-buiksloterham/>.
- [51] Finch Buildings, "Finch buildings," n.d.. [Online]. Available: <https://finchbuildings.com/>.
- [52] e. NEN 6069:2011+C1:2019 Brandwerendheid, 2019.
- [53] SteelConstructionInfo, "Fire and steel construction," [Online]. Available: https://www.steelconstruction.info/Fire_and_steel_construction.
- [54] SteelConstructionInfo, "Fire testing," [Online]. Available: https://www.steelconstruction.info/Fire_testing.
- [55] E. Borgström and J. Fröbel, *The CLT Handbook, CLT structures - facts and planning*, 2019.
- [56] V. Consolis, "Isolatieplaatvloer 200," VBI, [Online]. Available: <https://vbi.nl/download/isolatieplaatvloer-200/>.
- [57] PCE-instruments, "PCE-instruments," 2022. [Online]. Available: https://www.pce-instruments.com/dutch/meettechniek/meetapparatuur-voor-alle-parameters/vochtmeter-vochtigheidsmeter-absoluut-brookhuis-applied-technologies-b.v.-absolute-vochtigheidsmeter-fmd-6-ramelektrode-set-111.806-det_2213371.htm.
- [58] Brookhuis, Brookhuis, 2022. [Online]. Available: https://www.pce-instruments.com/dutch/meettechniek/meetapparatuur-voor-alle-parameters/houtvochtigheidsmeter-brookhuis-applied-technologies-b.v.-houtvochtigheidsmeter-fmw-t-det_2211373.htm?_list=qr.art&_listpos=3.
- [59] KNMI, "KNMI," [Online]. Available: <https://www.knmi.nl/nederland-nu/klimatologie/daggegevens>.
- [60] "Wood as a material," [Online]. Available: <https://www.britannica.com/science/wood-plant-tissue/Wood-as-a-material>.
- [61] "<https://www.fao.org/3/j8289e/J8289E05.htm>," [Online]. Available:

- <https://www.fao.org/3/j8289e/J8289E05.htm>.
- [62] R. Kingston, "Creep, relaxation, and failure of wood. Research applied in industry," 1962.
- [63] L. A. Soltis and T. D. Gerhardt, "Shear design of wood beams - State of the art," 1988.
- [64] S. Timoshenko, "Strength of materials - Part 1.," 1955.
- [65] B. Yang, P. Clauston and A. C. Schreyer, "Torsional shear test on laminated veneer lumber using a universal-type test machine," *Journal of materials in civil engineering*, p. 2, 2013.
- [66] Kuipers Funderingstechnieken, "Technische specificaties DPA schroefpalen," 2022. [Online]. Available: <https://www.kuiperslemmer.nl/producten/dpa-schroefpalen/technische-specificaties-dpa-schroefpalen>.
- [67] "BS EN 942 - General requirements of timber in joinery," 2007.
- [68] [Online]. Available: <https://www.betoninfra.nl/kennisportaal/betontechnologie/de-28-daagse-sterkte>.

Attachment A – Reading guide main and sub questions

To ensure the research goes smoothly a number of main and sub questions have been formulated. These questions are discussed in detail. For clarification this guide is provided to quickly find the answers to the questions. A table has been provided where the answer to the questions is located within the thesis and for convenience the questions are listed below.

Table 1 - Summary of questions with their corresponding sections.

Question	Section	Page
Main research question	8	116
1.1	Timber: 2.4, concrete: 3.5	24-31, 38-42
1.2	Timber: 2.4, concrete: 3.5, 4.14	24-31, 38-42, 81-82
1.3	2.4.3	27-31
1.4	4.7.3	81-82
1.5	4.7.3	81-82
1.6	4.13.2	74-76
2.1	4.13	72-82
2.2	4.13	72-82
2.3	Timber: 4.13.3.1, concrete: 4.13.2.1	76,74
2.4	4.8	63-64
2.5	4.9	65-66
3.1	2.4, 6	24-31, 95-101
3.2	2.4, 6	24-31, 95-101
3.3	6	95-101
4.1	4.12	69-71
4.2	4.13	72-82
4.3	4.13	72-82
5.1	4.10-4.11, 4.13.1	67-69, 72-73
5.2	6	95-101
6.1	4.11	68-69
6.2	4.7, 7.2	55-62, 106-115
6.3	7.2.1.4	110
6.4	7.2	106-115
7.1	7.2.2	112-115
7.2	4.11	68-69

Main research question

Various studies have been conducted into hybrid high-rise structures with wood. This research examines the settlement differences between a concrete core and the timber frame structure. A case study will be done to comprise a theoretical model based on experimental data. To ensure a proper flow of this research a main research question has been composed:

How can vertical straining differences in timber hybrid high-rise structures be minimized in practice by optimizing parameters by exploring a theoretical model?

Sub research questions

As the main question will provide a wide range of answers and cannot be answered with a simple yes or no. To support the main question a number of sub questions have been formulated. These sub questions can be found below and will be addressed during the research.

Sub question 1 (SQ1): Are the actual settlements located at the expected locations according to the theoretical expected settlements?

- SQ 1.1 What kind of settlements can be expected (elastic, plastic, time dependent etc.)?
- SQ 1.2 What kind of models exist to estimate these settlements?
- SQ 1.3 How do environmental influences impact the settlement?
- SQ 1.4 What are the theoretical expected locations where the settlement occurs?
- SQ 1.5 Where are the biggest settlements in practice?
- SQ 1.6 What are the expected settlements of the concrete core per level?

Sub question 2 (SQ2): How does the height of the structure affect the settlement for each floor?

- SQ 2.1 Is there a relation between the applied normal force and the expected deformation?
- SQ 2.2 What is the difference in settlement between the concrete core and the timber loadbearing structure?
- SQ 2.3 How does the elastic deformation relate to the total deformation?
- SQ 2.4 How does the stiffness of the foundation impact the settlement and deformations of the timber units?
- SQ 2.5 How does the stiffness of the core impact the settlement and deformations of the timber units?

Sub question 3 (SQ3): How will different load applications (parallel and perpendicular to the grain) influence the settlement behavior?

- SQ 3.1 What is the settlement behavior of wood when loaded perpendicular to the grain?
- SQ 3.2 What is the settlement behavior of wood when loaded parallel to the grain?
- SQ 3.3 How do the dimensions of the loaded specimen relate to the stress distribution?

Sub question 4 (SQ4): What is the common applied building order of the structure and how will changing the order effect the settlement behavior?

- SQ 4.1 What is the building order applied to Buiksloterham?
- SQ 4.2 What is the expected deformation during construction?
- SQ 4.3 Is there a relation between the building order and the expected deformation?

Sub question 5 (SQ5): What is the structural composition of the timber units and is it possible to improve settlement behavior by optimizing this composition?

- SQ 5.1 What is the current structural composition of the timber modular units?
- SQ 5.2 Can the structural composition be optimized by applying different kinds of wood (LVL, CLT)?

Sub question 6 (SQ6): How does the settlement impact the connections of the timber units?

SQ 6.1 What kind of connections are applied within the modular units?

SQ 6.2 What kind of loads do the applied connections transfer?

SQ 6.3 What kind of deformations/rotations are allowed in the connections?

SQ 6.4 What are the limitations to the connections currently applied within the system?

Sub question 7 (SQ7): How are the timber units attached to the concrete core?

SQ 7.1 What are the failure mechanisms of the connection?

SQ 7.2 How is vertical deformation allowed while limiting the horizontal deformation?

General loads				
Amount of floors	6			
Timber units	Material	Depth [mm]	g_k [kN]	q_k [kN]
Ceiling	CLT	80	0,50	0,00
Slab	CLT	120	1,20	0,00
Finish		60	0,60	0,00
Facade panels			0,50	0,00
General loadcase class	Class A - Floors			1,75
Partition walls				0,80
Roof			14,00	10,00
Concrete elements	Material	Depth [mm]	g_k [kN/m ¹]	q_k [kN/m ¹]
Slab	prefab	200	5	0
Finish		130	3,25	0
Walls	prefab	200	5	0
Facade panels			0	0
General loadcase class	Class A - Floors			1,75
Partition walls				0,8
Roof			7,5	5,2

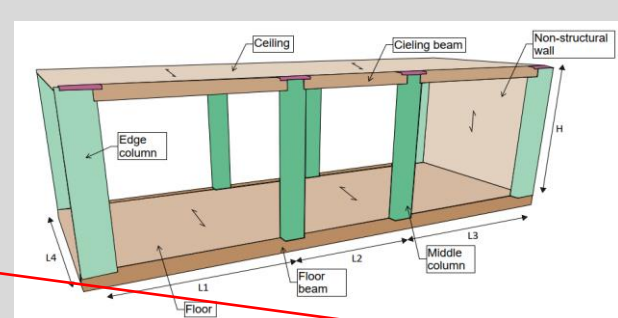
Generate output

After all the inputs are correct the output can be generated

General load tab for the timber units

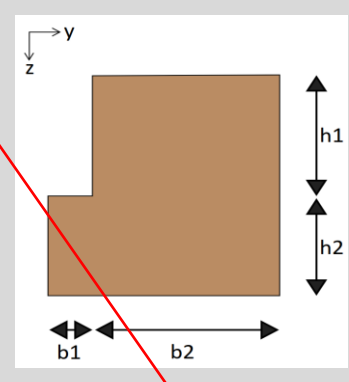
General load tab for the concrete units

Dimensions	
Timber units	[m]
H [m]	2,85
L1 [m]	3,2
L2 [m]	2,4
L3 [m]	3,2
L4 [m]	4
Climate class	1
Mc at final setting [%]	9,27
Season of installment	jun
Time between manufacturing and installment [days]	14
Installment cycle [days]	7
Creep calculation	Experimental
Timber floor Beam	
Material	LVL-KertoS
h1 [mm]	120
h2 [mm]	100
b1 [mm]	40
b2 [mm]	164
Compressive area A [mm ²]	84000
Continuous	Yes
Climate class	1
MC at production [%]	10
Perpendicular shrinkage coefficient	0,32



Dimensions input section for the timber units

Based on indoor conditions with relative humidity of 50% and a temperature of 20 degrees



Dimensions input for the timber beam

Based on the selected month the average relative humidity and temperature is taken to calculate the corresponding moisture content of the timber for these conditions. These average values are based on the weather in Amsterdam from 2021.

An option is given to calculate the creep as per Eurocode and experimentally based. The Eurocode does not have a time dependency while the experimentally based calculation does. If therefore the EC curve is selected the creep deformations during construction will automatically be 0. Another difference is that in the EC no distinction is made for timber loading parallel and perpendicular to the grain. If experimentally is selected the creep calculation for loading perpendicular to the grain is 4.5 times the creep parallel to the grain.

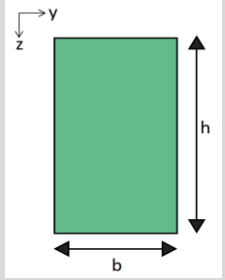
If continuous is selected the compressive area is increased by 60mm (30mm on each side)

Input tab 2-2

Timber column		
Material	GL24h	
h [mm]	360	
b [mm]	200	
A [mm ²]	72000	
Climate class	1	
MC at production [%]	12	
Longitudinal shrinkage coefficient	0,011	

Concrete slab		
Class	C55/67	
Prefabricated	Yes	
Span [m]	3,8	
Time between manufacturing and installment [days]	10	(Average of 10 days after casting)
Day at which curing ended [days]	1	If no curing: 1
RH at final setting [%]	65	

Concrete wall		
Class	C55/67	
Prefabricated	Yes	
Height [m]	2,8	
Age of concrete at time of loading [days]	10	
Day at which curing ended [days]	1	
RH at final setting [%]	65	



Input for the timber columns

Input for the concrete slab

Input for the concrete walls

Acoustic felt		
Level	E modulus [Mpa]	height [mm]
0	17	15
1	17	15
2	17	15
3	17	15
4	9,2	15
5	8,16	15
6	4,57	15

Depending on the amount of floors indicated at the top of the input tab the amount of different acoustic felts can be set up for each floor.

Loads tab 1-2

Timber units									
Load#	Type	g_k	q_k	m^2	F_{gk}	F_{qk}	F_k	$F_{qk,creep}$	$F_{k,construction}$
FC6	Roof	14,0	10,0	1,0	14,0	10,0	24,0	10,0	0,0
FC5	FC6				14,0	10,0	24,0	10,0	0,0
	Ceiling(80 mm CLT)	0,5	0,0	5,6	2,8	0,0	2,8	0,0	2,8
	Slab(120 mm CLT) +Finish	1,8	2,6	9,0	16,1	22,8	39,0	22,8	16,1
	Facade panels	0,5	0,0	10,4	5,2	0,0	5,2	0,0	5,2
					38,1	22,8	61,0	22,8	24,1
FC4	FC5				38,1	22,8	61,0	22,8	
	Ceiling(80 mm CLT)	0,5	0,0	5,6	2,8	0,0	2,8	0,0	2,8
	Slab(120 mm CLT) +Finish	1,8	2,6	9,0	16,1	22,8	39,0	22,8	16,1
	Facade panels	0,5	0,0	10,4	5,2	0,0	5,2	0,0	5,2
					62,2	45,7	107,9	45,7	24,1
FC3	FC4				62,2	45,7	107,9	45,7	
	Ceiling(80 mm CLT)	0,5	0,0	5,6	2,8	0,0	2,8	0,0	2,8
	Slab(120 mm CLT) +Finish	1,8	2,6	9,0	16,1	22,8	39,0	22,8	16,1
	Facade panels	0,5	0,0	10,4	5,2	0,0	5,2	0,0	5,2
					86,3	54,8	141,2	52,6	24,1
FC2	FC3				86,3	54,8	141,2	52,6	
	Ceiling(80 mm CLT)	0,5	0,0	5,6	2,8	0,0	2,8	0,0	2,8
	Slab(120 mm CLT) +Finish	1,8	2,6	9,0	16,1	22,8	39,0	22,8	16,1
	Facade panels	0,5	0,0	10,4	5,2	0,0	5,2	0,0	5,2
					110,5	64,0	174,4	59,4	24,1
FC1	FC2				110,5	64,0	174,4	59,4	
	Ceiling(80 mm CLT)	0,5	0,0	5,6	2,8	0,0	2,8	0,0	2,8
	Slab(120 mm CLT) +Finish	1,8	2,6	9,0	16,1	22,8	39,0	22,8	16,1
	Facade panels	0,5	0,0	10,4	5,2	0,0	5,2	0,0	5,2
					134,6	73,1	207,7	66,3	24,12

Weights

Live loads

Square meters of loading

Dead loads

Live loads based on ϕ_0 factor

Characteristic loads (no safety factors applied)

Live loads based on ϕ_2 factor

Dead loads of the corresponding floor

Loads tab 2-2

Concrete elements										
Load#	Type	g_k	q_k	m^2	F_{gk}	F_{qk}	F_k	$F_{qk,creep}$	$F_{k,construction}$	
WC6	Roof		7,5	5,2	1,0	7,5	5,2	12,7	5,2	0,0
WC5	WC6					7,5	5,2	12,7	5,2	0,0
	Walls(200 mm prefab)	5,0	0,0	2,8	14,0	0,0	14,0	0,0	0,0	14,0
	Slab(200 mm prefab) + Finish	8,3	2,6	1,9	15,7	4,8	20,5	4,8	4,8	15,7
	Facade panels	0,0	0,0	2,8	0,0	0,0	0,0	0,0	0,0	0,0
					37,2	5,2	42,4	5,2		29,7
WC4	WC5					37,2	5,2	42,4	5,2	
	Walls(200 mm prefab)	5,0	0,0	2,8	14,0	0,0	14,0	0,0	0,0	14,0
	Slab(200 mm prefab) + Finish	8,3	2,6	1,9	15,7	4,8	20,5	4,8	4,8	15,7
	Facade panels	0,0	0,0	2,8	0,0	0,0	0,0	0,0	0,0	0,0
					66,9	10,0	76,9	10,0		29,7
WC3	WC4					66,9	10,0	76,9	10,0	
	Walls(200 mm prefab)	5,0	0,0	2,8	14,0	0,0	14,0	0,0	0,0	14,0
	Slab(200 mm prefab) + Finish	8,3	2,6	1,9	15,7	4,8	20,5	4,8	4,8	15,7
	Facade panels	0,0	0,0	2,8	0,0	0,0	0,0	0,0	0,0	0,0
					96,5	12,0	108,5	11,5		29,7
WC2	WC3					96,5	12,0	108,5	11,5	
	Walls(200 mm prefab)	5,0	0,0	2,8	14,0	0,0	14,0	0,0	0,0	14,0
	Slab(200 mm prefab) + Finish	8,3	2,6	1,9	15,7	4,8	20,5	4,8	4,8	15,7
	Facade panels	0,0	0,0	2,8	0,0	0,0	0,0	0,0	0,0	0,0
					126,2	13,9	140,1	13,0		29,7
WC1	WC2					126,2	13,9	140,1	13,0	
	Walls(200 mm prefab)	5,0	0,0	2,8	14,0	0,0	14,0	0,0	0,0	14,0
	Slab(200 mm prefab) + Finish	8,3	2,6	1,9	15,7	4,8	20,5	4,8	4,8	15,7
	Facade panels	0,0	0,0	2,8	0,0	0,0	0,0	0,0	0,0	0,0
					155,9	15,9	171,7	14,4		29,7

Same principle as in the timber section.

Output tab 1-2

Level	Part	$u_{el,con}$	$u_{cr,con}$	$u_{sh,con}$	$u_{el, (t = \infty)}$	$u_{cr, (t = \infty)}$	$u_{sh, (t = \infty)}$	Elastic	Creep	Shrinkage	Total
roof	C	0,000	0,000	0,000	0,000	0,000	0,000	0,159	0,279	0,750	1,187
	T	0,000	0,000	0,000	0,000	0,000	0,000	12,159	24,352	8,890	45,402
6	C	0,000	0,000	1,203	0,005	0,007	1,410	0,159	0,279	0,750	1,187
	T	0,000	0,000	0,000	1,203	0,925	1,482	12,159	24,352	8,890	45,402
5	C	0,012	0,004	1,271	0,017	0,023	1,410	0,154	0,272	0,544	0,969
	T	0,725	0,039	0,000	1,833	2,197	1,482	10,956	23,427	7,409	41,792
4	C	0,012	0,004	1,290	0,030	0,042	1,410	0,149	0,254	0,404	0,807
	T	0,655	0,035	0,000	2,933	3,850	1,482	9,849	21,269	5,927	37,045
3	C	0,012	0,004	1,304	0,043	0,058	1,410	0,130	0,216	0,285	0,631
	T	0,405	0,021	0,000	2,370	4,774	1,482	7,571	17,454	4,445	29,470
2	C	0,012	0,004	1,316	0,055	0,075	1,410	0,099	0,163	0,179	0,441
	T	0,405	0,021	0,000	2,928	5,839	1,482	5,605	12,701	2,963	21,270
1	C	0,012	0,000	1,325	0,067	0,092	1,410	0,056	0,092	0,085	0,233
	T	0,405	0,020	0,000	3,487	6,903	1,482	3,082	6,884	1,482	11,447

Contribution by ratio	Deformation
floor of interest	1,000
Concrete wall	0,217
concrete slab	0,016
Timber column	2,714
Timber beam	6,192
Acoustic felt	2,541

A separate output file is generated based on the selected floor of interest (in this case floor 1), where all the individual contributions of the elements can be observed.

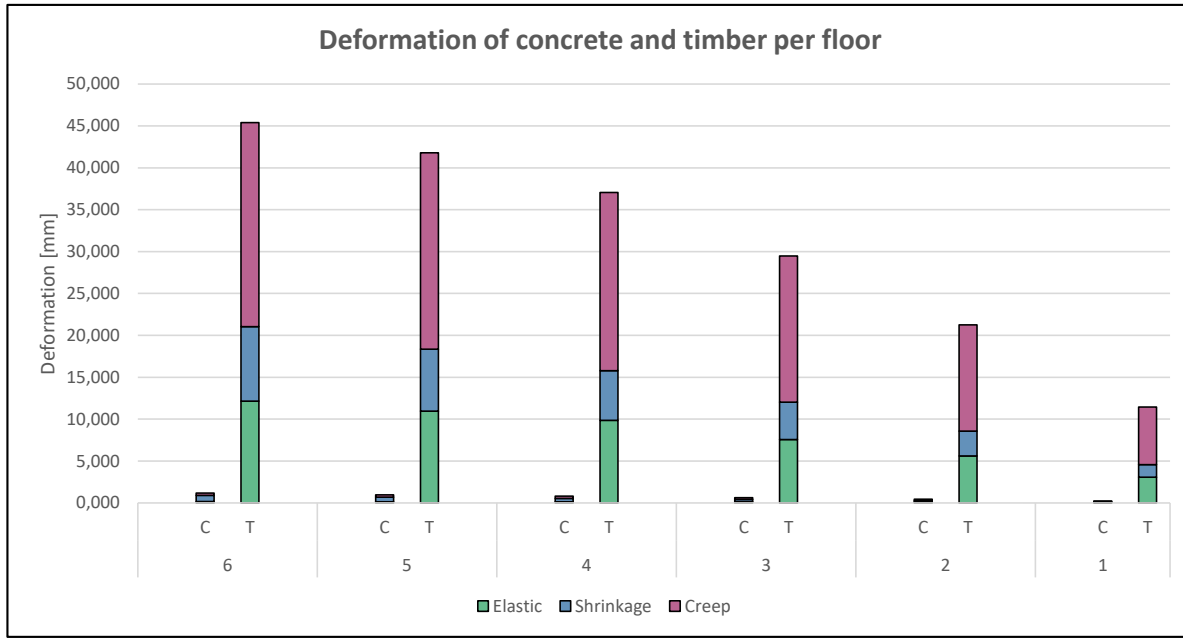
Indicated floor levels and their components (T for timber and C for concrete). The timber row consists out of the deformation of the beam, column and elastic felt. The concrete row consists out of the deformation in the slab and wall combined.

Construction mitigated deformations for elastic, creep and shrinkage deformations.

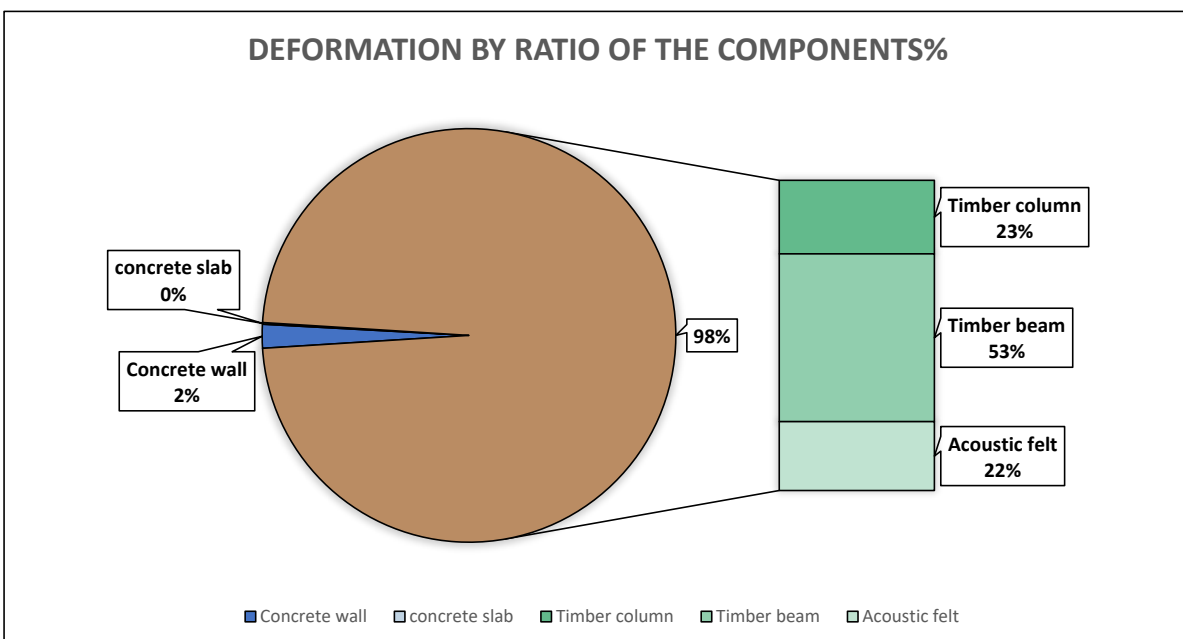
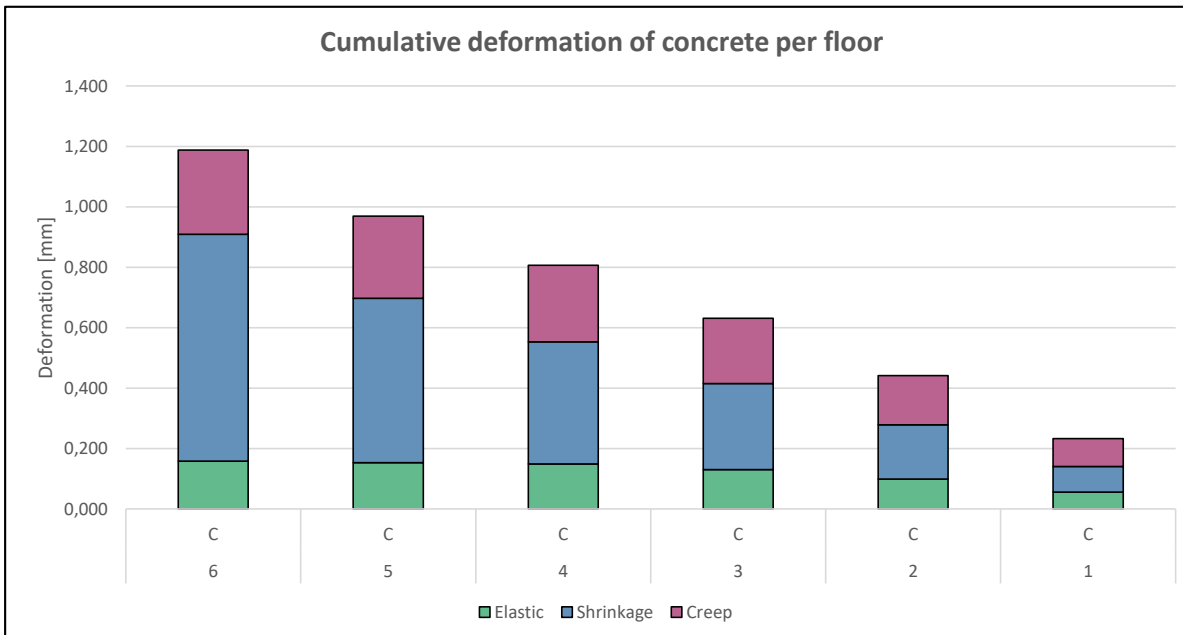
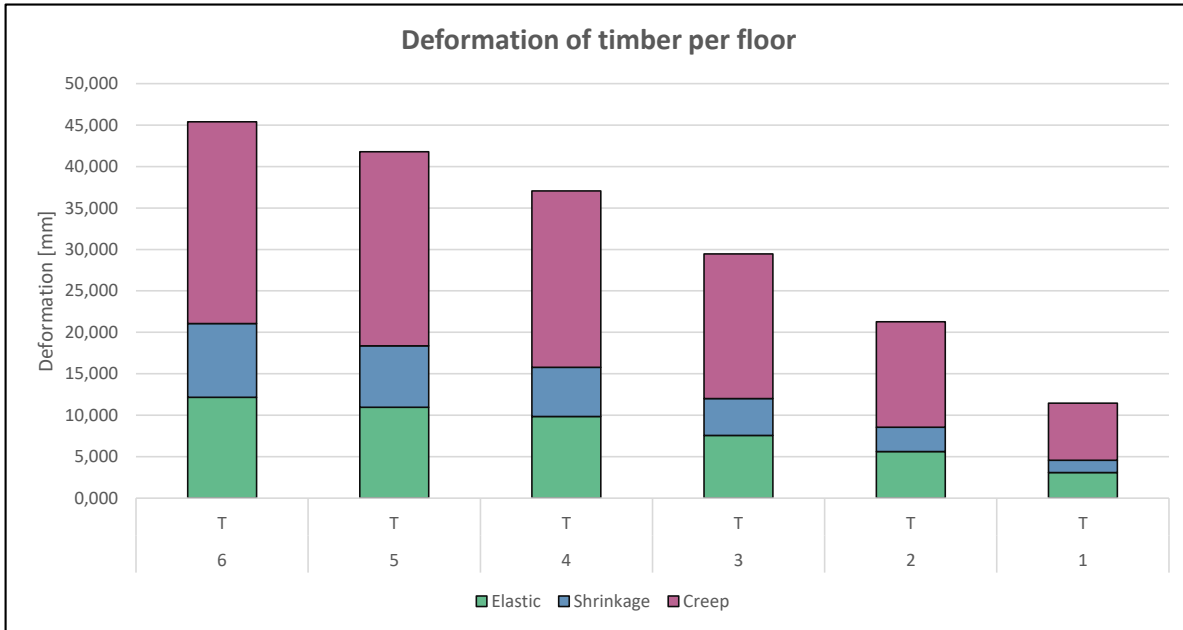
Elastic, creep and shrinkage deformations at $t = \infty$.

Summation of all the deformations, separated per category. The summation includes the deformation of the previous level. In other words, the deformation indicated for level 2 comprises out of the deformations of level 1 and 2 combined.

Summation of all the deformations. The summation includes the deformation of the previous level. In other words, the deformation indicated for level 2 comprises out of the deformations of level 1 and 2 combined.



A graphical overview is provided of the deformations per floor distinguished between the occurring deformations



Based on the floor of interest selected on the previous page, a graphical overview is provided to see the contribution of the components to the total deformation of that floor

Timber swelling tab 1-2

Input parameters			
Monthly increase in MC when fully wrapped and internally stored [%]		0,2	
Tangential (floor beam)		Longitudinal (column)	
MC ₀	10,00	MC ₀	12,00
MC _{∞,weather}	15,86	MC _{∞,weather}	15,86
MC _{low}	10,09	MC _{low}	12,09
Time from production to finish		days	
Time from production to installment	14		
Total installing cycle	42		
	56		

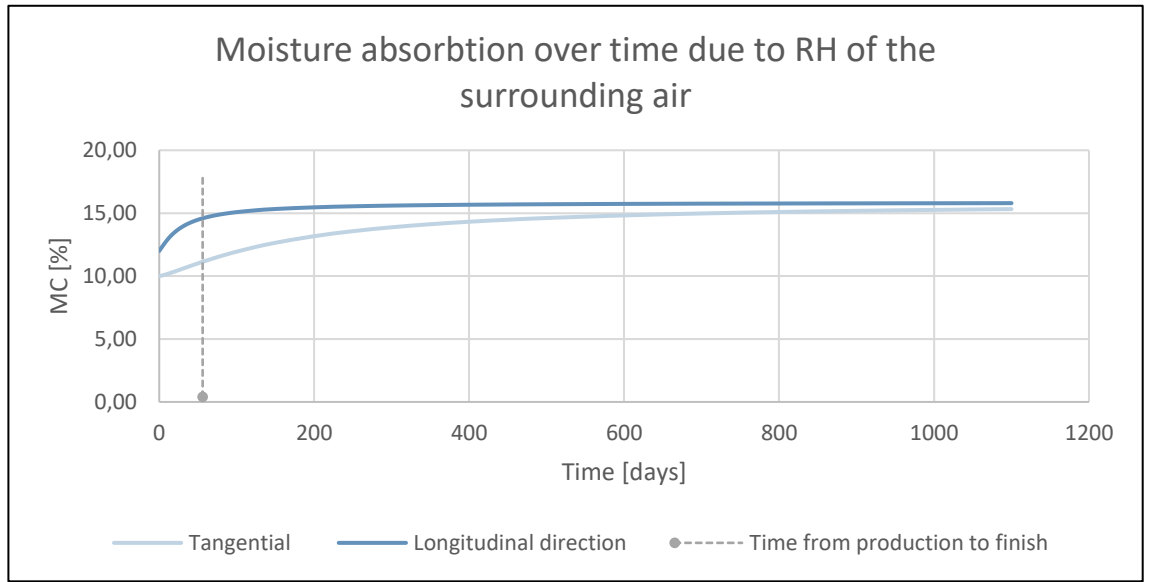
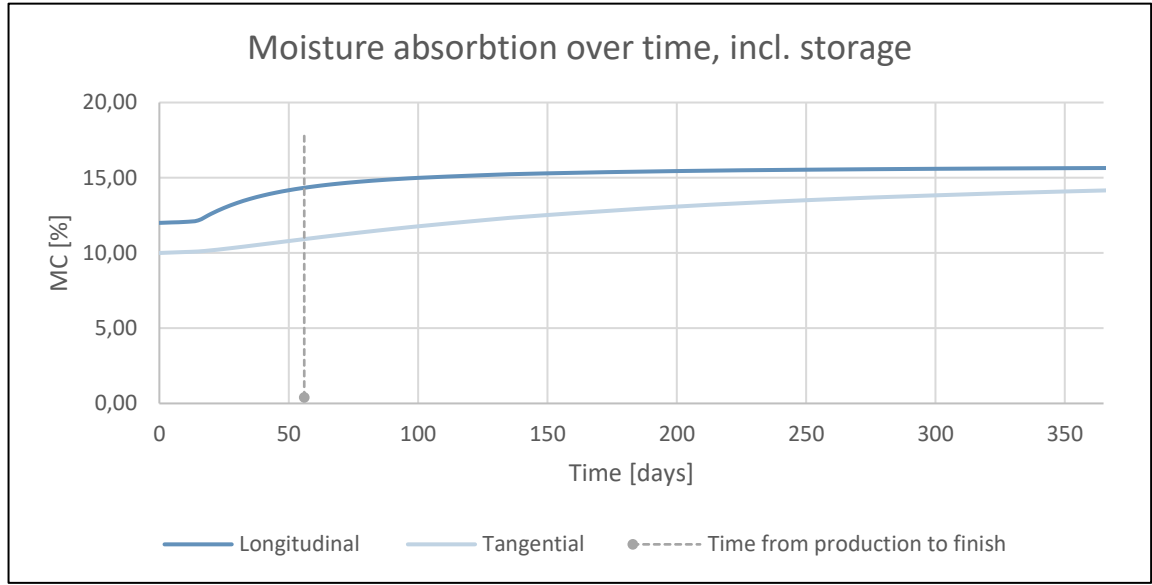
Input tab for calculating the timber swelling, these parameters are automatically taken from the input tab on the first page.

Dataset absorption				
time	Absorption regression		Including storage	
	Tangential	Longitudinal direction	Tangential	Longitudinal
0	10,00	12,00	10,00	12,00
5	10,07	12,44	10,03	12,03
10	10,16	12,85	10,07	12,07
15	10,26	13,20	10,10	12,17
20	10,36	13,49	10,18	12,60
25	10,47	13,73	10,27	12,99
30	10,58	13,93	10,37	13,32
35	10,69	14,10	10,47	13,59
40	10,80	14,24	10,58	13,82
45	10,91	14,37	10,69	14,01
50	11,01	14,48	10,79	14,17
55	11,12	14,57	10,90	14,31
60	11,22	14,66	11,01	14,43
65	11,32	14,73	11,11	14,53
70	11,41	14,80	11,21	14,62
75	11,51	14,86	11,31	14,70
80	11,60	14,91	11,41	14,77
85	11,69	14,96	11,50	14,84
90	11,78	15,01	11,59	14,89
95	11,86	15,05	11,68	14,95
100	11,94	15,08	11,77	14,99
125	12,32	15,23	12,18	15,17
150	12,65	15,33	12,52	15,29
200	13,17	15,47	13,08	15,45
250	13,57	15,55	13,51	15,54
300	13,88	15,60	13,83	15,59
350	14,12	15,64	14,09	15,64
400	14,32	15,67	14,29	15,67
450	14,48	15,69	14,46	15,69
500	14,61	15,71	14,60	15,71
600	14,82	15,74	14,81	15,74
700	14,98	15,76	14,97	15,76
800	15,09	15,77	15,09	15,77
900	15,19	15,78	15,19	15,78
1000	15,26	15,79	15,26	15,79
1100	15,32	15,80	15,32	15,80

Automatically generated data set to calculate the evolution of the swelling of the timber elements. (up to 1000 days) A distinction is made for the time from production to installment and during the installing itself. From production to installment the average increase is taken to be 0.2% per month and during installment the units are no longer wrapped and exposed to the elements so a different curve is generated. This curve is based on experimental values from literature.

Timber swelling tab 2-2

Moisture absorption during construction			
Time	floor	Experimental	
		Beam	column
14	6	10,09	12,15
14	5	10,09	12,15
14	4	10,09	12,15
14	3	10,09	12,15
14	2	10,09	12,15
14	1	10,09	12,15



The amount of swelling that occurs during construction.

Graphical overview of the increase in moisture content over the time. The swelling rate is derived from experiments

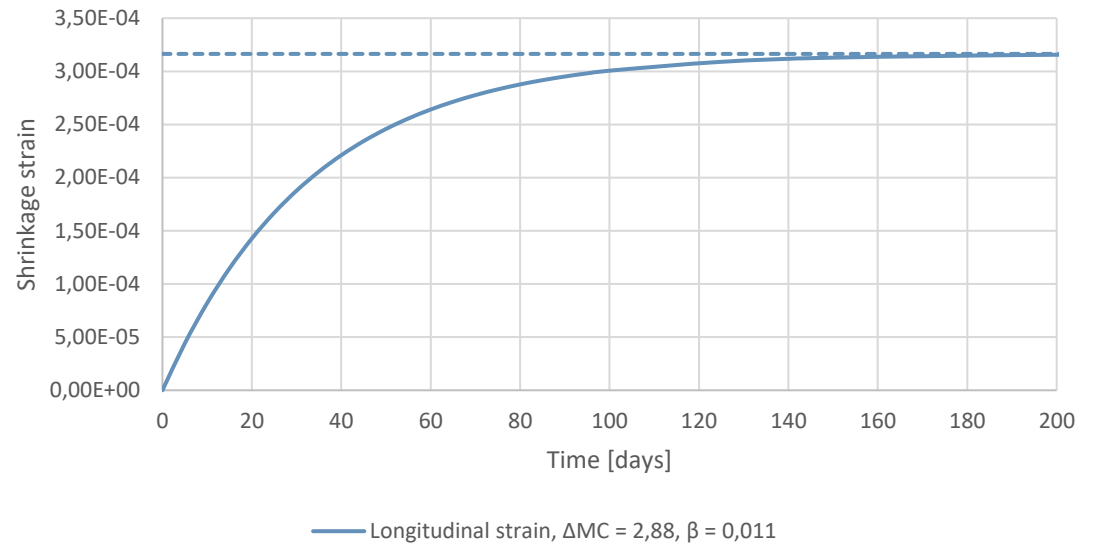
Timber shrinkage tab 1-1

Timber shrinkage during construction

MC _{∞,indoors} 9,27				
floor	MC high		Final strain	
	Beam	column	Beam	Column
6	10,09	12,15	0,0026	0,00032
5	10,09	12,15	0,0026	0,00032
4	10,09	12,15	0,0026	0,00032
3	10,09	12,15	0,0026	0,00032
2	10,09	12,15	0,0026	0,00032
1	10,09	12,15	0,0026	0,00032

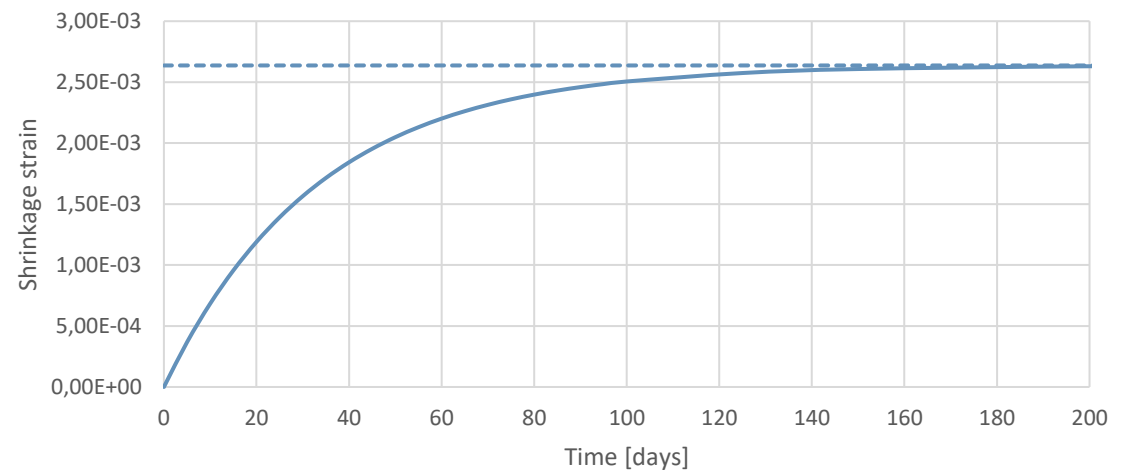
Same as in the swelling tab, the shrinkage curve is derived from experimental work. The MC_{indoors} is taken from the input tab on page 1.

Shrinkage strain timber column floor 1



— Longitudinal strain, $\Delta MC = 2,88$, $\beta = 0,011$

Shrinkage strain timber beam 1

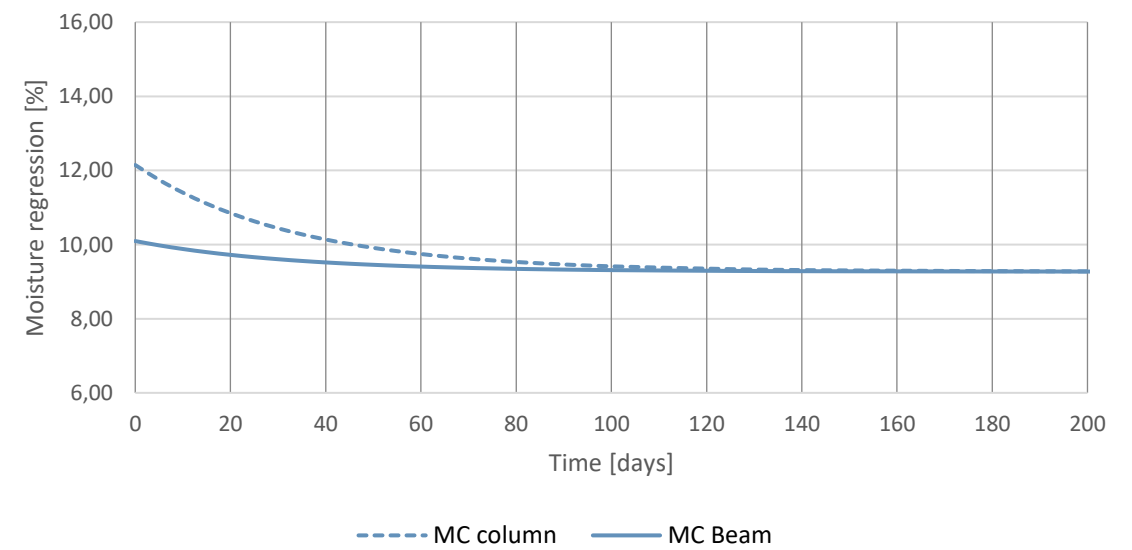


— Tangential strain, $\Delta MC = 0,82$, $\beta = 0,32$

Dataset MC and strain

days	LVL		CLT/GLh	
	MC Beam	Tangential strain	MC column	Longitudinal strain
0	10,09	0,00E+00	12,15	0,00E+00
5	9,98	3,67E-04	11,75	4,41E-05
10	9,88	6,83E-04	11,40	8,20E-05
15	9,80	9,56E-04	11,10	1,15E-04
20	9,72	1,19E-03	10,85	1,43E-04
25	9,66	1,39E-03	10,63	1,67E-04
30	9,61	1,56E-03	10,44	1,88E-04
35	9,56	1,71E-03	10,28	2,06E-04
40	9,52	1,84E-03	10,14	2,21E-04
45	9,48	1,95E-03	10,02	2,34E-04
50	9,45	2,05E-03	9,91	2,46E-04
55	9,43	2,13E-03	9,82	2,56E-04
60	9,41	2,20E-03	9,75	2,64E-04
65	9,39	2,26E-03	9,68	2,71E-04
70	9,37	2,31E-03	9,62	2,78E-04
75	9,36	2,36E-03	9,57	2,83E-04
80	9,34	2,40E-03	9,53	2,88E-04
85	9,33	2,43E-03	9,49	2,92E-04
90	9,33	2,46E-03	9,46	2,95E-04
95	9,32	2,48E-03	9,44	2,98E-04
100	9,31	2,51E-03	9,41	3,01E-04
125	9,29	2,57E-03	9,34	3,09E-04
150	9,28	2,61E-03	9,30	3,13E-04
200	9,27	2,63E-03	9,28	3,16E-04
250	9,27	2,64E-03	9,27	3,16E-04
300	9,27	2,64E-03	9,27	3,16E-04
350	9,27	2,64E-03	9,27	3,16E-04
400	9,27	2,64E-03	9,27	3,16E-04
450	9,27	2,64E-03	9,27	3,16E-04
500	9,27	2,64E-03	9,27	3,16E-04
600	9,27	2,64E-03	9,27	3,16E-04
700	9,27	2,64E-03	9,27	3,16E-04
800	9,27	2,64E-03	9,27	3,16E-04
900	9,27	2,64E-03	9,27	3,16E-04
1000	9,27	2,64E-03	9,27	3,16E-04
1100	9,27	2,64E-03	9,27	3,16E-04

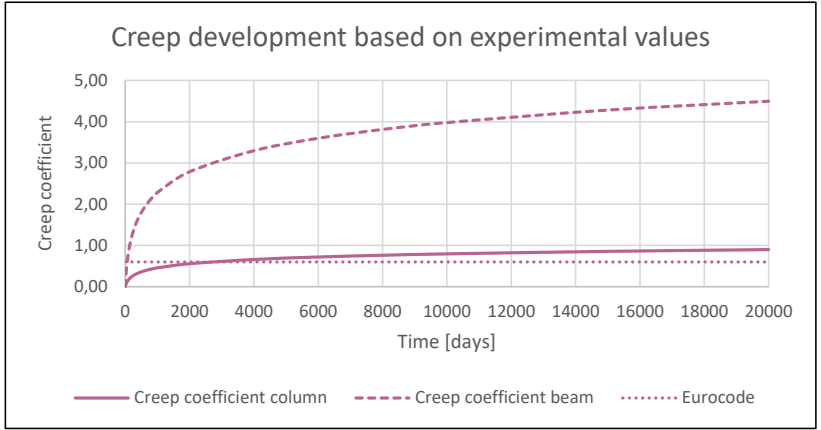
Moisture regression over time floor 1



--- MC column — MC Beam

Timber creep tab 1-1

Parameters according to input tab	
Element	Timber floor Beam
Material	LVL
kdef	0,6
Final creep coefficient	4,50
Element	Timber column
Material	CLT/GLh
Kdef	0,6
Final creep coefficient	0,90



Depending on whether the experimentally based creep curve is selected, this curve is used or a linear assumption is made when the EC is selected.

Dataset creep		
	LVL	CLT/GLh
days	Creep coefficient bear	Creep coefficient column
0	0,00	0,00
5	0,07	0,01
10	0,14	0,03
15	0,20	0,04
20	0,25	0,05
25	0,30	0,06
30	0,35	0,07
35	0,40	0,08
40	0,44	0,09
45	0,48	0,10
50	0,52	0,10
55	0,56	0,11
60	0,59	0,12
65	0,62	0,12
70	0,66	0,13
75	0,69	0,14
80	0,72	0,14
85	0,74	0,15
90	0,77	0,15
95	0,80	0,16
100	0,82	0,16
125	0,94	0,19
150	1,04	0,21
200	1,21	0,24
250	1,34	0,27
300	1,46	0,29
350	1,56	0,31
400	1,65	0,33
450	1,73	0,35
500	1,80	0,36
600	1,92	0,38
700	2,03	0,41
800	2,12	0,42
900	2,21	0,44
1000	2,28	0,46
2000	2,79	0,56
4000	3,30	0,66
6000	3,60	0,72
8000	3,81	0,76
10000	3,98	0,80
15000	4,28	0,86
20000	4,50	0,90

Mitigated during construction			
Time	floor	Experimental	
		Beam	column
7	6	0,10	0,02
7	5	0,10	0,02
7	4	0,10	0,02
7	3	0,10	0,02
7	2	0,10	0,02
7	1	0,10	0,00

Concrete creep & shrinkage tab 1-5

Input values	
Element	Concrete slab
fck [Mpa]	55
A _c [mm ²]	200000
u [mm]*	2000
t ₀ [days]	10
t _s [days]	1
t [days]	10
RH %	65
Cement class**	R

Input values	
Element	Concrete wall
fck [Mpa]	55
A _c [mm ²]	200000
u [mm]*	2000
t ₀ [days]	10
t _s [days]	1
t [days]	10
RH %	65
Cement class**	R

All input values are automatically taken from the input tab on the first page. The intermediate values are given so it is easier to see what is calculated.

*standard 2000 for two sides of a wall or slab

**If prefab then R, otherwise N is presumed.

Intermediate values Concrete slab	
Stiffness	
E _{cm} [Mpa]	38214
E _{cm} (t) [Mpa]	36701
E _c [Mpa]	40125
f _{cm}	63
f _{cm} (t)	55,06259978
β _{cc} (t)	0,87400952
s	0,2
Creep factor	
Creep factor t = inf	1,444
creep factor at t	0,000
Parameters	
φ _(t,t₀)	0,000
φ ₀	1,444
φ _{RH}	1,242
β(f _{cm})	2,117
β(t ₀)	0,550
β _c (t,t ₀)	0,000
β _H	489,765
h ₀	200
α ₁	0,663
α ₂	0,889
α ₃	0,745
t ₀	15
α	1
Drying shrinkage strain	
ε _{cd,t}	0,000348422
Parameters	
ε _{cd,0}	0,000421
k _h	0,85
β _{ds} (t,t _s)	0,974667164
α _{ds1}	6
α _{ds2}	0,11
f _{cmo}	10
f _{cm}	63
β _{RH}	1,124
h ₀	200
Autogenous shrinkage strain	
ε _{ca,t}	5,27304E-05
Parameters	
β _{as} (t)	0,47
ε _{ca} (inf)	0,000113

Intermediate values Concrete wall	
Stiffness	
E _{cm} [Mpa]	38214
E _{cm} (t) [Mpa]	36701
E _c [Mpa]	40125
f _{cm}	63
f _{cm} (t)	55,06259978
β _{cc} (t)	0,87400952
s	0,2
Creep factor	
Creep factor t = inf	1,444
creep factor at t	0,000
Parameters	
φ _(t,t₀)	0,000
φ ₀	1,444
φ _{RH}	1,242
β(f _{cm})	2,117
β(t ₀)	0,550
β _c (t,t ₀)	0,000
β _H	489,765
h ₀	200
α ₁	0,663
α ₂	0,889
α ₃	0,745
t ₀	15
α	1
Drying shrinkage strain	
ε _{cd,t}	0,000348422
Parameters	
ε _{cd,0}	0,000421
k _h	0,85
β _{ds} (t,t _s)	0,974667164
α _{ds1}	6
α _{ds2}	0,11
f _{cmo}	10
f _{cm}	63
β _{RH}	1,124
h ₀	200
Autogenous shrinkage strain	
ε _{ca,t}	5,27304E-05
Parameters	
β _{as} (t)	0,47
ε _{ca} (inf)	0,000113

Concrete creep & shrinkage tab 2-5

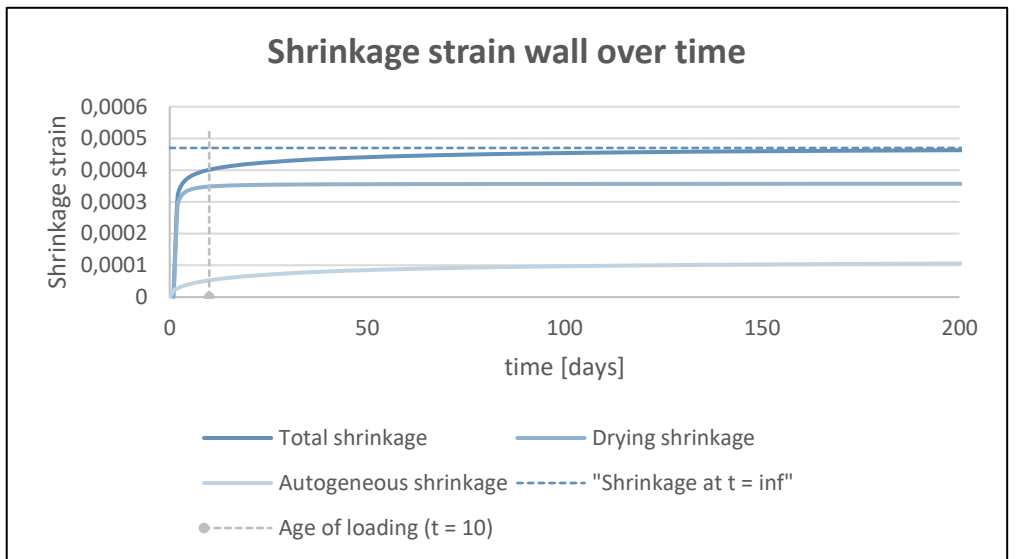
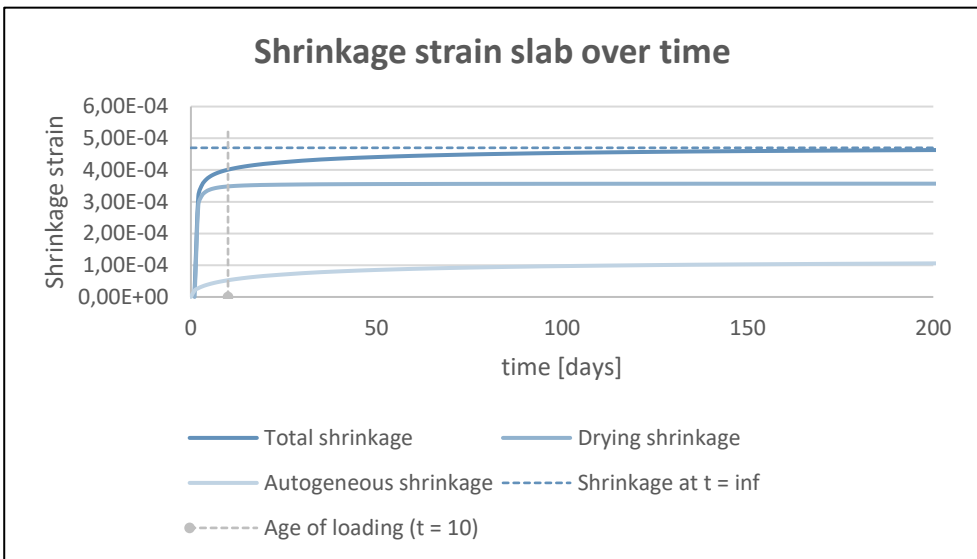
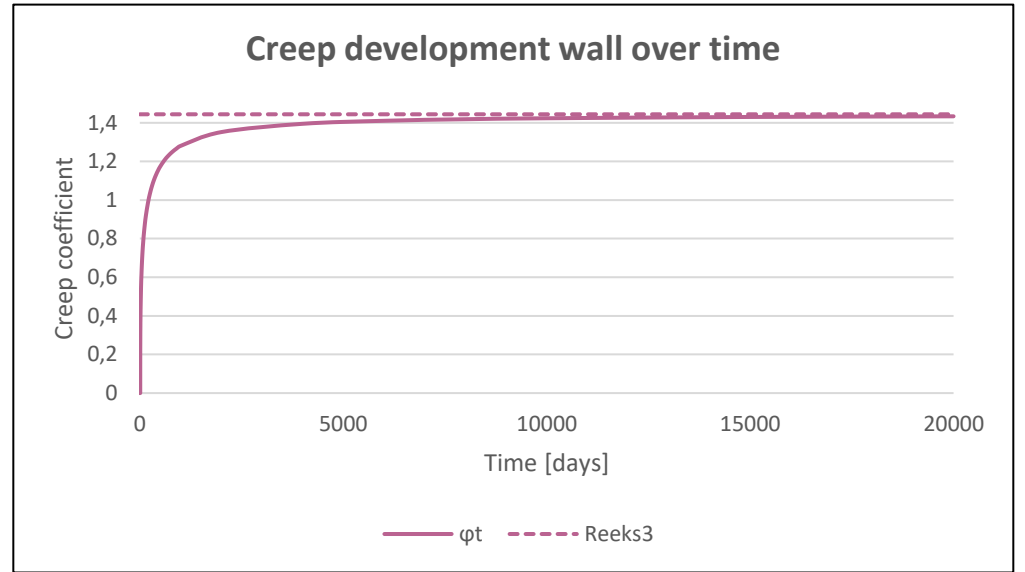
Dataset slab				
Days	φ_t	Total shrinkage	Drying shrinkage	Autogeneous shrinkage
0	0,000	4,012E-04	3,484E-04	5,273E-05
0	#GETAL!	4,67E-04	0,000466633	0
1	#GETAL!	2,04E-05	0	2,03928E-05
2	#GETAL!	3,17E-04	0,000289708	2,77157E-05
3	#GETAL!	3,53E-04	0,000320045	3,29375E-05
4	#GETAL!	3,69E-04	0,00033162	3,7089E-05
5	#GETAL!	3,78E-04	0,000337727	4,05667E-05
6	#GETAL!	3,85E-04	0,000341501	4,35725E-05
7	#GETAL!	3,90E-04	0,000344064	4,62256E-05
8	#GETAL!	3,95E-04	0,000345918	4,86033E-05
9	#GETAL!	3,98E-04	0,000347322	5,07587E-05
10	0	4,01E-04	0,000348422	5,27304E-05
11	0,225107019	4,04E-04	0,000349306	5,45472E-05
12	0,276970061	4,06E-04	0,000350034	5,62316E-05
13	0,312604721	4,08E-04	0,000350642	5,78011E-05
14	0,340575199	4,10E-04	0,000351159	5,927E-05
15	0,363933826	4,12E-04	0,000351603	6,06499E-05
16	0,384161404	4,14E-04	0,000351988	6,19505E-05
17	0,40210107	4,16E-04	0,000352326	6,31799E-05
18	0,418283567	4,17E-04	0,000352625	6,4345E-05
19	0,433066984	4,18E-04	0,000352891	6,54518E-05
20	0,446705565	4,20E-04	0,00035313	6,65053E-05
30	0,546700045	4,29E-04	0,000354617	7,4881E-05
40	0,613826146	4,36E-04	0,000355346	8,07453E-05
50	0,66534077	4,41E-04	0,000355779	8,51494E-05
60	0,707425491	4,45E-04	0,000356066	8,86028E-05
70	0,743093341	4,48E-04	0,00035627	9,13924E-05
80	0,774067461	4,50E-04	0,000356422	9,36955E-05
90	0,801437	4,52E-04	0,00035654	9,56292E-05
100	0,825939581	4,54E-04	0,000356635	9,72748E-05
125	0,877777581	4,57E-04	0,000356804	0,000100476
150	0,919890183	4,60E-04	0,000356917	0,000102787
200	0,985302476	4,63E-04	0,000357058	0,000105851
250	1,034569333	4,65E-04	0,000357142	0,000107738
300	1,073449008	4,66E-04	0,000357198	0,000108979
350	1,105117065	4,67E-04	0,000357238	0,000109832
400	1,131515544	4,68E-04	0,000357268	0,000110439
450	1,153918121	4,68E-04	0,000357291	0,000110883
500	1,173203631	4,69E-04	0,00035731	0,000111215
600	1,20478065	4,69E-04	0,000357338	0,000111661
700	1,229609563	4,69E-04	0,000357358	0,000111934
800	1,249684026	4,69E-04	0,000357373	0,000112107
900	1,2662709	4,70E-04	0,000357385	0,000112221
1000	1,280217904	4,70E-04	0,000357394	0,000112298
2000	1,352022562	4,70E-04	0,000357436	0,000112485
4000	1,394975177	4,70E-04	0,000357457	0,0001125
6000	1,4106246	4,70E-04	0,000357464	0,0001125
8000	1,418731049	4,70E-04	0,000357467	0,0001125
10000	1,423689784	4,70E-04	0,000357469	0,0001125
15000	1,430416026	4,70E-04	0,000357472	0,0001125
20000	1,433829577	4,70E-04	0,000357473	0,0001125

Automatically generated data sets which calculates the amount of shrinkage and creep. The error warning in the creep column is due to the indicated time before first loading from the input tab. In this case the elements get loaded after 10 days so no creep is present before that time.

Concrete creep & shrinkage tab 4-5

Dataset Wall				
Days	ϕ_t	Total shrinkage	Drying shrinkage	Autogeneous shrinkage
0	0,000	4,012E-04	3,484E-04	5,273E-05
0	#GETAL!	0,000466633	0,000466633	0
1	#GETAL!	2,03928E-05	0	2,03928E-05
2	#GETAL!	0,000317424	0,000289708	2,77157E-05
3	#GETAL!	0,000352982	0,000320045	3,29375E-05
4	#GETAL!	0,000368709	0,00033162	3,7089E-05
5	#GETAL!	0,000378294	0,000337727	4,05667E-05
6	#GETAL!	0,000385073	0,000341501	4,35725E-05
7	#GETAL!	0,000390289	0,000344064	4,62256E-05
8	#GETAL!	0,000394521	0,000345918	4,86033E-05
9	#GETAL!	0,00039808	0,000347322	5,07587E-05
10	0	0,000401152	0,000348422	5,27304E-05
11	0,225107	0,000403854	0,000349306	5,45472E-05
12	0,27697	0,000406265	0,000350034	5,62316E-05
13	0,312605	0,000408443	0,000350642	5,78011E-05
14	0,340575	0,000410429	0,000351159	5,927E-05
15	0,363934	0,000412253	0,000351603	6,06499E-05
16	0,384161	0,000413939	0,000351988	6,19505E-05
17	0,402101	0,000415506	0,000352326	6,31799E-05
18	0,418284	0,00041697	0,000352625	6,4345E-05
19	0,433067	0,000418343	0,000352891	6,54518E-05
20	0,446706	0,000419635	0,00035313	6,65053E-05
30	0,5467	0,000429498	0,000354617	7,4881E-05
40	0,613826	0,000436091	0,000355346	8,07453E-05
50	0,665341	0,000440928	0,000355779	8,51494E-05
60	0,707425	0,000444669	0,000356066	8,86028E-05
70	0,743093	0,000447662	0,00035627	9,13924E-05
80	0,774067	0,000450118	0,000356422	9,36955E-05
90	0,801437	0,00045217	0,00035654	9,56292E-05
100	0,82594	0,00045391	0,000356635	9,72748E-05
125	0,877778	0,000457281	0,000356804	0,000100476
150	0,91989	0,000459704	0,000356917	0,000102787
200	0,985302	0,000462908	0,000357058	0,000105851
250	1,034569	0,00046488	0,000357142	0,000107738
300	1,073449	0,000466177	0,000357198	0,000108979
350	1,105117	0,00046707	0,000357238	0,000109832
400	1,131516	0,000467708	0,000357268	0,000110439
450	1,153918	0,000468175	0,000357291	0,000110883
500	1,173204	0,000468525	0,00035731	0,000111215
600	1,204781	0,000468999	0,000357338	0,000111661
700	1,22961	0,000469292	0,000357358	0,000111934
800	1,249684	0,00046948	0,000357373	0,000112107
900	1,266271	0,000469606	0,000357385	0,000112221
1000	1,280218	0,000469692	0,000357394	0,000112298
2000	1,352023	0,000469921	0,000357436	0,000112485
4000	1,394975	0,000469956	0,000357457	0,0001125
6000	1,410625	0,000469964	0,000357464	0,0001125
8000	1,418731	0,000469967	0,000357467	0,0001125
10000	1,42369	0,000469969	0,000357469	0,0001125
15000	1,430416	0,000469972	0,000357472	0,0001125
20000	1,43383	0,000469973	0,000357473	0,0001125

Concrete creep & shrinkage tab 3-5



Graphical overviews of the creep and shrinkage strain development of the walls and slab. In this case identical as no distinction is made in material between the two.

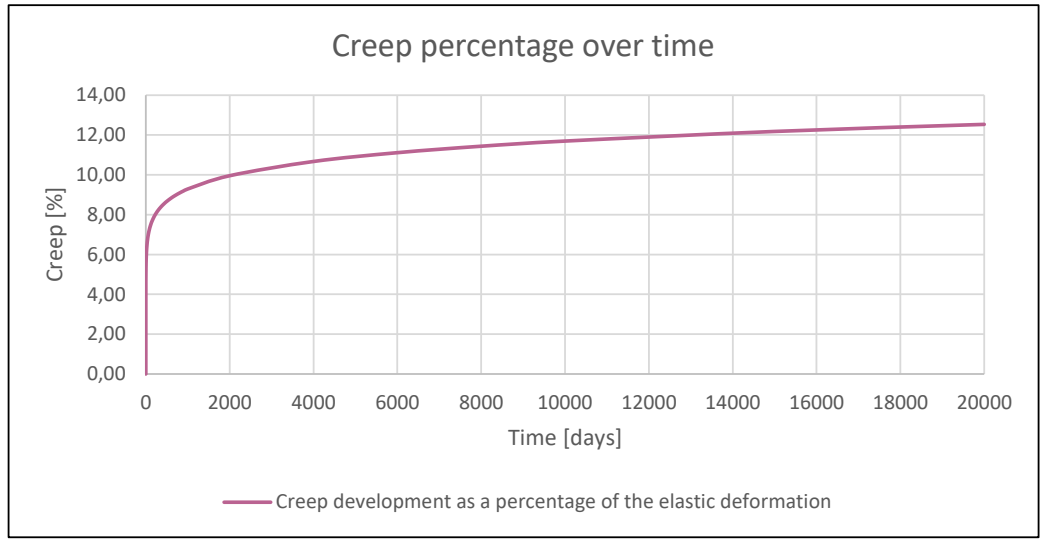
Concrete creep & shrinkage tab 5-5

Mitigated during construction						
Floor	Creep			shrinkage		
	Time	Creep,con,sla	Creep,con,wall	time	Slab	Wall
6	17	0,402	0,402	10	0,000401	0,00040
5	17	0,402	0,402	24	0,000424	0,00042
4	17	0,402	0,402	31	0,000430	0,00043
3	17	0,402	0,402	38	0,000435	0,00043
2	17	0,402	0,402	45	0,000439	0,00044
1	17	0,000	0,000	52	0,000442	0,00044

Generated datasets for the amount of creep and shrinkage strain is present during the construction phase.

Acoustic felt creep tab 1-1

Parameters	
Maximum creep [%]	12,53
Production to finish	days
Production to installment	14
Installing	42
	56



Dataset Acoustic creep	
t [days]	Creep development as a percentage of the elastic deformation
0	0,00
1	4,66
2	4,99
3	5,20
4	5,35
5	5,47
6	5,57
7	5,66
8	5,73
9	5,80
10	5,86
11	5,92
12	5,97
13	6,02
14	6,06
15	6,10
16	6,14
17	6,18
18	6,22
19	6,25
20	6,28
30	6,54
40	6,73
50	6,89
60	7,01
70	7,12
80	7,22
90	7,30
100	7,38
125	7,55
150	7,68
200	7,91
250	8,09
300	8,24
350	8,36
400	8,48
450	8,58
500	8,67
600	8,83
700	8,96
800	9,09
900	9,19
1000	9,29
2000	9,96
4000	10,67
6000	11,11
8000	11,44
10000	11,70
15000	12,18
20000	12,53

Creep development during construction		
Time [days]	floor	Creep _{con,felt}
7	6	5,656
7	5	5,656
7	4	5,656
7	3	5,656
7	2	5,656
7	1	5,656

Creep deflection as a percentage of the elastic deformation, given by the supplier. No distinction is made between different types of acoustic felt as these curves are all relatively close to each other.

Creep curve derived from the data provided by the supplier

Deformations tab 1-1

Timber column							timber beam					
level	z	$u_{el,(t=\infty)}$	$u_{el,con}$	$u_{cr,(t=\infty)}$	$u_{cr,con}$	$u_{sh,(t=\infty)}$	z	$u_{el,(t=\infty)}$	$u_{el,con}$	$u_{cr,(t=\infty)}$	$u_{cr,con}$	$u_{sh,(t=\infty)}$
Roof	0	0,00	0,00	0,00	0,000	0,00	0	0,00	0,00	0,00	0,000	0,00
6	2850	0,08	0,00	0,14	0,000	0,90	220	0,03	0,00	0,65	0,000	0,58
5	2850	0,21	0,08	0,36	0,002	0,90	220	0,07	0,03	1,64	0,003	0,58
4	2850	0,37	0,08	0,63	0,002	0,90	220	0,12	0,03	2,91	0,003	0,58
3	2850	0,49	0,08	0,82	0,002	0,90	220	0,15	0,03	3,74	0,003	0,58
2	2850	0,60	0,08	1,00	0,002	0,90	220	0,19	0,03	4,58	0,003	0,58
1	2850	0,71	0,08	1,18	0,000	0,90	220	0,23	0,03	5,41	0,003	0,58

Acoustic felt					Concrete wall						
z	$u_{el,(t=\infty)}$	$u_{el,con}$	$u_{cr,(t=\infty)}$	$u_{cr,con}$	z	$u_{el,(t=\infty)}$	$u_{el,con}$	$u_{cr,(t=\infty)}$	$u_{cr,con}$	$u_{sh,(t=\infty)}$	$u_{sh,con}$
0	0,00	0,00	0,00	0,00	0	0,000	0,000	0,000	0,000	0,000	0,000
15	1,09	0,00	0,14	0,000	2800	0,005	0,000	0,006	0,000	1,316	1,123
15	1,56	0,62	0,20	0,035	2800	0,016	0,011	0,021	0,004	1,316	1,186
15	2,44	0,55	0,31	0,03	2800	0,028	0,011	0,039	0,004	1,316	1,204
15	1,73	0,30	0,21	0,02	2800	0,040	0,011	0,054	0,004	1,316	1,217
15	2,14	0,30	0,26	0,02	2800	0,051	0,011	0,070	0,004	1,316	1,228
15	2,55	0,30	0,31	0,02	2800	0,063	0,011	0,086	0,000	1,316	1,237

Concrete slab							Construction compensation					
z	$u_{el,(t=\infty)}$	$u_{el,con}$	$u_{cr,(t=\infty)}$	$u_{cr,con}$	$u_{sh,(t=\infty)}$	$u_{sh,con}$	Timber, el	Timber, cr	concrete, el	concrete, cr	concrete, sh	
0	0,000	0,000	0,000	0,000	0,000	0,000	Roof	0,000	0,000	0,000	0,000	0,000
200	0,000	0,000	0,000	0,000	0,094	0,080	6	0,000	0,000	0,000	0,000	1,203
200	0,001	0,001	0,002	0,000	0,094	0,085	5	0,725	0,039	0,012	0,004	1,271
200	0,002	0,001	0,003	0,000	0,094	0,086	4	0,655	0,035	0,012	0,004	1,290
200	0,003	0,001	0,004	0,000	0,094	0,087	3	0,405	0,021	0,012	0,004	1,304
200	0,004	0,001	0,005	0,000	0,094	0,088	2	0,405	0,021	0,012	0,004	1,316
200	0,004	0,001	0,006	0,000	0,094	0,088	1	0,405	0,020	0,012	0,000	1,325

All deformations are collected based on the strains calculated in the previous tabs.

Tables tab 1-1

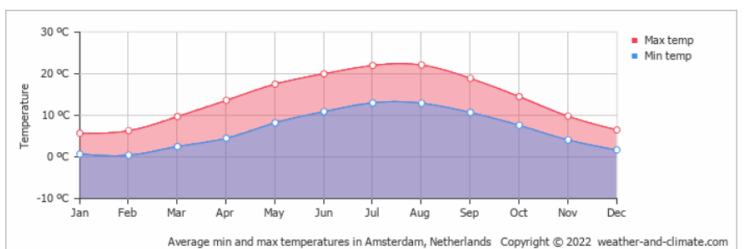
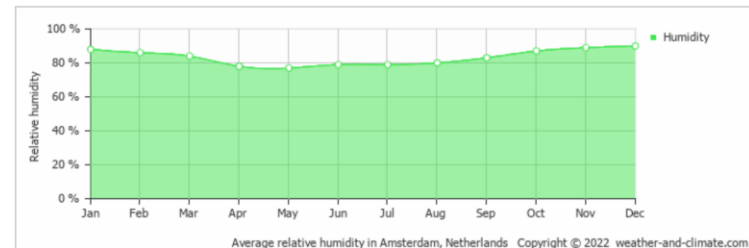
General loadcase classes	Q _k	ψ ₀	ψ ₁	ψ ₂	
Class A - Floors		1,75	0,4	0,5	0,3
Class A - Stairs		2	0,4	0,5	0,3
Class A - Bacony		2,5	0,4	0,5	0,3
Class B - Office		2,5	0,5	0,5	0,3
Class C - Meeting room		5	0,6	0,7	0,6
Class D - Shopping area		4	0,4	0,7	0,6
Class E - Stores		5	1	0,9	0,8
Class E - Library		2,5	1	0,9	0,8
Class E - Other		5	1	0,9	0,8
Class H - Roof			0	0	0

General tables tab. Several reference values are taken from these tables. These tables can be extended for further use.

Climate class			
	1	2	3
Sawn timber	0,6	0,8	2
CLT/GLh	0,6	0,8	2
LVL	0,6	0,8	2

kdef	
h ₀	kh
100	1
200	0,85
300	0,75
500	0,7

Average humidity, temperature and their corresponding MC's							
Month	MC	Temp	RH	W	K	K1	K2
jan	19,92	3,7	88	354,0	0,81	6,23	2,06
feb	18,94	4	86	354,4	0,81	6,23	2,07
mar	18,01	6,4	84	357,8	0,81	6,20	2,16
apr	15,39	9,7	77	362,8	0,81	6,15	2,28
mei	14,98	13,2	76	368,4	0,81	6,09	2,40
jun	15,86	15,8	79	372,8	0,82	6,05	2,48
jul	15,77	18	79	376,6	0,82	6,00	2,55
aug	16,13	17,8	80	376,2	0,82	6,01	2,54
sep	17,36	15,1	83	371,6	0,82	6,06	2,46
oct	19,26	11,2	87	365,1	0,81	6,13	2,33
nov	20,40	7,2	89	359,0	0,81	6,19	2,19
dec	21,00	4,4	90	354,9	0,81	6,22	2,08
Season	MC						
Winter	19,95						
Spring	16,13						
Summer	15,92						
Autum	19,01						



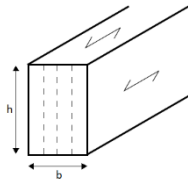
Materials	Density [kg/m ³]	E _{0,k}	E _{0,mean}	E _{90,edge,k}	E _{90,edge,me}	f _{m,0,k}	f _{c,0,k}	f _{c,90,k}	f _{t,0,k}	f _{t,90,k}	f _{v,90,k}	Category
Sawn timber												
C14	350		7000			230	14	16	2	8	0,4	3 Sawn timber
C16	370		8000			270	16	17	2,2	10	0,4	3,2 Sawn timber
C18	380		9000			300	18	18	2,2	11	0,4	3,4 Sawn timber
C20	390		9500			320	20	19	2,3	12	0,4	3,6 Sawn timber
C22	410		10000			330	22	20	2,4	13	0,4	3,8 Sawn timber
C24	420		11000			370	24	21	2,5	14	0,4	4 Sawn timber
C27	450		11500			380	27	22	2,6	16	0,4	4 Sawn timber
C30	460		12000			400	30	23	2,7	18	0,4	4 Sawn timber
C35	480		13000			430	35	25	2,8	21	0,4	4 Sawn timber
C40	500		14000			470	40	26	2,9	24	0,4	4 Sawn timber
C45	520		15000			500	45	27	3,1	27	0,4	4 Sawn timber
C50	550		16000			530	50	29	3,2	30	0,4	4 Sawn timber
Laminated timber												
GL20h	370		8400			300	20	20	2,5	16	0,5	3,5 CLT/GLh
GL22h	410		10500			300	22	22	2,5	17,6	0,5	3,5 CLT/GLh
GL24h	420		11500			300	24	24	2,5	19,2	0,5	3,5 CLT/GLh
GL26h	445		12100			300	26	26	2,5	20,8	0,5	3,5 CLT/GLh
GL28h	460		12600			300	28	28	2,5	22,3	0,5	3,5 CLT/GLh
GL30h	480		13600			300	30	30	2,5	24	0,5	3,5 CLT/GLh
GL32h	490		14200			300	32	32	2,5	25,6	0,5	3,5 CLT/GLh
LVL												
LVL-KertoS	510	11600	13800	350	2400	44	35	6	35	0,8	4,2	LVL
Concrete												
C12/15	2500							12		1,6		Concrete
C16/20	2500							16		1,9		Concrete
C20/25	2500							20		2,2		Concrete
C25/30	2500							25		2,6		Concrete
C30/37	2500							30		2,9		Concrete
C35/45	2500							35		3,2		Concrete
C40/50	2500							40		3,5		Concrete
C45/55	2500							45		3,8		Concrete
C50/60	2500							50		4,1		Concrete
C55/67	2500							55		4,2		Concrete
C60/75	2500							60		4,4		Concrete
C70/85	2500							70		4,6		Concrete
C80/95	2500							80		4,8		Concrete
C90/105	2500							90		5		Concrete

Attachment C – Manual verification timber straining

Loads

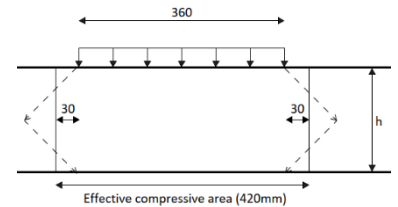
F_{gk}	134.6 kN
F_{qk}	73.1 kN
F_k	207.7 kN
$F_{k,cr}$	200.9 kN
$F_{k,construction}$	24.1 kN

LVL beam



Class	LVL
H	220 mm
B	204 mm
$E_{90,mean}$	2400 Mpa

Effective compressive area	$(30+30+360) \cdot 200 = 84000 \text{ mm}^2$
MC_0 after production	10%
MC_∞	9.27% (RH = 50%, T = 20 °C)
$MC_{surroundings}$	15.86% (RH = 79%, T = 15.8 °C)
K_{def}	0.6/4.5 [EC/experimental]
Time storage – instalment	14 days
Time instalment – heating	35 days
B	0.32
Increase in MC_0 after production	0.2% (assuming fully wrapped)



Elastic deformation

$$u_{el} = \frac{f_k \cdot h}{A \cdot E_{mean}} = \frac{207.7 \cdot 1000 \cdot 220}{84000 \cdot 2400} = 0.227 \text{ mm}$$

$$u_{el,con} = \frac{f_{k,construction} \cdot h}{A \cdot E_{mean}} = \frac{24.1 \cdot 1000 \cdot 220}{84000 \cdot 2400} = 0.0263 \text{ mm}$$

Creep deformation

$$u_{cr} = \frac{f_{k,cr} \cdot h \cdot \varphi}{A \cdot E_{mean}} = \frac{200.9 \cdot 1000 \cdot 220 \cdot 0.6}{84000 \cdot 2400} = 0.13 \text{ mm} \quad \text{[EC]}$$

$$u_{cr} = \frac{f_{k,cr} \cdot h \cdot \varphi}{A \cdot E_{mean}} = \frac{200.9 \cdot 1000 \cdot 220 \cdot 4.5}{84000 \cdot 2400} = 0.99 \text{ mm} \quad \text{[Experimental]}$$

$$\varphi_{cr} = 5 \cdot (\ln(1 + 0.02 \cdot t)) = 5 \cdot (0.15 \cdot \ln(1 + 0.02 \cdot 35)) = 0.398$$

$$u_{cr,con} = \frac{f_{k,con} \cdot h \cdot \varphi_{cr}}{A \cdot E_{mean}} = \frac{24.1 \cdot 1000 \cdot 220 \cdot 0.398}{84000 \cdot 2400} = 0.01 \text{ mm} \quad \text{[Experimental]}$$

Shrinkage and swelling

$$MC_1 = 10 + 0.2 \cdot \frac{12}{365} \cdot 14 = 10.092\% \quad \text{During production to instalment}$$

$$MC_2 = MC_{sur} - \frac{MC_{sur} - MC_1}{1 + \left(\frac{t}{175}\right)^{1.25}} = 15.86 - \frac{15.86 - 10.092}{1 + \left(\frac{35}{175}\right)^{1.25}} = 10.77\% \quad \text{After instalment}$$

$$u_{sh} = \frac{\beta}{100} \cdot (MC_2 - MC_{\infty}) \cdot h = \frac{0.32}{100} \cdot (10.77 - 9.27) \cdot 220 = 1.057 \text{ mm}$$

Final deformation beam

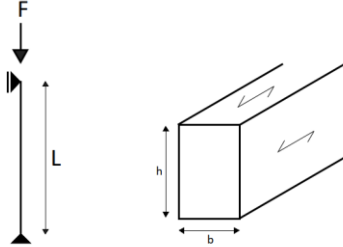
$$u_{fin} = u_{el} + u_{cr} + u_{sh} - u_{el,con} = 0.227 + 0.13 + 1.057 - 0.0263 = 1.39 \text{ mm}$$

[EC]

$$u_{fin} = u_{el} + u_{cr} + u_{sh} - u_{el,con} - u_{cr,con} = 0.227 + 0.99 + 1.057 - 0.026 - 0.01 = 2.24 \text{ mm}$$

[Experimental]

Glulam Column



Class	GL24h
H	360 mm
B	200 mm
L	2850 mm
$E_{0,mean}$	11500 Mpa
Compressive area	$360 \cdot 200 = 72000 \text{ mm}^2$
MC_0 after production	12%
MC_{∞}	9.27% (RH = 50%, T = 20 °C)
$MC_{surroundings}$	15.86% (RH = 79%, T = 15.8 °C)
K_{def}	0.6/0.9 [EC/experimental]
Time storage – instalment	14 days
Time instalment – heating	35 days
B	0.11
Increase in MC_0 after production	0.2% (assuming fully wrapped)

Elastic deformation

$$u_{el} = \frac{f_k \cdot L}{A \cdot E_{mean}} = \frac{207.7 \cdot 1000 \cdot 2850}{72000 \cdot 11500} = 0.71 \text{ mm}$$

$$u_{el,con} = \frac{f_{k,construction} \cdot L}{A \cdot E_{mean}} = \frac{24.1 \cdot 1000 \cdot 2850}{72000 \cdot 11500} = 0.083 \text{ mm}$$

Creep deformation

$$u_{cr} = \frac{f_{k,cr} \cdot L \cdot \varphi}{A \cdot E_{mean}} = \frac{200.9 \cdot 1000 \cdot 2850 \cdot 0.6}{72000 \cdot 11500} = 0.41 \text{ mm}$$

[EC]

$$u_{cr} = \frac{f_{k,cr} \cdot L \cdot \varphi}{A \cdot E_{mean}} = \frac{200.9 \cdot 1000 \cdot 2850 \cdot 0.9}{72000 \cdot 11500} = 2.24 \text{ mm}$$

[Experimental]

$$\varphi_{cr} = 0.15 \cdot (\ln(1 + 0.02 \cdot t)) = 0.15 \cdot (\ln(1 + 0.02 \cdot 35)) = 0.08$$

$$u_{cr,con} = \frac{f_{k,con} \cdot L \cdot \varphi_{cr}}{A \cdot 11500} = \frac{24.1 \cdot 1000 \cdot 2850 \cdot 0.08}{72000 \cdot 11500} = 0.0066 \text{ mm}$$

[Experimental]

Shrinkage and swelling

$$MC_1 = 12 + 0.2 \cdot \frac{12}{365} \cdot 14 = 12.09\%$$

During production to instalment

$$MC_2 = MC_{sur} - \frac{MC_{sur} - MC_1}{1 + \left(\frac{t}{30}\right)^{1.15}} = 15.86 - \frac{15.86 - 12.09}{1 + \left(\frac{35}{30}\right)^{1.15}} = 14.14\%$$

After instalment

$$u_{sh} = \frac{\beta}{100} \cdot (MC_2 - MC_{\infty}) \cdot L = \frac{0.011}{100} \cdot (14.14 - 9.27) \cdot 2850 = 1.53 \text{ mm}$$

Final deformation column

$$u_{fin} = u_{el} + u_{cr} + u_{sh} - u_{el,con} = 0.71 + 0.41 + 1.53 - 0.083 = 2.57 \text{ mm}$$

[EC]

$$u_{fin} = u_{el} + u_{cr} + u_{sh} - u_{el,con} - u_{cr,con} = 0.71 + 2.24 + 1.53 - 0.026 - 0.0066 = 4.45 \text{ mm}$$

[Experimental]

Acoustic felt



d	15 mm
H	360 mm
B	200 mm
E _{mean}	17 Mpa

Compressive area $360 \cdot 200 = 72000 \text{ mm}^2$

Elastic deformation

$$u_{el} = \frac{f_k \cdot d}{A \cdot E_{mean}} = \frac{207.7 \cdot 1000 \cdot 15}{72000 \cdot 17} = 2.55 \text{ mm}$$

$$u_{el,con} = \frac{f_{k,construction} \cdot d}{A \cdot E_{mean}} = \frac{24.1 \cdot 1000 \cdot 15}{72000 \cdot 17} = 0.30 \text{ mm}$$

Creep deformation

$$\varphi_{cr(35)} = 2.25 \cdot (t \cdot 1440)^{0.1} = 2.25 \cdot (35 \cdot 1440)^{0.1} = 6.64$$

6.64% of el. deformation

$$\varphi_{max} = 12.53$$

$$u_{cr} = \frac{f_{k,cr} \cdot d}{A \cdot E_{mean}} \cdot \frac{\varphi_{max}}{100} = \frac{200.9 \cdot 1000 \cdot 15}{72000 \cdot 17} \cdot \frac{12.53}{100} = 0.31 \text{ mm}$$

$$u_{cr,con} = \frac{f_{k,cr} \cdot d}{A \cdot E_{mean}} \cdot \frac{\varphi_{cr(35)}}{100} = \frac{200.9 \cdot 1000 \cdot 15}{72000 \cdot 17} \cdot \frac{6.64}{100} = 0.01 \text{ mm}$$

Final deformation acoustic felt

$$u_{fin} = u_{el} + u_{cr} - u_{el,con} - u_{cr,con} = 2.55 + 0.31 - 0.30 - 0.01 = 2.55 \text{ mm}$$

Final deformation floor 1

$$U = u_{beam} + u_{column} + u_{felt} = 1,47 + 2,82 + 2,55 = 6,51 \text{ mm}$$

[EC]

$$U = u_{beam} + u_{column} + u_{felt} = 6,67 + 3,39 + 2,55 = 9,24 \text{ mm}$$

[Experimental]

Appendix D – Creep in timber and loading direction

General

When subjected to a constant loading, timber behaves like a visco-elastic material. Meaning, that under constant stress the material will deform both elastically and viscously. This behavior is called creep. There are three main factors that contribute to the to the amount of creep of an timber element:

- | | |
|--------------------------------|--|
| The moisture content. | The moisture inside the timber acts as a plasticizer so with the increase in moisture content the creep increases as well. |
| Temperature. | The stiffness of wood is related to the temperature. A higher temperature alters the structure of the lignin and softens the hemicelluloses which reduces the stiffness. |
| Angle of loading to the grain. | With an increase of the angle of loading relative to the grain the more stress is taken by the gel inside the cells instead of the microfibrils. |

Creep in timber has 3 major stages which define the creep curve:

- Stage I: Primary phase. within the first phase the deformation develops fastest.
 Stage II: Secondary phase. The amount of deformation is hardly increasing and is almost constant.
 Stage III: Tertiary phase. The amount of creep rapidly increases and leads to failure.

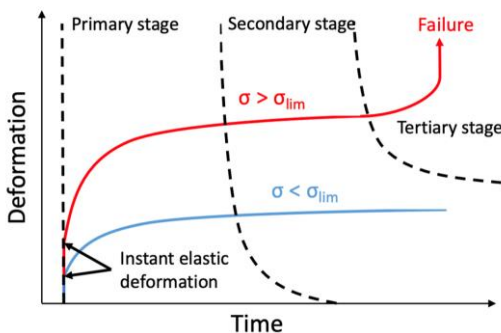


Figure 1 - Stages of creep over time

Boyd creep model

In order to describe the behavior of wood Boyd derived a microfibrils model to show the principles of creep in 1982. This principle can be observed in the figure below.

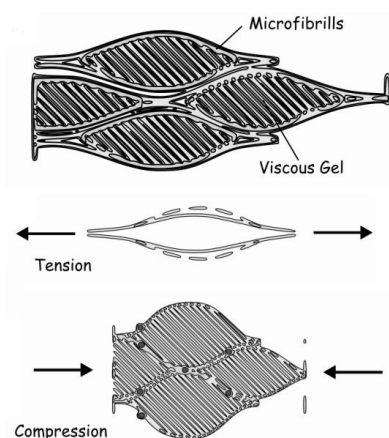


Figure 2 - Microfibrils model according to Boyd.

It can be observed that when loaded parallel to the grain the microfibrils take a large amount of the load. The amount differs in tension and compression. With creep determined by yielding of the viscous gel, it can be imagined that the amount of creep is less in tension than in compression. In case of loading perpendicular to the grain the microfibrils take even less of the load so the creep is increased even more compared to loading parallel to the grain.

Several code provisions

Across the world there are buildings being built with timber. Depending on region there are several standards provided in order to safely design timber structures. Standards like the Eurocode 5 (2004), New Zealand Timber Standard 3603 (1993) and National Design Specifications for Wood Construction (2018). These codes all provide standards for their own region for timber building. What these codes all have in common is that they take into account long term effects due to creep into their strength and deformation calculations.

In 2019 a comparison of the creep factor within these codes had been made by G. Granello and A. Palermo. The creep factors for each of the codes can be observed in Table 1. It should be noted that the New-Zealand code does not provide a distinction between service classes and is the same for all classes. The NDS only considers two service classes namely dry and wet.

Table 1 - Creep factors (intended as amplification factors of the elastic deflection).

Standard code	Service class I	Service class II	Service class III
NZS 3603	2	2	2
EC 5	1.6	1.8	3
NDS	1.5	2.41	2.41
Average	1.84	1.91	1.93
Max	NZS 3603	NDS	EC5
Min	NDS	EC 5	NZS 3603

The comparison concluded that generally there are no conservative codes. The Eurocode is most conservative for service class 3 but least conservative in service class 2. However, because the majority of the experiments in terms of creep are based on a period of observation lower than 10 years, it is difficult to identify which approach leads to the most accurate prediction over the life of a structure.

Creep factor perpendicular to the grain

It is well known that the angle to the grain matters in the amount of creep that is to be expected. Parallel to the grain provided to produce more creep than perpendicular to the grain. Below a few examples:

Wanninger et al. 2014.

Following is a brief summary of the following paper: Long-Term Behavior of Posttensioned Timber Connections, by Wanninger, F.; Frangi, A.; Fragiaco, M., 2014

In order to investigate the long-term behavior of timber connections, tests have been performed at the ETH in Zurich. This test setup consists out of a pre-tensioned column-beam connection. The column-beam connection consists out of glued laminated timber (spruce, Picea) with local hardwood strengthening using ash (Ash, Fraxinus), see Figure 3.



Figure 3 - Posttensioned timber connection made of glulam, darker areas indicate ash reinforcement.

In total 18 specimens were loaded using controlled conditions and 21 using uncontrolled conditions. The tests in the controlled environment were characterized by constant temperature of 20 degrees and a relative humidity of 65%. The uncontrolled environment was characterized by a constant temperature but fluctuating relative humidity.

The specimens were loaded by a constant distributed force of 3 Mpa, which accounts for approximately 35% of the characteristic compressive strength perpendicular to the grain of the ash timber column.

Creep results

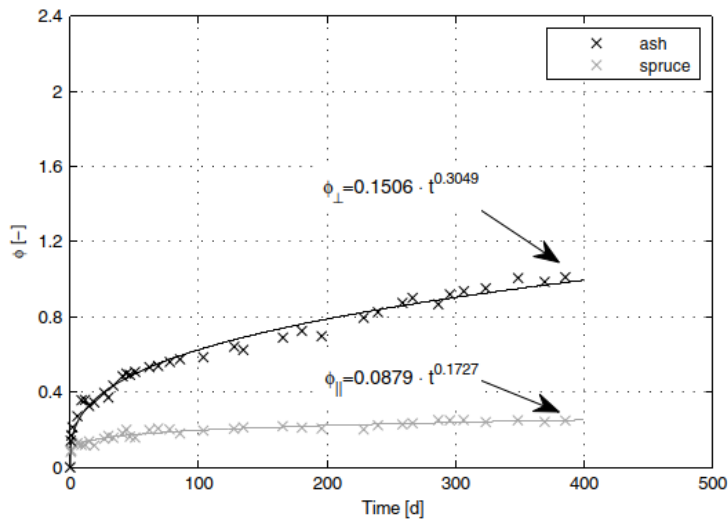


Figure 4 - Average creep results of the specimens using a logarithmic curve fitting.

The figure above depicts the average creep factor for the specimens loaded perpendicular (Ash) and parallel (Spruce) to the grain. When extrapolated to a 50 years, the creep coefficients become approximately 2.8 and 0.6 for the parallelly and perpendicularly loaded specimens.

A direct comparison was made between the Ash and Spruce creep coefficients. An assumption was made that the Ash and the Spruce share the same perpendicular creep coefficient. Although not verified by experimental testing this comparison is regarded as a conservative estimate because previous experimental testing carried out on glulam made from different softwood species (e.g., radiata pine) showed a creep coefficient perpendicular to the grain similar than monitored on Ash.

Massaro et al.

Following is a brief summary of the following paper: Long-Term Behavior of Norway spruce glulam loaded perpendicular to grain., Massaro, F.M.; Malo, K.A., 2019

The main objective of this study has been to quantify proper material parameters to describe the long-term behavior of timber under compression orthogonal to the grain and exposed to moisture variation. The model used in this paper is considered as a one-dimensional model. Examples of such applications are pre-stressed timber decks, header joists or more generally floors, beams and deck plates lying in between vertical load-bearing structures.

Test setup

In order to investigate this behavior a number of timber specimens are mechanically held together by steel rods, installed in pre-drilled holes in the perpendicular direction relative to the grain. The specimens consists out of Norway spruce classified as GL30c. The specimens were loaded through steel rods, which transfer the forces from the lever arms, passing the hollow steel coupler to the steel plates on top of the specimens. The test setup can be seen in Figure 5.

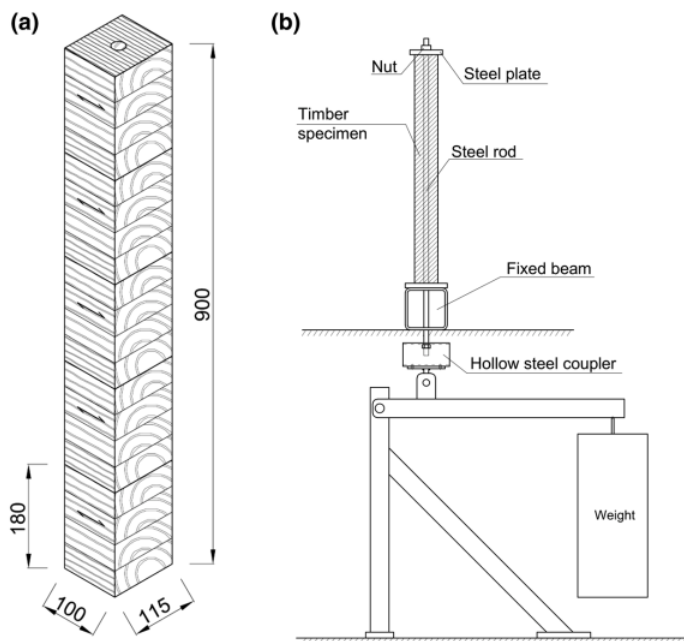


Figure 5 - a) Sketch of a timber specimen (units in mm); b) Lateral view of the test setup

The tests were performed in a climate-controlled room with a constant temperature of 20 degrees and continuous control of the relative humidity which was kept at 65% for 4 months. The specimens were tested under three different load conditions, which correspond to a uniform perpendicular compressive stress on the timber of 0.6, 0.8 and 1 MPa.

Results

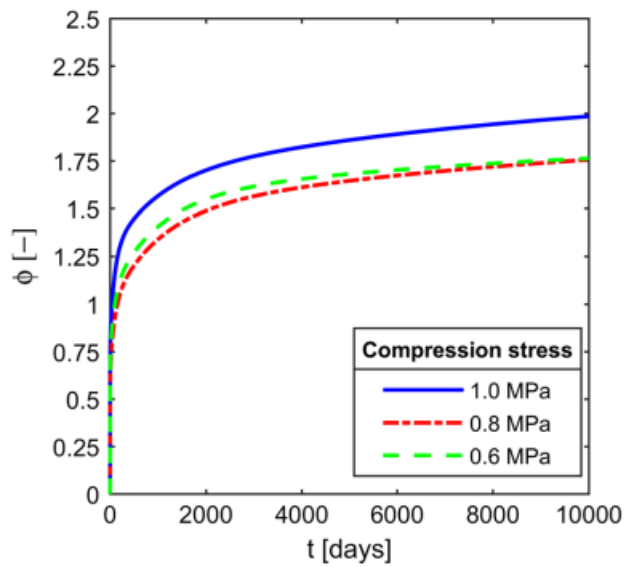


Figure 6 - Average creep results of the specimens using a logarithmic curve fitting.

In total there were 9 test specimens which have been loaded by 0.6, 0.8 and 1 MPa. The results can be observed in Figure 6 for all cases. It can be observed that when extrapolating the data to 50 years the creep factor reaches values of approximately 1.8, 1.8 and 2.1 for 0.6, 0.8 and 1 MPa loads respectively.